

Unmanned System Technologies

Zeeshan Kaleem
Ishtiaq Ahmad
Trung Quang Duong *Editors*



Intelligent Unmanned Air Vehicles Communications for Public Safety Networks

 Springer

Unmanned System Technologies

Springer's Unmanned Systems Technologies (UST) book series publishes the latest developments in unmanned vehicles and platforms in a timely manner, with the highest of quality, and written and edited by leaders in the field. The aim is to provide an effective platform to global researchers in the field to exchange their research findings and ideas. The series covers all the main branches of unmanned systems and technologies, both theoretical and applied, including but not limited to:

- Unmanned aerial vehicles, unmanned ground vehicles and unmanned ships, and all unmanned systems related research in:
- Robotics Design
- Artificial Intelligence
- Guidance, Navigation and Control
- Signal Processing
- Circuit and Systems
- Mechatronics
- Big Data
- Intelligent Computing and Communication
- Advanced Materials and Engineering

The publication types of the series are monographs, professional books, graduate textbooks, and edited volumes.

More information about this series at <https://link.springer.com/bookseries/15608>

Zeeshan Kaleem · Ishtiaq Ahmad ·
Trung Quang Duong
Editors

Intelligent Unmanned Air Vehicles Communications for Public Safety Networks

 Springer

Editors

Zeeshan Kaleem
Department of Electrical and Computer
Engineering
COMSATS University Islamabad
Wah, Pakistan

Ishtiaq Ahmad
Faculty of Engineering and Technology
Gomal University
Dera Ismail Khan, Pakistan

Trung Quang Duong
School of Electronics, Electrical
Engineering and Computer Science
Queen's University Belfast
Belfast, UK

ISSN 2523-3734

ISSN 2523-3742 (electronic)

Unmanned System Technologies

ISBN 978-981-19-1291-7

ISBN 978-981-19-1292-4 (eBook)

<https://doi.org/10.1007/978-981-19-1292-4>

© The Editor(s) (if applicable) and The Author(s), under exclusive license to Springer Nature Singapore Pte Ltd. 2022

This work is subject to copyright. All rights are solely and exclusively licensed by the Publisher, whether the whole or part of the material is concerned, specifically the rights of translation, reprinting, reuse of illustrations, recitation, broadcasting, reproduction on microfilms or in any other physical way, and transmission or information storage and retrieval, electronic adaptation, computer software, or by similar or dissimilar methodology now known or hereafter developed.

The use of general descriptive names, registered names, trademarks, service marks, etc. in this publication does not imply, even in the absence of a specific statement, that such names are exempt from the relevant protective laws and regulations and therefore free for general use.

The publisher, the authors and the editors are safe to assume that the advice and information in this book are believed to be true and accurate at the date of publication. Neither the publisher nor the authors or the editors give a warranty, expressed or implied, with respect to the material contained herein or for any errors or omissions that may have been made. The publisher remains neutral with regard to jurisdictional claims in published maps and institutional affiliations.

This Springer imprint is published by the registered company Springer Nature Singapore Pte Ltd.

The registered company address is: 152 Beach Road, #21-01/04 Gateway East, Singapore 189721, Singapore

Foreword

Unmanned air vehicles (UAVs) have shown great potential to enable numerous applications ranging from industry verticals to public-safety communications. However, various challenges also arise with its integration into the existing terrestrial networks such as efficient UAV positioning, power allocation, trajectory design, and resource allocation. The existing conventional optimization solutions are not intelligent enough to overcome those challenges. Thus, real-time optimization and machine-learning-assisted solutions, and emerging technologies are required to overcome those challenges.

In this regard, this book's arrival is timely, and it will build your knowledge about intelligent UAV communications for the public-safety network from the ground up. This book provides the state of the art of public-safety communication networks with the latest advances in intelligent UAV communications. This book also supplies a clear picture of future trends related to emergency communications that are assisted by the current research development of beyond 5G and upcoming 6G wireless networks. The book contents will help researchers and other stakeholders narrow down prospective concepts for employing intelligent UAV communications for public-safety networks.

The book also contains compelling use cases and insights developed by some of the leading researchers working in this exciting and pivotal research direction. It is now in your hand to use this book for enabling intelligent UAV networks.

Prof. Chau Yuen
IEEE Fellow
Singapore University of Technology
and Design (SUTD)
Singapore, Singapore

Introduction

UAVs have shown promising potential in enabling a wide range of applications, from industry verticals to public-safety communications. However, integrating it into current terrestrial networks poses a number of issues, including effective UAV placement, power distribution, trajectory design, and resource allocation. This book examines both conventional non-intelligent and intelligent UAV communication systems for public-safety networks. Furthermore, reconfigurable intelligent surfaces (RIS) have lately piqued the interest of researchers and academician due to their ability to improve the propagation environment and communication quality by intelligently reflecting received signals. By incorporating intelligence into RIS-assisted UAV communications, it will be able to satisfy the needs of intelligent, green, and sustainable 5G and upcoming 6G cellular networks, making it a viable choice for overcoming the fundamental flaws of older wireless systems.

Chapter “[Intelligent Unmanned Air Vehicles for Public Safety Networks: Emerging Technologies and Research Directions](#)” reviews the essential technologies that will enable public-safety communications by deploying intelligent UAVs. The authors pointed out the challenges related to them and also highlighted the future research directions for researchers. To enable public-safety communications, they highlighted that intelligence plays a critical role in increasing UAV performance in terms of coverage, throughput, mobility management, and edge computing. Moreover, they summarized that the existing traditional optimization algorithms are not sufficient enough to address the challenges like UAV positioning, power allocation, trajectory optimization, and resource allocation to enable emergency communications.

Chapter “[UAV Placement and Resource Management in Public Safety Networks: An Overview](#)” provided an overview about the features, applications, and enabling technologies for public-safety networks. The importance of safety networks is high when the existing terrestrial infrastructure is destroyed during the natural disasters. To timely reach a disaster area and rescue people, communication infrastructure quick deployment is desired. Hence, UAVs’ deployment is one of the finest solutions for reaching difficult-to-reach regions. The authors in this chapter discussed UAVs’ types, public-safety use cases, state-of-the-art positioning and resource allocation

schemes, as well as the security challenges to quickly overcome the communication challenges.

Chapter “[3D Unmanned Aerial Vehicle Placement for Public Safety Communications](#)” proposes a three-tier Aerial-HetNet to enable public-safety communications consisting of terrestrial macrocells and small cells carried by UAVs. This chapter, in particular, presents an Aerial-HetNet with strategically deployed UAVs to ensure quality of service. The proposed scheme also considers range expansion bias at small cells, various inter-cell interference coordination for interference mitigation, 3D beamforming for antennas, and 3D channel modeling for UAVs. The authors investigated the fitness of numerous algorithms for locating optimal or near-optimal 3D UAV placements. Based on the comparison of the brute-force technique and the heuristic algorithm examined in the chapter, it is necessary to discover a suitable algorithm that can solve the trade-off of decreasing computing complexity while finding the search problem’s near-global maxima.

Chapter “[Power-Efficient UAV Placement in Relay Assisted Heterogeneous Public Safety Networks](#)” discusses the placement of UAVs as a relay to enable emergency communications. The battery life of UAVs is a scarce resource that requires UAV BS transmit power optimization. To overcome this issue, a model which consists of a fixed base station, observation UAV, and relay UAV is adopted to enable long-distance communication. The optimal placement of relay UAV becomes requisite for reliable connectivity between observation UAV and ground base station. In this chapter, the authors minimize the sum power of observation and relay UAVs by using the optimal placement of relay UAVs. The optimized power ensures throughput requirements for real-time communication. They converted the non-convex problem into a convex optimization problem, and the optimal solution is acquired using the interior point method.

Chapter “[Location Prediction and Trajectory Optimization in Multi-UAV Application Missions](#)” explains multi-UAV cooperation applications and the way to perform drone location prediction and trajectory optimization using Kalman filtering and machine-learning approaches. These techniques facilitate the drones to follow intelligent paths and establish optimal trajectories while carrying out successful application missions under given resource and network constraints. Moreover, three scenarios are adopted to demonstrate the practicability of those techniques. The first scenario uses multiple Kalman filtering techniques with sensor fusion to provide location prediction-based intelligent packet transmission between drones in a disaster response scenario. The second scenario incorporates a learning-based trajectory optimization that employs a variety of reinforcement learning models to maintain excellent video resolution and network performance in a civil application scenario such as aerial monitoring of people or objects. The third scenario entails non-ML-based trajectory optimization approaches in UAV-based public-safety applications. The authors wrap up with a list of open issues and ongoing research on intelligent drone path planning using location prediction and trajectory optimization approach.

Chapter “[UAV Trajectory Optimization and Choice for UAV Placement for Data Collection in Beyond 5G Networks](#)” proposes collecting uplink traffic from disaster

points to reduce the overall network's Age-of-Information (AoI). Authors specifically examine the optimal trajectory of a UAV for data collection to ensure timely delivery of information to the destination, lowering the overall AoI. They compared the proposed trajectory performance with random trajectory and traveling salesman problem (TSP). Furthermore, as compared to Matern type-I hard-core process-based UAVs distribution, unsupervised learning-based UAVs distribution helps to reduce the AoI. Moreover, the proposed trajectory is less computationally expensive than a TSP-based trajectory design, making it suitable for the Internet of Things (IoT) applications.

Chapter “[Enhancing UAV-Based Public Safety Networks with Reconfigurable Intelligent Surfaces](#)” explains the fundamentals, design characteristics, and applications of reconfigurable intelligent surfaces (RIS) as a future wireless network enabling technology. Specifically, the authors focused on integrating RIS into UAV networks to flexibly move in the 3D space to achieve panoramic full-angle signals manipulation, while UAV users may rely on the available RISs within the environment in order to operate securely, at extended ranges, and with reduced communication and energy costs. Authors create two use cases related to public safety, namely, aerial surveillance and search-and-rescue UAV operations, to demonstrate their feasibility and usefulness. Finally, the author outlined the existing limitations of this integration as well as future research objectives for developing RIS-enabled UAV systems.

Chapter “[UAVs Path Planning by Particle Swarm Optimization Based on Visual-SLAM Algorithm](#)” The authors propose a two-step centralized approach for developing 3D path planning for a swarm of UAVs. Using the visual simultaneous localization and mapping (V-SLAM) method, they traced the UAV's position while simultaneously constructing an incremental and progressive map of the environment. Moreover, they offer a corner-edge points matching strategy for stabilizing the V-SLAM system in the least extracted map points. In this case, a single UAV fulfills the duty of mapping an area of interest using monocular vision. Furthermore, the particle swarm optimization (PSO) algorithm is adopted to optimize pathways for multi-UAVs systems. They also propose a path-updating method based on region sensitivity to avoid sensitive areas during final path execution.

Chapter “[UAV-Assisted Cooperative Routing Scheme for Dense Vehicular Ad hoc Network](#)” proposes UAV-assisted Cooperative Routing Scheme (UCRS), in which a flying ad hoc network (FANET) assists a vehicular ad hoc network (VANET). Here, each node in UCRS creates an Allied Node Table (ANT) based on the vehicles in the forwarding zone. Moreover, they selected the best node among several nodes available in ANT as an end-to-end route to forward the data traffic to the intended destination. They evaluated the proposal using the network simulator (ns-2.31) and proved that UCRS achieved better performance from U2RV and AODV with an increase in node density.

We believe that this contributed book will be helpful for both academic and industrial researchers. This book is made possible with the collaboration of several international professionals and research teams. It covers the potential use cases and intelligent technologies to enable UAV-assisted intelligent communications to enable public-safety communications. Moreover, the contributions include

machine/deep learning-assisted UAV 3D placement, trajectory optimization, path planning, UAV-assisted layered architectures, cooperative routing schemes, and 3GPP standardizations process to enable public-safety communications.

We expect this book to open the path for more study on reconfigurable and software-controlled meta-surfaces for intelligent UAV communications to enable public-safety networks in the future. This book also provides a clear picture of future trends related to emergency communications that assist in improving the efficiency and performance of beyond 5G and upcoming 6G wireless networks. The book contents will help researchers and other stakeholders narrow down prospective concepts for employing intelligent UAV communications for public-safety networks.

Contents

Intelligent Unmanned Air Vehicles for Public Safety Networks: Emerging Technologies and Research Directions	1
Zeeshan Kaleem, Ishtiaq Ahmad, and Trung Q. Duong	
UAV Placement and Resource Management in Public Safety Networks: An Overview	19
Rizwana Shahzadi, Mudassar Ali, and Muhammad Naeem	
3D Unmanned Aerial Vehicle Placement for Public Safety Communications	51
Abhaykumar Kumbhar and Ismail Güvenç	
Power-Efficient UAV Placement in Relay Assisted Heterogeneous Public Safety Networks	91
Yasir Iqbal, Ayaz Ahmad, and Zeeshan Kaleem	
Location Prediction and Trajectory Optimization in Multi-UAV Application Missions	105
Rounak Singh, Chengyi Qu, Alicia Esquivel Morel, and Prasad Calyam	
UAV Trajectory Optimization and Choice for UAV Placement for Data Collection in Beyond 5G Networks	133
Muhammad K. Shehzad, Syed Ali Hassan, Miguel Angel Luque-Nieto, and Pablo Otero	
Enhancing UAV-Based Public Safety Networks with Reconfigurable Intelligent Surfaces	145
Wael Jaafar, Lina Bariah, Sami Muhaidat, and Halim Yanikomeroglu	
UAVs Path Planning by Particle Swarm Optimization Based on Visual-SLAM Algorithm	169
Umair Ahmad Mughal, Ishtiaq Ahmad, Chaitali J. Pawase, and KyungHi Chang	

**UAV-Assisted Cooperative Routing Scheme for Dense Vehicular
Ad hoc Network 199**
Omer Chughtai, Muhammad Naem, and Kishwer Abdul Khaliq

Intelligent Unmanned Air Vehicles for Public Safety Networks: Emerging Technologies and Research Directions



Zeeshan Kaleem, Ishtiaq Ahmad, and Trung Q. Duong

Abstract Unmanned air vehicles (UAVs) has shown great potential to enable numerous applications ranging from industry verticals to public safety communications. However, various challenges also arises with its integration into the existing terrestrial networks such as efficient UAV positioning, power allocation, trajectory design, and resource allocation. The existing conventional optimization solutions are not intelligent enough to overcome those challenges. Thus, real-time optimization and machine learning assisted solutions, and emerging technologies are required to overcome those challenges. To address those challenges, we summarized key technologies and research directions for UAV deployment at the edge or in the cell center, the power allocation and localization schemes, and the federated learning solutions.

Keywords Federated learning · RIS · Intelligent UAVs · UAVs localization · Machine learning

1 Machine Learning for Wireless Communications

The worldwide requirement for data traffic has endured around 1000×-fold increase over the previous years [1]. Due to the development of modern wireless communication networks, data traffic requirements are supposed to increase the capacity of future networks. In addition to a notable increase in data traffic, the latest communications applications, such as autonomous networks, wearable gadgets, Internet of

Z. Kaleem (✉)

Electrical and Computer Engineering Department, COMSATS University Islamabad, Wah Campus, Wah Cantt., Punjab, Pakistan
e-mail: zeeshankaleem@gmail.com

I. Ahmad

Electrical Engineering Department, Gomal University, Dera Ismail Khan, Pakistan

T. Q. Duong

School of Electronics, Electrical Engineering and Computer Science, Queen's University Belfast, Belfast BT3 9DT, UK

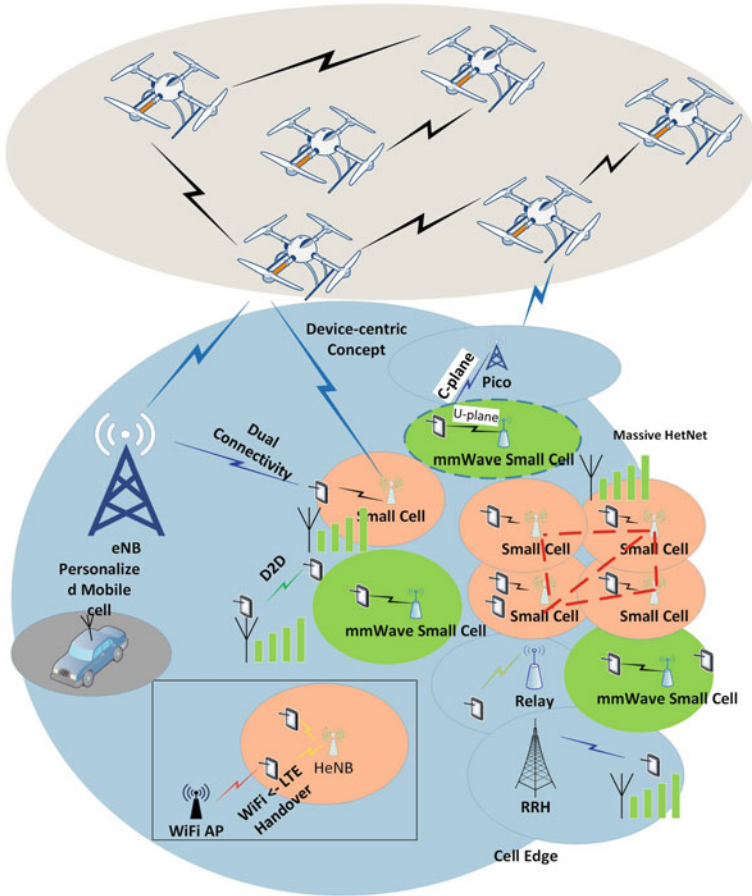


Fig. 1 Types of base stations to enable next-generation public safety networks

Things (IoT) devices, and cellular-connected unmanned air vehicles (UAVs) communications, continuously develop and produce immense data traffic with diverse requirements as shown in Fig. 1.

This development in communication applications demands an undeniable need for intelligent service, processing, and optimization of future communication systems. Using machine learning (ML), also known as artificial intelligence, into the design, planning, and optimization of future communication networks. The concept of ML has a lengthy and flourishing history. For instance, the use of neural networks (NN) for intelligent systems instead of utilizing a simple single-layer design to affect the state of one neuron. The idea of ML has established its powerful benefits in numerous fields, including robotics, computer vision, communications, and signal processing, where it is hard to find a detailed mathematical design for the characteristic pattern. In such areas, ML is considered a potential factor that does not demand any compre-

hensive model specification. The traditional methods that mainly depend on models and theories show weaknesses due to the extensive complexity of communication systems. Hence, research on ML for communication systems, particularly wireless communications, is currently encountering magnificent growth. For intelligent processing in a variety of scenarios, the emerging structure of ML acts as an enabler. The latest ML methods give a wide range of opportunities to develop intelligent communication systems that assists in addressing numerous challenges related to signal processing, classification, detection, channel estimation, resource allocation, routing protocols, configuring transport protocol, and user behavior interpretation. Various types of ML schemes have different usage in radio communication systems. It breaks the levels according to the kind of supervision demanded for training the ML models. Following are the three major categories of ML models.

1.1 Supervised Learning

Supervised learning model uses sample data with perceived results to estimate the output. Every sample data value is mapped to a single result value. The main purpose is to feed and train the model using sample data as input and with already known outcomes. After that, the already trained model predicts the results of the new input samples. Supervised learning is successful when there is a large amount of data to train the model. Hence, supervised learning is practical in deploying 6G to cope with rising traffic requirements. ML-based supervised learning collects performance computations such as throughput, outage probability, signal-to-interference and noise ratio, and pathloss for specific frequencies and bandwidth. ML-based supervised learning is used to predict the various performance matrix that a user will experience and adjust the different parameters accordingly [2]. ML-based supervised learning is adopted to train the models for pathloss prediction by considering channel state information (CSI) and approximate objective functions for associate propagation loss for 6G wireless systems.

1.2 Unsupervised Learning

An unlabeled collection of data is used to train the model with different characteristics and the system endeavors to identify subgroups with related features between the variables without having human involvement. Various schemes like generative deep neural network (DNN) and K-means clustering are advantageous when arranging devices for edge computing in a system. ML-based unsupervised learning is advantageous for uncertainty and detecting various faults in a system. It collects data in batches at data collection centers to decrease redundant data travel between distributed storage centers. It minimizes the latency by grouping nodes to automati-

cally determine the node with low powers that must be promoted to nodes with more power for resource management in ultra-dense small cells.

1.3 Reinforcement Learning

Reinforcement Learning (RL) constantly works in probabilistic situations of wireless systems. In order to obtain excellent performance, the network parameters are modeled by using a Markov decision process (MDP) as shown in Fig. 2. RL continuously communicates with the environment, calculating the decisions at periodic intervals of time. The RL model needs to determine action at each point, obtained at the current state, to which the model provides a positive or a negative reward and updates the state. The rewards are associated with SINR and data rate. The RL is a data-driven approach that is not completely modeled from physics and mathematical-based modeling. Undoubtedly, wireless communication networks are human-made with lots of compositions that lack fast learning and transparency. Moreover, the state transition probability is free of all prior actions and states. While we require to optimize the system, the RL holds a record of all probabilities and their outcomes to obtain the absolute optimum decision. The principal grounds for RL to be applied to a radio communication system problem consist of (i) the signaling for obtaining the valuable data sets required to accurately operate the system is too complicated, (ii) the mathematical analysis of the wireless environment is considerably complicated to use in an agent and (iii) the desired results of RL is presented as a scalar reward. For example, the extensive machine-type communication and cell deployment (mainly small cells) where comprehensive system preparation is not achievable. We also summarized and compared key features of these three ML schemes in Table 1.

Fig. 2 Reinforcement learning working procedure

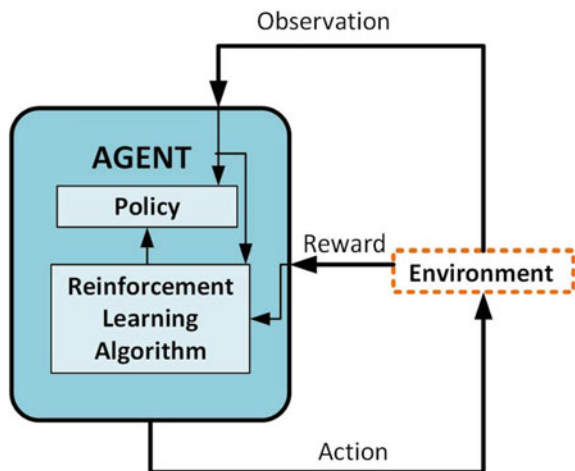
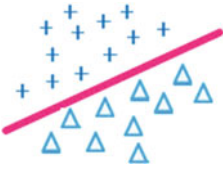
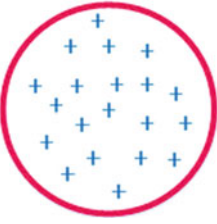
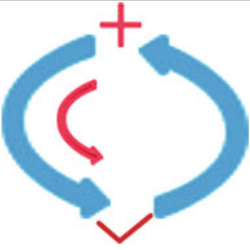


Table 1 Comparison of supervised, unsupervised and reinforcement learning

Supervised learning	Unsupervised learning	Reinforcement learning
		
Output is known	Output is not known	Interacts with the environment to make decision
Labelled data is used	Unlabelled data is used	Has no pre-defined data
Trained using past data	Trained using any data	Learning process rely on reward and policy
Algorithm is trained to predict output values	Algorithm is trained to discover similarities and differences in data	Algorithm learns by interacting with the environment using trial and error method
Highly supervised	Not supervised	Less supervised and rely on agent to find output
Learning predicts discrete value	Discover unknown patterns	Agent interacts with the environment to get rewards
Compute formula on the basis of inputs and outputs	Aim to find association among input and output value to sort them in groups	Aim to find the best possible reward by choosing suitable actions

2 Cellular-Connected UAVs for Emergency Communications

UAVs have applications in numerous fields ranging from civil to vertical industries as they can enhance coverage while supporting high mobility. UAVs also helps in enabling real-time sensing applications and emergency communications [3]. UAVs are getting popularity in provisioning emergency communications to the users in disaster-hit areas by serving as an aerial base station (ABS) [4]. UAVs can assist in carrying medical and food supplies to unreachable regions. With the assistance of ABS deployment, an emergency communication network is established to prevent further human lives and losses by connecting the victims with the emergency relief providing personals. Since, it is hard for a communication service provider to deploy a ground base station (BS) in a short time. Therefore, ABS are deployed to enable emergency communications or to increase the coverage of the functional BS as shown in Fig. 3.

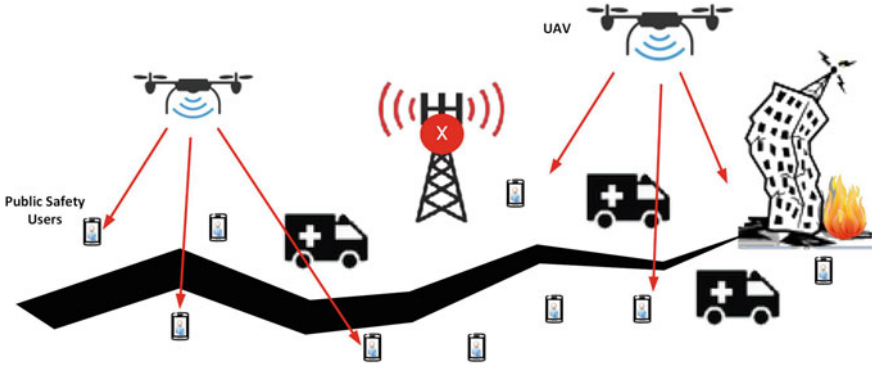


Fig. 3 UAVs-assisted public safety networks for coverage enhancement

Providing cellular connectivity to UAVs has enabled a plethora of applications ranging from online video streaming to enable emergency communications [5]. The Third Generation Partnership Project (3GPP), an industry-led consortium that standardises cellular networks, has been actively involved in identifying the key requirements, technologies, and protocols for aerial communications. To use enhanced Long Term Evolution (LTE) support for aerial vehicles, 3GPP successfully completed the first report in 2017 that led to 3GPP Release 15 Technical Report TR 36.777. That report highlighted the necessary requirements for UAVs to optimize their operations.

In 2019, 3GPP TR 22.829 identifies several UAV-enabled applications and use cases to improve and support 5G communications and networking technologies. During 2020 in Release 17, 3GPP mainly focused on two aspects: (1) infrastructure to support the connectivity and tracking in TR 23.754, and (2) application architecture to support UAV operations in TR 23.755 [6]. However, in order to provide UAVs with reliable wireless connectivity along with secure operation, a lot of challenges must be addressed, including interference management, mobility and handover management, and malware attacks prevention.

To enable these applications, multiple UAVs are required for zone monitoring during disaster situation. In addition, multiple UAVs system can boost the system efficiency through joint effort. However, number of challenges exists in multiple UAVs system that includes localization, data processing at the edge, and trajectory planning and 3D ABS placement optimization [7, 8]. When compared to normal operating conditions, user association plays a significant role in emergency scenarios. In the case of a disaster, when the traditional terrestrial base station (TBS) is out of service, it becomes necessary to deploy UAVs in that area. Enabling device-to-device (D2D) communications [9, 10], in addition to UAV deployment, could help to improve coverage. The user association for numerous types of base stations is the key challenge in co-existing D2D and UAVs network. To address this issue, the authors in [11] explored how to solve the user association problem for UAV-enabled networks using D2D connections by maximizing the weighted sum rate of UAV users and total

Table 2 Related works in UAV communications

References	Brief summary	Placement schemes	Localization approaches	AI and distributed learning	Emerging technologies
[17]	Survey on object detection for low-altitude UAVs			✓	
[7]	Comprehensive survey on UAV-assisted networks				✓
[18]	Survey on communication and networking technologies for UAVs				✓
[19]	Pervasive public safety communication technologies		✓		
[20]	Important issues in UAV communications	✓			
[21]	Survey on legacy and emerging technologies for public safety communications				✓
[22]	Issues in cybersecurity, Privacy, and Public Safety			✓	
[23]	Survey of public safety communications: User- and network-side solutions		✓		
[24]	Survey on channel modeling for UAV communications				
[25]	Survey on collaborative smart internet of drones			✓	
[26]	Survey on anti-drone systems: components, designs, and challenges	✓			
[27]	Survey on applications, databases, and open computer vision research from drone videos and image				✓
[28]	Survey on Collaborative UAV and wireless sensor network (WSN) for Monitoring		✓		
[29]	A Survey on machine-learning techniques for UAV-based communications	✓		✓	
[30]	Survey on security and privacy issues for UAV communications			✓	
[31]	Role of UAVs in public safety communications	✓	✓	✓	✓

D2D users. This difficult problem is tackled by presenting a learning-based clustering technique, which yielded sub-optimal results while being substantially simpler. As a consequence, this technique can be used to improve public safety wireless networks in the future.

In public safety communications, edge computing represents a paradigm change. Time taken to complete task is greatly minimize by placing edge computing centers in UAVs, which would minimize response time to consumers and save their lives. This strategy was described in [12], where the authors used user association, UAV trajectory, and user power to maximize offloaded bits from users to UAVs while considering the UAV's energy constraints and the users' QoS constraints. The trajectory of the UAV is significantly affected by various elements such as energy, flight time, and user needs.

UAVs equipped with Intelligent Reflecting Surface (IRS) are used in hazardous communication environments to provide public safety users with customizable services, quick deployment, low latency, coverage assurance, and a large amount of energy. UAVs-IRS defend mission-critical, high-priority public safety users from risks such as terrorism, natural disasters, and technological accidents. This communication helps to communicate and send the information (e.g., voice, data, and video) which improves the cooperation among of public safety users [13]. Due to malicious assaults or natural disasters [14], the BSs may be destroyed, leaving high-priority public safety users' without coverage. UAVs-IRS provide a direct or multi-hop by acting as a relay communication situation to address this issue [15]. When UAVs-IRS are used in conjunction with public safety networks, overall system congestion and communication coverage gaps are reduced. Adding flexible UAVs-IRS relays to disaster zones reduces the public safety users' outages dramatically. The coverage of public safety users' is significantly boosted after deploying UAVs-IRS relaying systems. UAVs-IRS can simultaneously give coverage to adjacent public safety users' and act as a relay to cover users that are positioned at a great distance by optimizing IRS reflection angle and phase shifts [16].

We summarize recent works related to UAV communications that covers various aspects such as ABS placement schemes, localization approaches, and artificial intelligence (AI)-assisted communications in Table 2.

3 ABS Placement, Power Allocation, and Localization for Emergency Communications

UAV-assisted communication infrastructure can provide high performance, capacity enhancements, and extended network coverage [32, 33]. They can explicitly provide mission-critical communications tasks with the facility of autonomous operations. Furthermore, UAVs play an important role in the distribution of critical information on the fringes of the fighting area as well as in the implementation of cellular networks. To provide the coverage extension, UAVs as a flying adhoc network (FANET)

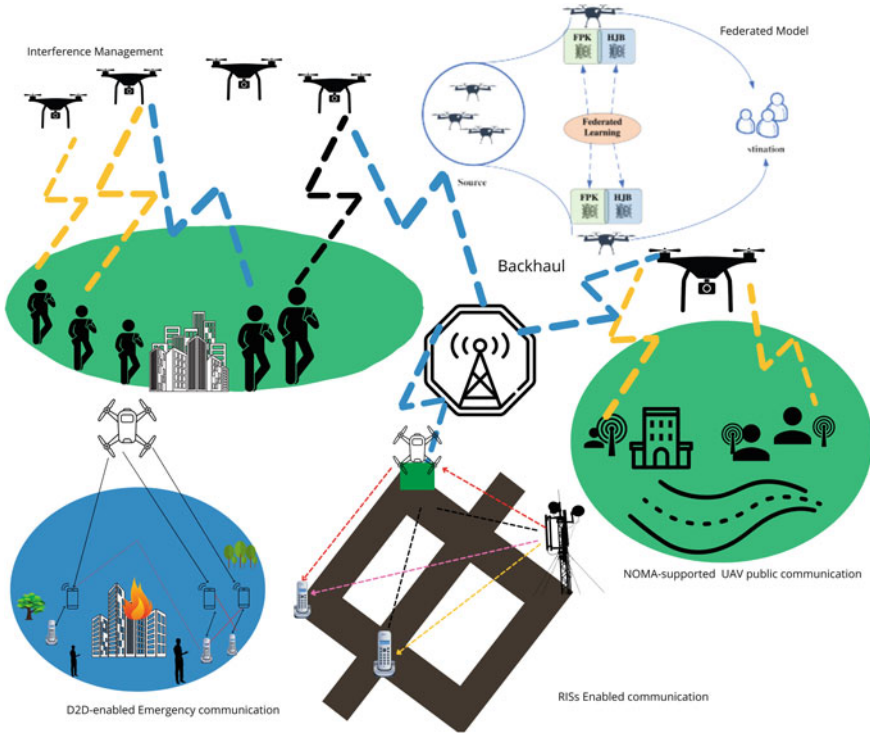


Fig. 4 UAVs-assisted public safety communication use cases

has gain the popularity [34]. We summarized some of the use cases to enable public-safety communications in Fig. 4.

A variety of future FANET communication architectures have been investigated including existing wireless technologies in the literature. However, selection of key communication technologies, architecture and core technology is truly a tedious problem to handle in FANET [35]. For instance, in [36] the authors presented a hybrid communication model, where they adopted features of 802.11 to meet high data rate requirements and 802.15.1 for low power consumption to enable FANET communications. This architecture considerably improved the network performance and reduced infrastructures costs.

In [37], the authors presented the advantage of coordination between UAVs and wireless sensor networks (WSNs). These two networks can support a wide range of applications, including search and rescue, navigation, control and recognition. The authors presented the solution for coverage enhancement using WSN-empowered UAV networks and argued that an efficient selection of way-points can solve several coverage issues.

To achieve high throughput gain during emergency situation, the authors in [38], presented the solution to optimally place the UAVs as an ABS in the disaster-hit

areas. They achieved the improved average as well as an edge throughput. Similarly, the authors in [31] summarized the key contributions of ABS to enable public safety communications by targeting energy efficiency perspective. Moreover, they also proposed the ABS-assisted architecture that can assist the emergency users by enabling emergency communication services.

To enhance the users' coverage and improve their connection, the matching game algorithm is proposed in [39]. Moreover, they also propose a medium access control framework to optimize emergency efficiency and priorities emergency communications users. The simulation results proved the efficacy of the proposal within the affected areas. In [40], the authors presented a solution for different path loss models and deployment situations to enable ABS-assisted public safety communications in heterogeneous networks. By system-level simulations, the authors proved that they successfully improved the system performance by reducing the co-channel interference.

For ABS-aided relay system to enable emergency communications [41], the authors in [42] presented the joint optimisation of real-time ABS deployment and resource allocation scheme by proposing a fast K-means-based user clustering model. They also provided the centralized and distributed models to maximise the energy efficiency of the considered network under the tight QoS constraints. Numerical results verified the effectiveness of the proposed scheme.

To solve the challenge of path planning during disaster situation with limited battery and unknown user distribution constraints, the authors in [43] converted this challenge into multi-armed bandit problem. Then to efficiently solve this problem, they proposed two path planning algorithms which significantly enhanced performance in terms of number of served users.

The back-haul-aware optimization problem is presented in [44] to minimize the delay and search the ABS optimum altitude to maximize the users' coverage. They selected the optimum altitude by considering the minimum transmit power constraint. In [45], the authors jointly optimized the user association, resource allocation and 3D UAV placement to maximize the downlink sum-rate. They divided the problem into the three sub-problems and proposed the iterative solution that significantly enhanced the sum rate by reducing the co-channel interference. In [46], the authors targeted to maximize the network throughput by jointly optimizing the transmit power and UAV trajectory subject to the mobility constraints. They proved that the proposed scheme achieved notable throughput gains as compared to the conventional static relaying system.

In [47], to jointly optimize the ABS elevation and power control with the goal of reducing the concentrated outage probability, an iterative algorithm centered on the block coordinate descent (BCD) technique was proposed. Simulation results revealed that the outage probability was considerably reduced. In [48], the author proposed a framework that optimizes UAV trajectory and transmits power in order to improve the minimum throughput among UAV aided users. An iterative algorithm was proposed with the goal of reducing access delay and improving throughput.

Localization of the users is key during the disaster situation. To address this challenge, the authors in [49] presented a solution to transmit the discovery message over

an ABS-to-user link. Simulation results proved that by using root-MUSIC algorithm the localization accuracy has been significantly improved. Similarly, in [50] data routing mechanism for localization in GPS-denied areas. The proposal focused on weighted centroid localization technique, where the position of unknown ABS are calculated using fuzzy logic. The proposed idea improves the localization efficiency by reducing the energy consumption and improving the lifetime.

4 Federated Learning for UAVs-enabled Public Safety Networks

UAVs as an ABS play key role in coverage improvement, capacity enhancement, and improving energy efficiency. During public safety communications, UAVs act as mobile terminal to enable applications like real-time video streaming for security personals. Here, UAV that act as an aggregator to globally train the model by collecting the locally trained model from the users, as shown in Fig. 5.

To efficiently implement this system, recently deep learning approaches has gained popularity to process the huge amount of received data. However, most of those processing are cloud centric, that in turn consumes huge power, consumes more bandwidth, introduce communication delay, and may pose security threats as it may contain UAV location and identity [51]. We compare the federated learning (FL) with the existing distributed and centralized learning schemes in terms of cost, accuracy, and latency in Table. 3.

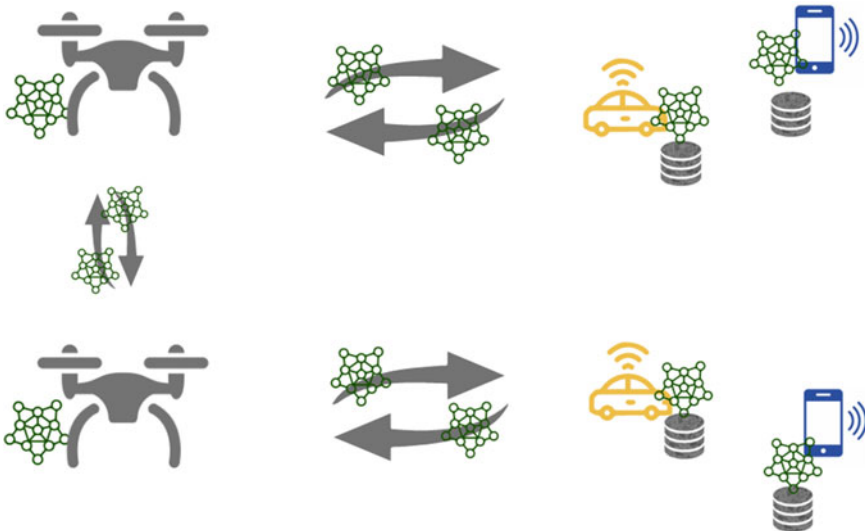


Fig. 5 Application of federated learning for UAV enabled public safety networks

Table 3 Comparison of FL with distributed and centralized learning

	Distributed learning	Centralized learning	Federated learning
Concept	Data is shared and process to multiple server parallel	Data collected at central server and process centralized manner	First client process their local data then local updates send to central server
Accuracy	Moderate	High	Low
Cost Feasibility	Cost effective	More costly	More cost effective due to locally sharing data
Latency	Less latency	More Latency than distributed learning	Latency is reduce to significant number from previous learning
Bandwidth	Less bandwidth require than centralized	More bandwidth needed	Updates are lighter so less bandwidth needed
Privacy	Privacy risk exist	Privacy risk exist	Due to exchange of Raw data privacy is not compromised

To overcome those challenges, recently Google introduced federated deep learning (FDL) or distributed deep learning concept [52] that has attracted huge popularity in communications, and specially in UAV communications during public safety, where only the locally trained models will be shared with the centralized entity for aggregation. This in turn significantly reduced the latency and power consumption as compared to centralized cloud processing as shown in Fig. 6 .

In FDL, deep neural network is collaboratively trained at the edge devices (UAVs in our case). Afterwards, the trained model is shared with the cloud to aggregate and create a global model. There are three main steps involved in this process; (1) training initialization, where as per requirements of the targeted application, hyper-parameters, initial global model, etc., are broadcasted to the UAVs by federated learning (FL) server, (2) each UAV collect new data and update parameters of local model based on the global model. Each UAV tries to optimize their parameters, and then shared those trained parameter with FL server, (3) after receiving those local parameters from UAVs, FL server aggregates them using the *FederatedAveraging* algorithm [53] and sends back the updated model parameters to UAVs. At FL server, the received parameters are optimized by minimizing the global loss function. More details about those steps are summarized in [51].

In public safety communications, UAVs have to execute various tasks that ranges from trajectory planning to target recognition. To address this challenge, the authors in [54] presented framework to implement FL algorithms for UAV swarms. In UAV swarm, one UAV as a leader gather the locally trained data from each of the following UAV, generate global FL model, and then transmit it among the followers UAVs. In order to optimize the the convergence rate of FL, joint power allocation and

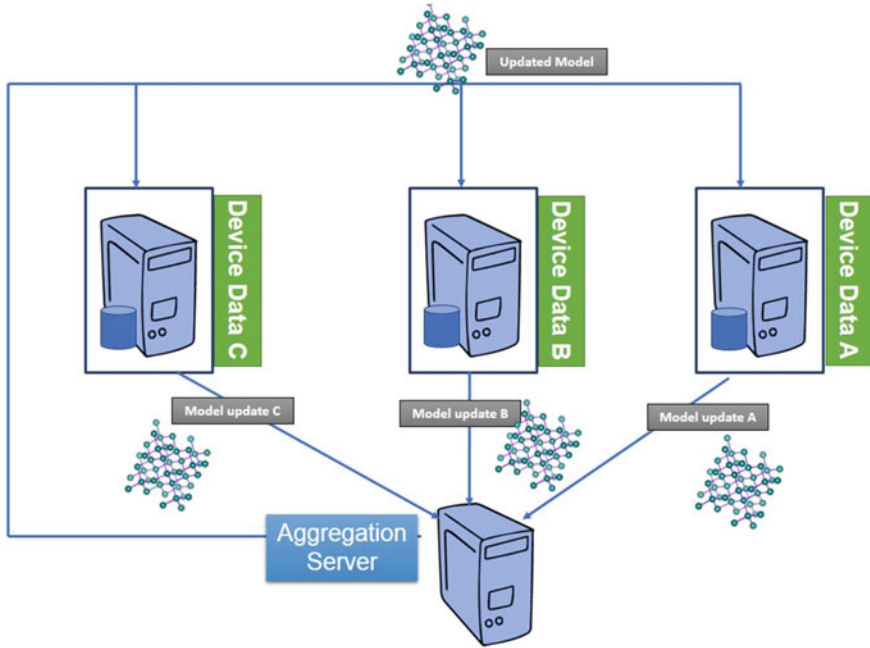


Fig. 6 Federated learning procedure for privacy preserving in safety networks

scheduling scheme was proposed by taking care of energy and delay constraints. Simulation results proved the effectiveness of the proposal by significantly reducing the communication rounds as compared to the baseline schemes.

Mobile crowd-sensing is key for successful implementation of emergency communications as it assists in indoor positioning and environment monitoring. Moreover, the combination of UAVs with AI has open ways for efficient mobile crowd-sensing [55]. However, the conventional existing AI models may arise serious security and privacy threats. To overcome this threat, FL proved a promising solution because of opening the possibilities of collaborative learning and training of the model without exposing the sense data. To improve this security further, the in this paper the authors introduced blockchain-based learning architecture that improves the privacy of local models. Results proved that the security was improved by introducing effective solution of model sharing as compared to the baseline schemes.

In [56], to reduce the processing load in multi-UAV networks the authors proposed an asynchronous federated learning (AFL) framework to enable asynchronous distributed computing that disallows transmitting the raw data to UAV servers and trained them locally. Moreover, to further improve the efficiency and maintain quality of service the device selection strategy was also introduced. The authors improved the convergence speed and accuracy considering asynchronous advantage actor-critic for joint device selection, UAVs placement, and resource management scheme [57].

In disaster hit areas, the thorough inspection of local updates at UAVs is necessary to guarantee privacy. To overcome this challenge, the authors in [58] combined blockchain with FL and replaced the centralized FL platform with a UAV-assisted FL with blockchain at edge. Results verified that the proposed framework was suitable to enable intelligent disaster communications that consumes less energy.

5 Conclusion

In this chapter, we have summarized the key technologies related to intelligent UAVs to enable public safety communications and also discuss future research directions for researchers. We have concluded that the intelligence plays key role in improving the UAVs performance in terms of coverage, throughput, mobility management, and computation at the edge to enable public-safety communications.

References

1. Saad W, Bennis M, Chen M (2019) A vision of 6G wireless systems: applications, trends, technologies, and open research problems. *IEEE Network* 34(3):134–142
2. Kaleem Z, Ali M, Ahmad I, Khalid W, Alkhayyat A, Jamalipour A (2021) Artificial intelligence-driven real-time automatic modulation classification scheme for next-generation cellular networks. *IEEE Access* 9:155584–155597
3. Nguyen LD, Duong TQ, Hoang TD (2022) Real time convex optimisation for 5G networks and beyond. *Telecommunications series. Institution of Engineering & Technology*
4. Shahzadi R, Ali M, Khan HZ, Naeem M (2021) UAV assisted 5g and beyond wireless networks: a survey. *J Netw Comput Appl* 103114
5. Challita U, Ferdowsi A, Chen M, Saad W (2019) Machine learning for wireless connectivity and security of cellular-connected UAVs. *IEEE Wirel Commun* 26(1):28–35
6. Aly Sabri Abdalla and Vuk Marojevic (2021) Communications standards for unmanned aircraft systems: the 3GPP perspective and research drivers. *IEEE Commun Stan Mag* 5(1):70–77
7. Hentati AI, Fourati LC (2020) Comprehensive survey of UAVS communication networks. *Comput Stand Interfaces* 103451
8. Shakoor S, Kaleem Z, Do D-T, Dobre OA, Jamalipour A (2020) Joint optimization of UAV 3D placement and path loss factor for energy efficient maximal coverage. *IEEE Internet Things J*
9. Kaleem Z, Qadri NN, Duong TQ, Karagiannidis GK (2019) Energy-efficient device discovery in D2D cellular networks for public safety scenario. *IEEE Syst J* 13(3):2716–2719
10. Hayat O, Kaleem Z, Zafarullah M, Ngah R, Hashim SZM (2021) Signaling overhead reduction techniques in device-to-device communications: paradigm for 5G and beyond. *IEEE Access* 9:11037–11050
11. Cheng F, Li D, Jiang F, Zhao N (2019) Learning-based user association in multi-UAV emergency networks with ground D2D. In: *IEEE international conference on communications workshops (ICC Workshops)*, pp 1–5. *IEEE*
12. Qian Y, Wang F, Li J, Shi L, Cai K, Shu F (2019) User association and path planning for UAV-aided mobile edge computing with energy restriction. *IEEE Wirel Commun Lett* 8(5):1312–1315
13. Li Y, Yin C, Do-Duy T, Masaracchia A, Duong TQ (2021) Aerial reconfigurable intelligent surface-enabled URLLC UAV systems. *IEEE Access* 9:140248–140257

14. Anwar MZ, Kaleem Z, Jamalipour A (2019) Machine learning inspired sound-based amateur drone detection for public safety applications. *IEEE Trans Veh Technol* 68(3):2526–2534
15. Ma D, Ding M, Hassan M (2020) Enhancing cellular communications for UAVs via intelligent reflective surface. In: *IEEE wireless communications and networking conference (WCNC)*, pp 1–6
16. Khalid W, Heejung Yu, Do D-T, Kaleem Z, Noh S (2021) RIS-aided physical layer security with full-duplex jamming in underlay D2D networks. *IEEE Access* 9:99667–99679
17. Mittal P, Sharma A, Singh R (2020) Deep learning-based object detection in low-altitude UAV datasets: a survey. *Image Vis Comput* 104046
18. Sharma A, Vanjani P, Paliwal N, Wijerathna Basnayaka CM, Jayakody DNK, Wang H-C, Muthuchidambaramanathan P (2020) Communication and networking technologies for UAVS: a survey. *J Netw Comput Appl* 102739
19. Masood A, Scazzoli D, Sharma N, Le Moullec Y, Ahmad R, Reggiani L, Magarini M, Alam MM (2020) Surveying pervasive public safety communication technologies in the context of terrorist attacks. *Phys Commun* 41:101109
20. Gupta L, Jain R, Vaszkun G (2015) Survey of important issues in UAV communication networks. *IEEE Commun Surv Tutor* 18(2):1123–1152
21. Kumbhar A, Koothifar F, Güven I, Mueller B (2016) A survey on legacy and emerging technologies for public safety communications. *IEEE Commun Surv Tutor* 19(1):97–124
22. Vattapparamban E, Güven I, Yurekli AI, Akkaya K, Uluğa S (2016) Drones for smart cities: issues in cybersecurity, privacy, and public safety. In: *2016 international wireless communications and mobile computing conference (IWCMC)*, pp 216–221. *IEEE*
23. Wei Yu, Hansong X, Nguyen J, Blasch E, Hematian A, Gao W (2018) Survey of public safety communications: user-side and network-side solutions and future directions. *IEEE Access* 6:70397–70425
24. Yan C, Lingang F, Zhang J, Wang J (2019) A comprehensive survey on UAV communication channel modeling. *IEEE Access* 7:107769–107792
25. Alsamhi SH, Ma O, Ansari MS, Almalki FA (2019) Survey on collaborative smart drones and internet of things for improving smartness of smart cities. *IEEE Access* 7:128125–128152
26. Park S, Kim HT, Lee S, Joo H, Kim H (2021) Survey on anti-drone systems: components, designs, and challenges. *IEEE Access* 9:42635–42659
27. Akbari Y, Almaadeed N, Al-maadeed S, Elharrouss O (2021) Applications, databases and open computer vision research from drone videos and images: a survey. *Artif Intell Rev* 54(5):3887–3938
28. Popescu D, Stoican F, Stamatescu G, Chenaru O, Ichim L (2019) A survey of collaborative UAV-WSN systems for efficient monitoring. *Sensors* 19(21):4690
29. Bithas PS, Michailidis ET, Nomikos N, Vouyioukas D, Kanatas AG (2019) A survey on machine-learning techniques for UAV-based communications. *Sensors* 19(23):5170
30. Zhi Y, Zhangjie F, Sun X, Jingnan Yu (2020) Security and privacy issues of UAV: a survey. *Mob Netw Appl* 25(1):95–101
31. Shakoor S, Kaleem Z, Baig MI, Chughtai O, Duong TQ, Nguyen LD (2019) Energy efficiency perspective. Role of UAVs in public safety communications. *IEEE Access* 7:140665–140679
32. Ali I, Kaleem Z, Khan S, Satti MA, Uddin Z (2020) Cognitive radios real-time implementation on software defined radio for public safety communications. *Telecommun Syst* 74(1):103–111
33. Duong TQ, Kim KJ, Kaleem Z, Bui M-P, Vo N-S (2021) UAV caching in 6G networks: a survey on models, techniques, and applications. *Phys Commun* 101532
34. Usman Q, Chughtai O, Nawaz N, Kaleem Z, Khaliq KA, Nguyen LD (2021) A reliable link-adaptive position-based routing protocol for flying ad hoc network. *Mob Netw Appl* 1–20
35. Kaleem Z, Yousaf M, Qamaf A, Ahmad A, Duong TQ, Choi W, Jamalipour A (2019) UAV-empowered disaster-resilient edge architecture for delay-sensitive communication. *IEEE Netw* 33(6):124–132
36. Khan MA, Qureshi IM, Khanzada F (2019) A hybrid communication scheme for efficient and low-cost deployment of future flying ad-hoc network (fanet). *Drones* 3(1):16

37. Sayeed M, Kumar R et al (2018) An efficient mobility model for improving transmissions in multi-UAVS enabled WSNS. *Drones* 2(3):31
38. Merwaday A, Guvenc I (2015) UAV assisted heterogeneous networks for public safety communications. In: *IEEE wireless communications and networking conference workshops (WCNCW)*, 329–334
39. Ali K, Nguyen HX, Vien Q-T, Shah P, Raza M (2020) Deployment of drone-based small cells for public safety communication system. *IEEE Syst J* 14(2):2882–2891
40. Kumbhar A, Guven İ, Singh S, Tuncer A (2018) Exploiting LTE-advanced HetNets and FeICIC for UAV-assisted public safety communications. *IEEE Access* 6:783–796
41. Do D-T, Nguyen T-TT, Le C-B, Voznak M, Kaleem Z, Rabie KM (2020) UAV relaying enabled NOMA network with hybrid duplexing and multiple antennas. *IEEE Access* 8:186993–187007
42. Do-Duy T, Nguyen LD, Duong TQ, Khosravirad SR, Claussen H (2021) Joint optimisation of real-time deployment and resource allocation for UAV-aided disaster emergency communications. *IEEE J Sel Areas Commun* 39(11):3411–3424
43. Lin Yu, Wang T, Wang S (2019) UAV-assisted emergency communications: an extended multi-armed bandit perspective. *IEEE Commun Lett* 23(5):938–941
44. Kumar S, Suman S, De S (2018) Backhaul and delay-aware placement of UAV-enabled base station. In: *IEEE conference on computer communications workshops (INFOCOM WKSHPs)*, pp 634–639. *IEEE*
45. Yin S, Li L, Yu FR (2020) Resource allocation and basestation placement in downlink cellular networks assisted by multiple wireless powered UAVs. *IEEE Trans Veh Technol* 69(2):2171–2184
46. Zeng Y, Zhang R, Lim TJ (2016) Throughput maximization for UAV-enabled mobile relaying systems. *IEEE Trans Commun* 64(12):4983–4996
47. Wang L, Bo H, Wang F, Chen S, Cui J (2020) Joint altitude, power control, and bandwidth allocation optimization for unmanned aerial vehicle-enabled reliable communications. *Trans Emerg Telecommun Technol* 31(7):e3983
48. Ji J, Zhu K, Niyato D, Wang R (2020) Joint cache placement, flight trajectory, and transmission power optimization for multi-UAV assisted wireless networks. *IEEE Trans Wirel Commun* 19(8):5389–5403, e3983
49. Masood A, Sharma N, Mahtab Alam M, Le Moullec Y, Scazzoli D, Reggiani L, Magarini M, Ahmad R (2019) Device-to-device discovery and localization assisted by UAVs in pervasive public safety networks. In: *Proceedings of the ACM MobiHoc workshop on innovative aerial communication solutions for First Responders network in emergency scenarios*, pp 6–11
50. Khelifi F, Bradai A, Singh K, Atri M (2018) Localization and energy-efficient data routing for unmanned aerial vehicles: fuzzy-logic-based approach. *IEEE Commun Mag* 56(4):129–133, e3983
51. Brik B, Ksentini A, Bouaziz M (2020) Federated learning for UAVs-enabled wireless networks: use cases, challenges, and open problems. *IEEE Access* 8:53841–53849, e3983
52. Bonawitz K, Eichner H, Grieskamp W, Huba D, Ingerman A, Ivanov V, Kiddon C, Konečný J, Mazzocchi S, Brendan McMahan H et al (2019) Towards federated learning at scale: system design. [arXiv:1902.01046](https://arxiv.org/abs/1902.01046)
53. McMahan B, Moore E, Ramage D, Hampson S, Aguera y Arcas B (2017) Communication-efficient learning of deep networks from decentralized data. In: *Artificial intelligence and statistics*, pp 1273–1282. *PMLR*
54. Zeng T, Semiari O, Mozaffari M, Chen M, Saad W, Bennis M (2020) Federated learning in the sky: joint power allocation and scheduling with UAV swarms. In: *IEEE international conference on communications (ICC)*, pp 1–6
55. Wang Y, Zhou S, Zhang N, Benslimane A (2021) Learning in the air: secure federated learning for UAV-assisted crowdsensing. *IEEE Trans Netw Sci Eng* 8(2):1055–1069, e3983
56. Yang H, Zhao J, Xiong Z, Lam K-Y, Sun S, Xiao L (2021) Privacy-preserving federated learning for UAV-enabled networks: Learning-based joint scheduling and resource management. *IEEE J Sel Areas Commun* 39(10):3144–3159, e3983

57. Kaleem Z, Khaliq MZ, Khan A, Ahmad I, Duong TQ (2018) PS-CARA: context-aware resource allocation scheme for mobile public safety networks. *Sensors* 18(5):1473
58. Pokhrel SR (2020) Federated learning meets blockchain at 6g edge: a drone-assisted networking for disaster response. In: *Proceedings of the 2nd ACM MobiCom workshop on drone assisted wireless communications for 5G and beyond*, pp 49–54

UAV Placement and Resource Management in Public Safety Networks: An Overview



Rizwana Shahzadi, Mudassar Ali, and Muhammad Naeem

Abstract Public safety networks (PSNs) can be deployed to help and rescue people in any trouble situation. These networks can be used by police, fire department or, a health service provider to instantly respond to an emergency situation. When a disaster occurs, either due to some natural or man-made reasons, the terrestrial infrastructure vanishes. The rapid deployment of communication infrastructure is required to reach a disaster scene to rescue people. In recent years, UAVs have emerged as a promising solution to this problem. UAVs fly independently without human pilot intervention; therefore they can be one of the best options to reach the difficult access areas. Even though UAVs offer numerous benefits of using them as an aerial base station, few important challenges e.g., efficient resource allocation, 3D placement, and security need to be addressed properly in order to efficiently utilize the UAVs. This chapter has focused the details on the UAV-supported public safety networks and state of the artwork related to UAV placement, resource allocation, and UAV-related security concerns in PSN.

Keywords UAV · PSN · BS · QoS · LoS · (SF ad DF Relay) · CRN

1 Public Safety Networks

Public Safety Networks (PSNs) are specially designed wireless networks that are used by first responders and emergency service providers in case of any disaster. PSNs can

R. Shahzadi (✉) · M. Ali
Department of Telecommunication Engineering, University of Engineering and Technology,
Taxila 47050, Pakistan
e-mail: rizwana.shahzadi@uettaxila.edu.pk

M. Ali
National University of Sciences and Technology, Islamabad 44000, Pakistan

M. Naeem
Department of Electrical Engineering, COMSATS University Islamabad, Wah Campus,
Rawalpindi 47040, Pakistan

© The Author(s), under exclusive license to Springer Nature Singapore Pte Ltd. 2022
Z. Kaleem et al. (eds.), *Intelligent Unmanned Air Vehicles Communications for Public Safety Networks*, Unmanned System Technologies,
https://doi.org/10.1007/978-981-19-1292-4_2

be useful in emergency situations to accomplish search and rescue activities. We are living in a world where the risk factor for any disaster is very high. Disasters can vary in nature, some are natural e.g., flood, storms, hurricanes, earthquakes and some are man-made e.g., transport accidents, war situations, blasts, industrial accidents, etc. There is also a new threat to society that is related to technology war. It is important for societies to identify and rectify the disastrous situation in an efficient manner. So, there is a great need for some kind of network that can be utilized in such a disastrous situation to deal with threats towards people's life and properties. Due to the immense need for such infrastructures, PSNs have emerged as an important future research direction. Public safety networks are used by different departments to provide emergency services such as:

- Police
- Fire brigades
- Medical emergency service

Personal devices (handheld computers, mobile cameras) and network utilization provide the greatest support towards the development of PSNs. The technological revolution in personal devices and connectivity has greatly improved the visibility and access to PSN service providers. Future PSN needs to efficiently collaborate the information chain to get access to the correct information via sensors and command chain to actually perform relief activities in a disaster scene. Public safety networks can be classified into two broad categories:

1. **Organizational perspective** From an organizational perspective, public safety network is a collaboration for information sharing and rescue functionality of PSN agencies associated with law enforcement, emergency rescue, and criminal activities. The factors that can affect the formation and operation of PSN may include official choices, priorities, and capabilities of technology.
2. **Communication perspective** From a communication perspective, PSN is a wireless communication network used by emergency service providers such as police, fire brigade, etc. The technological revolution in form of handheld and mobile cameras has greatly improved the efficiency of safety workers. Sensors deployment have revolutionized the data collection and act as eyes and ears of PSN service providers.

1.1 PSN Applications

Public safety networks involve several different operational sides in rural, urban, and suburban areas. Some of them are as following [1] (Fig. 1):

- **Law Agencies:** It is the responsibility of law enforcement agencies in any country to identify, investigate and keep away the culprits to make society a better place to live in. They can use PSN to maintain law and order in the state.



Fig. 1 PSN applications

- **Emergency Medical Services:** Medical services include immediate helpful care of sick and wounded individuals, and transferring them to the appropriate hospital sites where doctors, nurses, and other related staff can provide them detailed medical assistance.
- **Environment Protection:** This may include everyday observation of the environment to keep it healthy, particular area surveillance in order to support an endangered species, or maintaining the ecosystem of any area.
- **Border Security:** To protect the border area of any country by outsiders. This task is mainly the responsibility of law enforcement agencies and is usually performed by a specially formed force prepared for maintaining border security.
- **War Scene:** PSN can help people to rescue from war scenes either to safe places or rush the injured individuals to medical facilities.
- **Fire Fighters:** It is the responsibility of the fire department to extinguish fires erupted in any rural or urban area that is dangerous for people, animals, or people’s possessions. PSN can be used by firefighters to do their job in an efficient manner.
- **Search and Rescue:** The purpose of search and rescue is to locate, identify and rescue the lost individuals either due to a disaster or any crime scene.

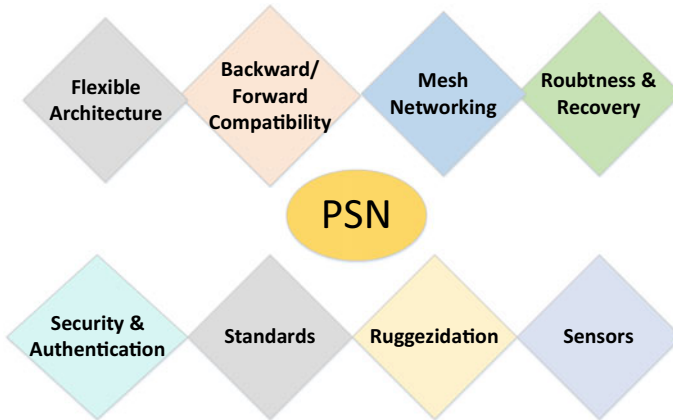


Fig. 2 PSN required features

- **Disaster Management:** In case of any disaster, it is the responsibility of the concerned department to help the individuals stuck in disaster areas either by search and rescue or necessary medical assistance.

Disaster management involves contributions from all modern-day communication and information techniques related to remote sensing, communication, video processing, database management, and security protocols. At present, radio communication related to risk management is totally a matter of state. Future coordination is only possible if the proposed scheme is flexible enough to address issues, risks, and resources of different nationals. Decision-making is an important part of risk management which requires a high level of spatial analysis techniques to identify the exact information for an accurate decision. Network reliability and security need to be incorporated in PSN to fulfill the QoS and DoE requirements of served individuals.

It involves a three-step procedure:

1. Pre-Disaster (Assessment, Observation, Prevention)
2. During Disaster (Response, Evacuation, Assistance)
3. Post Disaster (Recovery, Reconstruction, Development).

1.2 Desirable Features of Public Safety Networks

Some of the desire-able features of PSN are as following [1] (Fig. 2):

- **Flexible System Architecture:**

One major requirement of PSN is that different kind of devices and data types (voice and video) has to work together. Internet should have mixed media support. The architecture should be flexible enough to evolve with new technologies. Internet

packet transport should be more flexible to support high data rate (video streaming) demanding applications. It should support both IPV4 and IPV6 formats. PSN should be “bypass” and “talk around” enabled to exchange IP packets.

– **Backward and Forward Compatibility:**

It should have backward and forward compatibility towards new and old communications methods e.g., it can handle old telephone and IP-oriented sophisticated traffic at the same time.

– **Mesh Networking:**

Mesh networking improves the network experience by allowing packet relay capabilities at the edge devices and enabling the support for high frequency and high bandwidth utilization. PSN should support the joint working of IP and mesh networks.

– **Robustness and Recovery:**

PSN should be designed taking into account the chances of failure like power and malfunction of important network components e.g., towers, routers, switches. It should be robust to such failures and must be able to recover from them quickly.

– **Security and Authentication:**

PSN should be designed in such a manner that it ensures that the network designed for emergency services is only available to authenticated persons and the equipment related to PSN should be available after a strong authentication process. It should also have some strong distributed authentication processes as disaster scenes may require the involvement of individuals from different locations.

– **Standards:**

Standards need to be clearly defined for PSN. Compatibility between different connected devices can only be achieved via common standards to make PSN a worldwide success.

– **Ruggedization:**

Device Ruggedization is important in PSN as one cannot afford device failure in any critical situation. But it results in a high cost. Therefore, balance is required between Ruggedization, cost, and reliability.

– **Sensors and Location System:**

High-quality sensors and location systems need to be designed to identify and locate the individuals in any disaster situation. Better rescue services can only be provided after accurate location tracking.

– **High Density Radio Operation:**

Any PSN must be able to deal with high traffic due to the emergence of sudden heavy traffic volume in any particular area.

1.3 Key Enabling Standards and Technologies of PSN

Analog communication systems have been replaced by wireless digital communication systems. The main wireless communication standards for PSN are TETRA and TETRAPOL in Europe and APCO 25 in the USA. Nowadays, several other com-

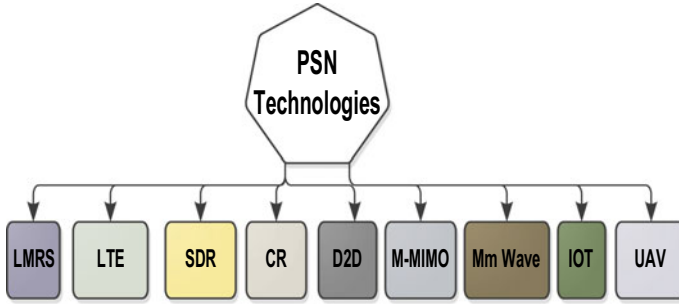


Fig. 3 Legacy and future PSN technologies, LMRS (Land Mobile Radio System), LTE (Long Term Evolution), SDR (Software Defined Radio), CR (Cognitive Radio), D2D (Device to Device), M-MIMO (Massive-Multiple Input Multiple Output), mm-wave, IoT (Internet of Things), UAV (Unmanned Aerial Vehicle)

munication systems other than these are used for Safety service provision (Fig. 3). Emergency service providers also include military standards using UHF and VHF. TETRA is a digital radio system standard that has an inter-operability feature enabled. Equipment from different vendors can operate at the same time using TETRA standards. It was designed by ETSI. It has a tendency to handle up to hundreds of users [2]. A talk group is one of the most famous features of TETRA. Since 1997 several networks based on TETRA have been deployed in Europe. It uses air as an interface for communication between TETRA and other communication networks. It has very strong security features such as encryption at the end to end and air interfaces. TETRA Release 2 provides high data rate services up to 473 Kbits/s along with backward compatibility and wideband data connectivity features [3].

APCO 25 is the USA-based wireless communication standard designed for public safety Networks. It has four main features:

- Improved functionality
- Better spectrum efficiency
- Healthy competition between vendors
- Support for inter-agency and intra-agency communication

APCO 25 is FDMA-based and supports the QPSK-C modulation method. It offers a limited data rate of up to 9.6 kb/s and several services e.g., messaging, group call, broadcast, etc. it is a fixed network-based method and can provide security to some extent. TETRAPOL was designed to satisfy French police requirements. It is FDMA-based and uses a 12.5 kHz/carrier channel. It offers both voice and data and several services similar to TETTRA which include messaging, broadcast, and group call [4]. It is FDMA base with a bit modulation rate of 8 Kbits/satellite are not terrestrial infrastructure dependent so it is used in PSN in case of natural disaster [5]. DMR (Digital Mobile Radio) unlicensed mode (in a 446.1–446.2 MHz band) and licensed mode and avionic communications in the VHF band (e.g., 118–136 MHz) can be used for PSN.

– **Land Mobile Radio System**

LMRS is an analog source to destination communication which is only for voice consisted of transmitter and receiver. The push to Talk button available on a microphone is pressed whenever a user wants to talk. LMRS uses VHF and UHF bands and Its range and power are limited.

– **LTE:**

LTE is one of the dominant future technology for commercial mobile networks. Due to high data rate support, it is becoming famous among PSN providers as high data rate-sensitive applications are emerging day by day. In Europe, LTE can be used with TETRA for PSN [6]. LTE can be adopted for PSN after the specification of services which are usually not defined in the commercial domain but are used in PSN. 3GPP is working on standardization work in three domains (1) Proximity services (2) Group Call (3) Public Safety Broadband. LTE has to support existing infrastructure. LTE is designed for reasons that are much more powerful as compared to PSN. Fears exist that PSN can't influence LTE standards. Technology evolution from TETRA to LTE is basically a five-step procedure in Europe, particularly in Finland. These steps are as following [7]:

- Due to rapid increases in data rate requirement first step is to set up Mobile Virtual Network Operator (MVNO).
- TETRA for critical and broadband for non-critical content.
- LTE core for dedicated broadband services for PSN in certain regions.
- Outclass voice services for both TETRA and LTE.
- Complete takeover of TETRA services by LTE broadband services.

– **Software Defined Radio:**

The broadband requirement of PSNs network is addressed by LTE. However, interoperability is an important aspect that needs to be developed. SDN is an important future technology that was designed to support interoperability factors. The author in [8] has covered important aspects of SDN. Furthermore, public safety aspects of SDN are covered in [9].

– **Cognitive Radio:**

Cognitive radio systems can identify, monitor, and adapt to the Radio frequency-changing conditions of the surrounding environment. It can cater to operations related to interference and availability when analyzing the radio frequency operation. CR-based devices can update their own RF parameters to adopt the surrounding RF changes. It can be used in PSN due to the main two features. (1) It can improve the spectrum utilization by detecting the spectrum availability (2) It promotes the interoperability feature [10].

– **D2D:**

In case of any catastrophic situation where wireless infrastructure has been damaged along with other facilities, D2D could serve the purpose of search and rescue. D2D devices communicate in a peer-to-peer fashion in an unlicensed band. It can provide a high data rate at a low price and latency features. An important feature of D2D that enhances the system capacity is spatial frequency reuse. Therefore, PSN D2D can be used to provide efficient search and rescue facilities [11]. The

agility feature of UAV has made UAV-assisted D2D implementation very flexible [12].

– **Massive-Multiple input multiple outputs (M-MIMO):**

It is an important future wireless technology that is designed to provide a better communication experience in the case of a high mobility environment. M-MIMO consists of multiple antenna arrays connected with BS, which can serve multiple users at the same time and frequency resource.

– **mm Wave:**

As spectrum is a scarce resource and with the passing time congestion in the already available spectrum is an important problem to be addressed. Mm-wave is an important way to solve the capacity problem of future 5G networks. The mm-wave spectrum ranges from 30 to 300 GHz. 250 GHz spectrum is available to be used under the mm-wave title which is a huge range but the propagation losses problem needs to be addressed in the mm-wave range.

– **IoT:**

IoT is a big future technology. It will transform the way we are living and can act as a game-changer for PSN. It can be used for surveillance purposes that help in the prevention of any disaster situation. If a disaster has happened, IoT can improve the first responder's experience. IoT sensors can help to actually locate the source and cause of any emergency situation. Academia and researchers can work together to combine two independently evolved streams IoT and PSN for the purpose of public benefit.

– **UAV:**

Recently a new trend has emerged in which unmanned aerial vehicles (UAV) can be used in PSN. If the infrastructure has completely vanished in any disaster and there is a need for immediate infrastructure deployment to continue the search and rescue operation, UAV can serve the purpose in a very efficient manner due to several benefits such as low-cost deployment, maneuverability, and LoS communication link.

1.4 PSN Implementation Challenges

Despite several advancements in PSN, still, several challenges are associated with PSN implementation. A disaster is a sudden event: therefore, immediate response from emergency service providers is required to handle the situation, which may cause several problems like Congestion, Connectivity, throughput, interoperability, Accurate positioning, Decision Making [13, 14].

- **Congestion** An emergency is a discrete random event, which causes a sudden spike in traffic volume. A competition starts for resources between public and emergency first responders (EFR), which may cause traffic congestion. The provision of a congestion-free network in an emergency is an important issue to be addressed.

- Emerging trends like the use of unlicensed bands, UAVs, small cells, and M-MIMO can help to solve the congestion problems.
- **Connectivity** Emergency is a discrete random event, which causes a sudden spike in traffic volume. A competition starts for resources between public and emergency first responders (EFR), which may cause traffic congestion. The provision of a congestion-free network in an emergency is an important issue to be addressed. Emerging trends like the use of unlicensed bands, UAVs, small cells, and M-MIMO can help to solve the congestion problems.
 - **Throughput** The high data rate is required in emergency service provision e.g., full-duplex communication link is required to maintain real-time communication in order to rescue distantly located users or if the fire erupts in an area EFR may require real-time video streaming to get to know about the exact situation at the disaster scene. Multimedia involvement in emergency service provision increases the efficiency of PSN up to several folds but at cost of a high data rate.
 - **Interoperability** PSN network may involve more than one EFR with different equipment types. Interoperability means coordination between every intended operator's parameters and equipment. Interoperability failure among different EFR may cause the failure of PSN and ultimately is a serious threat to the lives of people stuck in a disaster situation.
 - **Accurate positioning** Wise decisions can only be made if the exact location and situation of the disaster are known. Situational Awareness (SA) may help to identify the exact location of PSN members. Continuous analysis of situational awareness is required by EFR to get to know about the actual scenario at the disaster scene: therefore, it is essential for decision making in an emergency.
 - **Decision Making** Intelligence is required to make wise decisions at the disaster scene. Intelligent UAVs have served the purpose. They can hover the disaster area autonomously and intelligently can collaborate with other UAVs to cover the disaster area in an efficient manner e.g., Intelligent UAVs can take the decision to move from an empty to a crowded area to rescue a large no of individuals.

2 UAVs in PSN

PSN routine communication patterns are quite different in comparison with normal wireless communication scenarios. In PSNs traffic is usually low consisting of only the surveillance kind of messages to immediately get to know about any disastrous situation. However, the traffic volume of PSN suddenly increases once the disaster occurs. It is a non-practical and resource inefficient method to permanently depute high capacity fixed communication points for PSN even in normal times. However, it requires some immediately deployable communication means. UAVs are very useful communication nodes for PSNs because of the easy and immediate deployment, Los propagation, mobility, and maneuverability characteristics [15] (Fig. 4).

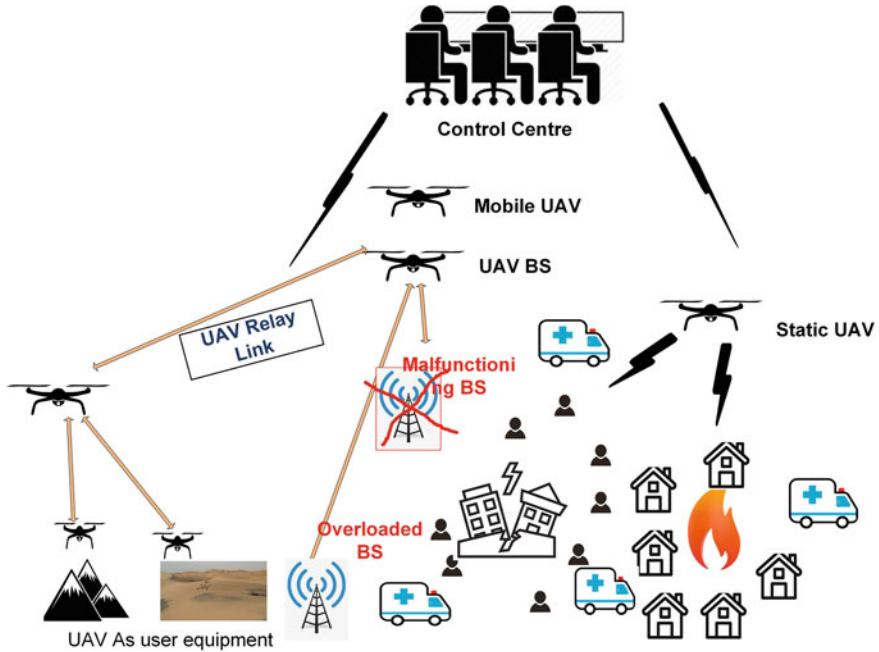


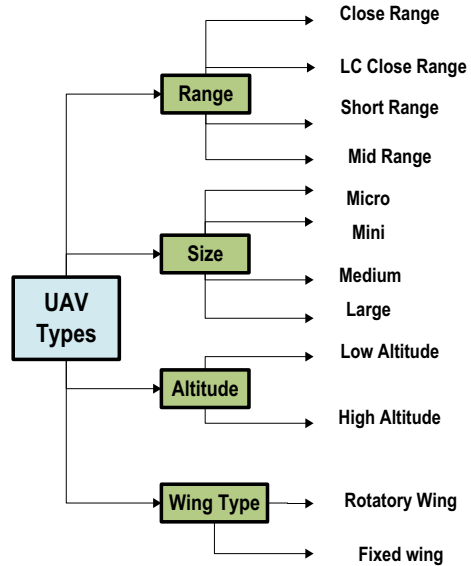
Fig. 4 UAV assisted PSNs

2.1 UAV Categories

A wide range of UAVs is available worldwide. They can be classified on the basis of four different parameters: (1) size (2) range (3) altitude (4) rotator type [16, 17]. It is important to utilize the application-specific UAVs for each scenario. Figure 5 shows the detail of UAV classification:

1. **Size:** UAVs can be classified With respect to size [17].
 - **Micro** Micro UAVs also known as very small UAVs range in size up to the size of small insect that is 30–50 cm in length. They look like insects and they provide options for both rotatory and flapping wings.
 - **Mini** Mini UAV is also known as a small UAV range in size up to 2 m not greater than that and it has a minimum of one side dimension larger than 50 cm.
 - **Medium** Medium size UAVs are heavy enough that they can't be handled by human hand but still, they are smaller as compared to small size aircraft. Their wings are 5–10 m long and they support payload to 100–200 kg.
 - **Large** This class of UAVs is very large in size usually of the size of aircraft and mostly they are used by the military.

Fig. 5 UAV types



2. **Range**

UAVs can be classified With respect to range as [17]:

- **Low-cost Close Range** They offer a range of up to 5 km. Endurance time 20–45 min and according to 2010 survey cost of 10000 dollars.
- **Close range** They offer a range of up to 50 km. Endurance time 1–6 h.
- **Short Range** They offer a range of up to 150 km. Endurance time 8–12 h.
- **Mid-range** They offer a range of up to 650 km.

3. **Altitude**

UAVs can be classified With respect to the altitude as [16]:

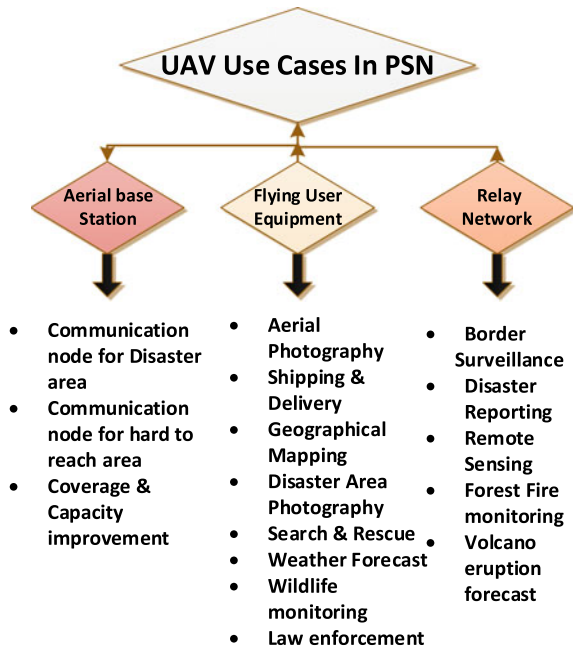
- **Low Altitude** Easy fast and flexible to install, they have a Small endurance time and coverage range.
- **High Altitude** Large deployment cost but larger range and endurance time.

4. **Rotator Type**

UAVs can be classified With respect to rotator type as [16]:

- **Fixed wing** Forwarding airspeed of wings is used to produce lift. Require runway for taking off and landing it has simple structure and support high payload.
- **Rotatory Wing** Lift is generated via blade it can hover in any required direction. It has a support of Vertical takeoff and higher payload.

Fig. 6 UAV use cases in PSNs



2.2 UAV Use Cases in PSN

We are living in an era of technology where demands of data rates are increasing at a very rapid rate due to the emergence of new multimedia applications on daily basis. As a result, the requirements for new communication means to satisfy such increasing demands are also high. Recently, UAV-assisted heterogeneous networks have attained much attention due to their easy deployment, low operational cost, low and maneuverability features. The purpose of PSNs is to maintain communication in a disaster area to locate and rescue the sufferers even if the communication infrastructure is completely or partially destroyed. In absence of Communication infrastructure UAVs have recently evolved as one of the best options to continue the communication services for first responders to help endangered people and their belongings. In any disaster area, UAV's can be utilized in three possible ways (Fig. 6):

1. **Flying BS** UAVs can be used as flying base stations to serve an area where the communication infrastructure is completely or partially destroyed due to a disaster situation or the area is difficult to approach due to its geographical facts. It can also facilitate the suddenly overloaded Macro Base Station due to the emergence of a large no of users e.g football matches.
2. **Relay** UAVs can act as a relay with either a single UAV or several UAVs to provide communication facilities or surveillance of distantly located users. It can be used in both store and forward (SF) and Decode and Forward (DF) modes.

3. **Aerial User Equipment** UAV can be used as aerial user equipment for delivery monitoring and rescue services.

As Aerial Base Station:

- Technological revolution has caused greater use of multimedia applications which resulted from the rapid increase in no of connected devices and their required data rate to satisfy QoS criteria. This is the major driving force towards the development of new and advanced communication methods to handling an increased no of devices and can provide a high data rate. In any disaster area, several methods and strategies such as M-MIMO, heterogeneous cellular network, orthogonal multiple access techniques, mm-wave communication, etc. [18] have been developed in past years. But each proposed method has some limitations. UAV-assisted networks have emerged as a new feasible solution to this problem because of their low operational cost, easy deployment, Los, and maneuverability features.
- ● UAV-assisted BS is a very viable solution in comparison with other broadband networks specially designed for public safety operations e.g., TETRA, First Net, APCO 25. UAV BSs can easily and immediately be deployed at any location to provide communication services to help the endangered people who are stuck in disaster scenes and can't communicate due to infrastructure failure [19].
- ● PSN require some reliable Los communication methods and shift towards a higher frequency band to provide more bandwidth capacity. UAV-assisted communication is one of the best solutions as it can provide Los communication [20].
- ● M-MIMO and 3D MIMO techniques enhance the network capacity by exploiting spatial diversity factors. Los communication is the key factor to implement spatial diversity. In this respect, UAVs serve the purpose in the most efficient way because of their Los communication technique which is the most important factor for beamforming [21].

As Flying User Equipment:

- ● Nowadays, photographers are focusing to use UAVs for photography purposes which were previously possible only with help of high-cost equipment such as helicopters. The cinematography of action scenes and sports coverage has been revolutionized. Another important development is the live coverage feature of any disaster scene. It is now possible in a very economical way with help of UAVs which was previously only possible with help of expensive satellites. This live coverage feature is of great help for PSN to perform the search and rescue operation.
- ● Big names in the field of delivery services are working on the option of UAV-assisted delivery. This can be used to deliver food, medicines, and instructions to the disaster scene where other transport means have vanished.
- ● It is now possible to gather information and 3D high-resolution images of hard-to-reach areas which need continuous monitoring such as mountains, coastlines with the help of UAVs.
- ● Due to the small size of drones they can be utilized to capture close-up images of the disaster areas and accurately collect victim's data with help of sensors, radars, and cameras.

- ● Infrared Sensors incorporated with UAVs help the farmers to continuously monitor crop health and take suitable measures for its betterment.
- ● UAVs can be utilized by PSN for the forecast of natural or man-made disasters e.g., hurricanes and tornadoes to inform the locals before any such situation actually happens.
- ● Drones can be used to protect endangered species from hunters with help of sensors and thermal cameras which can even work at night time. PSN can use the information about wild animals collected via UAVs to tell the tourist and locals about their presence in that particular area to avoid any mishap.
- ● PSN can use drones to monitor large public gatherings to avoid any mishap or criminal activity. Drug transportation, illegal smuggling across coastlines is monitored by border force with help of UAVs.

As Relay Node: UAVs can form a flying Ad-hoc network [22] to provide very reliable communication for far-flung areas which are difficult to reach due to their geographical facts. UAV relay network can greatly extend the communication range in a very economical and reliable way. They collect the data from far-flung areas and transmit it to nearby BS. It can be used in situations that require continuous monitoring e.g. borders, disaster areas, forest fire, Volcano, etc.

2.3 UAV Implementation Challenges in PSN

UAVs are becoming a potential candidate for PSN because of several advantages like Los communication, easy and immediate deployment, maneuverability, etc. Despite various benefits, there are certain challenges related to UAVs that need to be thoroughly investigated in order to maximize the efficiency of UAVs in PSN. Figure 7 shows challenges related to UAV-assisted PSN.

● **3D Placement:** UAV placement is one of the most important challenges. UAV placement is a 3D placement problem which means that height is an important parameter that needs to be adjusted along with other dimensions which makes it different and challenging from 2D placement problems. Several parameters which need to be addressed for UAV placement include User location, Channel conditions, Battery constraint, and Interference with other UAVs [23, 24].

● **Resource Management:** Efficient Resource Management of UAV-supported PSN is an important design challenge because UAV has to operate with resources that are also shared with existing infrastructure. Several researchers have recently worked on efficient resource utilization of UAV-assisted PSN to get the best out of it.

● **Trajectory Planning:** UAV Trajectory planning in PSN is a challenging task because it requires finding the large number (approaching to infinity) of variables via which UAV can fly during rescue operation [25]. Several important parameters which need to be considered while trajectory planning is energy constraint during flight time, collision avoidance in case of multiple UAVs taking part in the rescue operation, user demands, interference handling to maximize the network throughput, etc. Trajectory

Fig. 7 UAV implementation challenges in PSN



planning is basically an optimization problem of finding the optimized path between source and destination and this optimized path should maximize or minimize certain performance indexes e.g. energy, power, path length, time, delay, etc. The absence of proper laws resulted in illegal drone usage which is a serious threat to drone utilization and has made secure trajectory planning a challenging task [26].

- **Interference Handling:** Most of the time, PSN include multiple UAV operation at disaster scene to maximize the network throughput and coverage. Despite several benefits of multiple UAV operations, one important challenging factor is the interference management between multiple UAVs. UAV footprint should be placed in such a manner that it provides coverage to the larger area but not at cost of interference with neighboring UAV footprints. Researchers are working on several interference mitigation techniques to maximize network efficiency.

- **Channel Modeling:** Characteristics of the channel between transmitter and receiver have a great impact on the quality of communication and system efficiency. In UAV-assisted PSN, channel modeling is a complicated task as compared to ground-assisted PSNs because the air to ground channel is involved in UAV-assisted PSN whereas in ground-assisted PSN only ground to ground channel modeling is required. UAV-assisted PSN has both transmitter and receiver as mobile units whereas in the terrestrial network only the user is mobile [27].

- **Backhaul Connectivity:** In the case of UAV-assisted PSN, backhaul connectivity is another important factor. The mobile nature of UAVs demands wireless backhaul connectivity instead of wired backhauling [28]. Potential candidates for UAV wireless backhauling include the following options: mm-Wave, FSO (free-space optical fiber Communication), satellite links, Wi-Fi. Satellite offers large capacity but greater delays and high cost whereas low cost and small delays still make Wi-Fi backhauling the most potential candidate for backhauling.

- **Energy Limitation:** The limited battery is a significant challenge of UAV operation. Most of the time, UAVs are operated by onboard batteries that is why UAV

energy resources can't exceed certain limits. UAV onboard energy is used in several tasks e.g. information processing, mobility management, communication control, etc. Energy parameter is an important factor defining UAV lifetime. Researchers are working on efficient energy utilization methods to prolong the UAV lifetime [29]. UAV energy consumption depends upon several factors e.g. channel conditions, mission details, placement, and path planning strategies.

- **Security:** Security is an important factor related to UAV-assisted PSN. UAV communication links are broadcast in nature; therefore, hackers can easily launch attack an attack on them. Security is challenging and difficult to manage the task in UAV-assisted PSNs due to multi-layer topology involvement. Ensuring the security of SDN [30] controllers which are used for resource management in multi-layer networks is another challenging side in UAV-assisted PSNs. Researchers are working to protect UAV communication links from any kind of mischievous attacks, and have proposed different solutions based on artificial intelligence, signal processing, multi-antenna, relay selection, and friendly jamming techniques.

2.4 Intelligent UAVs

Unmanned Aerial Vehicles have been used to provide search and rescue services in Public safety networks due to their several advantages. Initially, UAVs were flying objects without human pilots onboard controlled manually by ground control stations. Recently a new concept of artificial intelligence combined with UAVs has emerged, which resulted in intelligent UAVs. Intelligent UAVs can be used in various fields. Artificial intelligence refers to a state where machines are capable of performing tasks intelligently without human involvement. Intelligent UAVs have modernized and updated aerial technology in several areas e.g., security, agriculture, disaster management, remote sensing, etc. Intelligence resulted in to increase in UAV utilization up to many folds. Intelligent UAVs can control their flight operation autonomously by intelligently controlling flying, trajectory planning, and battery replacement [31].

Computer Vision helps UAVs to incorporate intelligent behavior [32]. Intelligent UAVs can perform on-board image processing with help of neural networks which are used to implement several machine learning algorithms. Sensors also play a major role in UAV automation. They gather all necessary data and feed this collected data to a machine learning algorithm for appropriate action.

Intelligent UAVs have several uses. Some of them are as follows:

- **Search and Rescue:** In case of disaster intelligent UAVs can perform search operations in areas that are otherwise impossible to reach for human beings after a disaster. Intelligent drones can provide relief services in a better way by scanning the disaster scene in a faster way.
- **Military Uses:** Intelligent drones have the biggest application in military areas. Drones can replace pilots and save human costs in case of war. They can provide

continuous surveillance of border areas and even can enter in cross border areas because they are hard to notice due to their small size.

- **Agriculture:** UAVs can automate the agriculture sector by continuously monitoring the fields and scattering seeds pesticides etc. Intelligent drones can decide by themselves which treatment is needed for the crop and when the crop is ready to harvest or when the seed scattering is required.
- **Construction:** Intelligent drones can provide continuous monitoring of construction sites which will minimize human involvement. It will benefit the most in the monitoring of that construction site that is dangerous for human beings to monitor.
- **Delivery:** Big names like AMAZON are trying to update their delivery service with help of intelligent drones. They can identify the targeted user and deliver them the package. Drone delivery will not only save time but is also a suitable solution to the traffic problems of the modern world.

3 UAV 3D Placement in Public Safety Network

Among the major challenges associated with UAV-assisted PSN, placement is one of the major challenges due to several reasons. Firstly, in the case of the UAV-supported communication scenario, both end-user and BS are mobile whereas in conventional ground networks the end destined user is only mobile and BS is fixed. Therefore, placement is a difficult task in UAV-supported PSNs. Secondly, UAV placement in a 3D (length, width, height) placement problem is dissimilar from 2D (length, width) placement of ground networks which means that height (altitude) need to be adjusted in order to achieve optimized coverage and service quality along with other placement parameters in UAV networks. UAV placement is divided into two main problems altitude adjustment and 2D placement problem. Depending upon altitude, UAVs are classified into two main categories high altitude and low altitude platforms. The high altitude provides wider coverage and greater chances of Los but with increased path loss factor due to an increase in distance between end-user and UAV. Low altitude provides a narrow coverage area, fewer chances of a Los path, and fewer losses. Important network parameters e.g., network throughput, QoS, and DoE are directly linked with the UAV position [33]. SINR can be altered to adjust the varying demand of end-user by changing the position of UAV BS as it is a function of distances and locations of sender and receiver. Hence optimized placement problems can bring the best possible outcomes of UAV-assisted PSNs.

3.1 *State of the Art*

Single UAV BS Placement: The author [34] has analyzed UAV placement in disaster scenes with UAVs able to self-organize themselves. It has considered the circular disaster area with a 30km radius. It has utilized a simple search algorithm used

by bacteria to search the disaster space. Results indicate that vertical flexibility is not as efficient as finding the optimized altitude in maximizing spectral efficiency. Greater energy consumption is involved in vertical movements in comparison with horizontal movements due to a change in elevation angle. So, a trade-off is required between altitude performance improvement and energy consumption. The problem of maximizing the covered users with minimum involved power in terrain situations is discussed [35]. Averaged path loss model is used because of missing details related to its being LoS or NLoS due to terrain situation. The main 3D placement problem is divided into two small problems vertical and horizontal placement. In the horizontal direction, 2D circle placement (second-order cone) problem whereas in vertical direction optimized elevation angle is utilized to get the optimized altitude [36] has covered the 3D UAV placement to cover the users equally distributed within different floors of high rise building whose communication infrastructure is destroyed due to disaster situation. An algorithm is proposed to solve the placement problem based on particle swarm optimization algorithm [37]. The Convergence speed of PSO and gradient descent algorithm are compared to each other for variable building widths and heights. UAV-assisted ad hoc networks are useful research directions because they can easily be deployed to provide coverage in any disaster area where the infrastructure is partially or completely destroyed due to any natural or man-made disaster. UAV placement strategy has a very important impact on the ad hoc network lifetime due to its direct impact on utilized battery resources. Researchers in [38] have worked upon the recall frequency parameter which defines the lifetime of any battery-operated UAV-supported networks. Smaller UAV recall frequency refers to a larger lifetime of the corresponding ad-hoc network. UAV Placement is further distributed into horizontal placement and vertical placement. Results indicate that optimum altitude is a function of desired coverage area and slope depends upon the communication environment e.g. high altitudes are required for dense scattering situations. Results indicate that minimizing the onboard circuit power decreases the UAV recall frequency factor and hence results in a significant increase in ad-hoc network lifetime. Optimized 3D placement problem to support complete coverage for indoor users while keeping the transmitted power at a minimum level is discussed in [39]. UAV 3D Placement problem is optimized for two situations: (1) building location with highest path loss factor (2) users with the unvarying distribution. Simulation results have proved that in the first case required transmitted power is much higher and increases in a uniform manner with an increase in no of users. UAV placement problem to satisfy the user demands with different QoS requirements is presented in [40]. Optimized placement is done in two steps first is vertical optimized placement and horizontal placement. The horizontal direction optimized placement is achieved as a concentric circle placement problem. In [40], the designed algorithm is compared with the standard Genetic and MVX toolbox and has appeared much better than them when execution time and covered users factors are considered. In [41], the author has presented the placement problem in a situation in which the number of users and their demanded data rate is not stable but varies with time. Four diverse data rate cases HD video, VOIP, online gaming, and web surfing are considered. Knapsack-like problem is utilized for horizontal placement problem whereas verti-

cal placement problem is solved similar to [42]. 3D UAV BS placement to maximize the number of covered users based on the Honey bee algorithm [43] is presented in [44].

Multiple UAV BS Placement: UAV has emerged as a potential candidate to assist PSN due to several benefits like easy deployment, low cost, maneuverability, and Los communication. However, in some scenarios instead of one, multiple UAVs are involved to maximize the efficiency of PSN. The [45] problem of maximizing the no of covered users with a minimum number of UAVs, while maintaining the fairness of service is presented. A hybrid algorithm (greedy search and distribution motion) is utilized to achieve the optimized solution for the NP-Hard problem. Firstly, Greedy Search Algorithm is used to find the minimum number of UAVs and their optimized position in discontinuous space. Then, the optimized UAV placement in continuous space is achieved via the Distribution Motion algorithm. The proposed algorithm is tested for random and cluster distribution scenarios. Mean-field type game (MFTG) [46] to get the optimized placement for multiple UAVs is utilized [47]. Mean-field term is affected by each UAV decision value. Each UAV makes the decision of its optimized placement to achieve the Nash Equilibrium for optimized placement depending upon its status and mean-field term. The author [48] has presented the optimized multi UAV 3D placement while considering the energy constraint as well. 3D UAV placement problem within Network Flying platform is covered in [49]. Distributed placement and centric placement algorithms are utilized for optimized UAV placement decisions [49]. The existence of co-channel interference is an extremely important aspect to be addressed in real networks. UAV 3D placement problem in presence of co-channel interference is presented in [50]. Joint optimization of 3D placement and path loss factor to maximize the user up-link coverage is considered in [51]. Then UAV height is optimized in dense suburban cases. Results indicate improved coverage and throughput performance.

Ref. #	Object	Problem type	Algorithm	Use case	NO OF UAV'S
27	Optimized UAV Altitude	Non-Convex	Heuristic Bio inspired	BS	Single
28	Maximized Covered Users	MINLP	Heuristic	BS	Single
29	Indoor Coverage	Non Convex	PSO	BS	Single
31	Increases the ad hoc network lifetime	Optimization	Heuristic	BS	Single
32	Minimized Transmitted power	Minimum coverage circle	Iterative	BS	Single
33	Maximized users with diff QoS	Mixed Integer	Multi population Genetic	BS	Single
34	Maximized Users with diff QoS	knapsack	Density Aware Placement	BS	Single
37	Maximized Covered Users	optimization	Artificial Bee Colony	BS	Single
38	Maximized Coverage with minimum UAV's	NP Hard	Hybrid	BS	Multi
39	Minimized Cost	Optimized	Mean Field Type Game	BS	Multi
41	Maximized Coverage	Cooperative Coverage	Game Theory	BS	Multi
42	Maximum Coverage	Optimization	Distribute & Centric Placement	BS	Multi
43	Maximized Coverage	Optimization	Heuristic	BS	Multi
90	Maximized Coverage	Optimization	Round Robin/K-Mean	BS	Multi

3D Placement of UAV Flying Relay: UAVs are getting an important part of advanced networks at a very faster rate. An important use of UAVs in public safety networks is acting as a relay node and providing information to the ground control station or towards any other flying UAV. Due to limited storage and processing capabilities UAVs need to act as a relay node to provide relief services in any far-flung area under disaster situations. Placement is an important challenge for UAVs that are

acting lay nodes. The altitude optimization problem for flying relay node (UAV) to maximize the network reliability factor is presented in [52]. Both static and mobile cases are considered while optimizing the altitude. Numerical results have indicated that Decode and Forward (DF) is a better-relaying strategy than Amplify and Forward (AF). Variation in performance matrices results in the variation of optimum altitude. The author [52] has considered Bit error rate, outage probability, and power loss as performance matrices. Outage probability is used as a performance metric. Results have depicted that the power transmitted ratio among flying UAV and ground BS has a direct impact on placement optimization. Optimized placement in a wireless regenerative communication environment for a UAV relaying node in between relay station and mobile is presented [53]. Placement optimization for UAV acting lay node between users and fixed BS in terrain situation is discussed [54]. Placement Optimization is performed to get the maximum network throughput. Firstly, UAV collected information is used to estimate the location of end-users and information related to path loss. Then, an iterative algorithm is utilized to get the optimized placement. The work in [55] has presented the optimized placement of UAV relaying node to ensure the attainability of communication link among BS and user if there is any blockage due to terrain situation to maintain the QoS. Results have indicated substantial performance gains of actual Terrain situation considered in [55] instead of stochastic approach. Relay placement presented in [56] has considered the clustering model based approach with no of UAVs and network performance jointly acting as the performance metric. The researcher in [57, 58] has covered the UAV relay placement problem. Joint deployment and resource allocation for UAV aided relaying network in case of disaster is discussed in [59]. This research work has considered real-time scenarios and has proposed User clustering based on k-means along with joint power and time allocation transferring to recover the network after the occurrence of a disaster. Latter the energy efficiency is also maximized. Results have indicated the better performance of the proposed scheme as compared to other standard methods. Several obstacles on the communication path make it challenging to provide communication services to distantly located users. (Non-orthogonal multiple access) NOMA-enabled full-duplex UAV relaying strategy is proposed in [60] to provide communication services to faraway users. Outage probability and throughput performance are considered performance metrics. Results have indicated that a larger number of antennas on the receiver side results in better performance metrics (improved system throughput, reduced outage probability).

Ref #	Object	Problem type	Algorithm	Use case
44	Maximized network Reliability	NP Hard	Numerical Method	Relay
45	Minimized Outage Probability	Convex		Relay
46	Max Network Throughput	Cooperative Coverage	Heuristic	Relay
47	Ensured link in case of terrain	Quasi Convex	Non Convex	Relay
48	Optimized Placement	NP hard	Heuristic	Relay
91	Maximized EE	Non Convex	K-mean Clustering	Relay
96	Maximized Throughput/Minimized Outage	Optimization	Heuristic	Relay

UAV Placement as User Equipment: UAV-assisted networks where UAV is used as flying user equipment are an important part of PSNs. UAV can be deployed to collect actual information about a specific area either before any kind of disaster for forecast purposes (weather forecast, aerial photography, wildlife monitoring, geographical mapping, etc.) or after a disaster to accomplish search and rescue mission (search and rescue, delivery services, Photography of the disaster scene, etc.). UAVs have become one of the most suitable candidates for remote sensing and delivery networks due to ease of deployment, low cost, maneuverability, and several other benefits. In sensor networks, several nodes are deployed at different locations to monitor different objects. UAVs are deployed for remote sensing tasks to collect these node's data to transmit it to the control station. The work in [61] has discussed efficient UAV route planning in order to collect the data from these sensors. Efficient UAV route planning has a significant impact on network lifetime. Optimization problem is divided into small subproblem stages. The first stage is cluster formation. The second is the optimization of connections between clusters. The third step involves route optimization inside the clusters and the final stage involves UAV path optimization between clusters. Path planning strategy for UAV relay deployed for data collection in sensor networks is presented in [62]. PSO is used for path optimization. It has considered UAV flight time, energy, and BER as performance metrics. Floods are one of the biggest natural disasters that can cause huge destruction. As it is a very random situation so the only way to save lives is the accurate information collection from sensor nodes during the catastrophic event. The work in [63] has proposed a numerical-based strategy for UAV path planning deployed for flood sensing purposes. Path planning of remotely piloted aircraft (RPAS) used for surveillance of moving objects on the ground is discussed in [64]. Observer gets the raw data from RPAS and provides the data to the path planner for trajectory design. Path planning for Energy-efficient UAV swarms used for surveillance purposes is presented in [64] that has discussed the trajectory is planned while keeping the energy factor in all three stages of UAV life.

Ref #	Object	Problem type	Algorithm	Use case
44	Maximized network Reliability	NP Hard	Numerical Method	Relay
45	Minimized Outage Probability	Convex		Relay
46	Max Network Throughput	Cooperative Coverage	Heuristic	Relay
47	Ensured link in case of terrain	Quasi Convex	Non Convex	Relay
48	Optimized Placement	NP hard	Heuristic	Relay

4 Resource Management in UAV Assisted PSNs

UAV-assisted PSNs have several key challenges which must be addressed thoroughly to get the optimized network functionality. Among those, optimized resource allocation is a key challenge. Recently, several researchers have worked for optimized allocation of different resources in UAV-assisted networks. Some key resources are as following:

- • Energy
- • Power
- • Time Slot
- • Bandwidth
- • User association.

4.1 *State of the Art*

Energy Firstly UAVs have been utilized only in defense-related missions but later on, due to several advantages of UAVs as compared to conventional terrestrial communication nodes, UAVs have emerged into several other commercial applications. Recently UAVs have appeared as one of the most promising communication methods for PSNs due to their easy and immediate deployment characteristic. PSNs require a longer lifetime of flying nodes. Energy is a limited resource in the case of UAVs and directly defines operation lifetime. Therefore, optimized energy utilization can prolong the lifetime of UAV-assisted networks. The author in [65] has discussed energy allocation among UAV BS and terrestrial ground BS as a weight optimization problem. Weights of energy assignment are calculated via a proposed heuristic method. Each node SINR value serves as a metric to calculate the energy assignment weight of that node, more SINR referred to more weight. Optimized on-board energy allocation of UAV-supported eLAA (enhanced Licensed Assisted Access) network is presented in [66]. eLAA is an improved kind of LAA incorporated with IEEE 802.11e protocol. UAV is loaded with both Small Cell BS for VIP users and Wi-Fi access points for non VIP users. Joint resource and trajectory optimization is performed to ensure energy efficiency for the downlink communication links.

Power Optimized bandwidth and power allocation along with optimized placement for access and backhaul networks are presented in [67]. UAV Power used for relaying data from UAV controls its lifetime or UAV hover time. UAV hover time maximization (Convex problem) in UAV supported M2M communication is discussed in [68]. The results have shown that intelligent Selection causes the proposed scheme to outperform in terms of minimized transmitted power in comparison with RAS (resource allocation scheme. An algorithm is proposed in [69] to allocate power to IoT nodes in an intelligent manner towards Uplink direction based on deep reinforcement learning (DRL) algorithm for UAV assisted IoT networks. Optimized power allocation for

UAV relay networks based on alternating direction method of multipliers (ADMM) is presented in [70]. Results indicated that the presented algorithm has outperformed in no of iterations, throughput, stability, and convergence rate. Joint power and trajectory optimization to maximize the end-to-end throughput in the case of a relay (amplify and forward) is presented in [71]. The proposed optimization scheme has significantly increased the throughput up to 600+bits/s/Hz which is much higher in comparison with 500bits/s/Hz of fixed power and trajectory case. The author in [71] has discussed the joint beamforming and power allocation problem in case of the DF relay network. The maximum rasion combining approach is utilized to get the optimized result for beamforming, then these optimized results are used to address the power allocation problem. Optimized power allocation for indoor users getting service from UAV floating relay is presented in [72]. Joint power, Trajectory, and node scheduling in the UAV relay network for the minimum average rate maximization are discussed in [73]. In [74] network outage probability is minimized by the proposed optimization scheme of joint UAV trajectory and power allocation optimization for both devices and UAV. Proposed algorithm results are compared with circle trajectory with power allocation scheme (CT-PA) and fixed position with equal transmit power scheme (FT-EP). Results have indicated better performance in terms of outage probability. With the increase in transmitted power outage probability decreases. An iterative algorithm for joint optimization of power and trajectory for multiple UAVs behaving lay among source-destination pair to maximize the end to end throughput is discussed in [75]. Proposed scheme results have shown improved performance in comparison with static relay scheme $T > 205$ s ($P = 10$ dBm) and $T > 150$ s ($P = 0$ dBm).

Time Slot TDMA based QoS (Quality of Service) demand satisfaction of users along with maintained network throughput is presented in [76]. Dynamic time slot allocation is proposed and results are compared with the static time slot allocation scheme. The proposed scheme has shown higher data rates in comparison with the fixed time slot method which is as following for uplink channel (38, 435), downlink channel (50, 460), Voice channel (34, 633), and video channel (282, 502). Bisection method-based time slot allocation to maximize the spectrum along with energy efficiency for DF relay is presented in [76, 77]. Joint UAV time allocation, speed, and trajectory optimization are considered for optimizing the spectrum and energy efficiency. Wireless powered UAV time slot allocation problem is presented in [78]. Firstly, a closed-form solution based on the Albert function is used for optimized time allocation. Later on, placement is also optimized. In comparison with other benchmark schemes e.g., Dinkelbach based algorithm proposed algorithm outperforms while having the same convergence rate (5 iterations). UAV-supported IoT network Time allocation problem is presented in [79]. Firstly, UAV wirelessly powers IoT nodes, and later on, the nodes send information to UAVs. Comparison has shown that minimum throughput performance of wirelessly powered separated UAV is 28% higher than integrated UAV WPCN.15 iteration time is required by the proposed method to reach a stable point. In the first case, the same UAV is performing both wireless charging and information reception tasks. Whereas, two different UAVs are used for

these purposes in the second case. Minimum throughput maximization is achieved via both placement and resource allocation. An iterative algorithm is used to optimize the time allocation problem to facilitate information transfer along with charging.

Bandwidth Due to day by day increase in military and civilian UAV applications, UAV demand is continuously increasing. Referring to a report by Teal group that considers both military and Civilian UAV applications, UAV production in 2025 will be up to 20.3 billion dollars from 4.5 billion dollars of 2016, and this is likely to approach in a period of 10 years up to 135 billion dollars. With this rapid increase in UAV utilization, efficient bandwidth utilization schemes are mandatory due to the shortage of bandwidth resources. Cognitive Radio has appeared as a favorable candidate in UAV-assisted communication. Opportunities and challenges of CRN for UAV communication are presented in [80]. Reference [81] has discussed both sub-carrier allocation and UAV trajectory design problems and has proposed an algorithm “iterative subcarrier allocation and trajectory design” (ISACA). The carrier assignment problem consists of two steps: (1) carrier allocation from UAV to interface (2) carrier allocation form between UAVs. Results have indicated that the proposed algorithm has caused a 20% improvement in the uplink rate. Deep reinforcement learning (DRL) based channel and power allocation for UAV-assisted IoT nodes are presented in [70]. The key objective of the proposed algorithm is to achieve the max-min energy efficiency. Results show that the proposed algorithm is performing better in comparison to deep Q networks (DQN), and random methods. Subchannel allocation of UAV working as a relay node for ensuring QoS improvement for edge users is presented in [82]. NP-hard problem is solved via a Joint mode selection and sub-channel allocation, trajectory optimization, and power allocation (JMS-T-P) algorithm. Proposed algorithm results are compared with several other cellular schemes and standard random algorithms and have shown outperformance in throughput and fairness among users. Power and Bandwidth assignment in the backhaul and access network of UAV-assisted scenario is presented in [67]. The local optimum solution is achieved by using successive convex programming and alternating optimization. The proposed novel algorithm is compared with other benchmark schemes and has shown better performance as compared to them. Uplink network throughput maximization via joint subcarrier and power allocation of drone acting as amplify and forward relay for emergency communication scenario is presented in [83]. Results have indicated an increase in network throughput with an increasing number of users up to 8 users. The researcher in, [84] has considered the bandwidth optimization problem for heterogeneous UAV networks (Ad hoc networks). Heterogeneity refers to a network supporting satellite and ground networks along with UAVs. Three stages of Action networking and processing are considered. All sensing data is collected in the action stage and transferred to processing via the networking stage. The proposed strategy resulted in 75% spectrum efficiency. Joint user scheduling and bandwidth allocation for DF relay are discussed in [85]. The proposed block successive convex optimization algorithm (BSOA) outperforms other standard algorithms in terms of complexity and simulation time. Results have indicated that in comparison with other schemes proposed algorithm running time is 7 times small. Subcarrier allo-

cation optimization for UAV-assisted cognitive radio network is presented in [86]. Stochastic geometry and Game theory-based bandwidth allocation for UAV-based IoT network is covered in [87]. UAV-supported software-defined cellular network efficient bandwidth allocation problem (SDCN) is discussed in [88].

User Association Due to numerous advantages of UAV network including, easy deployment, maneuverability, and LoS communication, they are the most suitable candidate to serve the sudden increased no of users either due to some infrastructure failure or any natural or man-made disastrous situation. In [89], the user association problem is optimized via optimized UAV placement in Software-Defined Cellular Networks (SDCN) while maintaining the user QoS requirement as well. Three scenarios are considered (1) 3D optimized placement (2) optimization of resource allocation and 3D placement (3) optimized resource allocation and 2D placement. Case 2 has presented the best results in terms of downlink served users in Urban and dense urban situations. UAV-assisted power and wireless information transfer network, where both energy and information is wirelessly transferred to IoT nodes is considered in [90]. Joint user association and placement are optimized to obtain the maximum number of ground users and minimized data rate. UAV-supported mobile networks user association problem is discussed for the purpose of load balancing in [30]. Users are distributed in several clusters. Initial UAV placement is performed according to maximal user density. Then backtracking line algorithm is used to place the UAV in a way to get the minimized value of the maximum traffic demanded by a cluster of users. Optimum UAV position is achieved by the implementation of the location and load balancing algorithm in an alternate manner. The proposed Clustering approach resulted in 3.71% of users without service which is a lot better as compared to 6.94% of uniformly distributed methods.

5 Security Concerns in PSN

Public safety networks are used by emergency service providers and law enforcement agencies. They must support endpoint devices like laptops, mobile phones, cameras, and computers and they must also have strong support towards central support and emergency service providers. Different sensors and surveillance cameras are also part of public safety networks. This type of wide range of connected devices and personals in public safety results in a complicated network scenario, which causes a new type of security risk connected with PSNs. PSNs used by different departments like police, fire department and medical service providers are usually fixed networks. These fixed networks are usually interconnected for use by first responders in case of emergency by Long Term Evolution (LTE).

Why PSN Need to be secured Public safety networks usually carry information related to police, firefighters, or medical service providers.

- • Data related to the police department is extremely secret because it contains either criminal records or information about them or any future planning for an

operation to catch the culprits. So this kind of information is extremely confidential. Criminals will try to get it at any cost so good security schemes are required to keep this information private.

- ● Medical record of any patient used by PSN is extremely personal data and It must be only available to the patient guardian or its doctor. Secrecy maintenance of this critical data used by medical emergency providers is an important task.
- ● Data use by the fire department must only be available to departmental rescue providers and must not be publicly available as it can cause panic among people in case of a fire eruption at any location.

Public safety networks usually have very low traffic volume in case of no emergency but once an emergency situation arises there is a sudden increase in traffic. So allocating a larger resource pool permanently is not a good deal. So, researchers have worked on UAV-assisted PSNs because UAVs can easily and instantly be deployed in any hard-to-reach area. Despite several advantages associated with UAV-assisted public safety networks one major challenge which arises is a security concern because UAVs are broadcast communication devices. UAVs are flying platforms without human pilot intervention and also they have a broadcast nature. These two facts make them more prone to hackers attacks. Hackers can easily access the open links to launch eavesdropping, a man-in-the-middle attack, and several other malicious attacks. UAV-assisted public safety networks are examples of multi-layer network topologies in which nodes of dissimilar characteristics are connected to form one network. Security maintenance among this type of dissimilar characteristic nodes is a major challenge as nasty attacks can easily be launched on multi-layer topology networks. SDN controllers are used for managing the resources in multi-layer topology networks. Security maintenance in SDN controllers is another challenging task of UAV-assisted public safety networks.

The author in [30] has discussed different kinds of cyber-attacks that are possible in the case of UAV-assisted networks. Artificial Intelligence-based solution to address the UAV assisted communication security concerns is presented in [91]. UAV-assisted network's physical layer security in presence of eavesdroppers is discussed in [92]. Signal processing techniques are also investigated by several researchers to provide a secure UAV communication experience. Relay selection, friendly jamming, and multi-antenna type of signal processing techniques are discussed for UAV network's physical layer security in [93]. Finally, [94] has presented a dual UAV-based approach in which one UAV is used to jam the eavesdroppers and another one is used to continuing the routine communication service.

6 Conclusion

We are living in an extremely unpredictable world where several types of disasters happen every day around the world, some of them are natural whereas some occur due to human error or infrastructure failure. PSNs are designed for search and rescue

missions in any disaster situation. UAV-assisted PSN recently emerged as a promising candidate for search and rescue missions due to several advantages of UAVs like they fly without a human pilot, and can easily be deployed at any place and low deployment cost, etc., However, there are certain challenges associated with UAVs. This chapter has discussed the overview, features, applications, and enabling technologies of PSN. Furthermore, this chapter has presented types, use cases, state of the artwork, placement, and resource allocation of UAVs and the security challenges in PSNs.

References

1. Baldini G, Karanasios S, Allen D et al (1 more author) (2013) Survey of wireless communication technologies for public safety. *IEEE Commun Surv & Tut* 16(2):619–641. ISSN 1553-877X
2. Mayer-Schoenberger V (2002) Emergency communications: the quest for interoperability in the United States and Europe, BCSIA Discussion Paper 2002–7, ESDP Discussion Paper ESDP-2-2-03, vol John. Harvard University, F Kennedy School of Government
3. ETSI EN 300 392-1 V1.4.1 (2009-01), Terrestrial Trunked Radio (TETRA); Voice plus Data (V+D); Part 1: General network design
4. Kuypers D, Schinnenburg M (2005) Traffic performance evaluation of data links in TETRA and TETRAPOL. *Wireless Conference 2005 - Next Generation Wireless and Mobile*
5. Iapichino G, Bonnet C, Del Rio Herrero O, Baudoin C, Buret I (2008) A mobile ad-hoc satellite and wireless Mesh networking approach for public safety communications. In: 10th international workshop on signal processing for space communications, 2008. SPSC 2008, pp 1–6, 6–8
6. Nouri M (2013) Selection of a broadband technology for TETRA, Chairman of TC TETRA Working Group 4 (High-Speed Data). Presentation available online at TETRA Association website: <http://www.tetramou.com/Library/Documents/Files/Presentations/FutureVision2009Nouri.pdf>. Accessed 28 Jan 2013
7. Kaleem Z et al (2019) UAV-empowered disaster-resilient edge architecture for delay-sensitive communication. *IEEE Netw* 33(6):124–132. <https://doi.org/10.1109/MNET.2019.1800431>
8. Ulversoy T, Software defined radio: challenges and opportunities. *Commun Surv Tut IEEE PP(99):1–20, 0*
9. Baldini G, Picchi O, Luise M, Sturman TA, Vergari F, Moy C, Braysy T, Dopico R (2011) The EULER project: application of software defined radio in joint security operations. *Commun Mag, IEEE* 49(10):55–62
10. Federal Communication Commission, Cognitive Radio for Public Safety. <https://www.fcc.gov/general/cognitive-radio-public-safety>
11. Alnoman A, Anpalagan A (2017) On D2D communications for public safety applications. In: *IEEE Canada international humanitarian technology conference (IHTC)*, pp 124–127. <https://doi.org/10.1109/IHTC.2017.8058172>
12. Nguyen KK, Vien NA, Nguyen LD, Le M-T, Hanzo L, Duong TQ (2021) Real-time energy harvesting aided scheduling in UAV-assisted D2D networks relying on deep reinforcement learning. *IEEE Access* 9:3638–3648. <https://doi.org/10.1109/ACCESS.2020.3046499>
13. Kumbhar A, Koothifar F, Güvenç İ, Mueller B (2017) A survey on legacy and emerging technologies for public safety communications. *IEEE Commun Surv & Tutor* 19(1):97–124, Firstquarter. <https://doi.org/10.1109/COMST.2016.2612223>
14. Pérez MG, Huertas Celdán A, García Clemente FJ, Martínez Pérez G (1981) Review and open challenges of public safety networks to manage emergency settings in 5G. In: 2020 17th international conference on electrical engineering/electronics, computer, telecommunications

- and information technology (ECTI-CON), 2020, pp 555–558. <https://doi.org/10.1109/ECTI-CON49241.2020.9158213>. Subsequences. *J Mol Biol* 147:195–197 (1981) Integration. Technical report, Global Grid Forum (2002)
15. Shakoor S, Kaleem Z, Baig MI, Chughtai O, Duong TQ, Nguyen LD (2019) Role of UAVs in public safety communications: energy efficiency perspective. *IEEE Access* 7:140665–140679. <https://doi.org/10.1109/ACCESS.2019.2942206>
 16. Mozaffari M, Saad W, Bennis M, Nam Y, Debbah M (2019) A tutorial on UAVs for wireless networks: applications, challenges, and open problems. *IEEE Commun Surv Tut* 21(3):2334–2360. Thirdquarter
 17. PennState College of Earth and Mineral Sciences, Geospatial Applications of Unmanned Aerial Systems (UAS). <https://www.e-education.psu.edu/geog892/node/5>
 18. Agyapong PK, Iwamura M, Staehle D, Kiess W, Benjebbour A (2014) Design considerations for a 5G network architecture. *IEEE Commun Mag* 52(11):65–75
 19. Baldini G, Karanasios S, Allen D, Vergari F (2014) Survey of wireless communication technologies for public safety. *IEEE Commun Surv Tuts* 16(2):619–641. 2nd Quart
 20. Zhang L et al (2019) A Survey on 5G millimeter wave communications for UAV-assisted wireless networks. *IEEE Access* 7:117460–117504. <https://doi.org/10.1109/ACCESS.2019.2929241>
 21. Mozaffari M, Saad W, Bennis M, Debbah M (2019) Communications and control for wireless drone-based antenna array. *IEEE Trans Commun* 67(1):820–834
 22. Zafar W, Khan BM (2016) Flying ad-hoc networks: technological and social implications. *IEEE Technol Soc Mag* 35(2):67–74
 23. Kalantari E, Yanikomeroğlu H, Yongacoglu A (2016) On the number and 3D placement of drone base stations in wireless cellular networks. In: Proceedings of the IEEE vehicular technology conference, pp 1–6
 24. Kosmerl J, Vilhar A (2014) Base stations placement optimization in wireless networks for emergency communications. In: Proceedings IEEE international conference on communications (ICC), NSW, Australia, Sydney, pp 200–205
 25. Rucco A, Aguiar AP, Hauser J (2015) Trajectory optimization for constrained UAVs: a virtual target vehicle approach. In: Proceedings IEEE international conference on unmanned aircraft systems (ICUAS), pp 236–245
 26. Teng H, Ahmad I, Msm A, Chang K (2020) 3D Optimal surveillance trajectory planning for multiple UAVs by using particle swarm optimization with surveillance area priority. *IEEE Access* 8:86316–86327. <https://doi.org/10.1109/ACCESS.2020.2992217>
 27. Zheng Y, Wang Y, Meng F (2013) Modeling and simulation of pathloss and fading for air-ground link of HAPs within a network simulator. In: Proceedings of the IEEE International conference on cyber-enabled distributed computing and knowledge discovery (CyberC), Beijing, China, pp 421–426
 28. Horwath J, Perlot N, Knapek M, Moll F (2007) Experimental verification of optical backhaul links for high-altitude platform networks: atmospheric turbulence and downlink availability. *Int J Sat Commun Netw* 25(5):501–528
 29. Zeng Y, Zhang R (2017) Energy-efficient UAV communication with trajectory optimization. *IEEE Trans Wireless Commun* 16(6):3747–3760
 30. Javaid AY, Sun W, Devabhaktuni VK, Alam M (2012) Cyber security threat analysis and modeling of an unmanned aerial vehicle system. In: Proceedings of the IEEE conference on technologies for homeland security (HST), Waltham, MA, USA, pp 585–590
 31. Thakkar P, Balaji A, Narwane V (2019) Intelligent unmanned aerial vehicles: ICIMA 2018. https://doi.org/10.1007/978-981-13-2490-1_44
 32. Cao Y, Liang H, Fang Y, Peng W (2020) Research on application of computer vision assist technology in high-precision UAV navigation and positioning. In: 2020 IEEE 3rd international conference on information systems and computer aided education (ICISCAE), pp 453–458. <https://doi.org/10.1109/ICISCAE51034.2020.9236821>
 33. Rahman SU, Cho Y (2018) UAV positioning for throughput maximization. *J Wireless Com Netw* 2018:31

34. Gruber M (2016) Role of altitude when exploring optimal placement of UAV access points. *IEEE Wireless Commun Netw Conf 2016*:1–5. <https://doi.org/10.1109/WCNC.2016.7565073>
35. Alzenad M, El-Keyi A, Lagum F, Yanikomeroğlu H (2017) 3-D placement of an unmanned aerial vehicle base station (UAV-BS) for energy-efficient maximal coverage. *IEEE Wireless Commun Lett* 6(4):434–437
36. Shakhathreh H, Khreishah A, Alsarhan A, Khalil I, Sawalmeh A, Othman NS (2017) Efficient 3D placement of a UAV using particle swarm optimization. In: 2017 8th international conference on information and communication systems (ICICS), Irbid, pp 258–263
37. Kennedy J, Eberhart R (1995) Particle swarm optimization. In: *IEEE international conference on neural networks, 1995. Proceedings*, vol 4. IEEE, pp 1942–1948
38. J Lu J, Wan S, Chen X, Fan P (2017) Energy-efficient 3D UAV-BS placement versus mobile users' density and circuit power. In: 2017 IEEE globecom workshops (GC Wkshps), Singapore, pp 1–6
39. Cui J, Shakhathreh H, Hu B, Chen S, Wang C (2018) Power-efficient deployment of a UAV for emergency indoor wireless coverage. *IEEE Access* 6:73200–73209
40. Chen Y, Li N, Wang C, Xie W, Xv J (2018) A 3D placement of unmanned aerial vehicle base station based on multi-population genetic algorithm for maximizing users with different QoS requirements. In: 2018 IEEE 18th international conference on communication technology (ICCT), Chongqing, pp 967–972
41. Lai C, Chen C, Wang L (2019) On-demand density-aware UAV base station 3D placement for arbitrarily distributed users with guaranteed data rates. *IEEE Wireless Commun Lett* 8(3):913–916
42. Al-Hourani A, Kandeepan S, Lardner S (2014) Optimal LAP altitude for maximum coverage. *IEEE Wireless Commun Lett* 3(6):569–572
43. Artificial Bee Colony Algorithm Homepage. <https://abc.erciyes.edu.tr/>. Accessed 04 Dec 2018
44. Tahat A, Edwan T, Mbaideen D, Murrar N, Al-Qutob O, Ayman L (2019) Optimal decision on placement of an auxiliary aerial wireless base station using the artificial bee colony algorithm. In: 2019 international conference on advanced communication technologies and networking (CommNet), Rabat, Morocco, pp 1–6
45. Wang H, Zhao H, Wu W, Xiong J, Ma D, Wei J (2019) Deployment algorithms of flying base stations: 5G and beyond with UAVs. *IEEE Int Things J* 6(6):10009–10027
46. Xu Y, Li L, Zhang Z, Xue K, Han Z (2018) A discrete time mean field game in multi-UAV wireless communication system. In: *International conference on communications in China (ICCC)*, Beijing, China, pp 714–718
47. Sun Y, Li L, Xue K, Li X, Liang W, Han Z (2019) Inhomogeneous multi-UAV aerial base stations deployment: a mean-field-type game approach. In: 2019 15th international wireless communications and mobile computing conference (IWCMC), Tangier, Morocco, pp 1204–1208
48. Ruan L et al (2018) Energy-efficient multi-UAV coverage deployment in UAV networks: a game-theoretic framework. *China Commun* 15(10):194–209
49. Omri A, Hasna MO, Shakir MZ, Shaqfeh M (2018) 3-D placement schemes of multiple UAVs in NFP-based wireless networks. In: 2018 5th international conference on information and communication technologies for disaster management (ICT-DM), Sendai, Japan, pp 1–5. Aymen
50. Khuwaja AA, Zheng G, Chen Y, Feng W (2019) Optimum deployment of multiple UAVs for coverage area maximization in the presence of co-channel interference. *IEEE Access* 7:85203–85212
51. Shakoor S, Kaleem Z, Do D-T, Dobre OA, Jamalipour A (2021) Joint optimization of UAV 3-D placement and path-loss factor for energy-efficient maximal coverage. *IEEE Int Things J* 8(12):9776–9786. <https://doi.org/10.1109/JIOT.2020.3019065>
52. Chen Y, Feng W, Zheng G (2018) Optimum placement of UAV as relays. *IEEE Commun Lett* 22(2):248–251
53. Wei W, Chen S, Yan J, Ouyang J, Zhu W (2017) Optimal relay placement for UAV-assisted wireless regenerative communication system. In: 2017 13th international conference on natural computation, fuzzy systems and knowledge discovery (ICNC-FSKD), Guilin, pp 2850–2854

54. Esrafilian O, Gangula R, Gesbert D (2018) UAV-relay placement with unknown user locations and channel parameters. In: 2018 52nd Asilomar conference on signals, systems, and computers, Pacific Grove, CA, USA, pp 1075–1079
55. Chen J, Mitra U, Gesbert D (2019) Optimal UAV relay placement for single user capacity maximization over terrain with obstacles. In: 2019 IEEE 20th international workshop on signal processing advances in wireless communications (SPAWC), Cannes, France, pp 1–5
56. Gaofeng W, Xiaoguang G, Kun Z, Xiaowei F (2019) Multi-objective placement of unmanned aerial vehicles as communication relays based on clustering method. In: 2019 Chinese control and decision conference (CCDC), Nanchang, China, pp 1462–1467
57. Chen J, Gesbert D (2020) Efficient local map search algorithms for the placement of flying relays. *IEEE Trans Wireless Commun* 19(2):1305–1319
58. Rubin I, Zhang R (2007) Placement of UAVs as communication relays aiding mobile Ad Hoc wireless networks, MILCOM. In: 2007 IEEE military communications conference, Orlando, FL, USA, pp 1–7
59. Do-Duy T, Nguyen LD, Duong TQ, Khosravirad S, Claussen H, Joint optimisation of real-time deployment and resource allocation for UAV-aided disaster emergency communications. *IEEE J Select Areas Commun.* <https://doi.org/10.1109/JSAC.2021.3088662>
60. Do D-T, Nguyen T-TT, Le C-B, Voznak M, Kaleem Z, Rabie KM (2020) UAV relaying enabled NOMA network with hybrid duplexing and multiple antennas. *IEEE Access* 8:186993–187007. <https://doi.org/10.1109/ACCESS.2020.3030221>
61. Sujit PB, Lucani DE, Sousa JB (2013) Joint route planning for UAV and sensor network for data retrieval. In: 2013 IEEE international systems conference (SysCon), Orlando, FL, pp 688–692
62. Abdelkader M, Shaqura M, Ghommem M, Collier N, Calo V, Claudel C (2014) WiP abstract: optimal multi-agent path planning for fast inverse modeling in UAV-based flood sensing applications. In: 2014 ACM/IEEE international conference on cyber-physical systems (ICCPS), Berlin, pp 212–212
63. Haugen J, Imsland L (2016) Monitoring moving objects using aerial mobile sensors. *IEEE Trans Control Syst Technol* 24(2):475–486
64. Monwar M, Semiari O, Saad W (2018) Optimized path planning for inspection by unmanned aerial vehicles swarm with energy constraints. In: 2018 IEEE global communications conference (GLOBECOM), Abu Dhabi, United Arab Emirates, pp 1–6
65. Manzoor A, Kim DH, Hong CS (2019) Energy efficient resource allocation in UAV-based heterogeneous networks. In: 2019 20th Asia Pacific network operations and management symposium (APNOMS), Matsue, Japan, pp 1–4
66. Xu C, Chen Q, Li D (2019) Joint trajectory design and resource allocation for energy-efficient UAV enabled eLAA network. In: ICC 2019 - 2019 IEEE international conference on communications (ICC), Shanghai, China, pp 1–6
67. Li P, Xu J (2018) UAV-enabled cellular networks with multi-hop backhubs: placement optimization and wireless resource allocation. In: 2018 IEEE international conference on communication systems (ICCS), Chengdu, China, pp 110–114
68. Liu X, Ansari N (2019) Resource allocation in UAV-assisted M2M communications for disaster rescue. *IEEE Wireless Commun Lett* 8(2):580–583
69. Cao Y, Zhang L, Liang Y (2019) Deep reinforcement learning for channel and power allocation in UAV-enabled IoT systems. In: 2019 IEEE global communications conference (GLOBECOM), Waikoloa, HI, USA, pp 1–6
70. Gong J, Lin J, Chang T, Shen C, Chen X (2018) Distributed power allocation for UAV-assisted multi-user relay networks. In: 2018 11th international symposium on communication systems, networks and digital signal processing (CSNDSP), Budapest, pp 1–6
71. Jiang X, Wu Z, Yin Z, Yang Z (2018) Power and trajectory optimization for UAV-enabled amplify-and-forward relay networks. *IEEE Access* 6:48688–48696
72. Li Y, Feng G, Ghasemianmadi M, Cai L (2019) Power allocation and 3-D placement for floating relay supporting indoor communications. *IEEE Trans Mobile Comput* 18(3):618–631
73. Chen (2020) Joint trajectory and resource optimization for UAV enabled relaying systems. *IEEE Access* 8:24108–24119

74. Zeng S, Zhang H, Bian K, Song L (2018) UAV relaying: power allocation and trajectory optimization using decode-and-forward protocol. In: 2018 IEEE international conference on communications workshops (ICC Workshops), Kansas City, MO, pp 1–6
75. Zhang G, Yan H, Zeng Y, Cui M, Liu Y (2018) Trajectory optimization and power allocation for multi-hop UAV relaying communications. *IEEE Access* 6:48566–48576
76. Patra RK, Muthuchidambaranathan P (2018) Optimisation of spectrum and energy Efficiency in UAV-enabled mobile relaying using bisection and PSO method. In: 2018 3rd international conference
77. Zhang J, Zeng Y, Zhang R (2017) Spectrum and energy efficiency maximization in UAV-enabled mobile relaying. In: 2017 IEEE international conference on communications (ICC), Paris, pp 1–6
78. Jiang M, Li Y, Zhang Q, Qin J (2019) Joint position and time allocation optimization of UAV enabled time allocation optimization networks. *IEEE Trans Commun* 67(5):3806–3816
79. Amorosi L, Chiaraviglio L, D’Andreagiovanni F, Blefari Melazzi N (2018) Energy-efficient mission planning of UAVs for 5G coverage in rural zones. In: 2018 IEEE international conference on environmental engineering (EE), Milan, pp 1–9
80. Saleem Y et al (2015) Integration of cognitive radio technology with unmanned aerial vehicles: issues, opportunities, and future research challenges. *J Netw Comput Appl* 50:15–31
81. Zhang S, Zhang H, Di B, Song L (2018) Resource allocation and trajectory design for cellular UAV-to-X communication networks in 5G. In: 2018 IEEE global communications conference (GLOBECOM). Abu Dhabi, United Arab Emirates, pp 1–6
82. Zeng S, Zhang H, Song L (2019) Trajectory optimization and resource allocation for multi-user OFDMA UAV relay networks. In: 2019 IEEE global communications conference (GLOBECOM), Waikoloa, HI, USA, pp 1–6
83. He J, Wang J, Zhu H, Cheng W, Yue P, Yi X (2019) Resource allocation in drone aided emergency communications. In: ICC 2019 - 2019 IEEE international conference on communications (ICC), Shanghai, China, pp 1–6
84. Si P, Yu FR, Yang R, Zhang Y (2015) Dynamic spectrum management for heterogeneous UAV networks with navigation data assistance. In: 2015 IEEE wireless communications and networking conference (WCNC), New Orleans, LA, pp 1078–1083
85. Hu Q, Cai Y, Liu A, Yu G (2019) Joint resource allocation and trajectory optimization for UAV-aided relay networks. In: 2019 IEEE global communications conference (GLOBECOM), Waikoloa, HI, USA, pp 1–6
86. Wen J, Yu R, Wang Y, Zhou H, Zhou F (2019) Resource allocation and trajectory design for UAV-enabled wideband cognitive radio networks. In: 2019 IEEE Globecom Workshops (GC Wkshps), Waikoloa, HI, USA, pp 1–6
87. Yan S, Peng M, Cao X (2019) A game theory approach for joint access selection and resource allocation in UAV assisted IoT communication networks. *IEEE Int Things J* 6(2):1663–1674
88. Pan C, Yi J, Yin C, Yu J, Li X (2019) Joint 3D UAV placement and resource allocation in software-defined cellular networks with wireless backhaul. *IEEE Access* 7:104279–104293
89. Pan C, Yin C, Yu J, Kiran N (2018) 3D UAV placement and resource allocation in software defined cellular networks. In: 2018 IEEE/CIC international conference on communications in china (ICCC Workshops), Beijing, China, pp 136–141
90. Huang F, Chen J, Wang H, Ding G, Gong Y, Yang Y (2019) Multiple UAV-assisted SWIPT in internet of things: user association and power allocation. *IEEE Access* 7:124244–124255
91. Challita U, Ferdowsi A, Chen M, Saad W (2018) Artificial intelligence for wireless connectivity and security of cellular-connected UAVs. [arXiv:1804.05348](https://arxiv.org/abs/1804.05348)
92. Wang Q et al (2018) Joint power and trajectory design for physical-layer secrecy in the UAV-aided mobile relaying system. *IEEE Access* 6:82–849
93. Li B, Fei Z, Zhang Y, Guizani M (2019) Secure UAV communication networks over 5G. *IEEE Wireless Commun* 26(5):114–120. <https://doi.org/10.1109/MWC.2019.1800458>
94. Cai Y et al (2018) Dual-UAV enabled secure communications: joint trajectory design and user scheduling. *IEEE JSAC* 36(9):1972–85

3D Unmanned Aerial Vehicle Placement for Public Safety Communications



Abhaykumar Kumbhar and Ismail Güvenc

Abstract Emerging applications for public safety communications are further strengthened by integrating unmanned aerial vehicles (UAVs) into an existing terrestrial network infrastructure. UAV-based communications and networking can enhance wireless connectivity by integrating UAVs as aerial base stations and aerial user equipment into an existing 5G terrestrial heterogeneous network (HetNet). This chapter designs a public safety 3-tier aerial HetNet (Aerial-HetNet) composed of macrocells and picocells on the ground and small cells carried by UAVs. In particular, this chapter proposes an Aerial-HetNet with optimally placed UAVs for guaranteed quality-of-service. This proposed Aerial-HetNet also considers range expansion bias at small cells, various inter-cell interference coordination (ICIC) for interference mitigation, 3D beamforming for antennas, and 3D channel modeling for UAVs. Furthermore, the performance of designed Aerial-HetNet with optimally placed UAVs is evaluated in the coverage probability and fifth-percentile spectral efficiency (5pSE), using various heuristics algorithms and a brute-force. The Aerial-HetNet's system-wide coverage probability and 5pSE are computed and compared when the unmanned aerial base stations (UABS) are deployed on fixed hexagonal locations using computer-based Matlab simulations. UABS locations are optimized using an elitist harmony search genetic algorithm (eHSGA) and genetic algorithm (GA). The simulation results show that the heuristic algorithms (eHSGA and GA) outperform the brute-force approach and achieved higher peak values of 5pSE and coverage probability. Furthermore, simulation results reveal that the Aerial-HetNet performance of the low-altitude UABSs at 25 m is sparsely better than medium-altitude UABSs (50 m and 36 m). Finally, a trade-off is encountered between achieving the peak Aerial-HetNet performance and the computation time, while applying different heuristic algorithms.

A. Kumbhar (✉)

Motorola Solutions Inc, Plantation, FL 33322, USA
e-mail: abhaykumar.kumbhar@motorolasolutions.com

I. Güvenc

Department of Electrical and Computer Engineering, North Carolina State University Raleigh, Raleigh, NC 27606, USA
e-mail: iguven@ncsu.edu

Keywords Aerial base-stations · Brute force · Range expansion · Coverage · eICIC · FeICIC · Genetic algorithm · Harmonic search · Interference management · Location optimization · Public safety · Unmanned aerial vehicles

1 Introduction

Drones, also known as Unmanned Aerial Vehicles (UAVs), have numerous military, civilian, and commercial applications, such as telecommunications, public safety networks, and smart cities. In particular, 5G-equipped UAVs are stationed as unmanned aerial base stations (UABSs) to supplement the mobile data, satisfy coverage demands, and restore damaged infrastructure within a geographical area of interest. Thus, reducing stress on the existing terrestrial networks and reducing the cost of ultra-dense and dense distributions of small cells [19, 40, 41, 43, 47, 65]. For instance, in the aftermath of Hurricane Maria, AT&T deployed a UABS to restore LTE cellular coverage in Puerto Rico [9, 22, 31, 67]. Whereas, in the United States, Verizon has been experimenting with UABS that could provide broadband coverage with a range of one-mile [22, 29].

With reference to smart cities trends, mobile UAVs could be used as aerial user equipment (AUEs) for collecting data from sensors and Internet-of-Things (IoT) nodes, monitoring traffic, and support various public safety applications such as remote location sensing and search and rescue (SAR). During the Kilauea volcano eruption, the first responders were able to carry out the SAR operation of a Hawaiian man using a UAV [68]. Such practical applications have facilitated the original works to investigate the practicability of trajectory planning and deployment of AUEs in collaboration with 5G infrastructure in [8, 14, 38, 42, 46, 54, 60, 68].

The various application of UAVs in the field of SAR operations, disaster management and response, crowd control and monitoring, traffic monitoring, investigating and reconstructing crime scenes, and investigating active threats scenes are summarized in Table 1.

Given the developments with intelligent software and commercially viable hardware solutions have enabled UAVs to be seamlessly deployed in three-dimensional (3D), detect and avoid collisions, autonomous trajectory planning, and location-aware connectivity. The mobile capability of UAVs allows it to be integrated both as base stations and user equipment into a 5G heterogeneous network (HetNet) as illustrated in Fig. 1. UAVs such as gliders, quadcopters, and balloons are deployed as unmanned aerial base stations (UABSs) equipped with 5G new radio (5G NR) capabilities and AUEs. UAVs, together with a terrestrial 5G HetNet, is defined as a three-tier 5G air-ground HetNet (Aerial-HetNet). However, efficient UAV placement in the proposed Aerial-HetNet for guaranteed quality-of-service (QoS) requires expert network topology planning and optimal 3D deployment. However, optimized UAV placement with improved QoS requires addressing technical challenges such as interference management, performance characterization, handover management, cooperation between UAVs, and practical channel model.

Table 1 Literature review on techniques used for optimal 3D UAV location placement and trajectory planning for public safety communications

References	UAV goal	Techniques	Public safety applications
[39]	Path planning	Q-learning and directional antenna	Search and Rescue
[15]	Path planning	Heuristic algorithms	Collecting data from traffic sensors
[33]	Path planning, waypoint determination, 3D positioning	Multivariable optimization	Emergency data collection and transmission
[11]	Path planning	Double deep Q-network	Situational awareness from IoT sensor data
[7]	3D positioning	MAC-based communication optimization	Filling coverage holes
[32]	3D trajectory planning	proximal difference-of-convex algorithm with extrapolation	Video tracking and surveillance
[70]	–	mmWave antenna design	Sub-THz PSC
[69]	Path planning	MIMO	Data relaying
[61]	–	Deep-learning-based image processing	Search and rescue in forests
[26]	Path planning	Thermal image processing using deep convolutional neural networks	Real-time survivor detection system
[12]	Path planning	Image processing using convolutional neural network	Avalanche search and rescue operations
[38]	Path planning	Cooperative predictive model	Localizing malicious RF source
[3]	Path planning	Long short-term memory based machine learning	Localization of RF source
[48]	3D positioning	Random-forest based machine learning	Predictive crime deterrence and data acquisition
[35]	Ad-hoc network as cloudlet (data centers)	Disaster resilient three-layered architecture	Edge computing

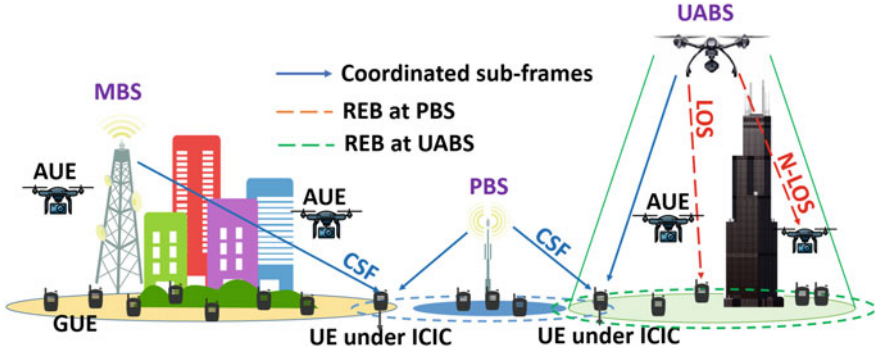


Fig. 1 An illustration of an Aerial-HetNet with GUE, PBS, and MBS as terrestrial nodes and AUE, and UABS as the aerial node. With inter-cell interference coordination techniques are considered at MBS and PBS. Small cell such as mobile UABSs and PBSs utilizes range expansion to offload users from congested cells

With an objective to design an Aerial-HetNet with ubiquitous broadband coverage, which is necessary to support mission-critical communication voice and data operations, this chapter aims to optimally deploy UABSs on 3D locations. To achieve this goal, a system-level understanding is required to alter and scale the network layout of the existing terrestrial infrastructure. To this end, in this chapter, an Aerial-HetNet wireless network in an urban environment and operating with public safety broadband frequency in LTE band class 14, as illustrated in Fig. 1, is defined and simulated. The illustrated Aerial-HetNet model leverages range expansion specified in 3GPP Release 8, intercell interference coordination (ICIC) specified in 3GPP Release 10/11, antenna 3D beamforming (3DBF) specified in 3GPP Release 12, and 3D channel model for UAVs specified in 3GPP Release 15. Consequently, to evaluate the performance of this Aerial-HetNet, the model considers *fifth percentile spectral efficiency (5pSE)* and *coverage probability* as the key performance indicators (KPIs). To maximize the two KPIs of the Aerial-HetNet, the UABS locations in two-dimension (2D), range expansion bias (REB), and ICIC parameters are jointly optimized using an elitist harmony search algorithm based on the genetic algorithm (eHSGA), genetic algorithm (GA), and brute-force. As seen in Table 5, the deployment altitude of the UABS is not considered as one search space parameter to minimize the overall complexity of the optimization algorithms. Nevertheless, the impact of UABS altitude on the overall performance of the Aerial-HetNet is reviewed by considering various practical deployment altitudes.

The remainder of the chapter is organized into the following sections. Section 2 discusses UABS placement techniques considered, Sect. 3 defines the problem of optimal 2D placement of UABS in the Aerial-HetNet using an eHSGA, GA, and brute-force. Section 4 describes the system model for the Aerial-HetNet model and outlines the KPIs as a function of system parameters. In Sect. 5, through extensive computer-based Matlab simulations, the two KPIs of the Aerial-HetNet are computed, compared, and analyzed for various deployment altitudes of UABS, ICIC

Table 2 Notations and symbols adopted in the chapter

Symbol	Description
$\Lambda_{mbs}, \Lambda_{pbs}$	MBS and PBS distribution density
$\Lambda_{gue}, \Lambda_{aue}$	GUE and AUE distribution density
$\mathbf{L}_{mbs}, \mathbf{L}_{pbs}, \mathbf{L}_{uabs}$	Locations of MBS, PBS, and UABS
$\mathbf{L}_{gue}, \mathbf{L}_{aue}$	Locations of GUE and AUE
N_{ue}	Cumulative users i.e., AUEs + GUEs
$P_{uabs}^{tx}, P_{pbs}^{tx}, P_{mbs}^{tx}$	Maximum transmit power of UABS, PBS, and MBS
$\vartheta(d_{un}), \vartheta(d_{pn}), \vartheta(d_{on})$	Path-loss in dB from UABS, PBS, and MBS
F	Nakagami-m fading
f_{psc}	PSC broadband frequency
h_{bs}	Altitude of the terrestrial base station
h_{uabs}	Altitude of the UABS station
h_{gue}	Altitude of GUEs
h_{aue}	Altitude of AUEs
d_{on}, d_{pn}, d_{un}	UE distance from its MOI, POI, and UOI
$A_{3DBF}(\phi, \theta)$	Transmitter antenna's 3DBF element
$P'_{mbs}(d_{on})$	RSRP from the MOI
$P'_{pbs}(d_{pn})$	RSRP from the POI
$P'_{uabs}(d_{un})$	RSRP from the UOI
I_{agg}	Aggregate interference at a UE from all base-stations, except BOI
$\Gamma_{usf}^{uabs}, \Gamma_{usf}^{pbs}, \Gamma_{usf}^{mbs}$	USF SIR from UOI, POI, and MOI
$\Gamma_{csf}^{uabs}, \Gamma_{csf}^{pbs}, \Gamma_{csf}^{mbs}$	CSF SIR from UOI, POI, and MOI
$\alpha_{pbs}, \alpha_{mbs}$	Power reduction factor of CSF for PBS and MBS
β_{pbs}, β_{mbs}	PBS and MBS Duty cycle for the transmission of USF
$\Upsilon_{pbs}, \Upsilon_{uabs}$	REB at PBS and UABS
$\rho_{mbs}, \rho_{pbs}, \rho_{uabs}$	MUE PUE, and UUE Scheduling threshold
$N_{usf}^{mbs}, N_{csf}^{mbs}$	Number of uncoordinated and coordinated MUEs
$N_{usf}^{pbs}, N_{csf}^{pbs}$	Number of uncoordinated and coordinated PUEs
$N_{usf}^{uabs}, N_{csf}^{uabs}$	Number of uncoordinated and coordinated UUEs
$C_{usf}^{mbs}, C_{csf}^{mbs}$	Aggregate SEs for uncoordinated and coordinated MUEs, respectively in a cell
$C_{usf}^{pbs}, C_{csf}^{pbs}$	Aggregate SEs for uncoordinated and coordinated PUEs, respectively in a cell
$C_{usf}^{uabs}, C_{csf}^{uabs}$	Aggregate SEs for uncoordinated and coordinated UUEs, respectively in a cell
$C_{5pSE}(\cdot)$	Objective function for 5pSE
$C_{cov}(\cdot)$	Objective function for coverage probability
T_{CSE}	Capacity threshold supporting broadband rates
\mathbf{S}^{ICIC}_{mbs}	ICIC parameter matrix for MBSs
\mathbf{S}^{ICIC}_{pbs}	ICIC parameters matrix for PBSs
\mathbf{S}^{ICIC}_{uabs}	ICIC parameters matrix for UABSs
S, BS_{KPI}	All possible states and best state of objective functions
POP	eHSGA and GA initial population
SZ_{GA}	GA population size
cxr, mr	GA crossover rate and mutation probability
SZ_{HM}	eHSGA population size
HM	eHSGA harmonic memory
R_{HMC}	eHSGA HM consideration rate
fr, par, N_{IMP}	eHSGA fret width, pitch adjustment rate, and number of improvisation
A_{sim}	Simulation area

techniques, and optimization techniques. Furthermore, the chapter explains the influence of UABS altitude on the KPIs and performance of the optimization techniques. Given in Table 2 are the lists of notations and symbols adopted throughout the chapter.

2 Literature Review

The advancements in UAV technology have made it possible to dynamically position mobile small cells such as UABSs as illustrated in Fig. 2 and enhance the overall performance of the Aerial-HetNet by offloading users in overcrowded and high-traffic locations and filling the coverage holes in the network. The UABSs placement in an Aerial-HetNet has two objectives: *deploying UABSs on optimized 3D locations* and *improving KPIs while addressing constraints* such as interference mitigation, performance characterization, handover management, cooperation between UAVs, and

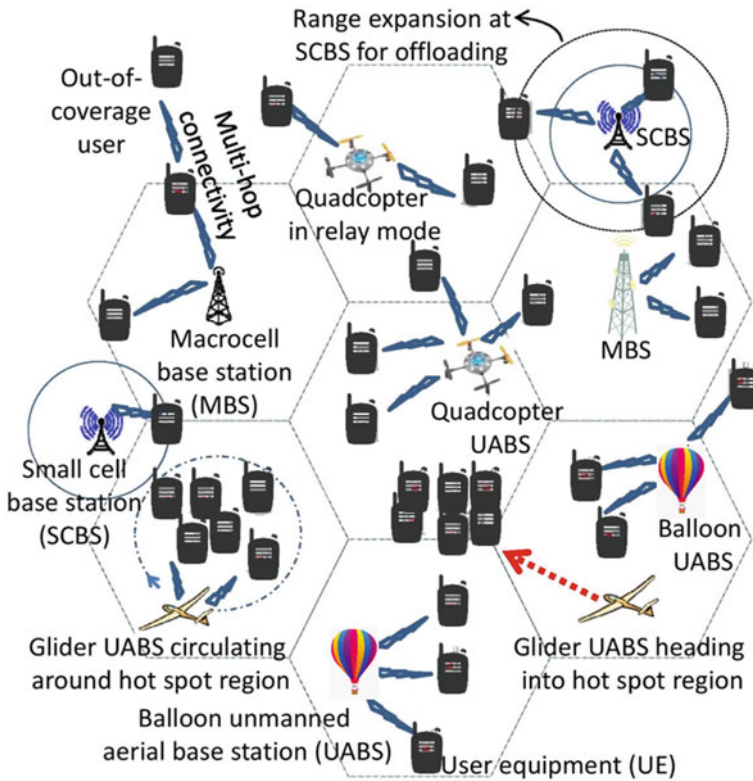


Fig. 2 An illustration of Aerial-HetNet with agile UABSs dynamically changing their locations to offload users in congested network, improving coverage, and providing seamless broadband connectivity

channel model. In this chapter, the literature review broadly classifies the optimized UABS placement in the Aerial-HetNet into two categories: mathematical modeling with numerical derivations and computer-based simulative study using algorithms-based iterative methods.

Several comprehensive simulation-based studies in the literature [17, 18, 18, 21, 30, 47, 52, 64, 74, 75] have investigated location optimization and UABS deployment altitude. However, important aspects like UE handover, 3GPP specified interference mitigation, and the air-ground path loss model are not explicitly considered. The advantages of enhanced ICIC (eICIC) specified in 3GPP Release 10, further-enhanced ICIC (FeICIC) specified in 3GPP Release 11, and range expansion at small cells have been examined in [41, 65] for LTE-Advanced Aerial-HetNet. Furthermore, the brute-force and heuristic algorithms were used to maximize the KPIs by jointly optimizing UABS locations in 2D and key ICIC parameters. Nevertheless, the deployment altitude of UABS in Aerial-HetNet was not taken into account. In literature [18, 41, 43, 47, 65, 74, 75] machine learning techniques are considered to jointly optimize UABS location and wireless network parameters. Although the Optimal 3D placement of UABS is studied in [20, 63], the other essential design aspects of Aerial-HetNet are not considered.

In [5, 17, 23, 50, 58, 66], the goal of UABS positioning was formulated into the numerical problem and was solved by using novel mathematical approaches. The results from the analytical derivations were verified against numerical simulations for accuracy. In particular, lower and upper bounds of the UABS altitude were determined; the KPI goal was limited only to maximize the coverage of users with varying QoS experiences. Furthermore, these literature does not consider a multi-tier Aerial-HetNet and techniques such as ICIC, CRE, and handover influencing the KPIs of a multi-tier Aerial-HetNet.

Our literature review of related works on techniques used for optimizing UABSs location placement and joint optimization of spectrum parameters in Aerial-HetNet is summarized in Tables 3, and 4. Given the summary and literature review earlier, the specific contributions of the chapter include the feasibility study of deploying UAVs as both UABS and AUEs with an existing 5G terrestrial infrastructure. Furthermore, the investigation of critical aspects such as the inter-cell interference, spectral efficiency, and coverage probability while considering key system parameters such as channel modeling support, antenna 3D beamforming, and range expansions. The system parameters under investigation and effectiveness technologies under consideration are also extended to cover both UABSs and AUEs as part of the Aerial-HetNet. Finally, the eHSGA, GA, and brute-force algorithms are modified to joint optimization the UABS locations in 2D, REB, and ICIC parameters to maximize the gains in KPIs defined in Sect. 3.

Table 3 Literature review on techniques used for optimal UABS location placement and joint optimization of spectrum parameters in Aerial-HetNet, wherein the optimization is presented using analytical approach and is also verified using simulation

References	Optimization techniques	Optimization goal	Approach
[72]	Strategyproof mechanism	UABS 3D placement	Analytical
[58]	–	Coverage, Throughput	Analytical
[66]	Region partition strategy, Backtracking line search algorithm	User load balancing, UABS locations	Analytical
[51]	Truncated octahedron	UABS 3D-locations	Analytical
[27]	particle swarm optimization, Hybrid fixed-point iteration	UABS 3D-locations, coverage, interference mitigation, spectral efficiency	Analytical
[59]	Integer linear programming optimization	UABS 3D-locations and antenna orientations	Analytical
[4]	Non-convex optimization using sequential exhaustive search, sequential maximal weighted area	UABS locations, number of users scheduled	Analytical
[23]	Mathematical modeling	UABS 3D-location, Transmit power	Both
[25]	fast k -means-based clustering model	UABS trajectory planning, power and time allocation	Both

3 UABS Optimal Placement in Aerial-HetNet

The simulative study in this chapter considers a public safety Aerial-HetNet during an emergency or large-scale events such as a Soccer World Cup or Super Bowl. Usually, during such an event, there is a surge in network activity and could cause traffic congestion in commercial cellular networks and public safety networks. In such a scenario, the existing terrestrial macrocell base stations (MBSs) and picocell base stations (PBSs) tend to get overloaded with several user equipments (UEs). Thus, resulting in scheduled UEs experiencing poor QoS. To address the network congestion in this scenario, the design considers optimizing UABSs location and maximizing the two KPIs. To this end, *elitist harmony search based on the genetic algorithm*, *genetic algorithm*, and *brute force algorithm* are considered. The pro-

Table 4 Literature review on techniques used for optimal UABS location placement and joint optimization of spectrum parameters in Aerial-HetNet, wherein the optimization is presented using simulative approach

References	Optimization techniques	Optimization goal	Approach
[47]	Genetic algorithm, Brute-force	Coverage, Throughput, UABS locations	Simulation
[64]	Neural model	UABS locations	Simulation
[65]	Deep Q-learning, Q-learning, Sequential algorithm, Brute-force	Throughput, UABS locations, interference mitigation, energy efficiency	Simulation
[41]	Genetic algorithm, Brute-force, Fixed hexagonal	Throughput, UABS locations, interference mitigation, energy efficiency	Simulation

(continued)

posed system design defines the KPI, 5pSE, as the worst fifth percentile UE capacity amongst all scheduled UEs. The coverage probability of the Aerial-HetNet is defined as the percentage of a geographical area having broadband rates and capacity larger than a threshold of T_{CSE} . Where T_{CSE} is the minimum guaranteed throughput needed to support mission-critical broadband applications.

For each UABS, $i \in \{1, 2, \dots, N_{uabs}\}$, individual location of a UABS is captured in (x_i, y_i) coordinate. The matrix \mathbf{L}_{uabs} would represent all the UABS locations in 3D and are placed within the simulation area regardless of the existing PBS locations (\mathbf{L}_{pbs}) and MBS (\mathbf{L}_{mbs}). Given the locations of base-station (\mathbf{L}_{uabs} , \mathbf{L}_{pbs} , and \mathbf{L}_{mbs}), individual ICIC parameters for each UABS can be represented in a matrix $\mathbf{S}_{uabs}^{ICIC} = [\boldsymbol{\rho}_{uabs}, \boldsymbol{\Upsilon}_{uabs}] \in \mathbb{R}^{N_{uabs} \times 2}$, individual ICIC parameters for each small cell PBS is captured in matrix $\mathbf{S}_{pbs}^{ICIC} = [\boldsymbol{\rho}_{pbs}, \boldsymbol{\Upsilon}_{pbs}, \boldsymbol{\beta}_{pbs}, \boldsymbol{\alpha}_{pbs}] \in \mathbb{R}^{N_{pbs} \times 4}$, and an individual ICIC parameters for each MBS is given by matrix $\mathbf{S}_{mbs}^{ICIC} = [\boldsymbol{\rho}_{mbs}, \boldsymbol{\beta}_{mbs}, \boldsymbol{\alpha}_{mbs}] \in \mathbb{R}^{N_{mbs} \times 3}$. The vectors $\boldsymbol{\rho}_{uabs} = [\rho_1, \dots, \rho_{N_{uabs}}]^T$ captures the scheduling threshold and $\boldsymbol{\Upsilon}_{uabs} = [\Upsilon_1, \dots, \Upsilon_{N_{uabs}}]^T$ the range expansion for each UABS. On the other hand, $\boldsymbol{\rho}_{pbs} = [\rho_1, \dots, \rho_{N_{pbs}}]^T$, captures the scheduling threshold, $\boldsymbol{\Upsilon}_{pbs} = [\Upsilon_1, \dots, \Upsilon_{N_{pbs}}]^T$ captures the the range expansion, $\boldsymbol{\beta}_{pbs} = [\beta_1, \dots, \beta_{N_{pbs}}]^T$ captures the USF duty cycle, and $\boldsymbol{\alpha}_{pbs} = [\alpha_1, \dots, \alpha_{N_{pbs}}]^T$ captures the power reduction for each PBS. Whereas, for each MBS, the vectors $\boldsymbol{\rho}_{mbs} = [\rho_1, \dots, \rho_{N_{mbs}}]^T$ captures the scheduling thresholds, $\boldsymbol{\beta}_{mbs} = [\beta_1, \dots, \beta_{N_{mbs}}]^T$ capture the power USF duty cycle, and $\boldsymbol{\alpha}_{mbs} = [\alpha_1, \dots, \alpha_{N_{mbs}}]^T$ captures the power reduction factor applied at CSF. Using these definitions, the initial state of the Aerial-HetNet can be given as $\mathbf{S} = [\mathbf{L}_{uabs}, \mathbf{S}_{mbs}^{ICIC}, \mathbf{S}_{pbs}^{ICIC}, \mathbf{S}_{uabs}^{ICIC}]$.

Given the range and step size of the search space parameters defined in Table 5, intuitively, it can be observed that a large search space needs to be considered for finding all feasible solutions. Therefore the system model is further simplified by applying the same \mathbf{S}_{mbs}^{ICIC} , \mathbf{S}_{pbs}^{ICIC} , and \mathbf{S}_{uabs}^{ICIC} parameters across all MBSs, PBSs, and

Table 4 (continued)

References	Optimization techniques	Optimization goal	Approach
[42]	Brute-force	UABS locations, spectral efficiency, coverage, energy efficiency, interference mitigation	Simulation
[30]	Brute-force, Gradient descent location optimization	Throughput, UABS locations	Simulation
[18]	Deep reinforcement learning	Energy efficiency, UABS locations, interference mitigation, wireless latency	Simulation
[74]	Centralized machine learning	Energy efficiency, UABS locations	Simulation
[75]	Wavelet transform machine learning	User load balancing, UABS locations	Simulation
[63]	Greedy approach	User load balancing, UABS 3D-locations	Simulation
[44]	Alternating optimization, Successive convex programming	Bandwidth allocation, UABS locations, energy efficiency	
[20]	Non-orthogonal and Orthogonal spectrum sharing	UABS 3D-locations	Simulation
[43]	eHSGA, Genetic algorithm, Brute-force	UABS locations, spectral efficiency, coverage, energy efficiency, interference mitigation	Simulation
[55]	Modified spiral algorithm	UABS locations, number of users scheduled, QoS of UEs, interference mitigation	Simulation
[56]	disaster mobility model	UABS placement, number of users scheduled, coverage	Simulation
[62]	modified k -means algorithm	UABS altitude, path-loss compensation factor	Simulation
[53]	proximal policy optimisation	Energy efficiency	Simulation

UABSs, respectively. Consequently, also reducing the algorithm complexity and the convergence time of the heuristic algorithms.

Using above understanding of the system-level parameters, the objective function C_{5pSE} and coverage probability is defined as

$$C_{5pSE} \left(\mathbf{L}_{uabs}, \mathbf{S}_{mbs}^{ICIC}, \mathbf{S}_{pabs}^{ICIC}, \mathbf{S}_{uabs}^{ICIC} \right), \quad (1)$$

Table 5 Upper bound values, lower bound values, and step size of parameters to be optimized within the search space

Search Variable	Variable Range	Search space size
α_{mbs}	$0, \delta\alpha_{\text{mbs}}, 2\delta\alpha_{\text{mbs}}, \dots, 1$	$1/\delta\alpha_{\text{mbs}} + 1$
β_{mbs}	$0, \delta\beta_{\text{mbs}}, 2\delta\beta_{\text{mbs}}, \dots, 1$	$1/\delta\beta_{\text{mbs}} + 1$
ρ_{mbs}	$\rho_{\text{mbs}}^{\text{low}}, \rho_{\text{mbs}}^{\text{low}} + \delta\rho_{\text{mbs}}, \rho_{\text{mbs}}^{\text{low}} + 2\delta\rho_{\text{mbs}}, \dots, \rho_{\text{mbs}}^{\text{high}}$	$\frac{(\rho_{\text{mbs}}^{\text{high}} - \rho_{\text{mbs}}^{\text{low}})}{(\delta\rho_{\text{mbs}})}$
α_{pbs}	$0, \delta\alpha_{\text{pbs}}, 2\delta\alpha_{\text{pbs}}, \dots, 1$	$1/\delta\alpha_{\text{pbs}} + 1$
β_{pbs}	$0, \delta\beta_{\text{pbs}}, 2\delta\beta_{\text{pbs}}, \dots, 1$	$1/\delta\beta_{\text{pbs}} + 1$
ρ_{pbs}	$\rho_{\text{pbs}}^{\text{low}}, \rho_{\text{pbs}}^{\text{low}} + \delta\rho_{\text{pbs}}, \rho_{\text{pbs}}^{\text{low}} + 2\delta\rho_{\text{pbs}}, \dots, \rho_{\text{pbs}}^{\text{high}}$	$\frac{(\rho_{\text{pbs}}^{\text{high}} - \rho_{\text{pbs}}^{\text{low}})}{(\delta\rho_{\text{pbs}})}$
Υ_{pbs}	$0, \delta\Upsilon_{\text{pbs}}, 2\delta\Upsilon_{\text{pbs}}, \dots, \Upsilon_{\text{pbs}}^{\text{high}}$	$\frac{\Upsilon_{\text{pbs}}^{\text{high}}}{\delta\Upsilon_{\text{pbs}}}$
ρ_{uabs}	$\rho_{\text{uabs}}^{\text{low}}, \rho_{\text{uabs}}^{\text{low}} + \delta\rho_{\text{uabs}}, \rho_{\text{uabs}}^{\text{low}} + 2\delta\rho_{\text{uabs}}, \dots, \rho_{\text{uabs}}^{\text{high}}$	$\frac{(\rho_{\text{uabs}}^{\text{high}} - \rho_{\text{uabs}}^{\text{low}})}{(\delta\rho_{\text{uabs}})}$
Υ_{uabs}	$0, \delta\Upsilon_{\text{uabs}}, 2\delta\Upsilon_{\text{uabs}}, \dots, \Upsilon_{\text{uabs}}^{\text{high}}$	$\frac{\Upsilon_{\text{uabs}}^{\text{high}}}{\delta\Upsilon_{\text{uabs}}}$
X coordinates in (x_i, y_i)	$-loc/2, -loc/2 + \delta_x, -loc/2 + 2\delta_x, \dots, loc/2$	$\frac{loc}{\delta_x}$
Y coordinates in (x_i, y_i)	$-loc/2, -loc/2 + \delta_y, -loc/2 + 2\delta_y, \dots, loc/2$	$\frac{loc}{\delta_y}$

$$C_{\text{COV}}(\mathbf{L}_{\text{uabs}}, \mathbf{S}_{\text{mbs}}^{\text{ICIC}}, \mathbf{S}_{\text{pbs}}^{\text{ICIC}}, \mathbf{S}_{\text{uabs}}^{\text{ICIC}}), C_{\text{COV}} > T_{C_{\text{SE}}}, \quad (2)$$

where $C_{5\text{pSE}}(\cdot)$ signifies 5pSE objective function, $C_{\text{cov}}(\cdot)$ signifies coverage probability objective function, and $T_{C_{\text{SE}}}$ is minimum capacity threshold. A generic definition of best state (\mathbf{BS}_{KPI}) from all possible states (\mathbf{S}) using objective functions is given as

$$\mathbf{BS}_{\text{KPI}} = \arg \max_{\mathbf{S}} C_{\text{KPI}}(\mathbf{S}), \quad (3)$$

where $C_{\text{KPI}}(\cdot)$ is a generic representation of objective function defined in (1) and (2) and $\mathbf{KPI} \in (5\text{pSE}, \text{COV})$.

In the Aerial-HetNet, UABSs are initially deployed on a fixed hexagonal locations within the simulation area (A_{sim}), as shown in Fig. 4a. Each UABS sends its 2D location coordinates and the system-level resources allocation for an users to an edge server, and using a brute-force described in the Algorithm 1, the two KPIs of the Aerial-HetNet will be determined at the edge server. The global maxima values of the best state (\mathbf{BS}_{KPI}) from all possible states \mathbf{S} are vectorized into $\mathbf{BS}_{\text{KPI}} = [\mathbf{L}_{\text{uabs}}^{\text{hex}}, \mathbf{BS}_{\text{mbs}}^{\text{ICIC}}, \mathbf{BS}_{\text{pbs}}^{\text{ICIC}}, \mathbf{BS}_{\text{uabs}}^{\text{ICIC}}]$.

Subsequent to this brute-force evaluation, an edge server would run *elitist harmony search genetic algorithm* (eHSGA) and *genetic algorithm* (GA). The pseudocode

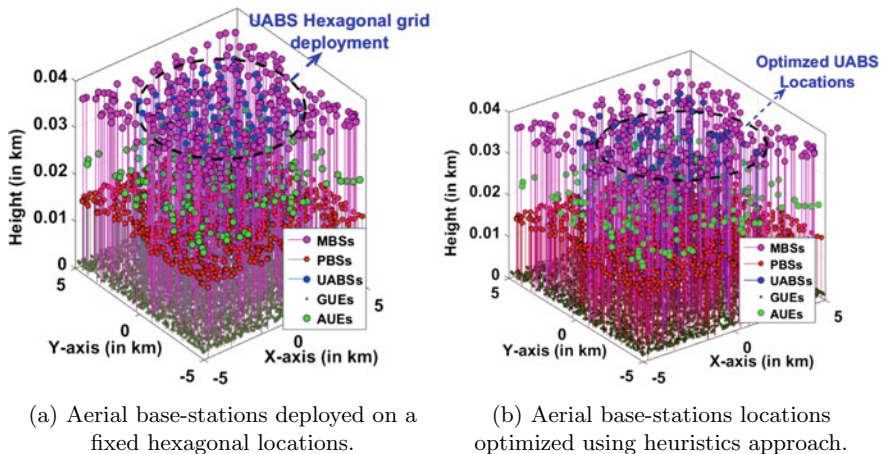


Fig. 3 A 3D simulative rendition of the base-stations and user equipments distributed in the designed Aerial-HetNet

Algorithm 1 Pseudocode for brute-force approach

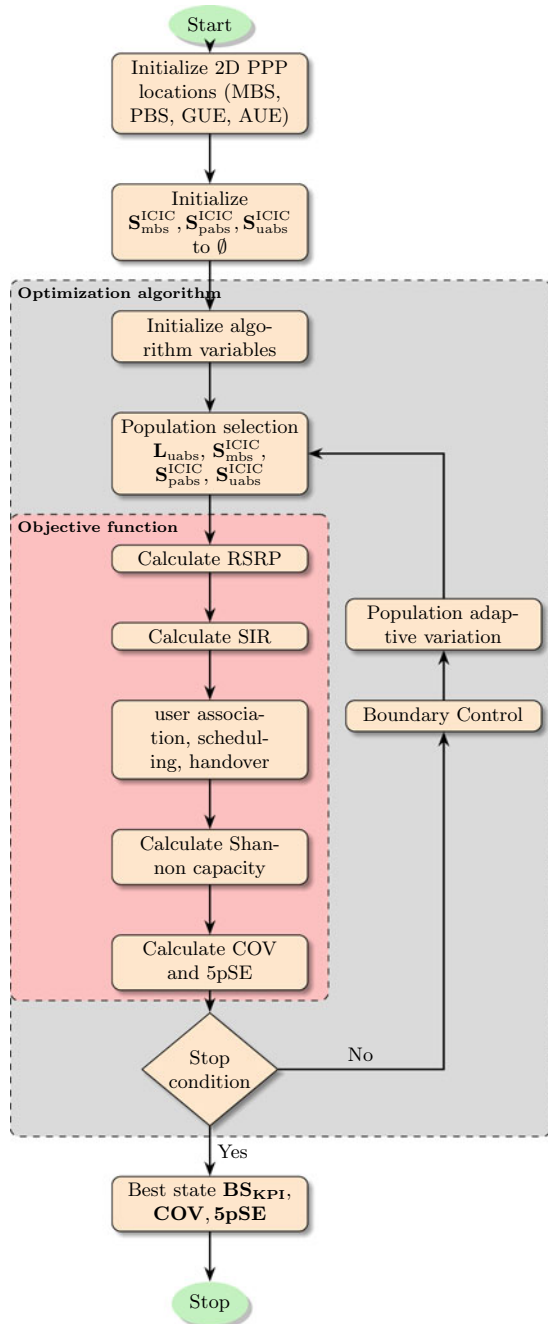
```

1: procedure  $C_{KPI}(\mathbf{L}'_{uabs}, \mathbf{S}^{ICIC}_{mbs}, \mathbf{S}^{ICIC}_{pbs}, \mathbf{S}^{ICIC}_{uabs})$ 
2:    $\mathbf{COV}, \mathbf{5pSE}, \mathbf{Best\ state\ BS} \leftarrow \emptyset$ 
3:   for all values of state  $\mathbf{S}$  do
4:     Current  $\mathbf{COV} \leftarrow C_{\mathbf{COV}}(\mathbf{S})$ 
5:     if Current  $\mathbf{COV} > \mathbf{COV}$  then
6:        $\mathbf{COV} \leftarrow$  Current  $\mathbf{COV}$ 
7:        $\mathbf{BS} \leftarrow \mathbf{S}$ 
8:     end if
9:     Current  $\mathbf{5pSE} \leftarrow C_{\mathbf{5pSE}}(\mathbf{S})$ 
10:    if Current  $\mathbf{5pSE} > \mathbf{5pSE}$  then
11:       $\mathbf{5pSE} \leftarrow$  Current  $\mathbf{5pSE}$ 
12:       $\mathbf{BS} \leftarrow \mathbf{S}$ 
13:    end if
14:  end for
15:  Return  $\mathbf{COV}, \mathbf{5pSE}, \mathbf{BS}$ 
16: end procedure

```

describing the optimization approach of these generic metaheuristic algorithms is given in Algorithms 2 and 3, respectively. The goal of the heuristics algorithm is to compute the global maxima of the best state (\mathbf{BS}_{KPI}) from all the possible states \mathbf{S} and is vectorized into $\mathbf{BS}_{KPI} = [\mathbf{L}'_{uabs}, \mathbf{BS}^{ICIC}_{mbs}, \mathbf{BS}^{ICIC}_{pbs}, \mathbf{BS}^{ICIC}_{uabs}]$. Where, \mathbf{L}'_{uabs} is the optimal 2D UABS locations as shown in Fig. 4b and $\mathbf{BS}^{ICIC}_{uabs}$, \mathbf{BS}^{ICIC}_{pbs} , and \mathbf{BS}^{ICIC}_{mbs} are the global maxima of ICIC parameters for UABSs, PBSs, and MBSs, respectively. With 2D optimization of UABS locations and ICIC parameters, the UABSs are reorganized at these optimal locations as illustrated in Fig. 4b. Lastly, a step-by-step representation of system flow given in Fig. 3 consisting the system-level details

Fig. 4 A step-by-step representation of system flow and optimization approach



Algorithm 2 Pseudocode for Genetic Algorithm

```

1: procedure OBJECTIVE FUNCTION (CKPI) : CCOV(Luabs, SmbsICIC, SpbsICIC, SuabsICIC),
   C5pSE(Luabs, SmbsICIC, SpbsICIC, SuabsICIC)
2: COV, 5pSE, Best state BS ← ∅
3: Selection strategy ← Roulette Wheel
4: Initialize variables:
   cxr, mr, and SZGA
5: Population (POP) Set of
   S ← Luabs, SmbsICIC, SpbsICIC, SuabsICIC
6: FITNESS = CCOV(.), C5pSE(.)
7: Evaluate POP FITNESS
8: Stop Condition ← number of iterations
9: while !Stop Condition do
10:   for k = 1 : SZGA do
11:     Parent1 (P1) ← SELECTION(POP, FITNESS)
12:     Parent2 (P2) ← SELECTION(POP, FITNESS)
13:     Child1 (C1), Child2 (C2) ←
       REPRODUCE(P1, P2, cxr)
14:     if rand() < mr then
15:       Children ← MUTATE(C1, mr)
16:       Children ← MUTATE(C2, mr)
17:     end if
18:     Evaluate Children FITNESS
19:     Choose best state BS from Children
20:     POP ← REPLACE(POP, Children)
21:   end for
22: end while
23: Best state BS ← Best FITNESS
24: Return COV, 5pSE, BS
25: end procedure

```

discussed in Sect. 4, objective functions, and optimization algorithms proposed in Algorithms 1–3.

3.1 Genetic Algorithm

Evolutionary algorithms are *generic* population-based metaheuristic algorithms and consider routines and procedures inspired by biological evolutionary stages, such as population generation, mutation, crossover, and selection. *Genetic algorithm* (GA) is one of the popular evolutionary algorithms used for solving search problems and produce high-quality optimal solutions. GA has been comprehensively investigated in [41, 43, 47] to obtain global maxima values of UABS locations in 2D and system-level ICIC parameters. The solution obtained using the GA approach showed meaningful improvement in system performance over the traditional brute-force approach. This proven GA approach is extended to consider the three-tier

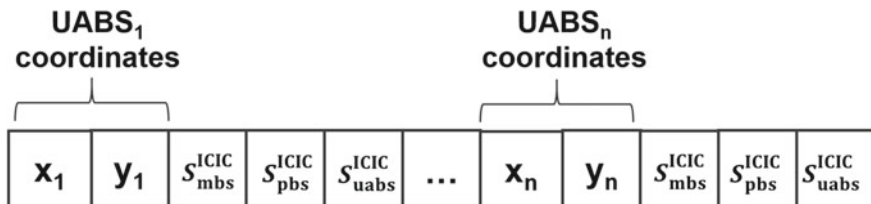


Fig. 5 An example of a GA chromosome with UABS locations and ICIC parameters S_{mbs}^{ICIC} , S_{pbs}^{ICIC} , and S_{uabs}^{ICIC}

Aerial-HetNet designed in Sect. 4 and the optimization goals to parameters and search space defined in Table 5.

GA considers a population of candidate solutions that are evolved towards a global maxima. Each candidate solution have a set of chromosomes and is assessed by the objective function. Illustrated in Fig. 5 is an example chromosome that is composed of UABS locations (L_{uabs}) and Aerial-HetNet ICIC parameters (S_{mbs}^{ICIC} , S_{pbs}^{ICIC} , S_{uabs}^{ICIC}) that form GA population (**POP**) and population size of SZ_{GA} . The initial steps of the optimization process include a population of randomly generated chromosomes that is altered and mutated to form the next-generation offspring [15]. This process considers enough iterations to avoid local maxima and achieve true global maxima. Given below are the step-by-step process involved in reaching global maxima and obtaining adaptive-fit individuals from the population.

1. The objective functions $C_{5pSE}(\cdot)$ calculated in (1) for 5pSE and $C_{cov}(\cdot)$ in (2) for coverage probability is referenced as the *fitness function* in Algorithm 2 and is used to evaluate the chromosomes.
2. Chromosome *selection* process is used for determining the most desirable set of the chromosome from the population, which provides global maxima for a given KPI. Furthermore, of the various selection strategies used in GA, the roulette wheel selection strategy is applied and is directly proportional to its fitness value. Let $P_n = \frac{f_n}{\sum_{n=1}^N f_n}$ be the probability of a n th chromosome being selected, where f_n is the fitness value of n th chromosome, and N is the total number of chromosomes in the population pool. After the chromosomes are picked, they are placed into a mating pool to generate a new set of chromosomes.
3. The genetic operator *crossover* is a process of recombining genetic information of two-parent chromosomes using a one-point crossover strategy to reproduce new generation chromosomes with a crossover rate of cxr .
4. Consequent to a reliable generation of new chromosomes using crossover operator, *mutation* genetic operator is applied for preserving genetic diversity in subsequent generations. The mutation process also helps to prevent the solution from converging at local maxima. During mutation, one or more gene values are modified in a chromosome with a mutation probability of mr from its initial state.

Algorithm 3 Pseudocode for eHSGA

```

1: procedure OBJECTIVE FUNCTION (CKPI) : CCOV( $\mathbf{L}_{uabs}, \mathbf{S}_{mbs}^{ICIC}, \mathbf{S}_{pbs}^{ICIC}, \mathbf{S}_{uabs}^{ICIC}$ ),
   C5pSE( $\mathbf{L}_{uabs}, \mathbf{S}_{mbs}^{ICIC}, \mathbf{S}_{pbs}^{ICIC}, \mathbf{S}_{uabs}^{ICIC}$ )
2: COV, 5pSE, Best state BS  $\leftarrow \emptyset$ 
3: Selection strategy  $\leftarrow$  Roulette Wheel
4: Initialize variables:
   RHMC, fr, par, and SZHM
5: Initial population S  $\leftarrow$  Set of
    $\mathbf{L}_{uabs}, \mathbf{S}_{mbs}^{ICIC}, \mathbf{S}_{pbs}^{ICIC}, \mathbf{S}_{uabs}^{ICIC}$ 
6: Evaluate Initial Population: CCOV(.), C5pSE(.)
7: Stop Condition  $\leftarrow$  number of iterations
8: while !Stop Condition do
9:   for itr = 1 : SZHM do
10:    if rand() < RHMC then
11:      Pick Best state, BS from HM
12:      if rand() < par then
13:        Pitch adjustment on BS
14:         $\mathbf{S}_{rand}^{new} = \mathbf{S}_{rand}' + (2 \times rand() - 1) \times fr_{rand}$ 
15:      else
16:        Crossover between  $\mathbf{S}^k$  and
17:        a random member  $\mathbf{S}^{rand}$ 
18:      end if
19:      else
20:        Random selection  $\mathbf{S}^{new}$ 
21:         $\mathbf{S}_j^{new} = (u_j - l_j) \times random() + l_j$ 
22:      end if
23:      Evaluate Population: CCOV(.), C5pSE(.)
24:    end for
25:    fr  $\leftarrow fr \times 99\%$ 
26:  end while
27: Best state BS  $\leftarrow$  Best solution
28: Return COV, 5pSE, BS
29: end procedure

```

Pseudocode describing the above step-by-step process is also described in Algorithm 2. Given GA's ability to achieve true global maxima, GA experiences high computation time and low convergence speed. Furthermore, to investigate any potential gain over GA, the chapter explores the eHSGA proposed in [16].

3.2 Elitist Harmony Search Genetic Algorithm (eHSGA)

The harmony search (HS) is based on the music harmony improvisation process and stochastic technique to diversify search population. In its initial step, the HS algorithm randomly creates a set of candidate solutions known as the harmony vectors (HV) within a search space and then vectorized in the harmony memory (HM).

Improving a candidate harmony vector within the HS happens in three main stages, i.e., HM creation/update, pitch adjustment, and randomization. Upon generation of a new vector, performance of the new vector performance is compared with other harmonies in the HM, and only the best-performing harmony vector is retained [16, 28]. Given this overview of the HS, a search strategy compiled by hybridizing HS and GA approaches is considered to improve the global maxima of search problems. The hybrid approach considers chromosomes and population structure from GA, whereas the aspects of pitch adjustment and HM phenomena are considered from HS. The *Hybrid eHSGA* proposed in [16] is extended to consider the Aerial-HetNet planned in Sect. 4 and the optimization goals to parameters and search space given in Table 5. The pseudocode of the proposed hybrid algorithm is described in Algorithm 3. The principal steps involved are:

1. In the initial steps, the first generation of population **POP** is produced using GA and is tagged as harmony memory (**HM**). The size of the **HM** is given by SZ_{HM} , and the chromosome shown in Fig. 5 form the HV.
2. Consider S_j as the j th element of harmony **S** and the lower and upper bounds of the j th element is given by l_j and u_j , respectively. The function $random()$ generates a uniformly-distributed real random number in closed interval $[0, 1]$ [16]. Then, the eHSGA initializes fret width (fr), maximum number of improvisation (N_{IMP}), HM consideration rate (R_{HMC}), and pitch adjustment rate (par).
3. The R_{HMC} and par are key variables for regulating the execution and convergence speed to global maxima during a harmony search. Variable R_{HMC} is updated linearly and is decreasing with each iteration. At the same time, par is dynamically adapted to increase at linear values. Thus guaranteeing hybrid search method can expeditiously avoid converging at local maxima, and the solution reached is diverse.
4. The objective functions $C_{5pSE}(\cdot)$ calculated in (1) for 5pSE and $C_{cov}(\cdot)$ in (2) for coverage probability are used to compute the fitness of every harmony in the **HM**. Subsequently, the **HM** is sorted in descending order of best fitness. Thus ensuring the best-fit harmony member is always at the head node of the **HM**.
5. A new **HM** is generated using selection, crossover, and mutation mechanism. Then a merge rule is used to combine previously sorted **HM** and newly generated **HM** to form an elitist **HM**. This aspect of elitism is applied through each iterative process to obtain the optimal value of search space parameters defined in Table 5. Pseudocode describing the above step-by-step process is also described in Algorithm 3.

3.3 Time Complexity of Algorithms

The range and step size of individual search space parameters α_{mbs} , β_{mbs} , ρ_{mbs} , α_{pbs} , β_{pbs} , ρ_{pbs} , Υ_{pbs} , Υ_{uabs} , ρ_{uabs} is defined in Table 5, where (δ_x, δ_y) , $\delta_{\alpha_{mbs}}$, $\delta_{\beta_{mbs}}$, $\delta_{\rho_{mbs}}$, $\delta_{\alpha_{pbs}}$, $\delta_{\beta_{pbs}}$, $\delta_{\rho_{pbs}}$, $\delta_{\Upsilon_{pbs}}$, $\delta_{\rho_{uabs}}$, and $\delta_{\Upsilon_{uabs}}$ refer to the step sizes for (x_i, y_i) UABS 2D

location Cartesian coordinates, α_{mbs} , β_{mbs} , ρ_{mbs} , α_{pbs} , β_{pbs} , ρ_{pbs} , Υ_{pbs} , ρ_{uabs} , and Υ_{uabs} , respectively. The lower bounds for ρ_{mbs} , ρ_{pbs} , and ρ_{uabs} is given by $\rho_{\text{mbs}}^{\text{low}}$, $\rho_{\text{pbs}}^{\text{low}}$, and $\rho_{\text{uabs}}^{\text{low}}$, respectively and the upper bounds for ρ_{mbs} , ρ_{pbs} , and ρ_{uabs} is given by $\rho_{\text{mbs}}^{\text{high}}$, $\rho_{\text{pbs}}^{\text{high}}$, and $\rho_{\text{uabs}}^{\text{high}}$, respectively.

The time complexity of the brute-force approach with fixed UABS on hexagonal locations is deterministic and is a function of the search space parameters and their step size and range specified in Table 5 and is given by

$$\begin{aligned} & \mathcal{O}\left(\left(1/\delta_{\alpha_{\text{mbs}}} + 1\right) \times \left(1/\delta_{\beta_{\text{mbs}}} + 1\right) \times \left(\frac{\rho_{\text{mbs}}^{\text{high}} - \rho_{\text{mbs}}^{\text{low}}}{\delta_{\rho_{\text{mbs}}}}\right) \times \right. \\ & \left. \left(1/\delta_{\alpha_{\text{pbs}}} + 1\right) \times \left(1/\delta_{\beta_{\text{pbs}}} + 1\right) \times \left(\frac{\rho_{\text{pbs}}^{\text{high}} - \rho_{\text{pbs}}^{\text{low}}}{\delta_{\rho_{\text{pbs}}}}\right) \times \right. \\ & \left. \left(\frac{\Upsilon_{\text{pbs}}^{\text{high}}}{\delta_{\Upsilon_{\text{pbs}}}}\right) \times \left(\frac{\rho_{\text{uabs}}^{\text{high}} - \rho_{\text{uabs}}^{\text{low}}}{\delta_{\rho_{\text{uabs}}}}\right) \times \left(\frac{\Upsilon_{\text{uabs}}^{\text{high}}}{\delta_{\Upsilon_{\text{uabs}}}}\right)\right). \end{aligned}$$

whereas the time complexity of a meta-heuristic algorithm considered in this chapter is directly proportional to the dimension of the search problem, search variables defined in Table 5, the population size ($SZ_{\text{GA}}/SZ_{\text{HM}}$), and the complexity cost of $C_{\text{cov}}(\cdot)/C_{5\text{pSE}}(\cdot)$ objective functions. Given these dependencies, it is challenging to determine the time complexity of a meta-heuristic algorithm trying to converge to a true global maximum while addressing a multi-dimensional and multi-objective optimization problem. With limited time and iterations restrictions, the meta-heuristics algorithms do not always assure convergence at the true global maxima. Nonetheless, eHSGA considered in this chapter demonstrated a better convergence efficiency than GA in reaching global maxima, and the results are reviewed in the upcoming Sect. 5.5.

4 Aerial-HetNet Design Guidelines

For each base-stations in three-tier Aerial-HetNet, the 3D locations of MBS, PBS, and UABS are recorded in matrices $\mathbf{L}_{\text{uabs}} \in \mathbb{L}^{N_{\text{uabs}} \times 3}$, $\mathbf{L}_{\text{pbs}} \in \mathbb{L}^{N_{\text{pbs}} \times 3}$, and $\mathbf{L}_{\text{mbs}} \in \mathbb{L}^{N_{\text{mbs}} \times 3}$, respectively. In these matrices, N_{uabs} , N_{pbs} and N_{mbs} are the number of UABSs, PBSs, and MBSs within the geographical area of interest Area_{sim} . The 3D locations of GUEs and AUEs are recorded in \mathbf{L}_{gue} and \mathbf{L}_{aue} matrices, respectively. Using the distribution densities of Λ_{gue} , Λ_{aue} , Λ_{pbs} and Λ_{mbs} , the Cartesian coordinate distribution of wireless nodes GUE, AUE, PBS, and MBS are modeled using a 2D Poisson point process (PPP). However, the RF antenna altitude remains fixed for these wireless nodes. The UABS cartesian coordinates are either on fixed hexagonal locations or optimized using an GA or eHSGA heuristic algorithm. Meantime low-

altitude and medium-altitude deployment altitudes are considered [45]. Given in the Table 7 are the simulation values considered for deployment altitudes and distribution densities for each of the wireless nodes.

Given the simulation area of Area_{sim} , the aggregate number of users (AUEs and GUEs) within the Area_{sim} is given by N_{ue} . Within, Area_{sim} consider an arbitrary n th UE, with the nearest distance from the UABS-cell of interest (UOI) is d_{un} , picocell of interest (POI) is d_{pn} , and macrocell of interest (MOI) is d_{on} . The signal attenuation in Aerial-HetNet is addressed by considering a Nakagami- m fading channel. The influence of fading on reference symbol received power (RSRP) from base-station of interest, i.e., the UOI, POI, and MOI at the arbitrary n th UE is given by

$$\begin{aligned} P'_{\text{uabs}}(d_{un}) &= \frac{P_{\text{uabs}}^{\text{tx}} A_{3\text{DBF}}(\phi, \theta) F}{10^{\vartheta(d_{un})/10}}, \\ P'_{\text{pbs}}(d_{pn}) &= \frac{P_{\text{pbs}}^{\text{tx}} A_{3\text{DBF}}(\phi, \theta) F}{10^{\vartheta(d_{pn})/10}}, \\ P'_{\text{mbs}}(d_{on}) &= \frac{P_{\text{mbs}}^{\text{tx}} A_{3\text{DBF}}(\phi, \theta) F}{10^{\vartheta(d_{on})/10}}, \end{aligned} \quad (4)$$

where variables $\vartheta(d_{un})$, $\vartheta(d_{pn})$, and $\vartheta(d_{on})$ are path-loss in dB and respectively observed from UABS, PBS, and MBS. The probability density function (PDF) for Nakagami- m fading F is given by [10]

$$f_N(\psi, q) = \frac{q^q \psi^{q-1}}{\Gamma(q)} \exp(-q\psi), \quad (5)$$

where ψ is the channel amplitude, q is the shaping parameter, and $\Gamma(q)$ is the standard Gamma function given as $\Gamma(q) = \int_0^\infty \exp(-u) u^{q-1} du$. Using q , the received signal power can be approximated to suitable fading conditions in Aerial-HetNet. When the shaping value equals 1 approximates to Rayleigh fading along non-LOS (NLOS), and when the shaping value is greater than 1, Nakagami- m fading approximates to Rician fading along line-of-sight (LOS).

In a Cartesian coordinate, let θ and ϕ be the zenith and azimuth of the spherical angles and unit vectors. Then the transmitter antenna's 3DBF element $A_{3\text{DBF}}(\phi, \theta)$ specified in [1] is defined by

$$\begin{aligned} A_{3\text{DBF}}(\phi, \theta) &= G_{3\text{DBF},\text{max}} - \min \left\{ (A_{\text{Hor}}(\phi) + A_{\text{Ver}}(\theta)), A_m \right\}, \\ G_{3\text{DBF},\text{max}} &= 8 \text{ dBi}, A_m = 30 \text{ dB}, \end{aligned} \quad (6)$$

where $A_{\text{Ver}}(\theta)$ and $A_{\text{Hor}}(\phi)$ are the vertical and horizontal antenna elements of the radiation pattern, respectively, and are defined as

$$A_{\text{Ver}}(\theta) = -\min \left[12 \left(\frac{\theta - \theta_{\text{tilt}}}{\theta_{3\text{-dB}}} \right)^2, SLAV \right], \theta_{\text{tilt}} = 90^\circ, \quad (7)$$

$$\theta_{3\text{-dB}} = 65^\circ, SLAV = 30, \quad (8)$$

$$A_{\text{Hor}}(\phi) = -\min \left[12 \left(\frac{\phi}{\phi_{3\text{-dB}}} \right)^2, A_m \right], \phi_{3\text{-dB}} = 65^\circ.$$

3DBF is an interference coordination method that can significantly improve signal-to-interference ratio (SIR) of the desired signal by calibrating $P_{\text{mbs}}^{\text{tx}}$, $P_{\text{pbs}}^{\text{tx}}$, and $P_{\text{uabs}}^{\text{tx}}$ transmission powers from MBS, PBS, and UABS, respectively [36]. Regulating the transmission power brings significant improvements to SIR for the UEs located at cell-edge or UEs in range expanded regions and checks the power transmitted into the neighboring cell sites.

4.1 Path Loss Model

To accurately investigate the signal reliability in the public safety network in an urban environment, well-defined any-to-air (ATA), air-to-ground (ATG), and ground-to-ground (GTG) communication links are considered between interfacing base-station of interest (BOI) and UEs available.

4.1.1 ATA Communication Link

ATA Communication Link is considered when an aerial user (AUE) is scheduled on any of the nearest MOI, POI, or UOI. To address the power loss experienced during ATA communication in the Aerial-HetNet, an urban-macro with aerial (UMa-AV) scenario specified in 3GPP Release 15 [2] is considered. The NLOS and LOS path loss estimate of this 3D channel model is presented as

$$\vartheta(d) = \begin{cases} \vartheta^{\text{NLOS}}(d) = -17.5 + (46 - 7\log_{10}(h_{\text{aue}}))10\log_{10}(d_{3\text{Dist}}) \\ \quad + 20\log_{10}\left(\frac{40\pi f_{\text{psc}}}{3}\right) \\ \vartheta^{\text{LOS}}(d) = 28.0 + 22\log_{10}(d_{3\text{Dist}}) + 20\log_{10}(f_{\text{psc}}) \end{cases}, \quad (9)$$

where $d_{3\text{Dist}}$ is the 3D distance between AUE and the base-station of interest (BOI), f_{psc} is the carrier frequency in MHz, and h_{aue} is the altitude of AUE in meter such that $22.5\text{m} < h_{\text{aue}} \leq 300\text{m}$ for $\vartheta^{\text{LOS}}(d)$ and $10.0\text{m} < h_{\text{aue}} \leq 100\text{m}$ for $\vartheta^{\text{NLOS}}(d)$. Finally, the LOS probabilities is given by

$$\mathbb{P}_{\text{LOS}}(\vartheta) = \begin{cases} 1, & d_{2\text{Dist}} \leq \text{dist}_1 \\ \frac{\text{dist}_1}{d_{2\text{Dist}}} + \exp\left(\frac{-d_{2\text{Dist}}}{\text{par}_1}\right)\left(1 - \frac{\text{dist}_1}{d_{2\text{Dist}}}\right), & d_{2\text{Dist}} > \text{dist}_1 \end{cases}, \quad (10)$$

where $d_{2\text{Dist}}$ is the 2D distance between AUE and the BOI such that $d_{2\text{Dist}} \leq 4\text{km}$, and the factors $dist_1$ and par_1 (in meters) are given by

$$\begin{aligned} dist_1 &= \max(460\log_{10}(h_{\text{aue}}) - 700, 18). \\ par_1 &= 4300\log_{10}(h_{\text{aue}}) - 3800, \end{aligned}$$

In the UMa-AV scenario for ATA communication link, the average path loss over the probabilities of NLOS and LOS is calculated using (9) and (10); the average path loss is given by

$$PL^{\text{avg}} = \mathbb{P}^{\text{LOS}} \times \vartheta^{\text{LOS}} + (1 - \mathbb{P}^{\text{LOS}}) \times \vartheta^{\text{NLOS}}. \quad (11)$$

4.1.2 ATG Communication Link

ATG Communication Link is considered when a terrestrial user (GUE) camps on an aerial base station (UOI). Under this communication link, a more simplified NLOS and LOS path loss model specified in [5, 34, 37] is considered, and the path loss estimate given by

$$\vartheta_{\text{uabs}}(d) = \prod_{x=0}^y \left[1 - \exp\left(-\frac{[h_{\text{uabs}} - \frac{(x+1/2)(h_{\text{uabs}} - h_{\text{gue}})}{y+1}]^2}{2\Psi^2}\right) \right], \quad (12)$$

where h_{uabs} is the UABS altitude, $y = \text{floor}(r\sqrt{\zeta\xi} - 1)$, r is the ground distance between the GUE and UABS, ζ is the ratio of construction area to the total land area, ξ is given as *buildings/km²*, and Ψ is distribution of building altitude (B_H) in meter and is based on a Rayleigh distribution: $f(B_H) = \frac{B_H}{\Psi^2} \exp(-\frac{B_H^2}{2\Psi^2})$. The LOS probability $\mathbb{P}^{\text{LOS}}(\vartheta_{\text{uabs}})$ is simplified and considered as a continuous function of Θ , and environment factors. By approximating the environment factors, the Sigmoid function (S-curve) is simplified and the LOS probability is presented as

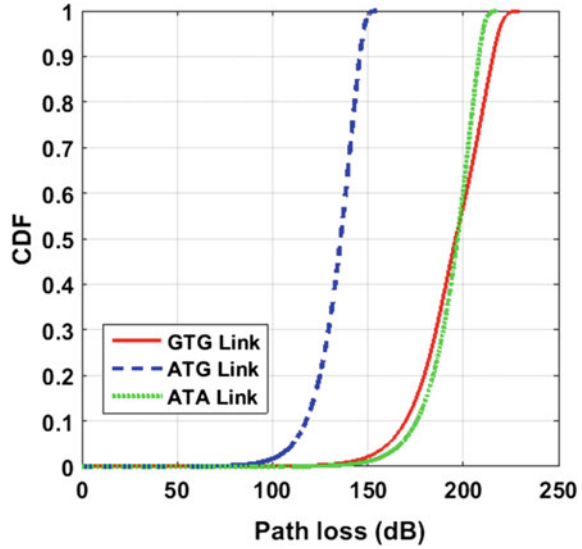
$$\mathbb{P}^{\text{LOS}}(\vartheta_{\text{uabs}}, \Theta) = \frac{1}{1 + p \exp(-q[\Theta - p])}, \quad (13)$$

where the S-curve is defined by parameters p and q .

4.1.3 GTG Communication Link

GTG communication link is considered when a terrestrial user (GUE) is scheduled on terrestrial MOI and POI. Okumura-Hata Path Loss (OHPL) is better suited for estimating the GTG communication link as the base-station altitude is constant [41, 71]. The path loss estimate using the Okumura-Hata model is given as

Fig. 6 CDF of the path loss values recorded between all base-stations and users scheduled in the public safety network



$$\vartheta(d) = U + V\log(d) + W, \quad (14)$$

where variables U , V , and W depends on frequency considered and antenna altitude of wireless node and is presented as

$$U = 69.55 + 26.16\log(f_{\text{psc}}) - 13.82\log(h_{\text{bs}}) - a(h_{\text{gue}}), \quad (15)$$

$$V = 44.9 + 6.55\log(h_{\text{bs}}), \quad (16)$$

$$a(h_{\text{gue}}) = \begin{cases} 8.29(\log(1.54h_{\text{gue}}))^2 - 1.1, & f_{\text{psc}} \leq 200 \text{ MHz} \\ 3.2(\log(11.75h_{\text{gue}}))^2 - 4.97, & f_{\text{psc}} \geq 200 \text{ MHz} \end{cases}, \quad (17)$$

$$W = 0 \quad (18)$$

where h_{gue} is the altitude of ground user in meter, f_{psc} is the PSC broadband frequency in MHz, and h_{bs} is the altitude of MBS (h_{mbs}) and PBS (h_{pbs}) in meter. The variable $a(h_{\text{gue}})$ and the factor C depends on the urban environment.

Using path loss model definition in (14)–(13), the cumulative distribution functions (CDFs) for the path loss observed is calculated over all the distances between base stations (\mathbf{L}_{uabs} , \mathbf{L}_{pbs} , and \mathbf{L}_{mbs}) and users (\mathbf{L}_{gue} and \mathbf{L}_{aue}). The path loss values in Fig. 6 reports distinct values for the maximum allowable path loss and are fundamentally due to the Aerial-HetNet environmental and NLOS/LOS experienced by

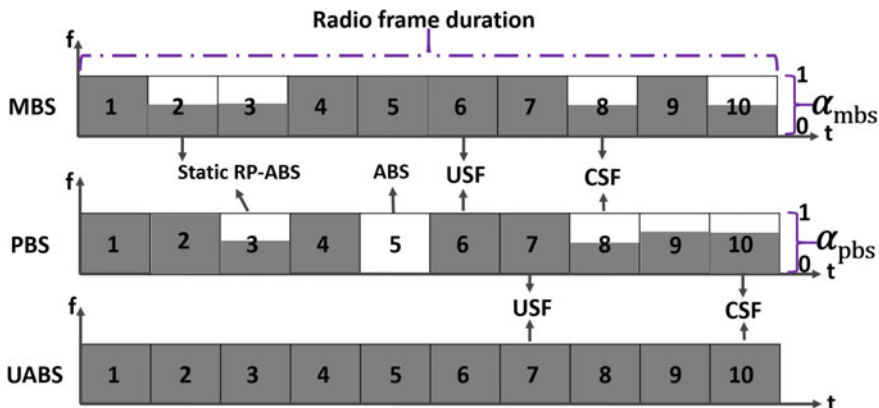


Fig. 7 Three-tier power reduction scheme applied to coordinate and uncoordinated LTE subframes at base-stations [43]

the users. From Fig. 6 it can be noted that the maximum path-loss experienced is 216 dB for ATA, 154 dB for ATG, and 255 dB for GTG link.

4.2 Inter-cell Interference Management in Aerial-HetNet

PBS and UABS illustrated in Fig. 1 are the small cell base-stations that have low transmission power and therefore can schedule fewer users compared to high-power MBSs. Applying positive REB specified in 3GPP Release 8, small cells can increase the cell capacity by extending the cell coverage and offloading traffic from overcrowded neighboring cell sites. However, applying REB also increases the SIR and interference at users located in the expanded cell region and at the cell edge. This issue of inter-cell interference is addressed by considering the ICIC mitigation schemes specified in 3GPP Release 10 and Release 11 [41, 43]. Using the ICIC at both MBS and PBS, the power levels of transmitting radio frames are reduced, as illustrated in Fig. 7.

Given the radio frames design in Fig. 7, the radio subframes transmitting with full power are tagged as uncoordinated subframes (USF) and radio subframes transmitting with reduced power as termed coordinated subframes (CSF). α_{mbs} is the power reduction factor applied to radio subframes at MBS and α_{pbs} at PBS. Specifically, when the power reduction factor $\alpha_{pbs} = 0$ and $\alpha_{mbs} = 0$ corresponds to eICIC specified in 3GPP Release 10, and the radio frames are referred to as almost blank subframes (ABS). The power reduction factor $\alpha_{mbs} = \alpha_{pbs} = 1$ corresponds to an absence of interference mitigation. Whereas, for $[0,1]$ open interval values i.e., $0 < \alpha_{mbs} < 1$ and $0 < \alpha_{pbs} < 1$, the power reduction factor corresponds to FeICIC specified in 3GPP Release 11 and radio frames are referred as reduced power sub-

frames. The reduced power subframes defined in Fig. 7 are designed to guard specific UABS radio subframes against transmit power from all other base stations and guard specific PBS subframes against MBS transmit power. The duty cycle of USF, and CSF radio subframes are coordinated using β_{pbs} and $(1 - \beta_{\text{pbs}})$ at PBS and β_{mbs} and $(1 - \beta_{\text{mbs}})$ at MBS. The user scheduling information, radio subframes' duty cycle, and power reduction strategy are shared over the X2 interconnecting interface.

The implementation of interference mitigation using ICIC techniques at every base-station reduces the interference into neighboring cell sites; however, it decreases the desired SIR at the users scheduled on cell-edge or in range expanded region. Consequently, to increase the desired SIR at these scheduled users, 3DBF is considered at all transmitting base-station to narrow the beamforming and restrict the power transmission at scheduled users [36].

4.3 Cell Selection, User Association, and Handover

Using the knowledge of interference mitigation using ICIC techniques defined across all 3GPP Releases and the design for reduced power CSF and USF specified in Fig. 7, the SIR experienced by the arbitrary n th user scheduled in either CSF or USF of base-stations of interest is defined in Table 6. Let $\Gamma_{\text{usf}}^{\text{mbs}}$, $\Gamma_{\text{csf}}^{\text{mbs}}$, $\Gamma_{\text{usf}}^{\text{pbs}}$, $\Gamma_{\text{csf}}^{\text{pbs}}$, $\Gamma_{\text{usf}}^{\text{uabs}}$, and $\Gamma_{\text{csf}}^{\text{uabs}}$ be the SIRs experienced by the users scheduled in the CSF or USF radio subframes of base-station of interest. In Table 6, \mathbf{I}_{agg} is the aggregate interference experienced at scheduled users from all base stations, except the base-stations of interest.

The process of cell selection uses the SIR definition given in Table 6 for each BOI and positive REB Υ_{uabs} at UABSs and Υ_{pbs} at PBSs. The positive REB Υ_{uabs} at UABSs and Υ_{pbs} at PBSs is applied to increase the SIR coverage. A user is always scheduled in the BOI that guarantees the best SIR experience during the cell selection process. After the cell selection process, an UABS-UE (UUE), PBS-UE (PUE), and MBS-UE (MUE) would be scheduled in either coordinated or uncoordinated radio subframes based on the scheduling threshold ρ_{uabs} , ρ_{pbs} , and ρ_{mbs} at UABS, PBS, and

Table 6 Shannon capacity definitions in terms of SIR and RSRP for USF/CSF radio frames

SIR ratio	Shannon capacity
$\Gamma_{\text{usf}}^{\text{mbs}} = \frac{R_{\text{mbs}}(d_{on})}{R_{\text{pbs}}(d_{pn}) + R_{\text{uabs}}(d_{un}) + \mathbf{I}_{\text{agg}}}$	$C_{\text{usf}}^{\text{mbs}} = \frac{\beta_{\text{mbs}} \log_2(1 + \Gamma_{\text{usf}}^{\text{mbs}})}{N_{\text{usf}}^{\text{mbs}}}$
$\Gamma_{\text{csf}}^{\text{mbs}} = \frac{\alpha R_{\text{mbs}}(d_{on})}{\alpha_{\text{pbs}} R_{\text{pbs}}(d_{pn}) + R_{\text{uabs}}(d_{un}) + \mathbf{I}_{\text{agg}}}$	$C_{\text{csf}}^{\text{mbs}} = \frac{(1 - \beta_{\text{mbs}}) \log_2(1 + \Gamma_{\text{csf}}^{\text{mbs}})}{N_{\text{csf}}^{\text{mbs}}}$
$\Gamma_{\text{usf}}^{\text{pbs}} = \frac{R_{\text{pbs}}(d_{pn})}{R_{\text{mbs}}(d_{on}) + R_{\text{uabs}}(d_{un}) + \mathbf{I}_{\text{agg}}}$	$C_{\text{usf}}^{\text{pbs}} = \frac{\beta_{\text{pbs}} \log_2(1 + \Gamma_{\text{usf}}^{\text{pbs}})}{N_{\text{usf}}^{\text{pbs}}}$
$\Gamma_{\text{csf}}^{\text{pbs}} = \frac{\alpha_{\text{pbs}} R_{\text{pbs}}(d_{pn})}{\alpha R_{\text{mbs}}(d_{on}) + R_{\text{uabs}}(d_{un}) + \mathbf{I}_{\text{agg}}}$	$C_{\text{csf}}^{\text{uabs}} = \frac{(1 - \beta_{\text{pbs}}) \log_2(1 + \Gamma_{\text{csf}}^{\text{uabs}})}{N_{\text{csf}}^{\text{uue}}}$
$\Gamma_{\text{usf}}^{\text{uabs}} = \frac{R_{\text{uabs}}(d_{un})}{R_{\text{mbs}}(d_{on}) + R_{\text{pbs}}(d_{pn}) + \mathbf{I}_{\text{agg}}}$	$C_{\text{usf}}^{\text{mbs}} = \frac{(\beta_{\text{mbs}} + \beta_{\text{pbs}}) \log_2(1 + \Gamma_{\text{usf}}^{\text{uabs}})}{N_{\text{usf}}^{\text{uue}}}$
$\Gamma_{\text{csf}}^{\text{uabs}} = \frac{R_{\text{uabs}}(d_{un})}{\alpha R_{\text{mbs}}(d_{on}) + \alpha_{\text{pbs}} R_{\text{pbs}}(d_{pn}) + \mathbf{I}_{\text{agg}}}$	$C_{\text{csf}}^{\text{uabs}} = \frac{(2 - (\beta_{\text{mbs}} + \beta_{\text{pbs}})) \log_2(1 + \Gamma_{\text{csf}}^{\text{uabs}})}{N_{\text{csf}}^{\text{uue}}}$

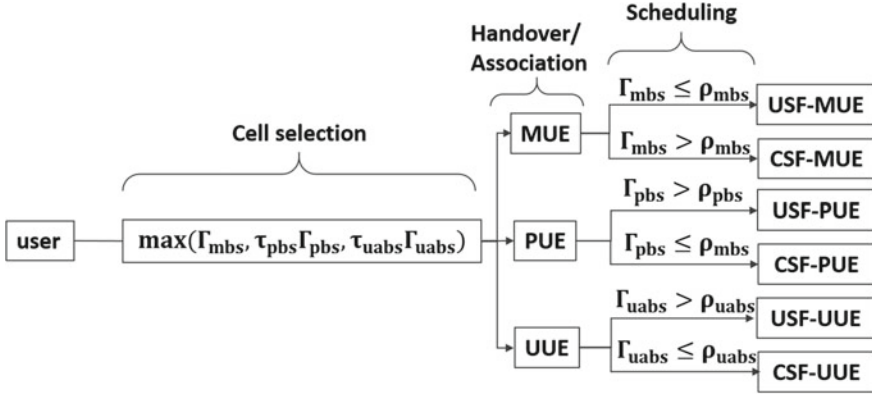


Fig. 8 Cell selection, association, and handover of users in coordinate and uncoordinated radio subframes at base-stations in Aerial-HetNet

MBS, respectively. This course of cell selection and user scheduling in CSF or USF and user handover to base-station of interest are summarized in Fig. 8.

Once the n th arbitrary user is scheduled in BOI i.e., either UOI, POI, or MOI and is assigned in USF or CSF radio subframes. Then using the SIR definitions, Shannon capacity of a user scheduled in the CSF and USF subframes is given by $C_{\text{usf}}^{\text{mbs}}$, $C_{\text{csf}}^{\text{mbs}}$, $C_{\text{usf}}^{\text{pbs}}$, $C_{\text{csf}}^{\text{pbs}}$, $C_{\text{usf}}^{\text{uabs}}$, and $C_{\text{csf}}^{\text{uabs}}$. In Table 6, $N_{\text{usf}}^{\text{uue}}$, $N_{\text{csf}}^{\text{uue}}$, $N_{\text{usf}}^{\text{pue}}$, $N_{\text{csf}}^{\text{pue}}$, $N_{\text{usf}}^{\text{mue}}$, and $N_{\text{csf}}^{\text{mue}}$ are the number of UUEs, PUEs, and MUEs scheduled in CSF or USF of the UABS, PBS, and PBS, respectively. Finally, the definition of these capacity equation are given in Table 6.

5 Simulation Results

The following section of the chapter reviews and compares the performance of the KPIs when UABSs are deployed on different practical altitudes of 50 m, 36 m, and 25 m. Additionally, the comparative analysis of the two KPIs is extended to Aerial-HetNet applying ICIC and without ICIC while considering eHSGA, GA, and brute-force algorithms. To this end, KPIs are evaluated using Matlab-based computer simulation, and the system parameters values specified in Table 7.

5.1 Brute Force for KPI Evaluation

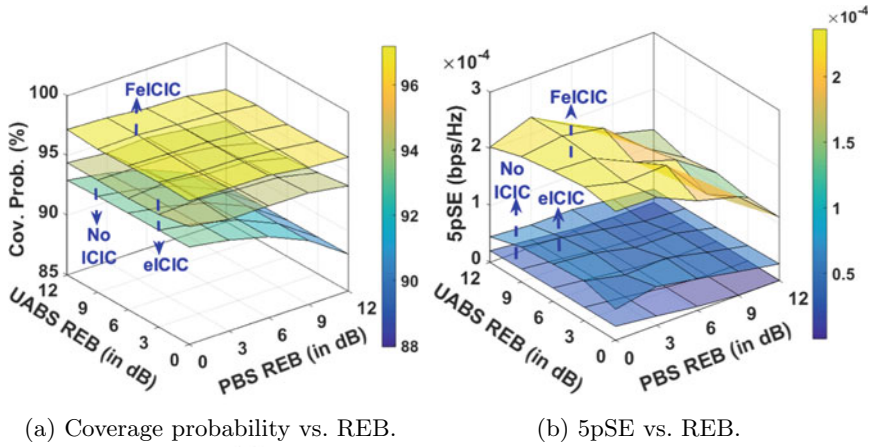
Aerial-HetNet performance when the UABS are deployed on fixed hexagonal locations and at altitudes of 50 m, 36 m, and 25 m is plotted in Figs. 11, 10, and 9. The

Table 7 System parameters and the values considered during simulation

System parameter	Value/Range
PSC broadband frequency	763 MHz (downlink)
Area of Simulation	100 km ²
Base station densities MBS	4 km ²
Base station densities PBS	12 km ²
Number of UABS	60
User densities AUE	1.8 per km ²
User densities GUE	100 km ²
Transmission power P_{mbs}^{tx}	46 dBm
Transmission power P_{pbs}^{tx}	30 dBm
Transmission power P_{uabs}^{tx}	26 dBm
UABS deployment altitude	25, 36, and 50 m
Base station altitude PBS	15m
Base station altitude MBS	36m
AUE altitude	22.5 m
GUE altitude	1.5 m
Power reduction at MBS α_{mbs}	closed interval [0, 1]
Power reduction at PBS α_{pbs}	closed interval [0, 1]
Duty cycle for uncoordinated subframe β_{mbs}	closed interval [0%, 100%]
Duty cycle for uncoordinated subframe β_{pbs}	closed interval [0%, 100%]
UUEs scheduling threshold ρ_{uabs}	-5 dB to 5 dB
PUEs scheduling threshold ρ_{pbs}	-10 dB to 10 dB
MUEs scheduling threshold ρ_{mbs}	20 dB to 40 dB
REB Υ_{pbs} at PBS, Υ_{uabs} at UABS	0 dB to 12 dB
GA (SZ_{GA}) and eHSGA (SZ_{HM}) population size	60
GA crossover(cxr) and mutation (mr) probabilities	0.7 and 0.1
GA generation number	100
HM fret (fr)	1
HM consideration rate (R_{HMC})	max = 0.8, min = 0.2
HM pitch adjustment rate (par)	max = 0.8, min = 0.4

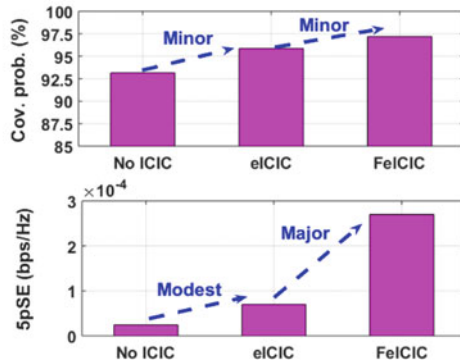
plotted results show the influence of positive REB at PBSs along the x-axis, UABSs along the y-axis, and KPI outcome along the z-axis.

Given the UABSs deployment at an altitude of 25m lower than MBS altitude, 36m same altitude as MBS altitude, and 50m higher than MBS altitude, the Aerial-HetNet with FeICIC experiences minor improvement in coverage probability and a significant improvement in 5pSE over other ICIC techniques and in the absence of ICIC as seen in Figs. 9c, 10c, and 11c. In particular, from Figs. 9, 10 and 11, it can



(a) Coverage probability vs. REB.

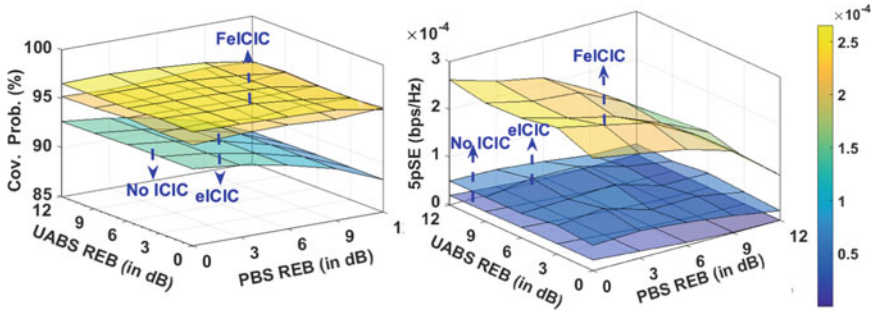
(b) 5pSE vs. REB.



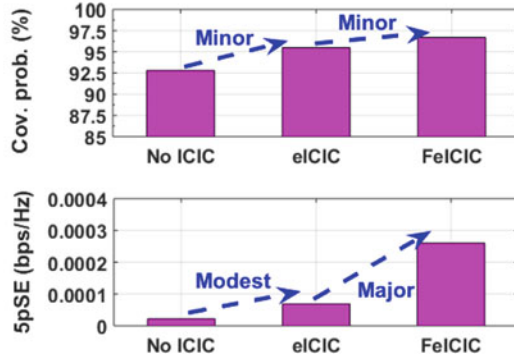
(c) KPI performance comparison.

Fig. 9 Aerial-HetNet performance when the UABS deployment locations are fixed on hexagonal locations and at an altitude of 25 m

be concluded that the overall peak performance of the Aerial-HetNet is when the UABS deployment is at a low altitude of 25 m. Increasing the positive REB at UABS and PBS increases the users associated with these small cells but also increases the interference. Therefore the applying optimal REB values at these small base stations is the key. Using the brute-force approach, the improved coverage probability is observed when UABS considers moderate to higher REB values between 3 and 12 dB, but low to moderate REB values of 0–6 dB is observed at PBS. Similarly, the peak values of 5pSE are observed for moderate to higher REB values between 3 and 12 dB at UABS and lower to moderate REB values between 3 and 6 dB at PBS.



(a) Coverage vs. REB. (b) 5pSE vs. REB.



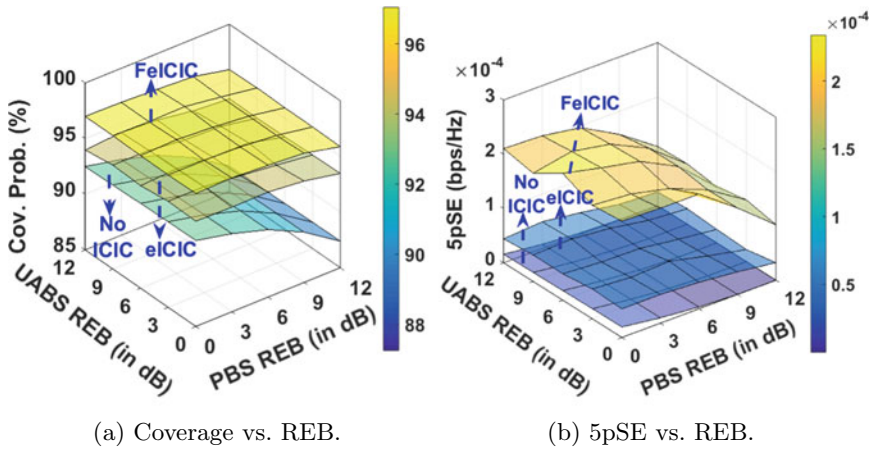
(c) KPI performance comparison.

Fig. 10 Aerial-HetNet performance when the UABS deployment locations are fixed on hexagonal locations and at an altitude of 36 m

5.2 Genetic Algorithm for KPI Evaluation

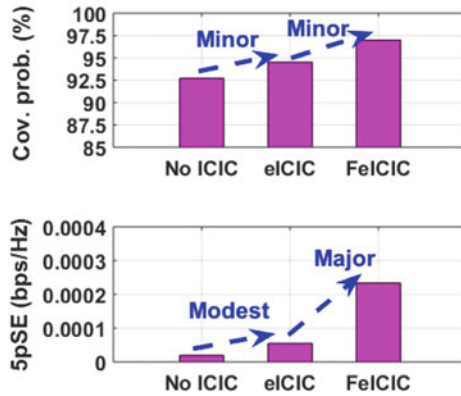
Aerial-HetNet performance is outlined in Fig. 12; the results demonstrate the influence of positive REB at PBSs along the x-axis, and UABSs along the y-axis, and KPI outcome along the z-axis. In particular, the result analysis was done when ICIC system parameters and UABS 2D locations are jointly optimized using the GA approach. The critical remarks are presented when the UABSs are deployed at an altitude of 25m lower than MBS altitude, 36m similar altitude as MBS elevation, and 50m higher than MBS altitude.

In the following, Fig. 12b, d, f capturing the comparative analysis from results in Fig. 12a, c, e, the Aerial-HetNet with FeICIC experiences modest improvement in coverage probability and a significant improvement in 5pSE over other ICIC techniques and in the absence of ICIC. In particular, from Fig. 12a, c, e, it can be concluded that the overall peak performance of the Aerial-HetNet is when the UABS deployment altitude is 25 m. Furthermore, increasing the positive REB at UABS and PBS increases the users associated with these small cells but also increases



(a) Coverage vs. REB.

(b) 5pSE vs. REB.



(c) KPI performance comparison.

Fig. 11 Aerial-HetNet performance when the UABS deployment locations are fixed on hexagonal locations and at an altitude of 50 m

the interference. Therefore the applying optimal REB values at these small base stations is the key. Using GA, the improved coverage probability is noted when UABS considers moderate REB values between 3 and 6 dB, but REB at PBS varies significantly between 0 and 12 dB. Similarly, the peak values of 5pSE are observed for moderate REB values between 3 and 6 dB at UABS and lower REB values between 0 and 3 dB at PBS.

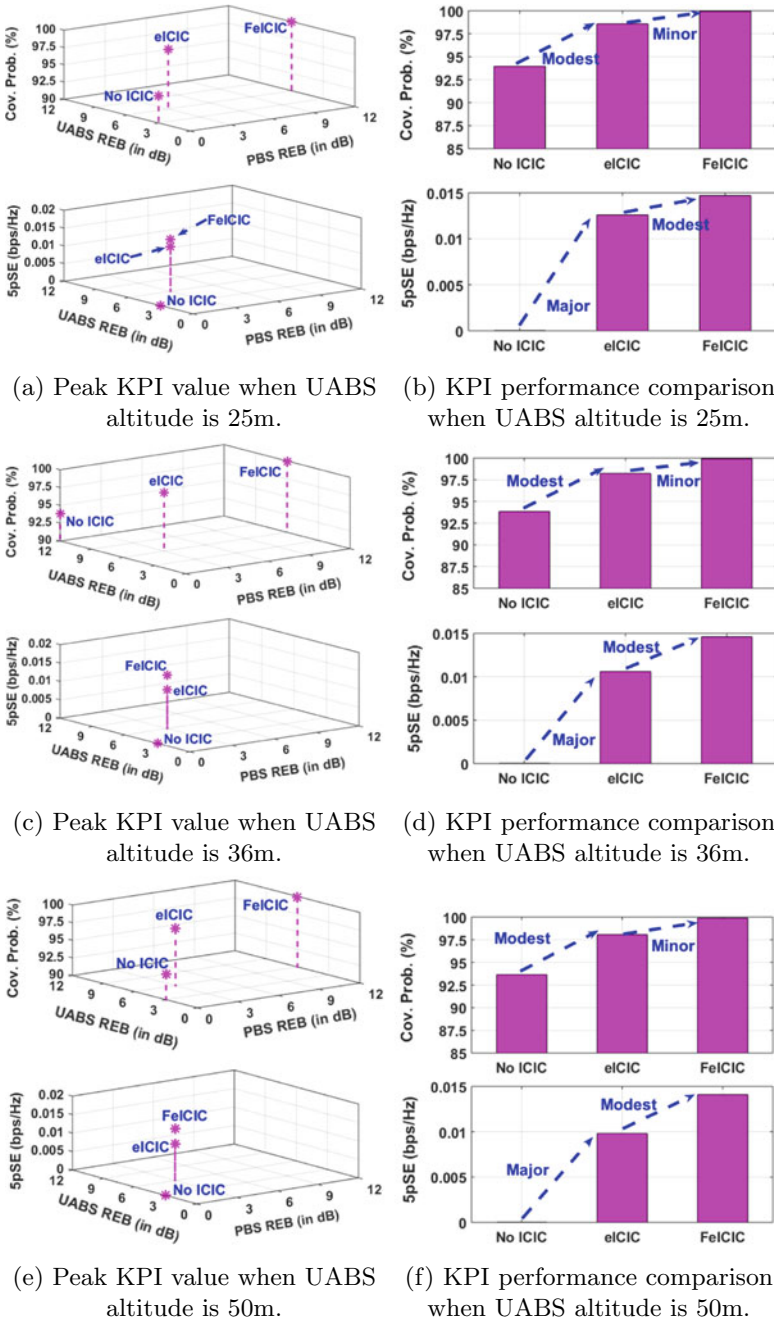


Fig. 12 Aerial-HetNet performance when the UABS deployment altitude is manually varied to 50 m, 36 m, and 25 m, and their locations are optimized in 2D using GA

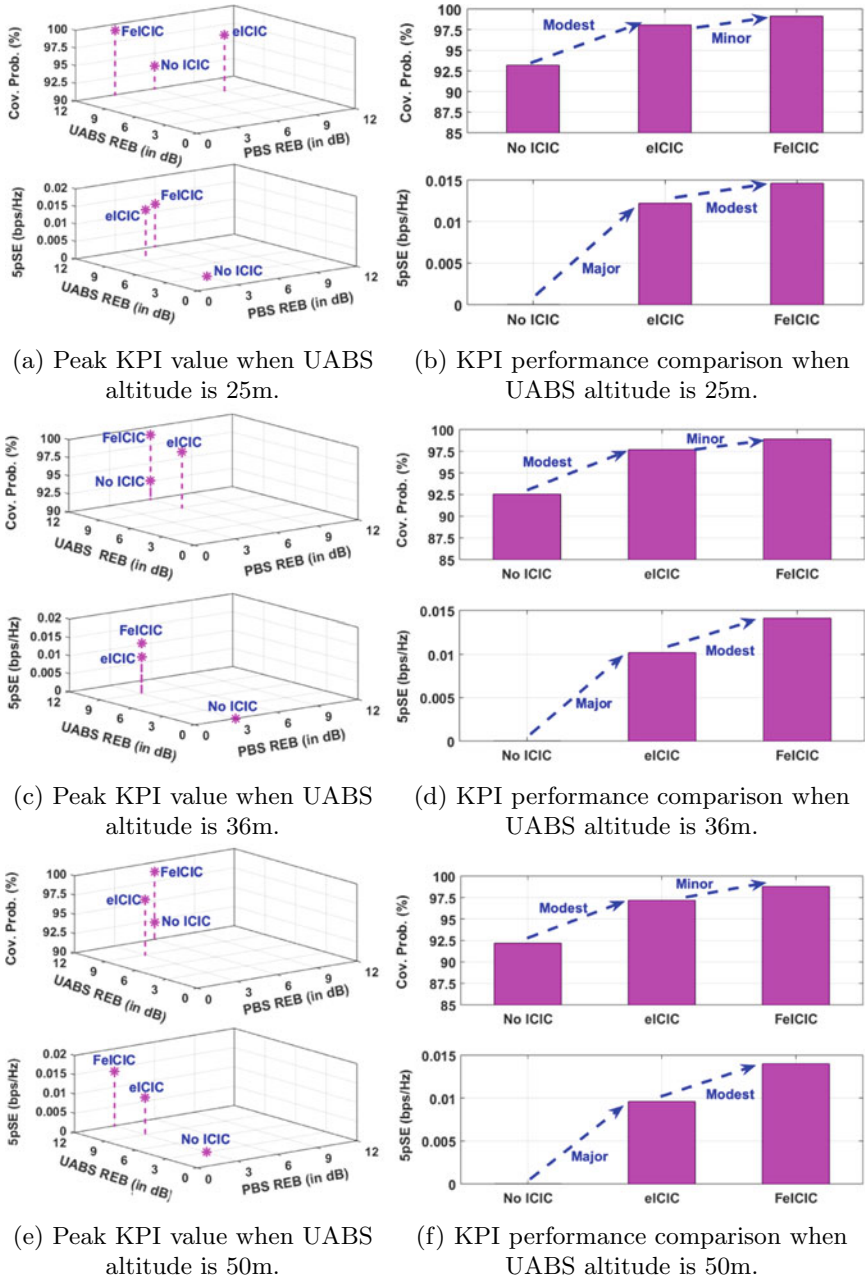


Fig. 13 Aerial-HetNet performance when the UABS deployment altitude is manually varied to 50 m, 36 m, and 25 m, and their locations are optimized in 2D using eHSGA

5.3 *eHSGA for KPI Evaluation*

Aerial-HetNet performance outlined in Fig. 13, the results demonstrate the influence of positive REB at PBSs along the x-axis, and UABSs along the y-axis, and KPI outcome along the z-axis. In particular, the result analysis was done when ICIC system parameters and UABS 2D locations are jointly optimized using the eHSGA approach. The key observations are made when the UABSs are deployed at an altitude of 25m lower than MBS altitude, at 36m, i.e., the same altitude as MBS, and 50m, which is higher than MBS.

In the following, Fig. 13b, d, f capturing the comparative analysis from results in Fig. 13a, c, e, the Aerial-HetNet with FeICIC experiences modest improvement in coverage probability and a significant improvement in 5pSE over other ICIC techniques and in the absence of ICIC. In particular, from Fig. 13a, c, e, it can be concluded that the overall peak performance of the Aerial-HetNet is when the UABS deployment altitude is 25 m. Furthermore, increasing the positive REB at UABS and PBS increases the users associated with these small cells but also increases the interference. Therefore the applying optimal REB values at these small base stations is the key. Using eHSGA, the improved coverage probability is noted when UABS considers higher REB values between 9 and 12 dB but moderate REB values between 3 – 9dB at PBS. Similarly, for the peak values of 5pSE, the REB at UABS values vary significantly between 0 and 12 dB, and lower REB values between 3 and 6 dB at PBS are considered.

5.4 *Comparative Analysis of KPIs*

From the analysis of Figs. 9, 10, 11, 12, and 13 given in Sects. 5.1, 5.2, and 5.3, the Aerial-HetNet with reduced power FeICIC in 3GPP Release 11 is seen to surpass other ICIC techniques and in the absence of ICIC with respect to overall coverage probability and 5pSE. Furthermore, closer inspection of Figs. 9, 10, 11, 12, and 13 and the results captured in Tables 9, and 8 confirms that the eHSGA and GA heuristic techniques outperform the brute-force approach and show significant improvement in 5pSE and coverage probability. Furthermore, the GA meta-heuristic technique achieved a marginal gains of up to 3% in 5pSE and coverage probability over the hybrid eHSGA optimization technique.

Using the optimization approach considered in this chapter, the Aerial-HetNet demonstrates peak performance when UABSs deployment altitude is 25 m, i.e., lower than any terrestrial base-station altitude. As the UABS deployment altitude is increased to 36 m and 50 m, which is higher than any terrestrial base-station altitude considered in Table 7, there is a gradual decrease in performance of coverage probability and 5pSE of the Aerial-HetNet. This is because a higher deployment altitude of UABS improves LOS and also the ability to associate more users. However, the improved LOS also increases the possibility of interference with users on cell-edge

Table 8 Summary of peak coverage probability in %, for different UABSs altitudes and interference coordination approaches

	Brute-force			GA			eHSGA		
	UABS Altitude			UABS Altitude			UABS Altitude		
ICIC	50 m	36 m	25 m	50 m	36 m	25 m	50 m	36 m	25 m
FeICIC	96.72	96.99	97.18	99.89	99.92	99.94	98.78	98.90	99.14
eICIC	94.52	95.62	95.85	98.06	98.24	98.58	97.17	97.69	97.89
No ICIC	92.71	92.86	93.15	93.64	93.83	93.95	92.19	92.54	93.19

Table 9 Summary of peak 5pSE values in bps/kHz, for different UABSs altitudes and interference coordination approaches

	Brute force			Genetic algorithm			eHSGA		
	UABS Altitude			UABS Altitude			UABS Altitude		
ICIC	50 m	36 m	25 m	50 m	36 m	25 m	50 m	36 m	25 m
FeICIC	$0.23e - 3$	$0.24e - 3$	$0.27e - 3$	$1.41e - 2$	$1.46e - 2$	$1.48e - 2$	$1.40e - 2$	$1.41e - 2$	$1.46e - 2$
eICIC	$0.55e - 4$	$0.69e - 4$	$0.70e - 4$	$0.98e - 2$	$1.06e - 2$	$1.26e - 2$	$0.96e - 2$	$1.02e - 2$	$1.22e - 2$
No ICIC	$1.92e - 5$	$2.21e - 5$	$2.45e - 5$	$3.44e - 5$	$3.53e - 5$	$4.01e - 5$	$1.98e - 5$	$2.30e - 5$	$2.63e - 5$

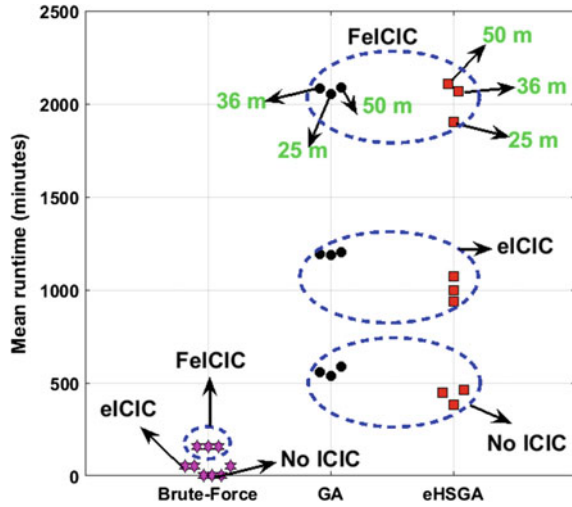
and in range expanded region, which could degrade the network level performance of the Aerial-HetNet.

Finally, in Tables 9 and 8, the peak 5pSE values in bps/kHz and coverage probability in % have been summarized for different UABSs deployment altitudes and interference mitigation schemes; while considering elitist hybridization harmonic search genetic algorithm, genetic algorithm, and brute force.

5.5 Computational Complexity Gain Analysis

Given the best state (\mathbf{BS}_{KPI}) definition in (3), algorithms given in Algorithms 1–3, and the simulation values specified in Table 7; a Matlab-based simulation is used to evaluate an individual KPI. Then the *mean runtime* is calculated from the Monte-Carlo simulation to determine the computational complexity gains. The comparative analysis of computational complexity gains is presented when the UABSs are deployed at different altitudes of 50m, 36m, and 25m, using eHSGA, GA, and brute-force approach, and in the presence of ICIC and absence of ICIC. The *mean runtime* needed for computing the peak KPI values with global maxima values of ICIC parameters and optimal 2D UABS locations is plotted in Fig. 14.

Fig. 14 Summary of KPI computational time, for different UABS altitudes and when 2D locations are optimized using different techniques



An initial review of Fig. 14 suggested that UABS deployed at a higher altitude of 50m require sparse to slightly higher computational time when compared to deployment altitude of 25 and 36. This higher computational time is needed to address the interference effects of better LOS from 50m altitude. Additional analysis of Fig. 14 reveals that joint optimization of 2D UABS locations and ICIC system parameters using the heuristic approach (eHSGA and GA) requires significantly higher computational time compared to the brute-force approach. This higher computational time is required for determining the best set of UABS locations L_{uabs} within a large search space A_{sim} . Whereas, the brute approach considers optimizing only the ICIC parameters while the UABS locations were fixed on a hexagonal grid. Similar observations were deduced while employing the reduced power FeICIC technique, which requires significantly higher computational time when compared to other ICIC techniques and in the absence of any ICIC. This increased computational time is mainly due to the step size of α_{mbs} and α_{pbs} within the closed interval as seen in Table 5, which expands the scope of the search space during simulation.

Finally, the computational complexity required to determine the optimal values to search parameters defined in the Table 5 is higher using heuristic algorithms (eHSGA and GA) but is capable of delivering broadband rates that could support mission-critical voice and data. The stringent requirement of 95% terrestrial coverage with broadband rates [49] for the public safety network could be met using the heuristic algorithms as reported in Table 8. From Fig. 14, Tables 8, and 9, it is observed that 3D optimal placement of UABS in the Aerial-HetNet is critical to improving the overall gains. Further analysis from Fig. 14, Tables 8, and 9, shown that eHSGA gives limited computational complexity gain over GA. Whereas GA has displayed marginal improvement in KPI gains over eHSGA. Therefore it becomes crucial to determine a suitable algorithm that could minimize the computational complexity and find the near-global maxima of the search problem in the real world.

Table 10 Summary of problem definition, application, and convergence KPI of various heuristic algorithms

Heuristic algorithm	Problem definition	Convergence characteristics
Nearest-neighbor	Data routing in D2D Networks	Accuracy [6]
Genetic algorithm	Terrestrial base-station deployment planning	Accuracy [43]
Elitist harmony search genetic algorithm	Restoring cellular infrastructure	Execution time [43]
Swarm intelligence	Search and localization of a mobile RF source	Accuracy and execution time [38]
Tabu search	Real-time dispatch of first-responders	Accuracy and execution time [24]
Genetic algorithm	Real-time dispatch of first-responders	Accuracy [13]
Hybrid genetic-simulated annealing	Data routing in D2D Networks	Accuracy and execution time [57]
Random Forest	Post-disaster localization and mapping of survivors	Accuracy and execution time [3]
Support Vector Machines	Post-disaster localization and mapping of survivors	Accuracy and execution time [73]

The entire postulation of proposing a heuristic algorithm is based on trade-offs, basically trading accuracy for computation time and vice-versa. However, given the problem definition and applications, convergence KPI of a heuristics can be adjusted to suit the requirements accordingly. The following Table 10 summarizes the problem definition, application, and convergence KPI of a heuristic algorithm.

6 Conclusion

This chapter investigated the fitness of different algorithms for finding optimal or close to the optimal 2D UAV locations. Based on the comparative analysis of the brute-force approach and the heuristic algorithm considered, it becomes essential to determine a suitable algorithm that could address the trade-off of minimizing the computational complexity and finding the near-global maxima of the search problem.

Using the system-level insight into designing the 5G Aerial-HetNet, low-altitude aerial vehicles were integrated into an existing terrestrial network as aerial users and aerial base stations. The UABS altitude variation contributed towards important design considerations such as interference mitigation, antenna 3D beamforming, and practical path loss model based on the type of user and base-station communication link. Using these design considerations and the Monte-Carlo approach, the simulation goal was to improve the coverage probability and 5pSE of the Aerial-HetNet using brute-force and heuristics algorithms.

Simulation and comparative analysis of results concluded that the Aerial-HetNet with UABS deployment altitude of 25 m performed sparsely better than deployment altitudes of 36 m and 50 m. The interference mitigation mechanisms considered for Aerial-HetNet attested that the reduced power subframes FeICIC generated better network 5pSE and coverage experiences than the other ICIC techniques and in the absence of ICIC. Lastly, the simulations results confirmed that the heuristic algorithms (eHSGA and GA) surpassed the brute force approach to accomplish practical peak values of 5pSE and coverage.

References

1. 3GPP (2017) Study on 3D channel model for LTE (Release 12). Technical Specification Group Radio Access Network 36.873, 3rd Generation Partnership Project (3GPP), version 12.7.0
2. 3GPP (2017) Study on Enhanced LTE Support for Aerial Vehicles (Release 15). Technical Specification Group Radio Access Network 36.777, 3rd Generation Partnership Project (3GPP), version 15.0.0
3. Acuna V, Kumbhar A, Vattapparamban E, Rajabli F, Guvenc I (2017) Localization of wifi devices using probe requests captured at unmanned aerial vehicles. In: Proceedings of IEEE wireless communication network conference (WCNC), San Francisco, CA, pp 1–6
4. Adam N, Tapparelo C, Heinzelman W, Yanikomeroglu H (2021) Placement optimization of multiple uav base stations. In: Proceedings of IEEE wireless communications and networking conference (WCNC), Nanjing, China, pp 1–7
5. Al-Hourani A, Kandeepan S, Lardner S (2014) Optimal LAP altitude for maximum coverage. *IEEE Wirel Commun Lett* 3(6):569–572
6. Alemayehu TS, Kim JH (2017) Efficient nearest neighbor heuristic tsp algorithms for reducing data acquisition latency of UAV relay WSN. *Wirel Pers Commun* 95(3):3271–3285
7. Ali K, Nguyen HX, Vien QT, Shah P, Raza M (2020) Deployment of drone-based small cells for public safety communication system. *IEEE Syst J* 14(2):2882–2891
8. Amorim R, Nguyen H, Wigard J, Kovács IZ, Sørensen TB, Biro DZ, Sørensen M, Mogensen P (2018) Measured uplink interference caused by aerial vehicles in LTE cellular networks. *IEEE Wirel Commun Lett* 7(6):958–961
9. AT&T (2017) Flying COW Connects Puerto Rico. Technical report. https://about.att.com/inside_connections_blog/flying_cow_puertori
10. Azari MM, Rosas F, Chiumento A, Pollin S (2017) Coexistence of terrestrial and aerial users in cellular networks. In: Proceedings of IEEE global communication conference, Singapore, pp 1–6
11. Bayerlein H, Theile M, Caccamo M, Gesbert D (2020) Uav path planning for wireless data harvesting: a deep reinforcement learning approach. In: Proceedings of IEEE global communications conference, pp 1–6
12. Bejiga MB, Zeggada A, Nouffidj A, Melgani F (2017) A convolutional neural network approach for assisting avalanche search and rescue operations with UAV imagery. *Remote Sens* 9(2):100
13. Benyahia I, Potvin JY (1998) Decision support for vehicle dispatching using genetic programming. *IEEE Trans Syst Man Cybernet-Part A: Syst Hum* 28(3):306–314
14. Van der Bergh B, Chiumento A, Pollin S (2016) LTE in the sky: trading off propagation benefits with interference costs for aerial nodes. *IEEE Commun Mag* 54(5):44–50
15. Binol H, Bulut E, Akkaya K, Guvenc I (2018a) Time optimal multi-UAV path planning for gathering its data from roadside units. In: Proceedings of IEEE 88th vehicular technology conference (VTC-Fall), Chicago, IL, USA, pp 1–5
16. Binol H, Guvenc I, Bulut E, Akkaya K (2018) Hybrid evolutionary search method for complex function optimisation problems. *IET Electron Lett* 54(24):1377–1379

17. Bor-Yaliniz RI, El-Keyi A, Yanikomeroglu H (2016) Efficient 3-D placement of an aerial base station in next generation cellular networks. In: Proceedings of IEEE international conference on communication (ICC), Kuala Lumpur, Malaysia, pp 1–5
18. Challita U, Saad W, Bettstetter C (2019) Interference management for cellular-connected UAVs: a deep reinforcement learning approach. *IEEE Trans Wirel Commun* 18(4):2125–2140
19. Chandrasekharan S, Gomez K, Al-Hourani A, Kandeepan S, Rasheed T, Goratti L, Reynaud L, Grace D, Bucaille I, Wirth T et al (2016) Designing and implementing future aerial communication networks. *IEEE Commun Mag* 54(5):26–34
20. Cherif N, Jaafar W, Yanikomeroglu H, Yongacoglu A (2020) On the optimal 3D placement of a UAV base station for maximal coverage of UAV users. In: Proceedings of IEEE global communication conference (GLOBECOM), Taipei, Taiwan, pp 1–6
21. Christy E, Astuti RP, Syihabuddin B, Narottama B, Rhessa O, Rachmawati F (2017) Optimum UAV flying path for Device-to-Device communications in disaster area. In: Proceedings of IEEE international conference signal system (ICSigSys), Bali, Indonesia, pp 318–322
22. CNBC (2018) AT&T and Verizon drones provide cell service in natural disasters. Technical report. <https://www.cnbc.com/2018/06/22/att-and-verizon-drones-provide-cell-service-in-natural-disasters.html>
23. Cui J, Shakhathreh H, Hu B, Chen S, Wang C (2018) Power-efficient deployment of a UAV for emergency indoor wireless coverage. *IEEE Access* 6:73200–73209
24. Dewinter M, Vandeviver C, Vander Beken T, Witlox F (2020) Analysing the police patrol routing problem: A review. *ISPRS Int J Geo-Inf* 9(3):157
25. Do-Duy T, Nguyen LD, Duong TQ, Khosravirad S, Claussen H (2021) Joint optimisation of real-time deployment and resource allocation for UAV-aided disaster emergency communications. *IEEE J Sel Areas Commun* 39(11):3411–3424
26. Dong J, Ota K, Dong M (2021) UAV-based real-time survivor detection system in post-disaster search and rescue operations. *IEEE J Miniatur Air and Space Syst*
27. Fouda A, Ibrahim AS, Güvenc İ, Ghosh M (2019) Interference management in UAV-assisted integrated access and backhaul cellular networks. *IEEE Access* 7:104553–104566
28. Gao XZ, Govindasamy V, Xu H, Wang X, Zenger K (2015) Harmony search method: theory and applications. *Computational intelligence and neuroscience* 2015
29. Gibbs C (2017) Verizon claims largest small cell deployment in the U.S. *Fierce Wireless*. <http://www.fiercewireless.com/wireless/verizon-claims-largest-small-cell-deployment-u-s-carrier>
30. Hanna S, Yan H, Cabric D (2019) Distributed UAV placement optimization for cooperative line-of-sight MIMO communications. In: Proceedings of IEEE international conference on acoustics, speech, and signal processing (ICASSP), Brighton, UK, pp 4619–4623
31. Heisler Y (2016) AT&T wants to use drones to improve its LTE network. *Yahoo Tech News*. <https://www.yahoo.com/tech/t-wants-drones-improve-lte-network-193203323.html>
32. Hu S, Ni W, Wang X, Jamalipour A, Ta D (2020) Joint optimization of trajectory, propulsion, and thrust powers for covert UAV-on-UAV video tracking and surveillance. *IEEE Trans Inf Forens Sec* 16:1959–1972
33. Huang Z, Chen C, Pan M (2020) Multiobjective UAV path planning for emergency information collection and transmission. *IEEE Internet of Things J* 7(8):6993–7009
34. ITU (2003) Propagation data and prediction methods required for the design of terrestrial broadband millimetric radio access systems. Technical specification ITU Radiocommunication Assembly P.1410-2, International Telecommunication Union (ITU)
35. Kaleem Z, Yousaf M, Qamar A, Ahmad A, Duong TQ, Choi W, Jamalipour A (2019) UAV-empowered disaster-resilient edge architecture for delay-sensitive communication. *IEEE Netw* 33(6):124–132
36. Kammoun A, Khanfir H, Altman Z, Debbah M, Kamoun M (2014) Preliminary results on 3D channel modeling: from theory to standard. *IEEE J Sel Areas Commun (JSAC)* 32(6):1219–1229
37. Khawaja W, Guvenc I, Matolak D, Fiebig UC, Schneckenberger N (2019) A survey of air-to-ground propagation channel modeling for unmanned aerial vehicles. *IEEE Commun Surv Tuts* 21:2361–2391

38. Koohifar F, Kumbhar A, Guvenc I (2017) Receding horizon multi-UAV cooperative tracking of moving RF source. *IEEE Commun Lett* 21(6):1433–1436
39. Kulkarni S, Chaphekar V, Chowdhury MMU, Erden F, Guvenc I (2020) UAV aided search and rescue operation using reinforcement learning. In: *Proceedings of IEEE SoutheastCon*, Raleigh, NC, USA, vol 2, pp 1–8
40. Kumbhar A, Koohifar F, Guvenc I, Mueller B (2016) A survey on legacy and emerging technologies for public safety communications. *IEEE Commun Surv Tuts* 18:97–124
41. Kumbhar A, Güvenç I, Singh S, Tuncer A (2018) Exploiting LTE-Advanced HetNets and FeICIC for UAV-assisted public safety communications. *IEEE Access* 6:783–796
42. Kumbhar A, Binol H, Guvenc I, Akkaya K (2019) Interference coordination for aerial and terrestrial nodes in three-tier LTE-advanced HetNet. In: *Proceedings of IEEE radio wireless symposium (RWS)*, Orlando, FL, pp 1–4
43. Kumbhar A, Binol H, Singh S, Güvenç I, Akkaya K (2020) Heuristic approach for jointly optimising FEICIC and UAV locations in multi-tier LTE-advanced public safety HetNet. *IET Commun* 14(20):3585–3598
44. Li P, Xu J (2018) Placement optimization for UAV-enabled wireless networks with multi-hop backhauls. *Springer J Commun Inf Netw* 3(4):64–73
45. Liu C, Ding M, Ma C, Li Q, Lin Z, Liang YC (2018) Performance analysis for practical unmanned aerial vehicle networks with LoS/NLoS transmissions. In: *Proceedings of IEEE International Conference on Communication Workshops (ICC Workshops)*, Kansas City, MO, pp 1–6
46. Menouar H, Guvenc I, Akkaya K, Uluagac AS, Kadri A, Tuncer A (2017) UAV-enabled intelligent transportation systems for the smart city: applications and challenges. *IEEE Commun Mag* 55(3):22–28
47. Merwaday A, Tuncer A, Kumbhar A, Guvenc I (2016) Improved throughput coverage in natural disasters: unmanned aerial base stations for public-safety communications. *IEEE Veh Technol Mag* 11(4):53–60
48. Miyano K, Shinkuma R, Shiode N, Shiode S, Sato T, Oki E (2020) Multi-UAV allocation framework for predictive crime deterrence and data acquisition. *Internet of Things* 11:100205
49. Moore LK (2014) The first responder network (FirstNet) and next-generation communications for public safety: issues for congress. *Congressional Research Service*
50. Mozaffari M, Saad W, Bennis M, Debbah M (2016) Optimal transport theory for power-efficient deployment of unmanned aerial vehicles. In: *Proceedings of IEEE International Conference on Communication (ICC)*, Kuala Lumpur, Malaysia, pp 1–6
51. Mozaffari M, Kargali ATZ, Saad W, Bennis M, Debbah M (2018) Beyond 5G with UAVs: foundations of a 3D wireless cellular network. *IEEE Trans Wirel Commun* 18(1):357–372
52. Narang M, Xiang S, Liu W, Gutierrez J, Chiaraviglio L, Sathiseelan A, Merwaday A (2017) UAV-assisted edge infrastructure for challenged networks. In: *Proceedings of IEEE Conference on Computer and Communications Workshops (INFOCOM Workshop)*, Atlanta, GA, pp 60–65
53. Nguyen KK, Vien NA, Nguyen LD, Le MT, Hanzo L, Duong TQ (2020) Real-time energy harvesting aided scheduling in UAV-assisted d2d networks relying on deep reinforcement learning. *IEEE Access* 9:3638–3648
54. Niu H, Gonzalez-Prelcic N, Heath RW (2018) A UAV-based traffic monitoring system-invited paper. In: *Proceedings of IEEE Vehicular Technology Conference (VTC Spring)*, Porto, Portugal, pp 1–5
55. Panda KG, Das S, Sen D (2020) Efficient UAV placement strategy for guaranteed QoS demand. In: *Proceedings of IEEE 92nd Vehicular Technology Conference (VTC2020-Fall)*, Victoria, BC, Canada, pp 1–5
56. Peer M, Bohara VA, Srivastava A (2020) Multi-UAV placement strategy for disaster-resilient communication network. In: *Proceedings of IEEE 92nd Vehicular Technology Conference (VTC2020-Fall)*, Victoria, BC, Canada, pp 1–7
57. Rahimunnisa K (2019) Hybridized genetic-simulated annealing algorithm for performance optimization in wireless adhoc network. *J Soft Comput Paradig (JSCP)* 1(01):1–13

58. Rupasinghe N, Yapıcı Y, Güvenç I, Kakishima Y (2019) Non-orthogonal multiple access for mm wave drone networks with limited feedback. *IEEE Trans Commun* 67(1):762–777
59. Sabzehali J, Shah VK, Dhillon HS, Reed JH (2021) 3D placement and orientation of mmWave-based UAVs for guaranteed LoS coverage. *IEEE Wirel Commun Lett*
60. Saputro N, Akkaya K, Uluagac S (2018) Supporting Seamless Connectivity in Drone-assisted Intelligent Transportation Systems. In: *Proceedings of IEEE Local Computer Networks Workshops (LCN Workshops)*, Chicago, IL, pp 110–116
61. Schedl DC, Kurmi I, Bimber O (2021) An autonomous drone for search and rescue in forests using airborne optical sectioning. *Sci Robot* 6(55)
62. Shakoor S, Kaleem Z, Do DT, Dobre OA, Jamalipour A (2020) Joint optimization of UAV 3d placement and path loss factor for energy efficient maximal coverage. *IEEE Internet of Things J*
63. Sharafeddine S, Islambouli R (2019) On-demand deployment of multiple aerial base stations for traffic offloading and network recovery. *Elsevier Comput Netw* 156:52–61
64. Sharma V, Bennis M, Kumar R (2016) UAV-assisted heterogeneous networks for capacity enhancement. *IEEE Commun Lett* 20(6):1207–1210
65. Singh S, Kumbhar A, Güvenç I, Sichitiu ML (2019) Distributed Approaches for Inter-cell Interference Coordination in UAV-based LTE-Advanced HetNets. In: *Proceedings of IEEE 88th Vehicular Technology Conference (VTC-Fall)*, Chicago, IL, pp 1–6
66. Sun Y, Wang T, Wang S (2018) Location optimization for unmanned aerial vehicles assisted mobile networks. In: *Proceedings of IEEE International Conference on Communications (ICC)*, Kansas City, MO, pp 1–6
67. The Drive (2018) AT&T and Verizon Test 4G LTE Drones in New Jersey. Technical report. <https://www.thedrive.com/tech/21756/att-and-verizon-test-4g-lte-drones-in-new-jersey>
68. The Drive (2018) Drone Saves Man’s Life From Kilauea Volcano Disaster in Hawaii. Technical report. <http://www.thedrive.com/tech/21276/drone-saves-mans-life-from-kilauea-volcano-disaster-in-hawaii>
69. Viana J, Cercas F, Correia A, Dinis R, Sebastião P (2021) MIMO relaying UAVs operating in public safety scenarios. *Drones* 5(2):32
70. Xia W, Semkin V, Mezzavilla M, Loianno G, Rangan S (2020) Multi-array designs for mmwave and sub-thz communication to uavs. In: *Proceedings of IEEE 21st International Workshop on Signal Processing Advances in Wireless Communications (SPAWC)*, pp 1–5
71. Xiro Online (2017) Okumura-Hata. Technical report. <https://www.xiro-online.com/help/en/okumurahata.html>
72. Xu X, Duan L, Li M (2018) UAV placement games for optimal wireless service provision. In: *WiOpt*, pp 1–8
73. Zagajewski B, Kluczek M, Raczko E, Njegovec A, Dabija A, Kycko M (2021) Comparison of random forest, support vector machines, and neural networks for post-disaster forest species mapping of the krkonoše/karkonosze transboundary biosphere reserve. *Remote Sens* 13(13):2581
74. Zhang Q, Mozaffari M, Saad W, Bennis M, Debbah M (2018a) Machine learning for predictive on-demand deployment of UAVs for wireless communications. In: *Proceedings of IEEE Global Communication Conference (GLOBECOM)*, Abu Dhabi, United Arab Emirates, pp 1–6
75. Zhang Q, Saad W, Bennis M, Lu X, Debbah M, Zuo W (2018b) Predictive deployment of UAV base stations in wireless networks: machine learning meets contract theory. [arXiv:1811.01149](https://arxiv.org/abs/1811.01149)

Power-Efficient UAV Placement in Relay Assisted Heterogeneous Public Safety Networks



Yasir Iqbal, Ayaz Ahmad, and Zeeshan Kaleem

Abstract During the disaster situation, there is a vital need for public safety communications to enable mission-critical search and rescue operations. In public safety networks, key challenge is to provide reliable and flexible wireless coverage to the affected areas. Unmanned aerial vehicles (UAVs) can act as aerial base station (BS) to provide the emergency communication services. Battery life of UAVs is a scarce resource that requires UAV BS transmit power optimization. To overcome this issue, a model which consist of fixed BS, observation UAV and relay UAV is adopted to enable long distance communication. The optimal placement of relay UAV becomes requisite for reliable connectivity between observation UAV and ground BS. In this chapter, our objective is to minimize the sum-power of observation and relay UAVs by using the optimal placement of relay UAV. The optimized power ensure throughput requirement for real-time communication. The proposed formulated non-convex problem is transformed into convex optimization problem, and the optimal solution is acquired using interior point method. The simulation result shows that the required targeted link-rate between relay UAV and observation UAV and also between relay UAV and ground BS is achieved at minimum sum power.

Keywords Overage enhancement · Heterogeneous networks · Public safety communications · Unmanned aerial vehicles (UAVs)

Y. Iqbal · A. Ahmad (✉) · Z. Kaleem
Department of Electrical and Computer Engineering, COMSATS University Islamabad, Wah
Campus, Wah Cantonment, Pakistan
e-mail: ayaz.uet@gmail.com

Z. Kaleem
e-mail: zeeshankaleem@ciitwah.edu.pk

© The Author(s), under exclusive license to Springer Nature Singapore Pte Ltd. 2022
Z. Kaleem et al. (eds.), *Intelligent Unmanned Air Vehicles Communications for Public Safety Networks*, Unmanned System Technologies,
https://doi.org/10.1007/978-981-19-1292-4_4

1 Introduction

Public safety networks have attracted researchers' attention because of their numerous applications during natural disasters such as earthquakes, tsunamis, and floods [1–3]. To enable emergency services, unmanned air vehicles act as an aerial base station (ABS) as it can easily meet the requirements of mobility, reliability, flexibility, and adaptive altitude [4]. Specifically, UAVs are emerging as a promising technology to monitor the disastrous areas by enhancing the coverage and capacity of wireless cellular networks [5].

To ensure a sustainable data rate for broadband real-time pervasive communications, efficient UAV placement is required to minimize the total transmit power of UAVs [6, 7]. In [8], the authors minimize the number of ABS required to provide wireless coverage for a group of distributed ground terminals, while ensuring that each terminal is within the communication range of at least one UAV. In [9], the main goal was to serve the maximum number of users by ABS with minimum transmit power to reduce the traffic demands of malfunctioned macro base station (BS). In [10], backhaul-aware optimal 3D placement of UAV is achieved by two approaches; user-centric and network-centric. In [11], the author proposed a heuristic algorithm that guarantees the quality-of-service (QoS) requirements of the targeted users by maximizing the minimum number of UAVs.

In [12], the authors proposed a 3D placement of UAVs that jointly optimize the height and path loss compensation factor. The proposed algorithm successfully reduces co-channel interference by varying UAV heights. In [13] author introduced attractive features of UAVs and their promising on-demand applications in the field of public safety communication. The author proposed a multi-layered network architecture that incorporates UAVs in public safety communication. In [14], UAV-aided disaster emergency communications is considered and a framework for joint optimisation of resource allocation and real-time UAV deployment has been proposed. The work in [15], proposes a deep reinforcement learning based approach for real-time energy harvesting aided scheduling in UAV-Assisted D2D Networks. In [16], UAV-empowered disaster-resilient edge architecture for delay-sensitive communication has been devised. In [17], particle swarm optimization algorithm is employed to perform 3D optimal surveillance trajectory Planning for multiple UAVs while taking the surveillance area priority into account. In [18] author describes the system model for UAV-enabled coordinate multipoint (CoMP) where the users may move on the ground, therefore the UAVs need to adjust their locations with respect to the user locations over time to maximize the network throughput. The work in [19] proposes an optimal 3D deployment of three UAV-base stations, these UAVs BS act as aerial access points for energy-efficient uplink communication in a given urban area.

The authors of [20] used an iterative method to jointly optimize the transmission power of Internet-of-things (IoT) devices and the altitudes of UAVs. The author also proposed an algorithm based on an improved k-means clustering method, where each cluster subgroup should have roughly the same number of IoT devices. In [21] author considered a system model of a cellular network consisting of an ABS coexisting

with multiple terrestrial base stations. A probabilistic channel-based model is used to design the 3D placement for the ABS and the transmit power allocation for all the nodes in the uplink (UL), downlink (DL), and combined UL and DL operations.

In [22], a latency aware drone BS placement is carried to enhance the QoS in a heterogeneous communication network. In [23], the authors formulate an optimization problem to connect multiple UAVs to the small BSs to enhance the sum rate of the overall network. The authors in [24] propose an architecture to form a composite heterogeneous network made up of several homogeneous networks. The basic purpose is to exploit drones to facilitate connectivity in a composite heterogeneous network. In [25], the mobility of UAV is catered for data gathering of sensor devices. It jointly optimizes the uplink power of sensors due to the optimal placement of UAVs.

The authors in [26] aim to deploy a robust system consist of quadcopter for environment remote monitoring to measure the fluctuating parameters. The authors in [27] model an optimization problem to minimize the number of deployed UAVs for gathering critical information from environmental sensors, and deliver it to the ground BS.

The main focus of this work is to ensure reliable wireless connectivity in disastrous areas. In that area, to establish a ground-based network in a short period is a difficult task. Therefore, our system model presents a UAV network that consists of observation UAV, relay UAV, and ground BS to provide connectivity of users in the affected area. In this heterogeneous network, relay UAV connects observation UAV and ground BS for real-time data transmission over longer distances. In a dynamic propagation environment, relay placement must be optimized to ensure end-to-end reliable communications. We propose an efficient algorithm for optimal placement of relay UAVs. This placement will be utilized to minimize the total power consumption of observation and relay UAVs. The parameters related to the observation area (e.g., area size, the distance between observation UAV and ground BS) and signal attenuation due to obstacles are also considered in the system model.

We performed the network performance evaluation by comprehensive simulations and analysis by varying different network parameters such as area size, the distance between a base station and observation area, and signal attenuation by obstacles (e.g., buildings, trees).

The rest of the chapter is organized as follows: We presented the system model of the proposed heterogeneous network in Sect. 2. Section 3 presents the proposed methodology for the optimal placement of relay UAVs for heterogeneous public safety communication networks. Section 4 highlights system parameters, numerical results, and analysis. Finally, we conclude and present future directions in Sect. 5.

2 System Model

In disaster-hit areas, the existing communication networks are damaged or even devastated which creates communication holes. Therefore, it is not possible for remaining ground BSs to provide cellular services in a disastrous area. It is also not feasible

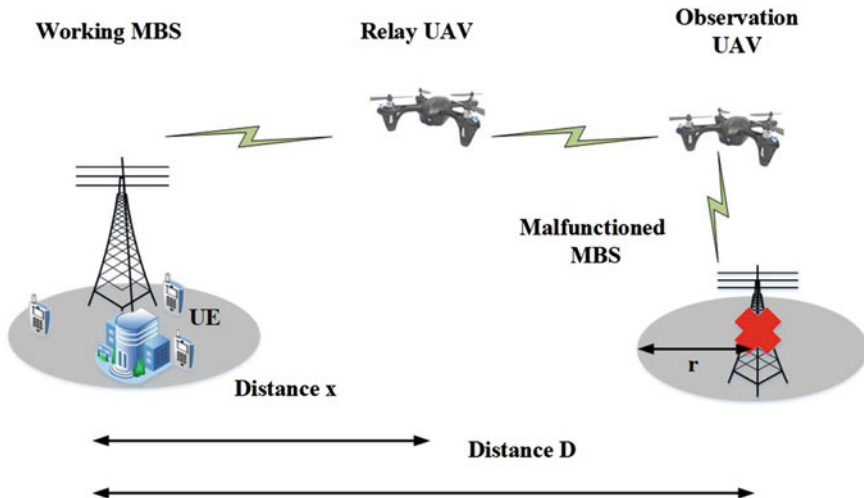


Fig. 1 System model

to install ground infrastructure in the affected area in a short time. Hence, we proposed a system model that consists of UAVs to serve as ABS in the disaster-hit areas as shown in Fig. 1. It comprises remote ground BS, observation UAV, and relay UAV.

Here, observation UAV monitors users in a circular region of radius r , termed as the observation area. The observation UAV transmits data to the nearby functional BS in real-time, but its communication range is limited. Therefore, to enable reliable data transmission, we placed the relay UAV between the observation UAV and nearby functional BS for reliable data transmission. The distance between ground BS and relay UAV is labeled as x , and distance between ground BS and observation UAV is denoted as D . The observation UAV moves in the assigned observation area to continuously gather the required information. It then transmits the information to the relay UAV positioned between observation UAV and ground BS. By using relay UAV, it is possible to transmit the real-time data to a longer distance.

The location of the relay UAV is always outside the radius of the observation area. Moreover, there are a lot of impediments between the BS, relay UAV, and observation UAV. These obstacles relatively attenuate the transmitted signal power. Therefore, we need to cater for this attenuation. When wireless infrastructure is malfunctioning, UAVs' battery life has major role in enabling communication services in the affected areas with ample flight time. Hence, to achieve the fidelity of mission-critical information, power consumption is the limiting factor. The link rate between the BS and relay UAV or between relay UAV and observation UAV is calculated by Shannon Theorem as follows:

$$R_r = B \log_2(1 + \gamma_r), \quad (1)$$

$$R_{GB} = B \log_2(1 + \gamma_{GB}), \quad (2)$$

where R_r is the link rate between relay UAV and observation UAV, R_{GB} is the link rate between nearby functional BS and relay UAV and B is the communication bandwidth. γ is the signal-to-noise ratio (SNR). To ensure a target link rate, we obtain the corresponding target SNR by optimizing the sum-power.

The SNR (γ_r) of relay UAV and observation UAV using Friis path loss model can be represented as

$$\gamma_r = \left(\frac{\lambda}{4\pi x} \right)^2 \frac{G_t G_r P_r}{N} \quad (3)$$

where λ is the wavelength of the transmitted signal, d is the transmission distance, G_t is the transmit antenna gain, G_r is the receiver antenna gain, N is the noise power, and P_r is the transmitted power. Let $g_r = \left(\frac{\lambda}{4\pi x} \right)^2 \frac{G_t G_r}{N}$ be the gain among the relay UAV and BS. So, Eq. (3) can be written as

$$\gamma_r = P_r g_r. \quad (4)$$

Similarly, for observation UAV, we can calculate the SNR as

$$\gamma_{obs} = \left(\frac{\lambda}{4\pi(D+r-x)} \right)^2 \frac{G_t G_r P_o}{N} (1 - A), \quad (5)$$

where A is the attenuation rate due to obstacles between the observation UAV and relay UAV. Where P_o is the transmitted power of observation UAV. Let $g_o = \left(\frac{\lambda}{4\pi(D+r-x)} \right)^2 \frac{G_t G_r}{N} (1 - A)$, so (5) can be represented as

$$\gamma_{obs} = P_o g_o, \quad (6)$$

where g_o is the channel gain between observation UAV and relay UAV. Thus, the achievable link rate depends upon the channel gain and SNR.

3 Power Efficient Optimal Placement of Relay UAV

3.1 Optimization Model

The main objective is to find the relay UAV optimal location that can minimize the sum power of observation and relay UAV to achieve the targeted link data rate R subject to various constraints. Therefore, the optimization problem is formulated as:

$$\min \quad (P_o + P_r) \quad (7)$$

$$\text{s.t. } B \log_2(1 + P_o g_o) \geq R \quad (8)$$

$$B \log_2(1 + P_r g_r) \geq B \log_2(1 + P_o g_o) \quad (9)$$

$$x \leq (D - r) \quad (10)$$

$$D \geq 10r \quad (11)$$

$$(P_o, P_r, D, x) \geq 0 \quad (12)$$

In the proposed optimization problem (7)–(12), our target is to minimize the sum power of observation UAV and relay UAV while satisfying the constraints (8)–(12). Constraints in (8) and (9) ensures that the link transmission rate between observation UAV and relay UAV should be greater than or equal to the required data rate R . The constraint in (10) guarantees that the relay UAV is placed outside the coverage area of observation UAV. The constraint in (11) force that the network size D is 10 times greater than the radius r of the observation area, so that network size is relatively large as compared to the observation area. Finally, the last constraint (12) highlights that the parameters P_o , P_r , x and D are non-negative.

3.2 Proposed Methodology

To optimize the defined problem in (7), we assume that the link rates of observation UAV and relay UAV are equal to the link rate between relay UAV and ground BS. This allows us to convert non-convex optimization problem into convex optimization problem. In order to determine the optimal solution, we equate the constraints in (9), and rewrite them as:

$$B \log_2(1 + P_r g_r) = B \log_2(1 + P_o g_o) \quad (13)$$

By simplification, we get

$$P_o g_o = P_r g_r \quad (14)$$

To find the received power at the relay UAV, we rearrange (14) as

$$P_r = \frac{P_o g_o}{g_r} \quad (15)$$

Using (8), we assume that $B \log_2(1 + P_o g_o)$ is equal to target data rate R . Thus, the power is calculated as

$$P_o = \frac{2^{\frac{R}{B}} - 1}{g_o} \quad (16)$$

Now, define C_o and C_r as:

$$C_r = \left(\frac{\lambda}{4\pi} \right)^2 \frac{G_t G_r P_t}{N} \quad (17)$$

$$C_o = \left(\frac{\lambda}{4\pi} \right)^2 \frac{G_t G_r P_t}{N} (1 - A) \quad (18)$$

Now Eq. (3) becomes:

$$g_r = \frac{C_o}{x^2} \quad (19)$$

Now Eq. (5) becomes:

$$g_o = \frac{C_o}{(D + r - x)^2} \quad (20)$$

Now, put g_o and g_r from (19) and (20) in (15) and (16) to get P_o and P_r . Finally, use P_o and P_r in the objective function to get the equivalent objective function in (16). This objective problem now becomes as given by:

$$\min k[(C_o + C_r)x^2 - 2C_r(D + x) + C_r(D + x)^2] \quad (21)$$

where $k = \frac{2^{\frac{R}{B}} - 1}{C_o} C_r$. The equivalent optimization problem in (21) is convex. This convex problem is solved using Interior point polynomial algorithm [28]. We propose an iterative algorithm for power efficient optimal relay UAV placement as given in Algorithm 1. As we solve the problem (21) by using Interior point polynomial method [28], the computational complexity of Algorithm 1 is very low and the solution is suited for practical systems with limited computational resources.

Input: $A, B, R, N, r, \lambda, G_t, G_o$

Output: P_t, P_o

1 Optimal placement of relay UAV

Obtain x by solving problem (21) by polynomial time integer point method [28]

2 Obtain g_r using (19)

3 Obtain g_o using (20)

4 Relay UAV power calculation

Obtain P_r by using (15)

5 Observation UAV power calculation

Obtain P_o by using (16)

6 Find sum power using steps 4 and 5

Table 1 Simulation parameters

Parameter	Specifications
Bandwidth (B)	20 MHz
Wavelength (λ)	0.125 m
Noise power (N)	1×10^{-10} W
TX antenna gain (G_t)	1
RX antenna gain (G_r)	1

4 Simulation Results and Analysis

4.1 Simulation Settings

Table 1 presents the parameters used in the simulations. For this simulation, 2.4 GHz frequency band is used for UAV communications. Bandwidth is set to 20 MHz as per wireless communication standards such as IEEE 802.11g/n and wavelength of 0.125 m is computed from 2.4 GHz frequency. Moreover, Noise power is fixed to 1×10^{-10} W, transmitter and receiver antenna gains are set to unity. We assume the usage of non-directional antennas in this evaluation.

Table 2 shows the analysis of optimized sum power for $A = 0.3$, $D/r = 10$ and $R = 800$ kbps.

4.2 Simulation Results

Firstly, the parameters related to observation area are varied to analyze the simulation results. Initially, network dimension parameter D is varied and D/r ratio is fixed to 10. Figure 2 shows the simulation results by varying network dimensions for fixed D/r ratio.

The performance metric in these curves is the optimized minimum power. These results are simulated for three different attenuation factors A , as shown in this Fig. 2. The numerical values of the results are formulated in Table 2.

It can be observed from these results that optimized sum power is minimum for $A = 0.3$. As parameter A increases, the optimized sum power increases correspondingly to achieve the target of link rate between relay UAV and observation UAV, and also between relay UAV and ground BS.

Figure 3 shows the advantage of optimal relay placement by varying network dimensions for fixed D/r ratio set to 10. The performance metric in these curves is the optimized minimum power. These results are simulated for $A = 0.6$. It is obvious from these results that sum power is largest when no relay is employed. For fixed relay placement, the performance of optimized sum power improves as compared

Table 2 Analysis of sum power

Radius of observation area r (m)	Optimal relay position x (m)	Network size D (m)	Sum power P (mW)
100	899.9998	1000	25.82978
200	1785.71	2000	102.6904
300	2500	3000	222.8173
400	3214.285	4000	393.0221
500	3928.571	5000	613.3051

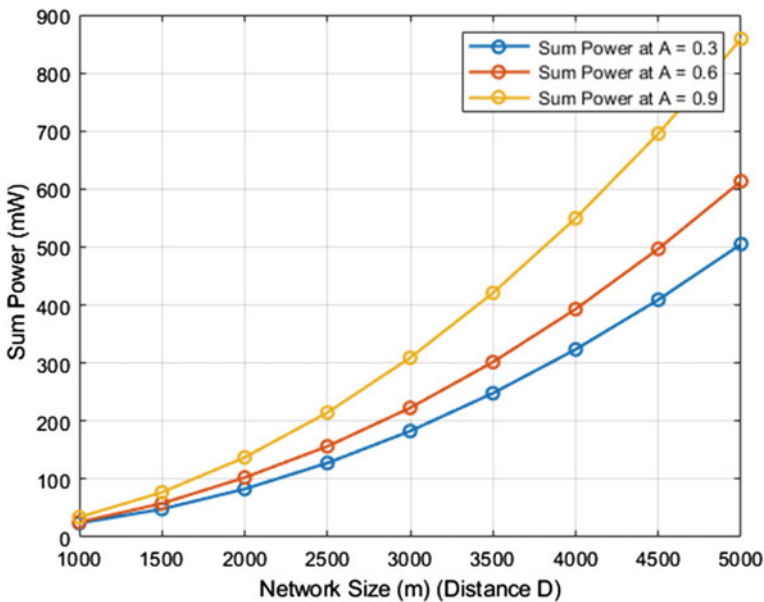


Fig. 2 Optimized power for different network dimensions for $A = [0.3, 0.6, 0.9]$; $D/r = 10$; $R = 800$ kbps

to the case when no relay is incorporated. Best results are obtained for optimized relay placement as compared to the other two scenarios. For instance, when the network size is 4000m, the sum power is 1374mW (no relay), 522.3mW (fixed relay location placed at $D/2$) and 393mW (optimized relay placement). It is obvious from these results that sum power decreases significantly for optimal relay placement as compared to the other two cases.

Figure 4 shows the advantages of optimal relay placement by varying D/r ratio from 10 to 20 for fixed radius of observation area ($r = 500$ m). Again, the performance measure in these curves is the optimized minimum power. These results are simulated for $A = 0.6$. It is observed from these results that sum power is largest when no relay

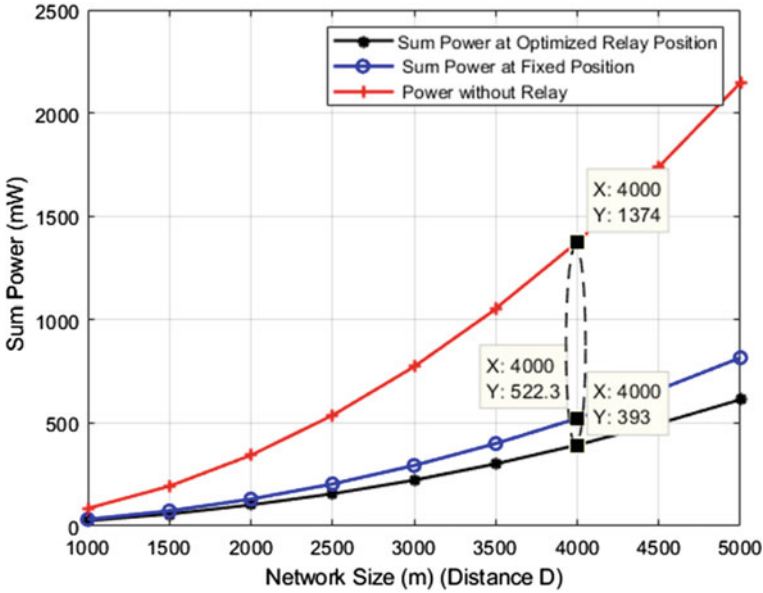


Fig. 3 Effect of optimal relay placement for for $A = 0.6$; $D/r = 10$; $R = 800$ kbps

is employed. For fixed relay placement, the performance of optimized sum power improves as compared to the case when no relay is incorporated. Best results are obtained for optimized relay placement as compared to the other two scenarios. For instance, when the D/r ratio is 15, the sum power is 4541 mW (no relay), 1681 mW (fixed relay location placed at $D/2$) and 1298 mW (optimized relay placement).

It is obvious from these results that sum power decreases significantly for optimal relay placement as compared to the other two cases. Figure 5 shows the advantages of optimal relay placement by varying D/r ratio from 10 to 20 for fixed radius of observation area ($r = 600$ m) and attenuation ($A = 0.9$). As network size (D/r ratio) increases, the observation area becomes far away from the ground BS. It is obvious from these results that sum power decreases significantly for optimal relay placement as compared to the other two cases.

5 Conclusion

In this chapter, we presented the role of UAVs in public safety communications. The main focus of this work is to ensure reliable wireless connectivity at disastrous areas to the remote ground BS. Therefore, our system model presents a UAV network which consists of observation UAV, relay UAV and ground BS to provide connectivity of users at affected area. An efficient algorithm is proposed in this research work

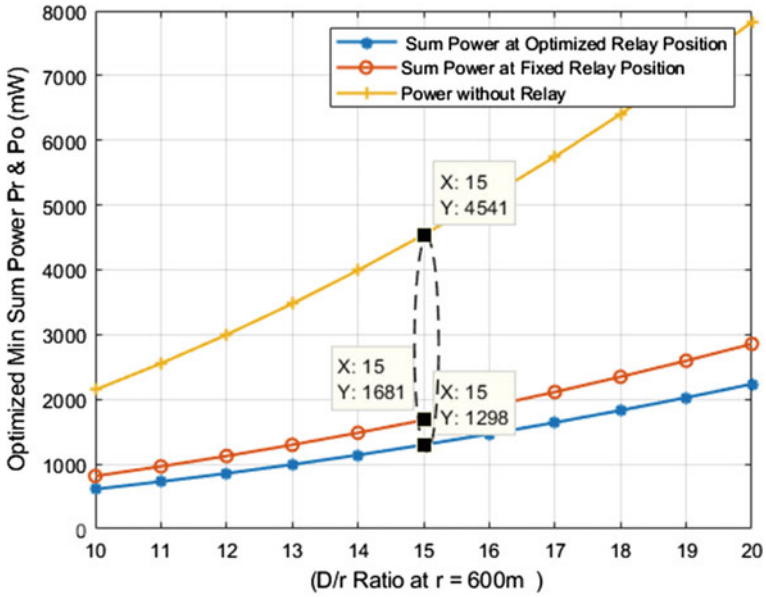


Fig. 4 Effect of relay UAV positions on sum power $A = 0.6$; $r = 500$; $R = 800$ kbps

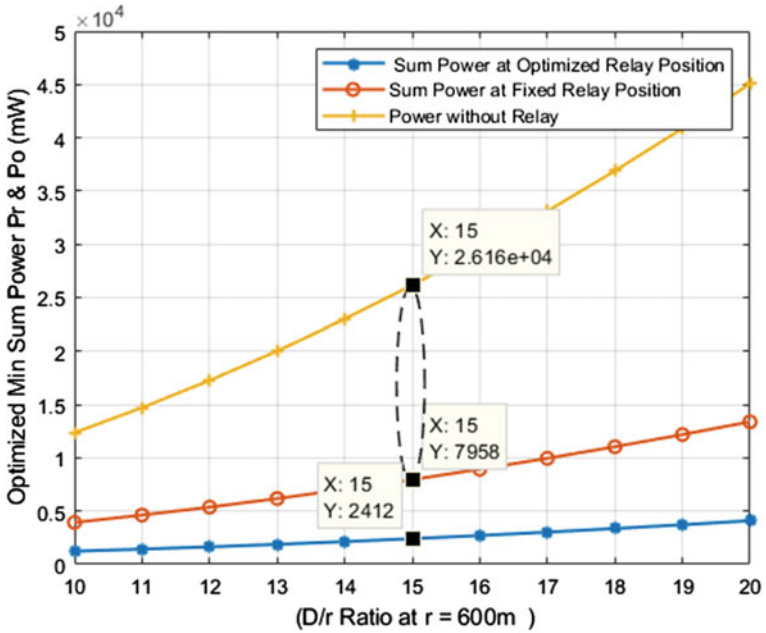


Fig. 5 Effect of optimal relay placement by varying D/r ratio for $A = 0.9$; $r = 600$; $R = 800$ kbps

for optimal placement of relay UAV. This optimal relay placement minimizes the sum power consumption of observation UAV and relay UAV. The optimized sum power ensures a target data rate for different network dimensions. The proposed algorithm is validated using MATLAB simulations. Furthermore, the performance with optimal relay placement significantly outperforms the fixed relay placement and no relay scenarios. Also, a noticeable performance gain is obtained for optimal relay placement for a range of D/r ratios, as compared to the fixed relay placement and the case when no relay is deployed. A formidable extension of this research work is to incorporate multiple relay UAVs over different network dimensions to provide connectivity at distant areas.

References

1. Baldini G, Karanasios S, Allen D, Vergari F (2013) Survey of wireless communication technologies for public safety. *IEEE Commun Surv & Tutor* 16(2):619–641
2. Merwaday A, Guvenc I (2015) UAV assisted heterogeneous networks for public safety communications. In: *Wireless communications and networking conference workshops (WCNCW)*. IEEE, pp 329–334
3. Sharma A, Vanjani P, Paliwal N, Basnayaka CMW, Jayakody DNK, Wang H-C, Muthuchidambaranathan P (2020) Communication and networking technologies for UAVs: a survey. *J Netw Comput Appl* 102739
4. Alzenad M, El-Keyi A, Yanikomeroglu H (2017) 3-D placement of an unmanned aerial vehicle base station for maximum coverage of users with different QoS requirements. *IEEE Wireless Commun Lett* 7(1):38–41
5. Do DT, Nguyen TTT, Le CB, Voznak M, Kaleem Z, Rabie KM (2020) UAV relaying enabled NOMA network with hybrid duplexing and multiple antennas. *IEEE Access* pp 1–1
6. Bor-Yaliniz RI, El-Keyi A, Yanikomeroglu H (2016) Efficient 3-D placement of an aerial base station in next generation cellular networks. In: *International conference on communications (ICC)*. IEEE, pp 1–5
7. Mozaffari M, Saad W, Bennis M, Nam Y-H, Debbah M (2019) A tutorial on UAVs for wireless networks: applications, challenges, and open problems. *IEEE Commun Surv & Tutor* 21(3):2334–2360
8. Lyu J, Zeng Y, Zhang R, Lim TJ (2016) Placement optimization of UAV-mounted mobile base stations. *IEEE Commun Lett* 21(3):604–607
9. Alzenad M, El-Keyi A, Lagum F, Yanikomeroglu H (2017) 3-D placement of an unmanned aerial vehicle base station (UAV-BS) for energy-efficient maximal coverage. *IEEE Wireless Commun Lett* 6(4):434–437
10. Kalantari E, Shakir MZ, Yanikomeroglu H, Yongacoglu A (2017) Backhaul-aware robust 3D drone placement in 5G+ wireless networks. In: *International conference on communications workshops (ICC workshops)*. IEEE, pp 109–114
11. Kalantari E, Yanikomeroglu H, Yongacoglu A (2016) On the number and 3D placement of drone base stations in wireless cellular networks. In: *84th Vehicular technology conference (VTC-Fall)*. IEEE, pp 1–6
12. Shakoor S, Kaleem Z, Do D-T, Dobre OA, Jamalipour A (2020) Joint optimization of UAV 3D placement and path loss factor for energy efficient maximal coverage. *IEEE Inter Things J*
13. Shakoor S, Kaleem Z, Baig MI, Chughtai O, Duong TQ, Nguyen LD (2019) Role of UAVs in public safety communications: energy efficiency perspective. *IEEE Access* 7:140 665–140 679
14. Do-Duy T, Nguyen LD, Duong TQ, Khosravirad SR, Claussen H (2021) Joint optimisation of real-time deployment and resource allocation for uav-aided disaster emergency communications. *IEEE J Select Areas Commun* 39(11):3411–3424

15. Nguyen KK, Vien NA, Nguyen LD, Le M-T, Hanzo L, Duong TQ (2021) Real-time energy harvesting aided scheduling in uav-assisted d2d networks relying on deep reinforcement learning. *IEEE Access* 9:3638–3648
16. Kaleem Z, Yousaf M, Qamar A, Ahmad A, Duong TQ, Choi W, Jamalipour A (2019) Uav-empowered disaster-resilient edge architecture for delay-sensitive communication. *IEEE Netw* 33(6):124–132
17. Teng H, Ahmad I, Msm A, Chang K (2020) 3d optimal surveillance trajectory planning for multiple uavs by using particle swarm optimization with surveillance area priority. *IEEE Access* 8:86 316–86 327
18. Liu L, Zhang S, Zhang R (2019) CoMP in the sky: UAV placement and movement optimization for multi-user communications. *IEEE Trans Commun* 67(8):5645–5658
19. Babu N, Papadias CB, Popovski P (2020) Energy-efficient 3D deployment of aerial access points in a UAV communication system. *IEEE Commun. Lett.*
20. Liu Y, Liu K, Han J, Zhu L, Xiao Z, Xia X-G (2020) Resource allocation and 3D placement for UAV-enabled energy-efficient IoT communications. *IEEE Inter Things J*
21. Ali MA, Jamalipour A (2020) UAV placement and power allocation in uplink and downlink operations of cellular network. *IEEE Trans Commun*
22. Sun X, Ansari N (2017) Latency aware drone base station placement in heterogeneous networks. In: *Global communications conference*. IEEE, pp 1–6
23. Shah SAW, Khattab T, Shakir MZ, Hasna MO (2017) A distributed approach for networked flying platform association with small cells in 5G+ networks. In: *Global communications conference*. IEEE, pp 1–7
24. Pandey S, Agrawal P (2006) A unifying architecture for maximal connectivity in heterogeneous Ad Hoc networks. In: *GLOBECOM*
25. Mozaffari M, Saad W, Bennis M, Debbah M (2017) Mobile unmanned aerial vehicles (UAVs) for energy-efficient internet of things communications. *IEEE Trans Wireless Commun* 16(11):7574–7589
26. Sajid M, Yang YJ, Kim GB, Choi KH (2016) Remote monitoring of environment using multi-sensor wireless node installed on quad-copter drone. In: *International symposium on robotics and intelligent sensors (IRIS)*. IEEE, pp 213–216
27. Zhang SQ, Xue F, Himayat NA, Talwar S, Kung H (2018) A machine learning assisted cell selection method for drones in cellular networks. In: *19th International workshop on signal processing advances in wireless communications (SPAWC)*. IEEE, pp 1–5
28. Nesterov Y, Nemirovskii A (1994) Interior-point polynomial algorithms in convex programming. *SIAM*

Location Prediction and Trajectory Optimization in Multi-UAV Application Missions



Rounak Singh, Chengyi Qu, Alicia Esquivel Morel, and Prasad Calyam

Abstract Unmanned aerial vehicles (a.k.a. drones) have a wide range of applications in e.g., aerial surveillance, mapping, imaging, monitoring, maritime operations, parcel delivery, and disaster response management. Their operations require reliable networking environments and location-based services in air-to-air links with co-operative drones, or air-to-ground links in concert with ground control stations. When equipped with high-resolution video cameras or sensors to gain environmental situation awareness through object detection/tracking, precise location predictions of individual or groups of drones at any instant possible is critical for continuous guidance. The location predictions then can be used in trajectory optimization for achieving efficient operations (i.e., through effective resource utilization in terms of energy or network bandwidth consumption) and safe operations (i.e., through avoidance of obstacles or sudden landing) within application missions. In this chapter, we explain a diverse set of techniques involved in drone location prediction, position and velocity estimation and trajectory optimization involving: (i) Kalman Filtering techniques, and (ii) Machine Learning models such as reinforcement learning and deep-reinforcement learning. These techniques facilitate the drones to follow intelligent paths and establish optimal trajectories while carrying out successful application missions under given resource and network constraints. We detail the techniques using three scenarios. The first scenario involves location prediction based intelligent packet transfer between drones in a disaster response scenario using the various Kalman Filtering techniques along with sensor fusion. The second scenario involves a learning-based trajectory optimization that uses various reinforcement learning models for maintaining high video resolution and effective network performance in

R. Singh · C. Qu · A. Esquivel Morel · P. Calyam (✉)
University of Missouri-Columbia, Columbia, MO, USA
e-mail: calyamp@missouri.edu

R. Singh
e-mail: rsft6@mail.missouri.edu

C. Qu
e-mail: cqy78@mail.missouri.edu

A. Esquivel Morel
e-mail: ace6qv@mail.missouri.edu

© The Author(s), under exclusive license to Springer Nature Singapore Pte Ltd. 2022
Z. Kaleem et al. (eds.), *Intelligent Unmanned Air Vehicles Communications for Public Safety Networks*, Unmanned System Technologies,
https://doi.org/10.1007/978-981-19-1292-4_5

a civil application scenario such as aerial monitoring of persons/objects. The third scenario involves salient non-ML-based trajectory optimization techniques that can be adopted within UAV-based applications for public safety networks. We conclude with a list of open challenges and future works for intelligent path planning of drones using location prediction and trajectory optimization techniques.

Keywords Drone swarms · Location-based services · Situational awareness · Deep reinforcement learning

1 Introduction

The use of drones has been increasing at a rapid pace for a diverse range of applications in e.g., aerial surveillance, mapping, imaging, monitoring, maritime operations, parcel delivery, and disaster response management. Many applications involve multi-UAV configurations [1], wherein several drones act as either carrier devices to carry supplies [2], or are used for aerial surveillance for intelligent information gathering [3]. They also are deployed as aerial base stations to provide bandwidth and network coverage for ground users in certain applications [4]. An example of air-to-air links with co-operative drones surveying over a designated area is shown in Fig. 1. These operations require location-aided drone movement and optimal drone paths for reduced energy consumption and efficient resource allocation. We discuss salient challenges in realizing these drone location prediction and trajectory optimization techniques and show their advantages through two scenarios involving: (i) network and video analytics orchestration, and (ii) intelligent packet transfer in a disaster response management scenario. This chapter will illustrate how various predicted location information and intelligent path planning schemes help in achieving efficient performance of application missions.

1.1 How Can Drone's Location Prediction Be Useful in Networking Environments and Application Scenarios?

To explain the significance of drone location prediction in real-time applications, we consider a multi-drone co-ordination and networking system for a critical application mission such as e.g., a disaster response scenario (DRS) [5, 6]. This scenario involves critical tasks such as monitoring the disaster affected area, search and rescue operations, and providing supplies to victims. This system features a Flying Ad-Hoc Network Topology (FANET) [7] to support air-to-air, as well as air-to-ground links. The ground control station (GCS) sends requests to the drones to execute certain tasks and the drones send back situational awareness information to the GCS. Such a scenario, however involves challenges related to drone positioning and path plan-

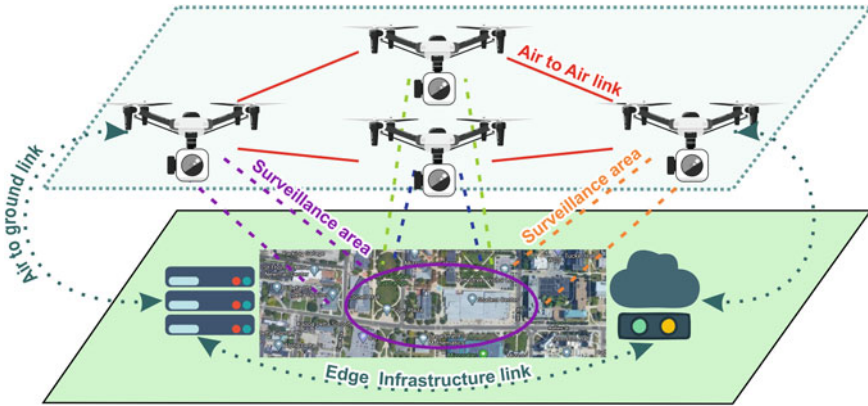


Fig. 1 Overview of multi-drone setup based on air-to-air and air-to-ground links

ning. Particularly, the *location estimation of drones* is necessary for multi-drone co-operation in order to stay on-course and avoid mid-air collisions. Furthermore, *trajectory planning and optimization* is required to efficiently carry out the application mission considering the limitations of energy and resources. To explicitly understand how these two essential methods impact the performance of drones in application missions, we elaborate them in the following:

1. **Location Estimation and Prediction:** Tracking and predicting the locations of drones is important in order to get real-time estimates of drone positions for autonomous control and to improve the accuracy of delivery tasks execution in a specific application scenario. It measures how closely the drones are being monitored and also measures the reliability of the path computation algorithm performance. This can be achieved by using motion models of the drone movements, and by using such models within a tracking algorithm or a recursive filter. To get the near-optimal estimates with the motion model, prior works use the Kalman Filter [8] technique which is widely-used for estimation purposes. The popularity of Kalman Filter is due to the fact that this technique takes in the current values as input data (i.e., measurement) along with noises (i.e., measurement noise and process noise) to produce unbiased estimates of system states [9]. Leveraging this state estimation technique can help achieve predicted positions of drones.
2. **Trajectory Optimization** The path that a drone follows during its operation is crucial for effective communication, computation offloading [10], energy consumption and information transfer. A drone’s trajectory design unquestionably plays an important role in the application performance enhancement and effectiveness. During its operation, the drone flies over areas which are prone to network and communication vulnerabilities such as signal-loss, cyber-attacks, coverage and range limitations that could severely impact the drones’ performance and put the application mission at risk. Machine learning techniques such as model-free

reinforcement learning [11] and deep reinforcement learning [12] provide effective reliable solutions for tackling these implications. They use trial-and-error path learning techniques for a drone to establish optimal and intelligent trajectory during its overall flight time during an application mission.

1.2 Chapter Organization

This book chapter aims to address the concepts of drone position and trajectory optimization techniques related to intelligent path planning. The chapter will first discuss the challenges related to drone location prediction and trajectory optimization. Next, methods for location prediction will be discussed that involve various Kalman filtering techniques and methods of trajectory optimization using reinforcement and deep reinforcement learning techniques. In this context, we also discuss non-ML-based methods for trajectory optimization. They together provide motivation for localization and intelligent path planning of drones for a given application scenario. Furthermore, we discuss how trajectory optimization of UAVs can aid the operations of public safety networks. These techniques are based on the theoretical and experimental research conducted by the authors in the Virtualization, Multimedia and Networking (VIMAN) Lab at University of Missouri Columbia. Lastly, we discuss the main findings of this chapter and list out the open challenges and future works that can be implemented using our approaches to carry out drone-based application missions effectively and efficiently.

2 Challenges in Drone Location Prediction and Trajectory Optimization

Since drones are classified under unmanned aerial vehicles, it can be presumed that the navigation, operation and controlling is carried out externally by a ground control station or a ground (human) pilot. In most of the applications today, however the drones flight is increasingly becoming autonomous and may require minimal or almost no external (human) guidance. This is possible due to the variety of sensors on-board that constitute the inertial measurement unit (IMU), global positioning system (GPS), inertial navigation system (INS), gyroscope, accelerometer, barometer and high resolution cameras. These sensors facilitate the autonomous drone flights with high accuracy. Nevertheless, these sensors are prone to external noises that can cause inaccuracies malfunctioning. Another critical elements on which a drone's flight is dependent is the battery that powers the drones flying mechanism, its flight controller and the above-mentioned sensors. Some of the major challenges pertaining to localization and path-planning relating to the above issues are:

Collision avoidance: Real-world application missions are carried out in complex environments and sometimes, civil applications involving drones are conducted in urban areas. The UAVs are only dependent on their on-board sensor capabilities for their traversal through these environments. It is not always feasible to rely on these sensor readings for navigation and the drones may run into obstacles, hit trees, buildings or other drones mid-operation. Many techniques have been proposed for collision avoidance using decentralized control [13, 14]. The drone has to be aware of the location of its neighbor (drone) and itself at any given instant of time. Leveraging this information can help tackle the problem of mid-air collisions. Object detection using computer vision can help in identifying certain objects by training on datasets of images of common environment obstacles [15]. However, drone's system reliance and communication within the network is usually difficult and challenging in large-scale application missions involving complex environments.

System Security: A wide range of drone-based applications are carried out by the military that operate on highly confidential information gathering within classified missions. Also, many civil applications involve sensitive data collection when drones are deployed as aerial base stations or network providers that handle ground user data (e.g., faces and postures of individuals in crowds). Drones are at risk of cyber-attacks and can be hacked, without the drone being physically captured. The information gathered can become vulnerable and exposed to hackers. Mostly, the camera modules are targeted and video captured is received by hackers which may expose the operations that are carried out in the surveillance area. The work in [16] uses Blockchain technology that encrypts the data being transmitted to base stations. An approach for threat analysis of drone based systems is described in [17]. Countermeasures to security issues in professional drone based networks are shown in [18].

Energy Limitations: Drones require energy for total flight time including hovering over an area for surveillance and data transmission. Additionally, the on-board sensors constantly consume energy to function properly and provide localization of the drones. Energy consumption can also be increased due to attached payloads [19], wind resistance [20] and network issues [21]. The total energy on a drone is limited thus restricting the flight-time of the application mission. The work in [22] provides an energy-aware approach that uses trajectory planning of drones used as mobile anchors to save energy.

Location Awareness and Blockage of Line-of-Sight: In the context of location estimation of drones, blockage of line-of-sight for drones is a very trivial problem that surfaces in the rarest of times [23]. As drones tend to fly long distances based on their application missions, the location awareness becomes essential in order for them to remain in their trajectory and under a predefined network connection for information transfer. It is necessary that they avoid collisions and interference. It becomes a problem if a drone's flight is affected due to external factors and it might become susceptible to unknown attacks. In the worst case scenario, the drone can be thrown off-path and after consuming all its power, it can land or fall in an unknown

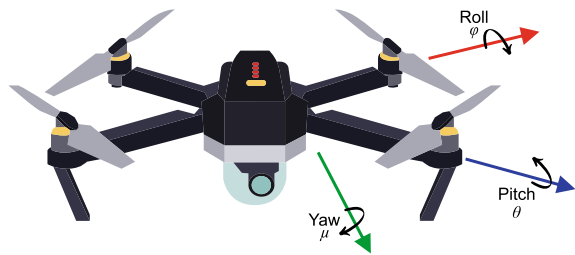
territory. Thus, it can render itself and the information collected vulnerable, and any expensive sensors or video camera components are subject to expensive damage or loss. Various types of research is being conducted by many groups to realize location awareness [24] of drones.

3 Methods for Drone Location Estimation and Prediction

In our DRS application the drone environment is considered to be a 2D dynamic and non-linear horizontal plane. As discussed in Sect. 1.1, we assume that all the drones are connected forming a FANET. They communicate the mapping and monitoring information over the same network to the delivery drones in order to carry out a delivery task. Consequently, the network topology of the multi-drone system keeps on changing based on the mobility of the drones. The position estimation of the drones must be performed in very short intervals of time using the new coordinates being updated rapidly within the FANET. Each drone in the FANET is considered to have a GPS module and an IMU to record its current location. This information is broadcast to the FANET so that the other drones in the vicinity are recognized for packet or information transfers when needed. We get the initial measurement data of the drone using GPS and other on-board sensors such as gyroscope, barometer, accelerometer and magnetometer that are all part of the IMU. The drone's rotational movement angles observed and controlled by a gyroscope and rotary movements, for stability are shown in Fig. 2. The accelerations and rotations of the drone can be observed over time to give an estimated position by learning the next measurement values for different time-steps.

The position, velocity, acceleration and heading of a UAV are considered as dynamic states at a given time-step. In order to get the location prediction of an UAV, a state estimator is required to get the true values along with a prediction of these states for the next time-step. Kalman filter can be used to observe state estimates over time along with process noise and measurement noise from sensors to give estimates on which drone position state estimates are closer to true values that cannot be calculated directly [25]. Since the inception of Kalman filter in 1960, it has evolved over time, and the most popular Kalman filters for UAV location esti-

Fig. 2 Motion angles of a drone responsible for movement with six degrees of freedom controlled by the gyroscope and flight controller



mation are the original Kalman filter, the extended Kalman filter (EKF) [26] and the unscented Kalman filter (UKF) [27].

3.1 State Estimation of Drone Parameters Using Original Kalman Filter

The functionality of Kalman filter relies on consecutive iterations of prediction and filtering i.e., it follows a sequence of prediction and update equations. Along with the inertial navigation system (INS) data, a predefined motion model of the drones' movement is given as input to the Kalman filter. The motion model is basically a state transition matrix having time-periods of the states i.e., x and y coordinate, acceleration and angular velocity. The prediction equations give priori estimates and the update equations give posterior estimates. The update equations take up the previous state's mean and noise covariance and produce the updated mean and noise covariance values for the next state. The filter then combines the predicted states and noisy measurements to produce unbiased estimates of drone system states. In this process, data with process noise and measurement noise from sensors is used as input, and the Kalman filter produces a statistically optimal estimate of the underlying state by recursively acting on the series of observed inputs.

For simplicity, the Kalman Filter can be used to get position and velocity estimates of UAVs but only in a 2D plane, assuming it is flying at a fixed altitude. Other applications of Kalman filter include guidance and navigation systems, tracking of maneuvering targets, dynamic positioning, sensor data fusion and signal processing. An approach for path planning of UAV using a Kalman filter is given in [28].

3.2 Extended Kalman Filter for Non-linear Drone State Estimation

The major limitation of a Kalman filter is that it can only process estimates of linear systems, and it suffers from linearization when operated on nonlinear models. Drone flight operation is generally non-linear and time varying and system parameters with a dynamic motion model cannot be measured directly with on-board sensors because they may be subject to noise and malfunctioning. To overcome this non-linearity issue of drone position estimation, one of the widely used filter for non-linear state estimation, i.e. the extended Kalman filter (EKF) is used. It uses Taylor series expansion and linearizes and approximates the state estimates of a non-linear function around the conditional mean. EKF can be reliable while estimating the drone positions using the drones' dynamic state parameters.

The dynamic motion model is solved by learning the non-linear transition of measurement noise covariance and process noise covariance along with the change

in states to give an optimal estimate of the UAV position. The EKF also follows a series of prediction and update equations. The priori estimates calculated during the prediction process are updated to give the posterior estimates and their covariance. Additionally, Jacobians of dynamic functions are used with respect to system state of the UAV to map its states to observations. Additionally, by recursive operations, the covariance of the estimated error is minimized. Hence, the EKF can be used to get the more accurate positions of the drones through prediction of future positions with insignificant errors, when compared to the original Kalman filter.

The work in [29] shows the non-linear estimation of drone's state along with sensor data for localization and [30] shows an approach for determining the locations of drones using inter-drone distances in 2D co-ordinates.

3.3 Unscented Kalman Filter for Improved Position Estimation and Orientation Tracking of UAVs

The EKF is computationally complex and takes longer to produce estimates, also its accuracy is reliable in real-time but can still be improved. The unscented Kalman filter (UKF) is used for the same applications requiring higher accuracy. It is a deterministic sampling approach involving sampling of distributions using a Gaussian random variable. It employs the unscented transform method to select a set of samples called sigma points around the mean to calculate the mean and covariance of the estimation that eradicates the requirement of using Jacobians, as in the EKF. This preserves the linear update structure of the original Kalman of estimates filter unlike the EKF. Table 1 shows the comparison of various Kalman filtering schemes used for location estimation of UAVs; for a detailed comparison, readers can refer to [31].

In drone localization application, the system dynamics is expanded as the drone's cartesian location i.e., position, velocity and acceleration. These provide a non-linear relationship between the system states and measurements, and thereby the implementation becomes simpler. The orientation tracking of a drone is also carried out using the UKF [32] by considering rigid body dynamics using various types of measurements like acceleration, angular velocity and magnetic field strength. It uses quaternions and UKF, thus proving its computational effectiveness of tracking. Another approach for position estimation using UKF samples images uses a visual target. It uses weights (difference of observed value and estimated value of vision sensor) for observations to prevent divergence in estimated values by UKF [33].

3.4 Sensor Fusion for UAV Localization

Multi-sensor fusion is another technique that shows the importance of using data from distinct sensors to predict the dynamic state estimates of drones for aerial

Table 1 Comparison of Kalman filtering scheme variants for location estimation and prediction of UAVs

Type of filter	Type of system	Accuracy	Model design
Kalman Filter	Linear	Least accurate	Least complex
Linearized Kalman Filter	Non-linear	Moderately accurate	Moderately complex
Extended Kalman Filter (EKF)	Non-linear	Accurate	Most complex
Unscented Kalman Filter (UKF)	Non-linear	Most accurate	Complex

applications. The work in [34] shows how data collected from the GPS, IMU, and INS are fused together for UAV localization using state-dependent Riccati-equation non-linear filter along with a UKF. Drone path planning involves navigating the drone to a desired destination travelling over a predefined path that constitutes obstacles and other environment constraints. The work in [35] shows how the sensor fusion along with real-time kinematic GPS sensors is used to accurately calculate the altitude and position of the drone. They generate a data-set using instantaneous positions of the drone in different directions along with the roll, pitch and yaw angles. Further, they compare this data with the output of the sensor fusion model estimations that are carried out using an EKF to produce position and altitude estimates of drones.

3.5 Location Prediction Based Intelligent Packet Transfer

The location prediction algorithm embedded with the above drone position models along with the position and velocity estimation by Kalman filter and location prediction by EKF, can be run online to make advance decisions by using future location information of the mapping drones, monitoring drones and the delivery drones in the FANET. UKF along with sensor fusion methods can alleviate potential inconsistencies in the dynamic state estimation and can help the algorithm produce accurate results. Thus, the FANET in the DRS scenario can utilize these location estimation techniques to facilitate efficient packet transfer.

Table 2 summarizes how different methods of location prediction of drones have been proposed in prior works to achieve goals in different application missions. The details of the salient methods used to perform drone location prediction while operating in an application are described in the following:

Table 2 Methods and applications of location estimation of drones

Case study	Method	Solution	Application	Goal
Xiong et al. [25]	Kalman Filter	Linear estimation	State estimation	Autonomous flight
Mao et al. [30]	Extended Kalman Filter	Non-linear estimation	Localization of UAVs	Localization without GPS
Kraft et al. [32]	Unscented Kalman Filter	Linearized estimation	Localization of UAVs	Orientation computation
Abdelfatah et al. [35]	Sensor Fusion	Non-linear estimation	Localization of UAVs	Altitude, position estimation

4 Methods for Drone Trajectory Optimization Using Machine Learning

In context of drone trajectory optimization, we consider an area that is prone to signal-losses, cyber-attacks and potential obstacles like trees, buildings, tall-standing structures which affect the drones’ performance and cause hindrance in the application mission. An overview of a drone’s trajectory during an application is shown in Fig. 3. To overcome these problems there is a need for intelligent path planning that can enable the drones follow an optimal trajectory, flying in areas free of all the impediments and attacks.

The details of the salient methods used to optimize the drones’ trajectories while operating in an application are described in the following:

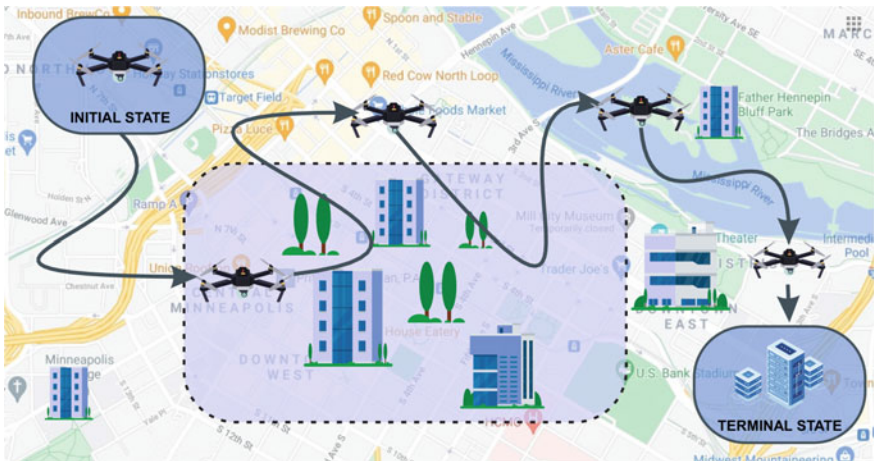


Fig. 3 Overview of drone’s trajectory in a learning based environment comprising of potential obstacles

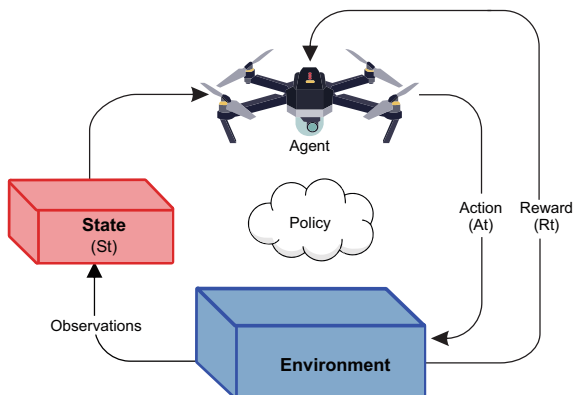
Reinforcement Learning: Path planning of drones is a crucial aspect of research in drone-based applications because the efficiency of missions is dependent on the traversal of the drones in a given area. It correlates with autonomy and has a profound impact on guidance, operation and endurance of the drones. Most drone based application missions are defined in unknown environments. Therefore, Markov Decision Process (MDP) is employed to solve such environments and the Q-Learning algorithm is used that follows the Markov property [36]. It is a model-free reinforcement learning algorithm that puts emphasis on an agent to learn actions under given circumstances to handle problems with stochastic transitions. For any finite MDP, the Q-learning algorithm finds an optimal policy by maximizing the expected value of cumulative rewards over successive actions taken in given states, starting from a current state. There has been a wide usage of reinforcement learning algorithms in varied areas of drone-based application research where drones are allowed to directly and continuously interact with the environment.

Deep Reinforcement learning (DRL): This concept can be considered as a combination of deep learning and reinforcement learning. It employs a deep neural network (DNN) to estimate the Q function $Q(s, a)$ for a given set of state-action pairs. Often reinforcement learning requires the state space and the action space to be fixed and discrete, and the agent learns to make decisions by using a trial and error method. It basically involves employing a Q learning algorithm that maintains a record of values of what actions have been taken in given state spaces and also the rewards associated with the corresponding states and actions in a limited format where the state space is predefined. The DRL method allows the agent to act in an environment that has a continuous and mostly undefined state space. It also uses a set of discrete or continuous actions which are given as a stack of inputs in contrast to the single inputs in case of a simple reinforcement learning. In other words, the DRL makes sure that the agent performs well with extensive input data coming from a large state space to optimize the given objective of any application e.g., it uses pixels as input data in Atari games [37]. The DNN approximates the Q function which estimates the cumulative reward for each state-action pair. A DNN may often suffer with divergence, so it uses a set of experience replay memory and target network to overcome this issue. DQN based RL solutions for drones are necessary because a drone's operation in a given environment is considered as a continuous state space and multi drone scenarios require more robust algorithms such as the multi-agent DQN [38] and the actor-critic [39] networks, which also employ DNNs to generate an optimal policy solution.

4.1 Q-Learning

Q-learning is a type of model-free reinforcement learning as described in [40], which is used to solve MDP based problems with dynamic programming. The Q-learning algorithm creates a table (i.e., Q-table) containing the corresponding values of each

Fig. 4 Overview of Reinforcement learning showing the agent's interaction with the environment corresponding to given states and actions to generate a policy



state-action pair and keeps updating them along with the reward values. The scores obtained in the Q-table are represented as the values of the Q-function $Q(s_t, a_t)$, and are given by -

$$Q(s_t, a_t) = E \left[\sum_k \gamma^k R_{t+k+1} | (s_t, a_t) \right] \quad (1)$$

where t is the time step and k is the episode. The Q-function is updated for each episode when the agent performs certain actions in a given state to maximize its cumulative reward using the Bellman's equation [41], which is given as -

$$Q(s_{t+1}, a_{t+1}) \leftarrow (1 - \alpha)Q(s_t, a_t) + \alpha[R_t + \gamma \cdot \max_a Q(s_{t+1}, a_{t+1}) - Q(s_t, a_t)]; \quad (2)$$

The algorithm converges when maximum reward is reached. The policy encourages the agent to choose optimal actions and receive greater scores in an iterative fashion, which results in the model rendering high Q-values. The interaction of the agent with the environment to generate rewards and to establish a policy is shown in Fig. 4. The output of the Q-learning is the drone trajectory update guidance that is used to keep the drones as much as possible in the optimal trajectory.

Ensuing the design of the drone's optimal trajectory selection scenario using an MDP, we can evaluate the overall performance by tuning the values of the discount factor γ for obtaining the optimal policy $\pi_t^* : S_t \rightarrow A_t$, which maps the state space with best suitable actions.

4.2 *Deep Q-Network*

To implement the Q-Learning based algorithm that render optimal trajectories of the drones, we choose a DQN that allows for maximum exploration and exploitation [42] of the learning environment by the agent. The actions in this case are dependent on the weights of the primary DNN, which adds flexibility in the overall learning process i.e., as the weights update, the rewards update accordingly. The intelligent trajectory learning application for DRS scenario renders network performance in terms of throughput and the video quality scores (i.e., rewards) obtained in the process of learning. The DQN is trained using a experience replay, which is memory buffer that stores the sequence of state-action pairs from previous episodes. The process of utilizing replay memory to gain experience by random sampling is called experience replay.

The DQN utilizes the mini-batch from experience replay with the observed state transition samples to update its DNNs after each episode during the training process. Thereby, it breaks any correlation made using sequential state-action pairs in the previous episodes. Sometimes, drones are used as swarms in application missions that are connected via wireless links. For any broken link, the drones have to position themselves to make up the broken link to maintain the same QoS requirements. The work in [43] gives an approach that uses DQN to determine optimal links between drones in swarms and to localize the drones to improve overall network performance of the swarm's wireless network.

4.3 *Double Deep Q Network*

The Deep Q Network has a single action value function and while updating the primary DNN, same values are used for selection and evaluation of actions. This in turn leads to overestimation that renders over optimistic action value estimates. To avoid this issue, Double Deep Q Learning decouples the selection and evaluation of value function using two separate DNNs (primary and target). It employs two value functions that learn by selecting random experiences that produce two set of weights [44]. It aims to get the most out of Double Q learning with slight increase in computation. For civil and military based application missions, Double Deep Q Network (DDQN) is used for 3 Dimensional path planning of drones using greedy exploitation strategy to improve learning in complex environments [45].

4.4 *Dueling Deep Q Network*

The Dueling Deep Q Network (Dueling DQN) is another form of a deep reinforcement learning algorithm. It consists of two separate estimators (DNNs) for state value

function and action value function. It is used to overcome the impact caused by similar action values in multiple episodes [46]. Some application missions involve multi-drone connections using cellular networks with each drone acting as a base station. To improve the connectivity over the cellular network, Dueling DQN is used to provide trajectory optimization and coverage-aware navigation for radio mapping [47]. Also in other dynamic environments with unrealized threats, Dueling DQN can provide intelligent path-planning using epsilon greedy policy to render optimal trajectories of the drones [48].

4.5 Actor Critic Networks

Some of the most recent and popular reinforcement learning algorithms are the actor critic networks that aim to achieve optimal policies using low-gradient estimates. The actor network is a DNN that takes in the current environment state and computes continuous actions and the critic judges the performance of the actor network with respect to the input states. It also provides feedback to determine the best possible actions that render higher rewards [49, 50]. An approach to achieve efficient communication and band allocation in the drone network involves determining their 3D trajectory under energy constraints using deep deterministic policy gradient (DDPG) [51] actor-critic networks as shown in [52].

4.6 Orchestration Motivation for Online Learning

The performance in the network links across multi-drone FANETs vary due to certain factors such as, application requirements, weather conditions, obstacles in the path, etc. that cause frequent or intermittent outages in transmission and reception of crucial information inside the FANET. This could also affect the drone's video analytics, when used for civil applications for aerial surveillance. Our proposed orchestration process solves the network links and video analytics disruption by employing an online learning based technique. It analyzes the trajectory during the drone flight, and find ways to optimize the drone's path and even the video quality by selection of pertinent network protocol and video properties during the drone flight.

The Q-learning algorithm forms the basis of the trajectory learning of the drones in different areas and can be applied across all the drones in the FANET. An approach for path planning and obstacle avoidance is shown here [53]. However, Q-learning cannot be used for complex learning environments as it would not allow exploration and exploitation [54] of the total area that the drones are covering during their flights.

To achieve intelligent trajectory learning, we propose a Deep Q-Network based method. The path selection aids the drones to learn and make necessary sequence of decisions under uncertainty in FANET conditions. The learning involved in path selection by the drones can be represented as a Markov Decision Process (MDP) [39]

which forms the basis for the DQN algorithm and is defined as a tuple containing the following-

$$M=(s_t, a_t, p_t, r_t, s'_t) \quad (3)$$

where s_t is the state space, a_t is the action space, r_t is the reward, p_t is the probability of transition of states and s'_t is the next state. The MDP aims to maximize the cumulative rewards that are received by the drones along their trajectories during the operation over a surveillance area. The drones are assumed to be fully charged before they enter the initial state. The learning environment comprises of all the states and actions.

(1) *States*: For any MDP, the states used are the current state s_t and the next state s'_t .

(2) *Actions*: These are the actions that the drone chooses to perform during its flight operation.

(3) *Reward*: It is a feedback parameter, received either as an award or penalty which is a consequence of taking certain actions in the learning environment state-space.

(4) *Probability of State Transition*: It is defined as the probability distribution of the next state s'_t given the current state s_t and current action a_t .

The video and network analytics of drones can be formulated as states s_t , actions a_t along with corresponding reward functions in a civil application based on requirements. A DQN with pre-defined weights can take state space values (s_t) of drones as input, forward pass the values and generate optimal action value function $Q(s_t, a_t)$, and compare it with optimal action value function $Q^*_\pi(s_t, a_t)$. Through back-propagation, it can perform updates to the weights of the neurons so that in the later iterations the output values come close to the optimal value. The DQN algorithm converges when an optimal value is reached. The DQN model can be further extended to Double DQN, Dueling DQN and Actor-Critic network using the same learning environment based on the requirements for network and video orchestration.

An approach that uses deep reinforcement learning for optimizing UAV trajectories is detailed in [55] and uses flow-Level modeling for UAV base station deployments. A similar approach in [56] uses a deterministic policy gradient (DPG) on a model-free reinforcement learning scenario to obtain intelligent UAV trajectories. Deep reinforcement learning can also be applied to more complex scenarios involving tedious tasks such as real-time resource-allocation in multi-UAV scenarios [57]. We consider a scenario that aims to achieve optimal solution for 'energy harvest time scheduling' in a UAV assisted device-to-device (D2D) communications setup by conceiving a system model that can reflect dynamic positions of UAVs along with unknown channel state information. The system model also uses the deep deterministic policy gradient (DDPG) algorithm to solve the energy efficient optimization game for the D2D communications scenario.

5 Non-ML-Based Trajectory Optimization Techniques for Drones

Although machine learning is gaining traction in solutions for autonomous vehicles, trajectory optimization of UAVs in real-time scenarios is challenging because it is a non-convex optimization problem. There have been advances in drone trajectory planning and optimization techniques for single-UAV, dual-UAV and multi-UAV based applications. A survey for long-distance trajectory optimization of small UAVs is given in [58], and a survey of techniques involving joint trajectory optimization with resource allocation is given in [59]. An approach to perform joint trajectory and communication co-design can be found in [60]. Advances in path-planning techniques feature techniques that are quite different from learning-based methods. To provide high-mobility and flexibility in FANETs, many techniques have been proposed. However, there are several open challenges when it comes to path planning of UAVs. A series of latest works that try to solve the open challenges are as follows.

5.1 *Trajectory Optimization Using Quantization Theory-Lagrangian Approach*

An approach to provide optimal UAV positions in static networks under spatial user density is described in [61]. This approach uses uniform distribution of ground terminals at zero altitude and determines optimal placement of UAVs in static environments along with ways to reduce power consumption. The optimizations for the static case are done by considering the UAVs at varying altitudes, followed by characterizing optimal UAV deployments in dynamic scenarios. These optimizations are performed by varying ground terminal density in any given dimension for a fixed number of UAVs which are placed at moderate distances from each other. Two cases are considered: (i) UAVs with no movement, and (ii) UAVs with unlimited movement. This approach aims to achieve lowest possible average power consumption followed by providing a Lagrangian-based descent trajectory optimization technique. The Lagrangian technique is similar to Voronoi based coverage control algorithms and is based on time discretization.

5.2 *Joint Optimization of UAV 3D Placement and Path Loss Factor*

An approach in [62] aims to fill the gaps of joint aerial base station (ABS) deployments and path loss compensation for ABS placements at certain heights. It puts stress on the power control mechanism needed to establish reliable communication, and on the propagation path-loss that hinders the overall communication performance. The

3D UAV placement procedure involves altitude optimization for maximum coverage along with horizontal position optimization for 2D placement that uses a modified K-means algorithm for aerial base station height with a compensation factor.

5.3 Flexible Path Discretization and Path Compression

This technique considers a piecewise-linear continuous trajectory of a UAV whose path comprises of consecutive line segments connected through a finite number of points in 3D called way-points. It provides a solution to render an optimal path by using a flexible path discretization technique to optimize number of way-points in the path to reduce the complexity in the design of the UAV trajectory [63]. The variables that tend to solve the path-planning are considered in two sets of design-able and non-design-able way-points. The way-points are generated using their sub-path representations that ensure a desired trajectory discretization accuracy. They also help to obtain utility and constraint functions that retain accuracy in e.g., aerial data harvesting using distributed sensors. Following this, a path compression technique is performed that takes the 3D UAV trajectory and decomposes it into a 1D (sub-path) signal to further reduce the path-design complexity.

5.4 Connectivity Constrained Trajectory Optimization

This technique provides a solution to optimize an UAV's trajectory in an energy and connectivity constrained application to reduce the overall mission completion time. It uses graph theory and convex optimizations to achieve high-quality solutions in various scenarios involving: (i) altitude mask constraints, (ii) coordinated multi point (CoMP)-based cellular enabled UAV communications, (iii) QoS requirements based communication using UAVs, and (iv) non-LoS channel model. The degree of freedom of UAV movement is exploited to increase the design flexibility of UAV trajectories with respect to the locations of GCS, and ground users for effective communication. By applying structural properties, effective bounding and approximation techniques, the non-convex trajectory problem is converted into a simple shortest path problem between two vertices and solved using two graph theory based algorithms [64]. A similar technique involving effective trajectory planning under connectivity constraints using graph theory is shown in [65].

5.5 3D Optimal Surveillance and Trajectory Planning

Public safety is another crucial application domain for designing drone based communication systems. Prior works such as [66] have proposed approaches to solve

Table 3 Methods and applications of trajectory optimization of drones

Case study	Objective	Solution	Method	Performance
Koushik et al. [43]	Node Positioning	MHQ-PRP Queuing	Deep Q-Network	Increased throughput of dynamic UAV swarming network
Zhao et al. [45]	3D Path Planning	Greedy Exploration (DRL)	Double Deep Q-Network	Better convergence compared to DQN and DDQN
Yan et al. [48]	Real-time path planning	STAGE scenario	Dueling DDQN	Efficient dynamic environment path planning
Ding et al. [52]	3D Trajectory Planning	DDPG (DRL)	Actor-Critic Network	Increased throughput under fairness conditions
Saxena et al. [55]	Traffic-aware UAV trajectories	Leveraging UAV Base Station Network (UAVBSN)	Deep Reinforcement Learning	Three fold increase in throughput of UAVBSN
Nguyen et al. [57]	UAV Trajectory Optimization	Energy Harvesting Time Scheduling	Deep Deterministic Policy Gradient	Efficient resource allocation under energy and flight-time constraints
Xu et al. [60]	2D Trajectory Planning	Semi-definite Programming	Monotonic Optimization (various)	Significant power saving
Koyuncu et al. [61]	Multi-UAV Trajectory Optimization	Lagrangian Approach (1D)	Quantization Theory	Minimized power consumption
Shakoore et al. [62]	3D Placement and Path-Loss	Placement Compensation Factor	Various Optimization techniques	Improved coverage and performance
Guo et al. [63]	3D Trajectory Design	Flexible Path Discretization and Path Compression	Graph Theory (Shortest path)	Reduced path design complexity
Zhang et al. [64]	3D UAV Trajectory Design	Graph Theory	Optimization - (various)	Improved connectivity
Yang et al. [65]	3D UAV Trajectory Design	Graph Theory, Inequality property	Optimization - (various)	Improved connectivity
Teng et al. [66]	3D Optimal Trajectory Planning	Particle Swarm Optimization	Trajectory Planner	Improved dynamic environment adaptability

challenges for the public safety application domain. Specifically, a swarm optimization based trajectory planner is provided with surveillance-area-importance updating apparatus. The apparatus aims to derive 3D surveillance trajectories of several monitoring drones along with a multi-objective fitness function. The fitness function is used as a metric for various factors of the trajectories generated by the planner such as energy consumption, area priority and flight risk. This approach renders collision-free UAV trajectories with high fitness values and exhibits dynamic environment adaptability and preferential important area selection for multiple drones. Table 3 summarizes how different methods of trajectory estimation and optimization have been proposed to achieve certain goals in various applications.

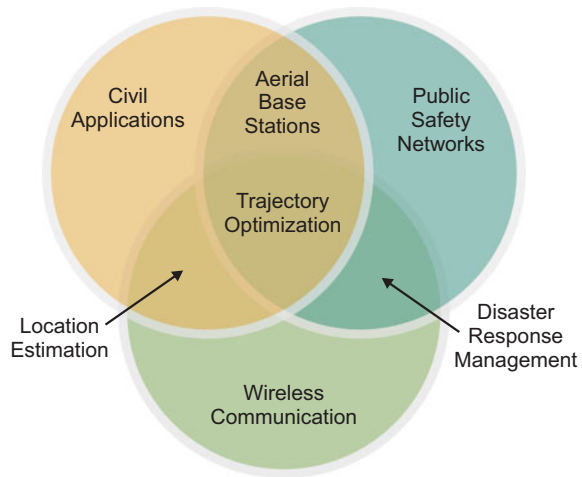
6 How Can Trajectory Optimization Aid UAV-Assisted Public Safety Networks?

Public safety networks (PSNs) are established for public welfare and safety. They are essential means of communication for first responders, security agencies and health-care facilities. Nowadays, PSNs have been widely relying on wireless technologies such as long range WiFi networks, mobile communication and broadband services that use satellite-aided communication links. In addition, PSNs operate extensively during natural disasters, during times when there is a threat to national security such as terrorist attacks, and any large-scale hazards caused due to human activities. As wireless communication is the backbone of PSNs, advanced and efficient communication technologies such as LTE and 5G-based communications can help establish broadband services that provide improved situational awareness with security and reliability characteristics in the network. In this section, we will discuss how UAVs could be a choice for public safety networks in terms of various use cases, provide case studies on trajectory optimization and localization for UAV-assisted PSNs, and discuss open challenges in UAV-assisted PSNs. Figure 5 provides an overview of multi-UAV operations spanning diverse applications ranging from civil applications to public safety networks.

6.1 UAV-Assisted Public Safety Networks

Since wireless communications play a fundamental role in PSN operations, their effectiveness and responsiveness to emergency situations becomes critical [67]. A few issues that affect the functioning of PSNs include: communication equipment deployment costs, spectrum availability, network coverage and quality of service (QoS). A few of these issues can be solved by improving the ground-based communication systems by fully exploiting the potential of situational awareness and enabling advanced tracking, navigation and localization services [68]. However, to

Fig. 5 Overview of multi-UAV operations across various applications ranging from civil applications to public safety networks



eradicate these issues of PSNs as a whole, UAVs with enhanced functionalities that can operate as aerial base stations with high-end communication equipment can be used to amplify the effectiveness of communication, improve coverage, reliability, and energy efficiency of wireless networks. In such UAV-assisted PSNs, UAVs are operated by acting as flying mobile terminals within a cellular network or broadband service while monitoring the area, simultaneously. The other advantage on UAV-assisted PSNs is that the UAV base stations are faster and easier to deploy, which provides effectively on cost and can be flexibly reconfigured based on mobility.

6.2 *Trajectory Optimization and Path-Planning for UAV-Assisted PSNs*

Trajectory Optimization and localization of UAVs can significantly impact the 3D-deployment of the aerial base-stations serving non-stationary users. Optimal path planning can help strengthen the carrier channel transmitting and receiving characteristics. The cellular networks involving aerial base stations can be converted to FANETs, which can help to establish efficient wireless communication in the PSNs. A case study in [69] used path-planning for UAVs in a disaster resilient network. They showed how drones can be used in an wireless infrastructure, allowing a large number of users to establish line-of-sight links for communication. Another approach in [70] uses fast K-means based user cluster model for joint optimization of UAV deployment and resource allocation along with joint optimal power and time transfer allocation for restoring network connectivity during a disaster response scenario. Similarly, research in [71] discusses the role of UAVs in PSNs in terms of energy efficiency and provides a multi-layered architecture that involves UAVs to establish efficient communication by considering the energy consumption considerations.

6.3 *Open Challenges in UAV-Assisted PSNs*

As we can observe from the previous subsections, UAVs when used as aerial base stations can significantly improve the performance and operation of PSNs. However, there are still open challenges that need to be resolved. For example, the monitoring of moving objects/target-users becomes an issue after deployment in a disaster scenario. Few challenges such as traffic estimation, frequency allocation and cell association are addressed in [72]. An approach in [73] propose a disaster resilient communications architecture that facilitates edge-computing by providing a UAV cloudlet layer to aid emergency services communication links. Another approach in [74] has a uplink/downlink architecture for a Full-Duplex UAV relay to facilitate ground base stations around the UAVs. The UAVs communicate to distant ground users using non-orthogonal multiple access (NOMA) assisted networks.

Another important concern raised with UAV-based PSNs is security (see Sect. 2). In most cases, These PSNs are handling confidential information and may become vulnerable. They can also be subject to cyber and physical attacks. A variety of security concerns and challenges in drone-assisted PSNs are addressed in [75] such as: WiFi attacks, channel-jams, grey hole attacks, GPS spoofing and other issues relating to interruption, modification, interception and fabrication of information along with procedures to handle them.

7 Conclusion and Future Outlook

In this chapter, we have presented multi-UAV co-operation applications and explained how drone location prediction and trajectory optimization can be performed. We have learnt how location estimation prediction and trajectory optimization of drones can be beneficial in diverse application missions such as disaster response and other civil applications relating e.g., transportation. Various challenges in drone localization, path-planning and trajectory prediction were detailed.

To cope up with the challenges of localization of drones in application scenarios, we studied how techniques such as non-linear dynamic parameter state estimation of drones using distinct Kalman filtering techniques and sensor fusion can solve the drone localization and position prediction problem. We have also seen how Kalman filter can be used for position and velocity estimation of drones followed by location prediction with inter-drone distances and sensory measurements using the Extended Kalman filter. To cope up with sensory malfunctions and other inconsistencies of the filtering techniques, we detailed various machine learning techniques such as reinforcement learning and deep reinforcement learning. Furthermore, to cope up with the challenges of collision avoidance, trajectory optimization and path planning as well as handling of energy constraints, we have seen how a variety of reinforcement and deep reinforcement learning techniques can be used to realize the potential of multi-UAV co-operation.

Further, we presented a scenario corresponding to online orchestration and learning of network and video analytics for civil applications using multi-agent reinforcement learning techniques. These techniques feature prominent mechanisms that can be used for the 2-D and 3-D path-planning of UAVs along with network and resource allocation under bandwidth and energy constraints. Moreover, we discussed non-ML-based trajectory optimization techniques and explained how UAV-based applications can aid public safety networks.

The Road Ahead to More Open Challenges: We conclude this chapter with a list of more open challenges for multi-drone co-ordination in application missions. Addressing these challenges is essential for a variety of multi-drone applications such as aerial surveillance, deployment of UAVs as base stations and aerial mapping and monitoring that are relevant for location estimation and path planning. Few approaches such as [76] shows how joint positioning of UAVs as aerial base stations is done to provide a smart backhaul-fronthaul connectivity network. Other issues are shown in the following-

- **Excessive movements during flight with no hovering:** When the drones are in complex environments or unknown territories with unrealized threats, they tend to fly more rapidly and in different directions in a short span of time. This may be a result of collision avoidance of obstacles in the path or ineffectual attempts to explore the environment to learn threats. This leads to increased energy consumption and affects the battery capacity of drones, thus shortening their overall flight time. To avoid this issue, dynamic programming and scheduling algorithm could be useful if the drone flight plan in the mission is known apriori. The work in [77] provides two cases that show how data services using UAVs is maximized using hover time management for resource allocation, where the optimal hover time can be derived using service load requirements of ground users.
- **Air-resistance due to strong winds:** Severe wind gusts can throw the drones off-course and deviate a drone from following its optimal path. The on-board sensors are subject to vibrations during severe wind conditions and can produce noisy data that may lead to inaccurate estimates of drones parameters. Unexpected wind resistance can also hinder the trajectory learning of the drone using DRL techniques. This hindrance is possible when the drone traversing in optimal path may change course due to the impacts wind. Further research on EKF and UKF based state estimation of gyroscope readings to study the effects of wind could help in developing suitable solutions. The approach in [78] addresses the altitude control problem of UAVs in presence of wind gusts and proposes a control strategy along with stability analysis to solve the issue of air-resistance.
- **Combining LSTMs with Kalman Filters and DQN:** The non-linear state estimation of drone's dynamic parameters is done using individual time-steps of data by on-board sensors and use of the Kalman filter. Also, for the DRL techniques, the drone (agent) takes actions in a given state in independent episodes. Long short term memorys (LSTMs) can be used to utilize the information of previous time-steps of drones instead of just one time step or one episode to make predictions. This way LSTM based Kalman Filtering mechanisms and LSTMs based DRL

mechanisms can use past information of the drone(s) and make much accurate predictions. There are works that show how coupling a Kalman Filter with LSTM network improves performance and provides faster convergence of algorithms for various application purposes [79, 80].

- **Multi-drone Co-ordination under energy constraints:** In missions involving a drone swarm or a fleet of drones, it is difficult to monitor each of the drones' parameters. Factors such as malfunctioning or loss of one drone due to total battery utilization can affect the operation of other drones and compromise the overall application mission. Off-line path planning along with online path-planning can help UAVs find the nearest base stations with recharge units and help alleviate this issue and support multi-drone co-ordination even under available energy limitations. One such approach to solve the issue of multi-drone coordination under energy constraints is detailed in [81].

References

1. Yoo S, Kim K, Jung J, Chung AY, Lee J, Lee SK, ... Kim H (2015) Poster: a multi-drone platform for empowering drones' teamwork. In: Proceedings of the 21st annual international conference on mobile computing and networking, pp 275–277
2. Sorbelli FB, Corò F, Das SK, Pinotti CM (2020) Energy-constrained delivery of goods with drones under varying wind conditions. *IEEE Trans Intell Transp Syst*
3. Abiodun TF (2020) Usage of drones or unmanned aerial vehicles (UAVs) for effective aerial surveillance, mapping system and intelligence gathering in combating insecurity in Nigeria. *Afr J Soc Sci Humanit Res* 3(2):29–44
4. Bor-Yaliniz RI, El-Keyi A, Yanikomeroglu H (2016) Efficient 3-D placement of an aerial base station in next generation cellular networks. In: 2016 IEEE international conference on communications (ICC). IEEE, pp 1–5
5. Mayor V, Estepa R, Estepa A, Madinabeitia G (2019) Deploying a reliable UAV-aided communication service in disaster areas. *Wirel Commun Mob Comput*
6. Mishra B, Garg D, Narang P, Mishra V (2020) Drone-surveillance for search and rescue in natural disaster. *Comput Commun* 156:1–10
7. Kim GH, Nam JC, Mahmud I, Cho YZ (2016) Multi-drone control and network self-recovery for flying Ad Hoc networks. In: 2016 eighth international conference on ubiquitous and future networks (ICUFN). IEEE, pp 148–150
8. Ribeiro MI (2004) Kalman and extended kalman filters: concept, derivation and properties. *Inst Syst Robot* 43:46
9. Kalman RE (1960) A new approach to linear filtering and prediction problems
10. Qu C, Calyam P, Yu J, Vandanapu A, Opeoluwa O, Gao K, Palaniappan K (2021) DroneCO-CoNet: learning-based edge computation offloading and control networking for drone video analytics. *Future Gener Comput Syst* 125:247–262
11. Strehl AL, Li L, Wiewiora E, Langford J, Littman ML (2006) PAC model-free reinforcement learning. In: Proceedings of the 23rd international conference on machine learning, pp 881–888
12. Li Y (2017) Deep reinforcement learning: an overview. [arXiv:1701.07274](https://arxiv.org/abs/1701.07274)
13. Liu W, Gu W, Sheng W, Meng X, Wu Z, Chen W (2014) Decentralized multi-agent system-based cooperative frequency control for autonomous microgrids with communication constraints. *IEEE Trans Sustain Energy* 5(2):446–456
14. Abouheaf M, Gueaieb W, Lewis F (2020) Online model-free reinforcement learning for the automatic control of a flexible wing aircraft. *IET Control Theory Appl* 14(1):73–84

15. Zhu P, Wen L, Bian X, Ling H, Hu Q (2018). Vision meets drones: a challenge. [arXiv:1804.07437](https://arxiv.org/abs/1804.07437)
16. Rana T, Shankar A, Sultan MK, Patan R, Balusamy B (2019) An intelligent approach for UAV and drone privacy security using blockchain methodology. In: 2019 9th international conference on cloud computing, data science and engineering (confluence). IEEE, pp. 162–167
17. Samland F, Fruth J, Hildebrandt M, Hoppe T, Dittmann J (2012) AR. Drone: security threat analysis and exemplary attack to track persons. In: Intelligent robots and computer vision XXIX: algorithms and techniques, vol 8301. International Society for Optics and Photonics, p 83010G
18. Rodday NM, Schmidt RDO, Pras A (2016) Exploring security vulnerabilities of unmanned aerial vehicles. In: NOMS 2016–2016 IEEE/IFIP network operations and management symposium. IEEE, pp 993–994
19. Di Franco C, Buttazzo G (2015) Energy-aware coverage path planning of UAVs. In: 2015 IEEE international conference on autonomous robot systems and competitions. IEEE, pp 111–117
20. Ware J, Roy N (2016) An analysis of wind field estimation and exploitation for quadrotor flight in the urban canopy layer. In: 2016 IEEE international conference on robotics and automation (ICRA). IEEE, pp 1507–1514
21. Artemenko O, Dominic OJ, Andryeyev O, Mitschele-Thiel A (2016) Energy-aware trajectory planning for the localization of mobile devices using an unmanned aerial vehicle. In: 2016 25th international conference on computer communication and networks (ICCCN). IEEE, pp 1–9
22. Kouroshnezhad S, Peiravi A, Haghighi MS, Jolfaei A (2020) An energy-aware drone trajectory planning scheme for terrestrial sensors localization. *Comput Commun* 154:542–550
23. Ivancic WD, Kerczewski RJ, Murawski RW, Matheou K, Downey AN (2019) Flying drones beyond visual line of sight using 4g LTE: issues and concerns. In: 2019 integrated communications, navigation and surveillance conference (ICNS). IEEE, pp 1–13
24. Kato N, Kawamoto Y, Aneha A, Yaguchi Y, Miura R, Nakamura H, Kitashima A (2019) Location awareness system for drones flying beyond visual line of sight exploiting the 400 MHz frequency band. *IEEE Wirel Commun* 26(6):149–155
25. Xiong JJ, Zheng EH (2015) Optimal kalman filter for state estimation of a quadrotor UAV. *Optik* 126(21):2862–2868
26. Fujii K (2013) Extended kalman filter. *Refernce Manual*, 14–22
27. Julier SJ, Uhlmann JK (1997) New extension of the Kalman filter to nonlinear systems. In: *Signal processing, sensor fusion, and target recognition VI*, vol 3068. International Society for Optics and Photonics, pp 182–193
28. Wu Z, Li J, Zuo J, Li S (2018) Path planning of UAVs based on collision probability and Kalman filter. *IEEE Access* 6:34237–34245
29. Abdelkrim N, Aouf N, Tsourdos A, White B (2008) Robust nonlinear filtering for INS/GPS UAV localization. In: 2008 16th mediterranean conference on control and automation. IEEE, pp 695–702
30. Mao G, Drake S, Anderson BD (2007) Design of an extended kalman filter for uav localization. In: 2007 information, decision and control. IEEE, pp 224–229
31. St-Pierre M, Gingras D (2004) Comparison between the unscented Kalman filter and the extended Kalman filter for the position estimation module of an integrated navigation information system. In: *IEEE Intelligent Vehicles Symposium*, 2004. IEEE, pp 831–835
32. Kraft E (2003) A quaternion-based unscented Kalman filter for orientation tracking. In: *Proceedings of the sixth international conference of information fusion*, vol 1, no 1. IEEE Cairns, Queensland, Australia, pp 47–54
33. Tang SH, Kojima T, Namerikawa T, Yeong CF, Su ELM (2015) Unscented Kalman filter for position estimation of UAV by using image information. In: 2015 54th annual conference of the society of instrument and control engineers of Japan (SICE). IEEE, pp 695–700
34. Nemra A, Aouf N (2010) Robust INS/GPS sensor fusion for UAV localization using SDRE nonlinear filtering. *IEEE Sens J* 10(4):789–798
35. Abdelfatah R, Moawad A, Alshaer N, Ismail T (2021) UAV tracking system using integrated sensor fusion with RTK-GPS. In: 2021 international mobile, intelligent, and ubiquitous computing conference (MIUCC). IEEE, pp 352–356

36. Gurvits L, Ledoux J (2005) Markov property for a function of a Markov chain: a linear algebra approach. *Linear Algebra Appl* 404:85–117
37. Mnih V, Kavukcuoglu K, Silver D, Graves A, Antonoglou I, Wierstra D, Riedmiller M (2013) Playing atari with deep reinforcement learning. [arXiv:1312.5602](https://arxiv.org/abs/1312.5602)
38. Tampuu A, Matiisen T, Kodelja D, Kuzovkin I, Korjus K, Aru J, Vicente R (2017) Multiagent cooperation and competition with deep reinforcement learning. *PloS One* 12(4):e0172395
39. Sutton RS, Barto AG (2018) Reinforcement learning: an introduction. MIT press
40. Roderick M, MacGlashan J, Tellex S (2017) Implementing the deep q-network. [arXiv:1711.07478](https://arxiv.org/abs/1711.07478)
41. González RLV, Aragone LS (2000) A Bellman's equation for minimizing the maximum cost. *Indian J Pure Appl Math* 31(12):1621–1632
42. Osband I, Blundell I, Pritzel A, Van Roy B (2016) Deep exploration via bootstrapped DQN. *Adv Neural Inf Process Syst* 29:4026–4034
43. Koushik AM, Hu F, Kumar S (2019) Deep Q-learning-based node positioning for throughput-optimal communications in dynamic UAV swarm network. *IEEE Trans Cogn Commun Netw* 5(3):554–566
44. Mnih V, Badia AP, Mirza M, Graves A, Lillicrap T, Harley T, ... Kavukcuoglu K (2016) Asynchronous methods for deep reinforcement learning. In: International conference on machine learning. PMLRpp, 1928–1937
45. Zhao L, Ma Y, Zou J (2020) 3D Path planning for UAV with improved double deep Q-network. In: Chinese intelligent systems conference. Springer, Singapore, pp 374–383
46. Wang Z, Schaul T, Hessel M, Hasselt H, Lanctot M, Freitas N (2016) Dueling network architectures for deep reinforcement learning. In: International conference on machine learning. PMLR, pp 1995–2003
47. Zeng Y, Xu X, Jin S, Zhang R (2021) Simultaneous navigation and radio mapping for cellular-connected UAV with deep reinforcement learning. *IEEE Trans Wirel Commun*
48. Yan C, Xiang X, Wang C (2020) Towards real-time path planning through deep reinforcement learning for a UAV in dynamic environments. *J Intell Robot Syst* 98(2):297–309
49. Grondman I, Busoniu L, Lopes GA, Babuska R (2012) A survey of actor-critic reinforcement learning: Standard and natural policy gradients. *IEEE Trans Syst Man Cybern Part C (Appl Rev)* 42(6):1291–1307
50. Konda VR, Tsitsiklis JN (2000) Actor-critic algorithms. In: Advances in neural information processing systems, pp 1008–1014
51. Hou Y, Liu L, Wei Q, Xu X, Chen C (2017) A novel DDPG method with prioritized experience replay. In: 2017 IEEE international conference on systems, man, and cybernetics (SMC). IEEE, pp 316–321
52. Ding R, Gao F, Shen XS (2020) 3D UAV trajectory design and frequency band allocation for energy-efficient and fair communication: a deep reinforcement learning approach. *IEEE Trans Wirel Commun* 19(12):7796–7809
53. Zhao YJ, Zheng Z, Zhang XY, Liu Y (2017) Q learning algorithm based UAV path learning and obstacle avoidance approach. In: 2017 36th chinese control conference (CCC). IEEE
54. Coggan M (2004) Exploration and exploitation in reinforcement learning. Research supervised by Prof. Doina Precup, CRA-W DMP Project at McGill University
55. Saxena V, Jaldèn J, Klessig H (2019) Optimal UAV base station trajectories using flow-level models for reinforcement learning. *IEEE Trans Cogn Commun Netw* 5(4):1101–1112
56. Yin S, Zhao S, Zhao Y, Yu FR (2019) Intelligent trajectory design in UAV-aided communications with reinforcement learning. *IEEE Trans Veh Technol* 68(8):8227–8231
57. Nguyen KK, Vien NA, Nguyen LD, Le MT, Hanzo L, Duong TQ (2020) Real-time energy harvesting aided scheduling in UAV-assisted D2D networks relying on deep reinforcement learning. *IEEE Access* 9:3638–3648
58. Langelan J (2007) Long distance/duration trajectory optimization for small UAVs. In: AIAA guidance, navigation and control conference and exhibit, p 6737
59. Lakew DS, Masood A, Cho S (2020) 3D UAV placement and trajectory optimization in UAV assisted wireless networks. In: 2020 international conference on information networking (ICOIN). IEEE, pp 80–82

60. Xu D, Sun Y, Ng DWK, Schober R (2020) Multiuser MISO UAV communications in uncertain environments with no-fly zones: robust trajectory and resource allocation design. *IEEE Trans Commun* 68(5):3153–3172
61. Koyuncu E, Shabanighazikelayeh M, Seferoglu H (2018) Deployment and trajectory optimization of UAVs: a quantization theory approach. *IEEE Trans Wirel Commun* 17(12):8531–8546
62. Shakoor S, Kaleem Z, Do DT, Dobre OA, Jamalipour A (2020) Joint optimization of UAV 3D placement and path loss factor for energy efficient maximal coverage. *IEEE Internet Things J*
63. Guo Y, You C, Yin C, Zhang R (2021) UAV trajectory and communication co-design: flexible path discretization and path compression. *IEEE J Sel Areas Commun*
64. Zhang S, Zeng Y, Zhang R (2018) Cellular-enabled UAV communication: a connectivity-constrained trajectory optimization perspective. *IEEE Trans Commun* 67(3):2580–2604
65. Yang D, Dan Q, Xiao L, Liu C, Cuthbert L (2021) An efficient trajectory planning for cellular-connected UAV under the connectivity constraint. *China Commun* 18(2):136–151
66. Teng H, Ahmad I, Msm A, Chang K (2020) 3D optimal surveillance trajectory planning for multiple UAVs by using particle swarm optimization with surveillance area priority. *IEEE Access* 8:86316–86327
67. Fantacci R, Gei F, Marabissi D, Micciullo L (2016) Public safety networks evolution toward broadband: sharing infrastructures and spectrum with commercial systems. *IEEE Commun Mag* 54(4):24–30
68. Laoudias C, Moreira A, Kim S, Lee S, Wirola L, Fischione C (2018) A survey of enabling technologies for network localization, tracking, and navigation. *IEEE Commun Surv Tutor* 20(4):3607–3644
69. Naqvi SAR, Hassan SA, Pervaiz H, Ni Q (2018) Drone-aided communication as a key enabler for 5g and resilient public safety networks. *IEEE Commun Mag* 56(1):36–42
70. Do-Duy T, Nguyen LD, Duong TQ, Khosravirad S, Claussen H (2021) Joint optimisation of real-time deployment and resource allocation for UAV-aided disaster emergency communications. *IEEE J Sel Areas Commun*
71. Shakoor S, Kaleem Z, Baig MI, Chughtai O, Duong TQ, Nguyen LD (2019) Role of UAVs in public safety communications: energy efficiency perspective. *IEEE Access* 7:140665–140679
72. Mozaffari M, Saad W, Bennis M, Nam YH, Debbah M (2019) A tutorial on UAVs for wireless networks: applications, challenges, and open problems. *IEEE Commun Surv Tutor* 21(3):2334–2360
73. Kaleem Z, Yousaf M, Qamar A, Ahmad A, Duong TQ, Choi W, Jamalipour A (2019) UAV-empowered disaster-resilient edge architecture for delay-sensitive communication. *IEEE Netw* 33(6):124–132
74. Do DT, Nguyen TTT, Le CB, Voznak M, Kaleem Z, Rabie KM (2020) UAV relaying enabled NOMA network with hybrid duplexing and multiple antennas. *IEEE Access* 8:186993–187007
75. He D, Chan S, Guizani M (2017) Drone-assisted public safety networks: the security aspect. *IEEE Commun Mag* 55(8):218–223
76. Shehzad MK, Ahmad A, Hassan SA, Jung H (2021) Backhaul-aware intelligent positioning of UAVs and association of terrestrial base stations for fronthaul connectivity. *IEEE Trans Netw Sci Eng*
77. Mozaffari M, Saad W, Bennis M, Debbah M (2017) Wireless communication using unmanned aerial vehicles (UAVs): optimal transport theory for hover time optimization. *IEEE Trans Wirel Commun* 16(12):8052–8066
78. Shi D, Wu Z, Chou W (2018) Super-twisting extended state observer and sliding mode controller for quadrotor uav attitude system in presence of wind gust and actuator faults. *Electronics* 7(8):128
79. Pérez-Ortiz JA, Gers FA, Eck D, Schmidhuber J (2003) Kalman filters improve LSTM network performance in problems unsolvable by traditional recurrent nets. *Neural Netw* 16(2):241–250

80. Coskun H, Achilles F, DiPietro R, Navab N, Tombari F (2017) Long short-term memory kalman filters: recurrent neural estimators for pose regularization. In: Proceedings of the iee international conference on computer vision, pp 5524–5532
81. Scherer J, Rinner B (2016) Persistent multi-UAV surveillance with energy and communication constraints. In: 2016 IEEE international conference on automation science and engineering (CASE). IEEE, pp 1225–1230

UAV Trajectory Optimization and Choice for UAV Placement for Data Collection in Beyond 5G Networks



Muhammad K. Shehzad, Syed Ali Hassan, Miguel Angel Luque-Nieto, and Pablo Otero

Abstract Unmanned aerial vehicles (UAVs) evolution has shown potential in many applications of wireless communication because of their high coverage, promising rates, and flexible installation. Owing to the drastic increase of this technology, one of the major challenges is the availability of on-board energy levels to UAVs to stay aloft for a prolonged time. Due to their limited on-board energy, many of the UAVs can go down, and as a result, many associated ground users can face coverage issues etc. Considering this problem, in this study, we give an idea of collecting the uplink traffic from these disaster-points (where active UAVs were serving previously) with the objective of minimizing the Age-of-Information (AoI) of the entire network. Specifically, we address the optimum trajectory of a UAV for collecting data so that the timely delivery of information to the destination can be possible, which will ultimately reduce the overall AoI. We use three different kinds of trajectories namely, *random trajectory*, *travelling salesman problem (TSP)-based trajectory*, and *proposed trajectory*. Simulations show that the proposed trajectory outperforms in the scenario, where disaster-points are less. Additionally, unsupervised learning-based UAVs distribution helps in reducing the AoI as compared to *Matern type-I hard-core process-based UAVs distribution*. Furthermore, the *proposed trajectory* is computationally less expensive than *TSP-based trajectory*; thus, it can be viable in many applications, e.g., Internet of Things (IoT).

Keywords Age-of-Information (AoI) · Backhaul network · Drones · Internet of Things (IoT) · Small cell base stations (SBs) · Travelling salesman problem (TSP) · Unmanned aerial vehicles (UAVs) · Unsupervised learning · 5G

M. K. Shehzad (✉) · S. A. Hassan
School of Electrical Engineering and Computer Science, National University of Sciences and Technology, Islamabad, Pakistan
e-mail: mshehzad.msee17seecs@seecs.edu.pk

M. A. Luque-Nieto · P. Otero
Instituto de Ingenieria Oceanica, University of Malaga, Malaga, Spain

© The Author(s), under exclusive license to Springer Nature Singapore Pte Ltd. 2022
Z. Kaleem et al. (eds.), *Intelligent Unmanned Air Vehicles Communications for Public Safety Networks*, Unmanned System Technologies,
https://doi.org/10.1007/978-981-19-1292-4_6

1 Introduction

Within a short span of time, unmanned aerial vehicles (UAVs) communication emerged as a new paradigm shift because of their instant deployment, flexible to change position and high probability of line-of-sight (LoS); thus, improving the coverage and rate performances [1–8]. Seeing the popularity of UAV communications, [9] address the real-time deployment of UAVs and a resource allocation scheme. By utilizing deep reinforcement learning, [10] propose a solution for energy harvesting time scheduling in a UAV-aided device-to-device communication. The non-orthogonal multiple access (NOMA)-based UAV network is evaluated in [11], where a detailed theoretical analysis is provided with simulation-based results. Teng et al. [12] propose a particle swarm optimization (PSO)-based UAV trajectory algorithm, where priority is given to surveillance areas. Motivated by the inaccurate channel state information (CSI) at the transmitter side [13–15] address a twin-channel prediction-based CSI acquisition algorithm for UAV communications. Recently, a scalable idea of replacing terrestrial backhaul network with an aerial network is proposed, in which small cell base stations (SBs) will be routing the uplink/downlink traffic of cellular users via UAV-hubs to the ground core-network [16].

In [6, 17–19], the association (serving a group of network entities) of SBs with the UAVs is addressed for the idea given in [16]. On the one hand, on-demand deployment of UAVs in this kind of backhaul network will result in saving deployment cost constraints and time; however, on the other hand, their limited battery life or on-board energy levels cannot help them stay aloft for a prolonged time [20]. Therefore, notably, the UAVs will be replaced with the new ones when there is battery depletion in the older ones. This replacement of UAVs will greatly affect the overall network's performance in terms of delay for the ground users or SBs.

Considering such kind of network, in which UAVs are unable to provide the services to ground SBs due to their limited on-board energy levels, we propose an idea of collecting the information from the disaster-points (where a few UAVs went down or unavailable to provide services) with the help of one UAV in the uplink scenario of the network discussed in [6, 17–19]. This collection of information from ground SBs shall be delivered timely to the destination to avoid mismatch and is proposed as Age-of-Information (AoI) in the literature, which is defined as “the measure of the freshness of data” [21, 22]. AoI metric has become more important in the network, where live updates are needed to be delivered without any delay from the source (SBs) to the destination (ground core-network). Hence, in such kinds of scenarios, the trajectory of the UAV for the collection of data from different disaster-points plays a vital role.

In this book chapter, the optimum trajectory of a UAV is addressed to minimize the AoI within the context of our work discussed in [19]. Nevertheless, it is important to note that our proposed trajectory is also useful in the Internet of Things (IoT) environment [23, 24] for the collection of data from various IoT-based devices (e.g., smart transportation systems, smart homes and buildings). Specifically, we use three different kinds of trajectories to minimize the values of AoI metric. Firstly, we use

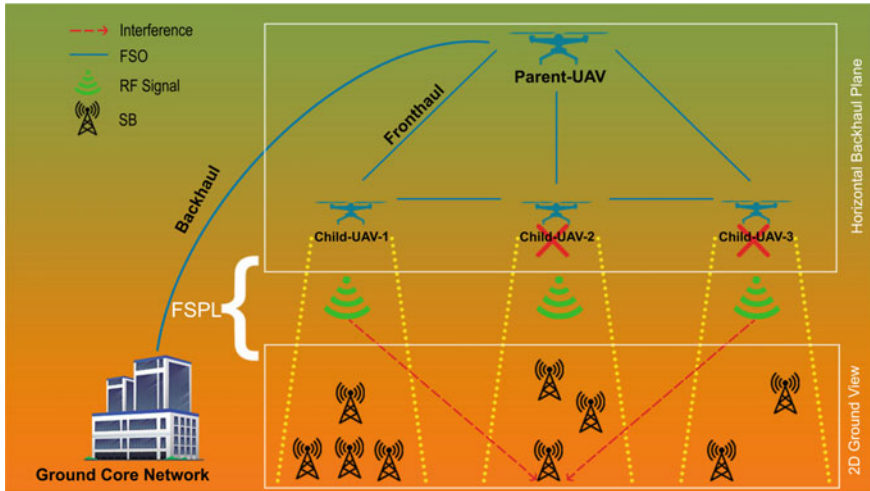


Fig. 1 Pictorial representation of a wireless backhaul network, where multiple UAVs are serving different SBs. Failure of different UAVs is marked with the cross sign

random trajectory for the collection of data, then we give the idea of using famous *travelling salesman problem (TSP)* as a UAV trajectory. Finally, we address *proposed trajectory* to meet the objective of minimizing AoI. Simulations show that for a smaller network, having few disaster-points, *proposed trajectory* gives better performance in terms of minimizing AoI and computation cost. Also, UAVs distribution used in [19] outperforms the one used in [17].

The remainder of the book chapter is organized as follows: In Sect. 2, we describe disaster scenario and path-loss model. In the same section, we also elaborate AoI and the algorithms to minimize AoI. Section 3 focuses on the outcomes of algorithms discussed in Sect. 2 and their computation cost. Additionally, it compares AoI with the types of UAVs distributions used in [17, 19]. The conclusion is given in Sect. 4 with some future outlooks.

2 System Model

2.1 Scenario

Consider the uplink scenario of a UAV-assisted heterogeneous network (HetNet), as shown in Fig. 1, where C child-UAVs are flying at an altitude H from the ground level to collect the uplink traffic of S ground SBs. A parent-UAV P is flying at an altitude higher than the child-UAVs, and it is connected with the child-UAVs via a free-space optical (FSO) link. The purpose of placing parent-UAV at a higher altitude

is to make an LoS connection with the child-UAVs and the ground core-network. Each child-UAV will directly send the collected information from its associated SBs to the parent-UAV. Further, parent-UAV is connected through a single-hop FSO link with ground core-network. Let us denote the set of child-UAVs as $\mathcal{C} \triangleq \{1, \dots, C\}$ and set of ground SBs as $\mathcal{S} \triangleq \{1, \dots, S\}$. Moreover, $\mathbf{c} \in \mathcal{C}$ has horizontal coordinate $\mathbf{u}_c = (s_c, t_c)$, with H altitude, and $\mathbf{s} \in \mathcal{S}$ has $\mathbf{v}_s = (x_s, y_s)$, with zero altitude.

We assume that in such a network, all the child-UAVs will not be providing the services all the time because of their low on-board energy levels. Therefore, we assume that $C - 1$ child-UAVs go down and the remaining only one child-UAV $\mathbf{c} \in \mathcal{C}$ has to collect the data from the rest of the points called as disaster-points, where $C - 1$ child-UAVs were serving previously. In the rest of the book chapter, we model our system by considering only one child-UAV $\mathbf{c} \in \mathcal{C}$.

2.2 Path-Loss Model

In the considered case, the distance from child-UAV \mathbf{c} , which will collect the data from the disaster-points, to the SB \mathbf{s} is

$$d_{\mathbf{c},\mathbf{s}} = \sqrt{H^2 + \|\mathbf{u}_c - \mathbf{v}_s\|^2}, \quad \mathbf{c} \in \mathcal{C}, \mathbf{s} \in \mathcal{S} \quad . \quad (1)$$

In addition, the probability of LoS, denoted by P_{LoS} , presented in [25, 26], is given as

$$P_{\text{LoS}} = \frac{1}{1 + \alpha \cdot \exp\{-\beta(\varphi - \alpha)\}} \quad , \quad (2)$$

where the values of α and β depend on the operational environment. Also, the elevation angle (measured in degrees) is represented by φ . It is important to note that $P_{\text{NLoS}} = 1 - P_{\text{LoS}}$.

Next, we consider the wireless channel between child-UAVs and SBs; therefore, we use the air-to-ground (ATG) path-loss model presented in [25, 26]. The total path-loss is written as

$$\Psi_{\mathbf{c},\mathbf{s}} = \text{FSPL} + P_{\text{LoS}} \cdot \zeta_{\text{LoS}} + P_{\text{NLoS}} \cdot \zeta_{\text{NLoS}}, \quad \mathbf{c} \in \mathcal{C}, \mathbf{s} \in \mathcal{S} \quad , \quad (3)$$

where free-space-path-loss (FSPL) is obtained as $\text{FSPL} = 20 \log_{10} \left(\frac{4\pi \cdot d_{\mathbf{c},\mathbf{s}}}{\lambda} \right)$, ζ_{LoS} and ζ_{NLoS} are the attenuation factors for the LoS and NLoS links, respectively.

The signal-to-noise ratio (ψ) of the \mathbf{s}^{th} SB at the \mathbf{c} child-UAV is written as

$$\psi_{\mathbf{c},\mathbf{s}} = \frac{\mu}{\sigma^2}, \quad \mathbf{s} \in \mathcal{S}, \mathbf{c} \in \mathcal{C} \quad , \quad (4)$$

where $\mu_{s,c} = \Omega_t - \Psi_{c,s}$ is the received power at child-UAV c from s^{th} SB, Ω_t is the transmit power of each SB, and σ^2 is the noise power between their communication link.

The outage probability (P_{out}) of each SB at child-UAV c can be calculated by comparing the received power with predefined threshold τ , which is formulated as

$$P_{out} = \mathbb{P}\{\mu < \tau\} \quad . \quad (5)$$

The uplink data rate is given by

$$R_{c,s} = w \cdot \log_2(1 + \psi_{c,s}) \quad , \quad s \in S, c \in C \quad . \quad (6)$$

where w is the available bandwidth to each SB to upload their data.

2.3 Age-of-Information (AoI)

AoI is the measure of the freshness of data at a particular base station. In other words, it means that how much collected information at time t is old after $t + 1$ time. Within the scope of our problem, we consider two types of AoI. The one because of movement of UAV from one disaster-point to other and here we call it as Age-of-Information due to the movement (AoI_M) and is calculated as

$$AoI_M = \frac{1}{v} \sum_{c \in C} d_{c,j} \quad , \quad (7)$$

where $d_{c,j}$ is the distance from the location of c child-UAV to j^{th} disaster point, v is the speed of child-UAV with which it moves from one disaster-point to the other, and C is the set of all disaster points to be visited. The other Age-of-Information is called as AoI_C, which is the age to collect the data, from s^{th} SB by c child-UAV at a particular disaster-point and is defined as

$$AoI_C = L \sum_{s \in S} \frac{1}{R_{s,c}} \quad . \quad (8)$$

It can be observed that the second age is dependent on the rate of each SB with which it sends the data to child-UAV and the size of the transmitted packet L of that SB. Therefore, our focus would be to minimize the first age in the rest of the book chapter.

The total Age-of-Information (AoI_T) by adding (7) and (8) is, therefore, given as

$$AoI_T = AoI_M + AoI_C \quad . \quad (9)$$

2.4 Algorithms for AoI Minimization

In the disaster scenario, where only one child-UAV is left to collect the uplink traffic of SBs, child-UAV \mathbf{c} moves to the first disaster-point and associates the SB with itself by using Equation (5). Afterwards, it collects the data from associated SBs and then moves to the next disaster-point. Our objective is to minimize AoI_M . Therefore, below we describe three algorithms to minimize this age.

2.4.1 Random Trajectory

In this algorithm, once the disaster has occurred, child-UAV \mathbf{c} moves to collect the information to the disaster-point next to it. In this method, child-UAV does not calculate distances to take its next turn; it simply moves to the next point and collects the information and from there to next and so on. Hence, in this way, child-UAV collects the data from all disaster-points and handovers to the parent-UAV P . Therefore, this trajectory of child-UAV for collection of data is called as *random trajectory*.

2.4.2 Travelling Salesman Problem's Trajectory

The *travelling salesman problem (TSP)*-based trajectory is the way in which child-UAV computes the minimum cost (distance) to its all disaster-points before starting the walk. In other words, it calculates the minimum cost in which child-UAV can cover all disaster-points. Therefore, in this trajectory, child-UAV makes intelligent decisions to collect the data from its disaster-points before leaving, which is commonly known as *TSP* [27].

2.4.3 Proposed Trajectory

In the *proposed trajectory*, we use the idea of minimum distance-based planning to meet the objective of minimizing AoI. In this trajectory, child-UAV calculates the distance from its initial point P_{init} to its disaster-points and then moves to the nearest neighboring point $P_{\text{init}+1}$ to collect the data and after collecting the data from $P_{\text{init}+1}$, the child-UAV again measures the distance at $P_{\text{init}+1}$ from un-visited disaster points; therefore, moves to the nearest neighbor, which is at the minimum distance from $P_{\text{init}+1}$. This is how the algorithm works until it visits all the disaster-points to collect the information, and at the last disaster-point, child-UAV handovers the collected information from all SBs to its parent-UAV P . Later on, parent-UAV sends the data to the ground core-network, which we do not consider in our work.

3 Simulation Results and Discussion

The area of 16 km^2 is considered, where the distribution of SBs is considered using *Matern type-I* hard-core process [28]. The intensity of SB and the distance between two SBs is ς and d_{\min} (in meters), respectively [19]. Next, in scenario-1, the child-UAVs are distributed using *Matern type-I* hard-core process used in [17], and in scenario-2, utilizing unsupervised learning used in [19]. Then one child-UAV c is kept, and the rest of them are removed because of the assumption that they went out of battery, and hence one remaining child-UAV c has to collect the data from the rest of the positions (disaster-points) where $C - 1$ child-UAVs were collecting the data previously. Table 1 shows the simulation parameters. The results are scrutinized using three trajectories, i.e., *random trajectory*, *TSP trajectory*, and *proposed trajectory*.

Figure 2 shows the 3D view of the distribution of disaster-points using an unsupervised learning-based algorithm and the optimal path is represented by using *TSP trajectory*. The disaster points are depicted by integers, where 1 represents the start position of a UAV. It can be observed that by using *TSP trajectory*, the optimal trajectory of a UAV for data collection is 9, 1, 4, and so on.

Table 1 Simulation parameters

Parameter	Value	Parameter	Value
λ	0.15 m	τ	-120 dB
α	9.61	σ	-125 dB
β	0.16	μ_{LoS}	1 dB
μ_{NLoS}	20 dB	L	100 Kb
ς	$2 \times 10^{-6} / \text{m}^2$	d_{\min}	250 m
v	20 Kmph	Ω_t	5 W

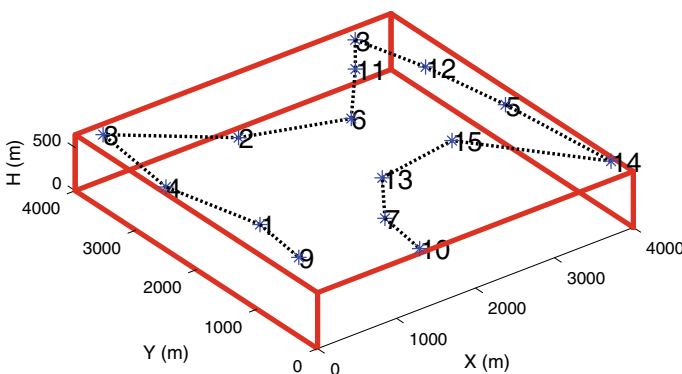


Fig. 2 Three dimensional (3D) view of distribution of disaster-points using unsupervised learning and optimal path of UAV for data collection using *TSP trajectory*

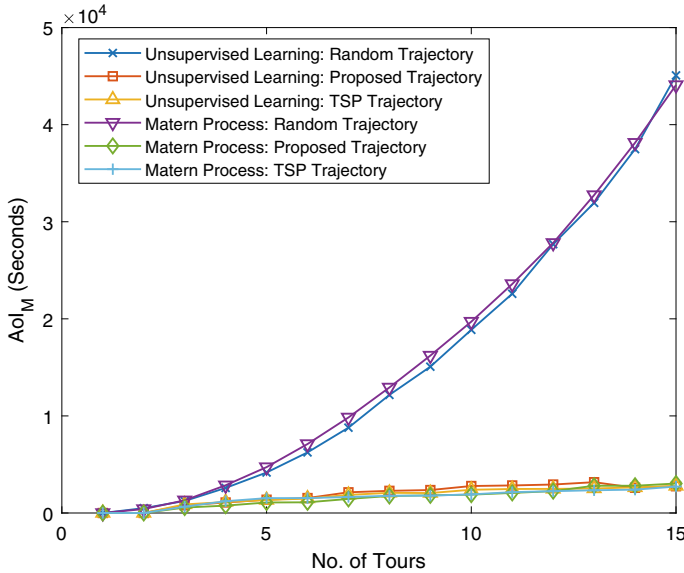


Fig. 3 Age-of-Information due to movement versus disaster-points in all trajectories

Figure 3 depicts that as more number of UAVs go into outage, then AoI_M for the collection of data increases, for one UAV. However, in the case of *random trajectory*, AoI_M increases exponentially, which means that data collected by this trajectory will be very old. On the other hand, AoI_M for the *proposed* and *TSP trajectory* increases very slowly, which is almost constant. However, there is a little difference in both the trajectories, which we evaluate in the next figure.

Figure 4 reveals that as the number of tours for the collection of data increases, *TSP trajectory* performs better in both types of UAVs distribution. However, for a smaller number of tours (up to 6), *proposed trajectory* has a smaller value of AoI_M , for both types of UAVs distribution, which is good if we consider the scenario of [19], where only four UAVs are present (and we assume that three are not serving because of battery depletion). Later in this section, we also evaluate the computation cost of both the trajectories to see the positive side of the *proposed trajectory*.

Figure 5 uncovers the positive side of using unsupervised learning-based UAVs distribution when the packet size is varied. The trend shows that as the uploading packet size L of SBs increases, AoI_C increases as well. However, AoI_C increases slowly in unsupervised learning-based distribution; on the other hand, it increases gradually in *Matern type-I* hard-core process-based UAVs distribution.

Finally, in Fig. 6, the trend for AoI_T can be observed, for both types of trajectories i.e., *TSP-based trajectory* and the *proposed trajectory*. It can be noticed that total Age-of-Information, AoI_T for the *proposed trajectory* is very less, which means that received data at the destination will be fresher. Conversely, *TSP trajectory* has higher value of AoI_T . Nonetheless, the curves for both the trajectories are almost constant,

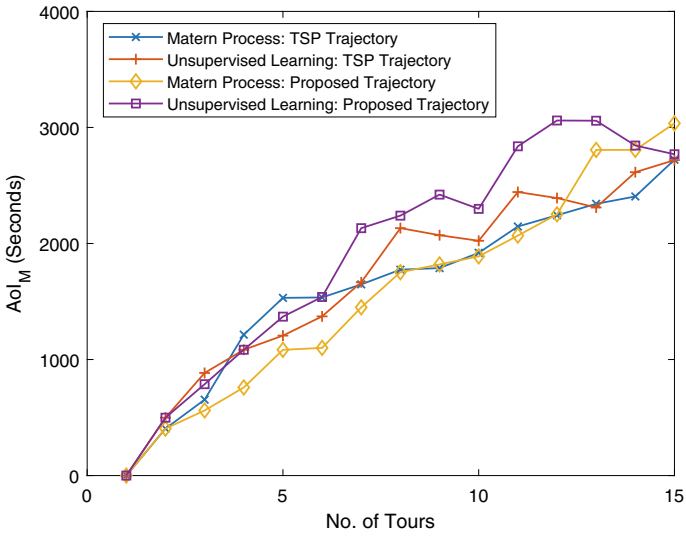


Fig. 4 Age-of-Information due to movement versus disaster-points in two trajectories

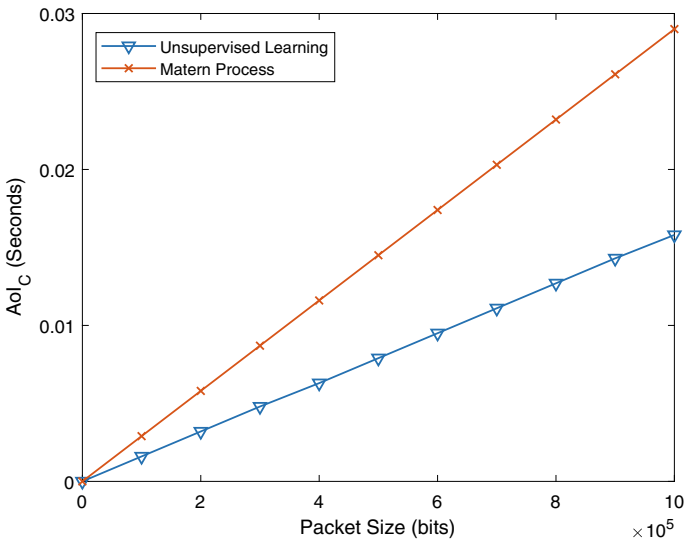


Fig. 5 Age-of-Information due to collection of data versus packet size in both distributions. (Disaster-Points 3)

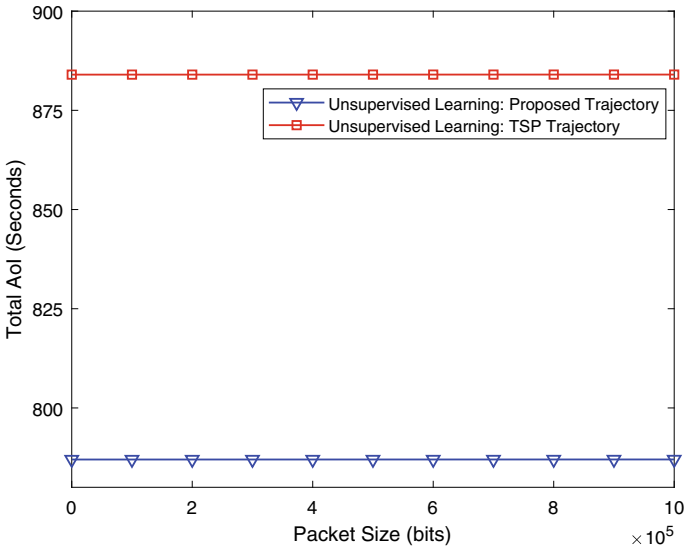


Fig. 6 Total AoI versus packet size using two trajectories. (Disaster-Points 3)

which is due to the reason that we kept disaster-points to three, and there is a very small increase (in milliseconds) in AoI_C ; therefore, when AoI_C adds up with a bigger value of AoI_M , then it does not make any big difference. Thus, curves are constant. In a nutshell, unsupervised learning-based UAVs distribution used in [19] gives better results for minimizing the overall AoI.

3.1 Computational Complexity

The computational complexity of both the trajectories is analyzed using the elapsed time for three disaster-points, which is a perfect fit in the worst-case scenario for the network used in [19]. Importantly, both the trajectories are implemented on MATLAB R2018a (Windows 10 platform). The laptop, core 2, had 4 logical processors clocked at 1 GHz and having RAM = 4 GB. It can be observed from Table 2 that unsupervised learning-based UAVs distribution achieves the better AoI, for both kinds of trajectories. Additionally, the *proposed trajectory* results in saving computation time up to 1.85 s. Similarly, in *Matern type-I* hard-core process-based UAVs distribution, firstly, the *proposed trajectory* saves AoI due to movement (AoI_M) up to 90 s. Secondly, the computational time of the *proposed trajectory* is also very little, which makes a difference of 1.3 s. In short, the *proposed trajectory* is beneficial in saving computation cost and AoI_M when we use unsupervised learning-based UAVs distribution and with *Matern type-I* process-based distribution, *proposed trajectory* not only saves the computation time but also AoI_M .

Table 2 Computational complexity of *TSP* and the *proposed trajectory* using 3 disaster-points

Method	AoI_C (S)	AoI_M (S)	Elapsed time (S)
Unsupervised learning: <i>Proposed</i>	1.6×10^{-3}	0.787×10^3	0.69
Unsupervised learning: <i>TSP</i>	1.6×10^{-3}	0.884×10^3	2.54
<i>Matern type-I</i> process: <i>Proposed</i>	2.9×10^{-3}	0.560×10^3	0.88
<i>Matern type-I</i> process: <i>TSP</i>	2.9×10^{-3}	0.654×10^3	2.18

4 Conclusions and Future Directions

In this book chapter, AoI minimization in UAV-assisted backhaul network is addressed. Initially, a few UAVs are collecting the uplink traffic of SBs, but due to battery depletion, three UAVs go in outage, we have one UAV to cover the entire region. Hence, in such kind of scenario, we tried to collect the information by using one UAV with the aim of minimizing AoI of the entire network. To minimize AoI, three different trajectories are used, that is, *random trajectory*, *travelling salesman problem's*-based trajectory, and the *proposed trajectory*. Numerical results showed that the unsupervised learning-based UAVs distribution resulted in saving AoI than using the *Matern type-I* based UAVs distribution. Additionally, the *proposed trajectory* is computationally less expensive than the *TSP trajectory*. Further, the *proposed trajectory* has given better values of AoI due to mobility for a fewer number of visits.

In this book chapter, focus was solely on the minimization of age due to the mobility of a UAV. In the future, we will also address minimization of age due to the collection of data. In addition to this, we will focus on providing a comprehensive analysis of different UAV trajectories proposed in the literature, e.g., PSO.

References

1. Fitzpatrick A (2018) The drone age, May 2018. <https://time.com/longform/time-the-drone-age>
2. Cheema MA, Shehzad MK, Qureshi HK, Hassan SA, Jung H (2021) A drone-aided blockchain-based smart vehicular network. *IEEE Trans Intell Transp Syst* 22(7):4160–4170
3. Shakoor S, Kaleem Z, Baig MI, Chughtai O, Duong TQ, Nguyen LD (2019) Role of UAVs in public safety communications: energy efficiency perspective. *IEEE Access* 7:140 665–140 679
4. Naqvi SAR, Hassan SA, Pervaiz H, Ni Q (2018) Drone-aided communication as a key enabler for 5G and resilient public safety networks. *IEEE Commun Mag* 56(1):36–42
5. Kaleem Z, Yousaf M, Qamar A, Ahmad A, Duong TQ, Choi W, Jamalipour A (2019) UAV-empowered disaster-resilient edge architecture for delay-sensitive communication. *IEEE Netw* 33(6):124–132

6. Shehzad MK, Ahmad A, Hassan SA, Jung H (2021) Backhaul-aware intelligent positioning of UAVs and association of terrestrial base stations for fronthaul connectivity. *IEEE Trans Netw Sci Eng* 8(4):2742–2755. <https://doi.org/10.1109/TNSE.2021.3077314>
7. Shakoor S, Kaleem Z, Do D-T, Dobre OA, Jamalipour A (2021) Joint optimization of UAV 3-D placement and path-loss factor for energy-efficient maximal coverage. *IEEE Int Things J* 8(12):9776–9786
8. Shehzad MK, Akhtar MW, Hassan SA (2021) Performance of mmWave UAV-assisted 5G hybrid heterogeneous networks, pp 97–118. <https://onlinelibrary.wiley.com/doi/abs/10.1002/9781119751717.ch6>
9. Do-Duy T, Nguyen LD, Duong TQ, Khosravirad S, Claussen H (2021) Joint optimisation of real-time deployment and resource allocation for UAV-aided disaster emergency communications. *IEEE J Sel Areas Commun* 1–1
10. Nguyen KK, Vien NA, Nguyen LD, Le M-T, Hanzo L, Duong TQ (2021) Real-time energy harvesting aided scheduling in UAV-assisted D2D networks relying on deep reinforcement learning. *IEEE Access* 9:3638–3648
11. Do D-T, Nguyen T-TT, Le C-B, Voznak M, Kaleem Z, Rabie KM (2020) UAV relaying enabled NOMA network with hybrid duplexing and multiple antennas. *IEEE Access* 8:186 993–187 007
12. Teng H, Ahmad I, Msm A, Chang K (2020) 3D optimal surveillance trajectory planning for multiple UAVs by using particle swarm optimization with surveillance area priority. *IEEE Access* 8:86 316–86 327
13. Shehzad MK, Rose L, Assaad M (2021) A novel algorithm to report CSI in MIMO-based wireless networks. In: *ICC 2021—IEEE international conference on communications*, pp 1–6
14. Shehzad MK, Rose L, Assaad M (2021) “Dealing with CSI compression to reduce losses and overhead: an artificial intelligence approach. In: *IEEE international conference on communications workshops (ICC Workshops) 2021*:1–6
15. Shehzad MK, Rose L, Assaad M (2021) RNN-based twin channel predictors for CSI acquisition in UAV-assisted 5G+ networks. *IEEE GLOBECOM*, pp 1–6
16. Alzenad M, Shakir MZ, Yanikomeroglu H, Alouini M-S (2018) FSO-based vertical backhaul/fronthaul framework for 5G+ wireless networks. *IEEE Commun Mag* 56(1):218–224
17. Shah SAW, Khattab T, Shakir MZ, Khafagy MG, Hasna MO (2018) Small cell association with networked flying platforms: novel algorithms and performance bounds. [arXiv:1802.01117](https://arxiv.org/abs/1802.01117)
18. Shehzad MK, Hassan SA, Luque-Nieto M, Poncela J, Jung H (2020) Energy efficient placement of UAVs in wireless backhaul networks. In: *Proceedings of the 2nd ACM MobiCom workshop on drone assisted wireless communications for 5G and beyond*, pp 1–6
19. Shehzad MK, Hassan SA, Mahmood A, Gidlund M (2019) On the association of small cell base stations with UAVs using unsupervised learning. In: *IEEE vehicular technology conference (VTC-Spring)*, May 2019
20. Zeng Y, Zhang R (2017) Energy-efficient UAV communication with trajectory optimization. *IEEE Trans Wirel Commun* 16(6):3747–3760 June
21. Kaul S, Gruteser M, Rai V, Kenney J (2011) Minimizing age of information in vehicular networks. In: *2011 8th annual IEEE communications society conference on sensor, Mesh and Ad Hoc communications and networks*. IEEE, pp 350–358
22. Kaul S, Yates R, Gruteser M (2012) Real-time status: how often should one update? In: *Proceedings IEEE INFOCOM*. IEEE, pp 2731–2735
23. Wortmann F, Flüchter K (2015) Internet of things. *Bus Inf Syst Eng* 57(3):221–224
24. Abbas Q, Hassan SA, Pervaiz H, Ni Q (2021) A Markovian model for the analysis of age of information in IoT networks. *IEEE Wirel Commun Lett*
25. Al-Hourani A, Kandeepan S, Jamalipour A (2014) Modeling air-to-ground path loss for low altitude platforms in urban environments. In: *IEEE GLOBECOM*, pp 2898–2904
26. Al-Hourani A, Kandeepan S, Lardner S (2014) Optimal LAP altitude for maximum coverage. *IEEE Wirel Commun Lett* 3(6):569–572
27. Dantzig G, Fulkerson R, Johnson S (1954) Solution of a large-scale traveling-salesman problem. *J Oper Res Soc Am* 2(4):393–410
28. Matérn B (2013) Spatial variation. Springer Science & Business Media, p 36

Enhancing UAV-Based Public Safety Networks with Reconfigurable Intelligent Surfaces



Wael Jaafar, Lina Bariah, Sami Muhaidat, and Halim Yanikomeroglu

Abstract Recently, reconfigurable intelligent surface (RIS) has emerged as a 6G enabling technology, which is capable of enhancing communication reliability, extending coverage, and improving security, while maintaining high energy and spectral efficiency. RIS comprises a number of artificially engineered meta-atoms that achieve diverse functionalities, including beam shaping, signal splitting, reflection, absorption, and polarization. These functionalities shed the light on the advantageous integration of RIS into future wireless networks. Specifically, integrating RIS into unmanned aerial vehicle (UAV) networks can be attractive, in the sense that RIS and UAV networks are intertwined, i.e., being enabled by each other. In fact, RIS-equipped UAVs can flexibly move in the 3D space to achieve panoramic full-angle signals manipulation, while UAV users may rely on the available RISs within the environment in order to operate securely, at extended ranges, and with reduced communication and energy costs. Consequently, the integration of RIS with UAV networks is advocated as a key enabler for critical public safety services, where highly resilient, reliable, secure, and low latency communications are mandatory. In this chapter, we aim to articulate the fundamentals, design aspects, and applications of RIS as an enabling technology for future wireless networks. Furthermore, we will present an in-depth discussion about the integration of RIS into UAV networks, with emphasis on the mechanisms, advantages, and related challenges. Finally, practical

W. Jaafar · S. Muhaidat · H. Yanikomeroglu

Department of Systems and Computer Engineering, Carleton University, Ottawa, ON K1S 5B6, Canada

e-mail: waeljaafar@sce.carleton.ca

S. Muhaidat

e-mail: muhaidat@ieee.org

H. Yanikomeroglu

e-mail: halim@sce.carleton.ca

L. Bariah (✉) · S. Muhaidat

KU Center for Cyber-Physical Systems, Khalifa University, Abu Dhabi, United Arab Emirates

e-mail: lina.bariah@ieee.org

L. Bariah

Electrical and Computer Engineering Department, University at Albany, Albany, NY 12222, USA

© The Author(s), under exclusive license to Springer Nature Singapore Pte Ltd. 2022

145

Z. Kaleem et al. (eds.), *Intelligent Unmanned Air Vehicles Communications for Public Safety Networks*, Unmanned System Technologies,

https://doi.org/10.1007/978-981-19-1292-4_7

public safety related use cases will be studied, providing performance insights and future research directions.

Keywords Reconfigurable intelligent surface · RIS · Unmanned aerial vehicle · UAV · Phase-shift · Public safety

1 Introduction

The speculative vision of future sixth-generation (6G) wireless networks is tailored for provisioning massive-scale ubiquitous connectivity, with the aim to cater for the massive increase in the number of connected devices. This explosive growth is a consequence of the emergence of novel data-hungry applications, which require seamless on-demand wireless connectivity, with guaranteed high-reliability and ultra-low latency requirements [1]. Such applications call for the development of efficient technologies to provide enhanced connectivity, in order to cover wider areas at the earth, from urban and suburban to rural areas, and therefore, support a wider range of new use cases. Over the last decade, unmanned aerial vehicle (UAV) networks has attracted a considerable attention from the research and industrial communities. This stimulated from the evolution of aerial-based applications that are supported by UAV networks, including security inspection, packet delivery, traffic control, as well as connectivity support to rural and disaster-hit areas [2]. The ability of UAVs to fly in a three-dimensional (3D) space with flexible altitudes, in the range of few hundred meters, enables them to realize a 360° panoramic full-angle communication, and hence, provide on-demand backhaul connectivity to ground nodes, fronthaul links for aerial nodes, and an interface between satellite and ground networks. Energy efficiency constitutes a major limiting factor in the design of efficient UAV networks, given their limited on-board battery capacity, which limits the flying time between a few minutes and a few hours. This is particularly pronounced when the UAV acts as a flying base station (BS) or an amplify-and-forward (AF) relay, due to the increased amount of consumed power needed for signals generation, transmission, and processing. Extensive research efforts have approached the energy efficiency issue, with the aim to enable UAVs to enjoy uninterrupted long flying time and to widen the range of functionalities supported by flying BSs and relays.

Motivated by the recent advancement in the field of reconfigurable intelligent surfaces (RISs), RIS-enabled UAV networks have emerged as a promising candidate in order to realize energy-efficient, reliable, cost effective, and low-complex wireless communication at the sky [3]. In addition to the earlier mentioned features, the integration of RIS into aerial networks was motivated by other several advantages offered by these intelligent surfaces. Inspired by their basic operational principle, RISs promise to offer enhanced reliability to UAV-supported ground communication, by ensuring the availability of a line-of-sight (LoS) link between the UAV and terrestrial nodes. It is worth recalling that the existence of a LoS is essential for the realization of efficient aerial-ground communication. Such links might be unavail-

able or blocked by an obstacle, particularly in crowded urban areas. Furthermore, the utilization of an RIS, mounted at the UAV, enables the UAV to extend its coverage area, by employing a number of functionalities supported by the RIS, e.g., wave focusing and splitting. This attractive property can be significantly boosted by the employment of a larger number of reflective elements (REs), which are the main building blocks of an RIS [4].

1.1 RIS-Enabled UAVs for Public Safety Networks

Public safety networks are a critical type of wireless networks that are essential for emergency scenarios such as, fires or natural disasters, and are characterized by their fast deployment, guaranteed coverage and energy supply, availability, low latency, and adaptivity. UAV networks have been extensively studied in the literature as key enablers for public safety networks. This is motivated by the swift deployment, the availability of a line-of-sight (LoS) communication, the availability of on-demand 360° panoramic full-angle communication, and the scalability features offered by UAV systems, which perfectly fit the needs of public safety networks. Nevertheless, the limited battery capabilities and the short communication distances constitute a limiting factor in the deployment of UAV networks for public safety communications. In this regard, the integration of RIS into UAV networks represents an appealing solution for public safety systems. This is motivated by the seamless, flexible, wide-coverage, and reliable communication that can be offered by RIS-aided UAV networks to the first responders (FRs) when an emergency occurs, either in urban or rural areas. Furthermore, various RIS functionalities can be exploited to enable enhanced signal strength and hence, longer communication distances. Inspired by this, the aim of this chapter is to lay down the fundamentals of RIS-enabled UAV networks, as an enabler for resilient and low-latency communication in public safety networks. In particular, the main chapter contributions can be summarized as follows:

- Articulate the fundamentals of RIS-enabled wireless networks, in addition to a thorough discussion on metasurfaces, trade-offs between RIS and relaying systems, and path-loss modeling. In the latter, we investigated the 3GPP models for terrestrial and non-terrestrial networks.
- Study the integration of RIS into UAV wireless networks. In particular, we will shed lights on the fundamentals, advantages, and major limitations of RIS-assisted and RIS-equipped UAV systems.
- To demonstrate the performance of RIS-assisted and RIS-equipped UAV communications, we present two case studies as enablers for surveillance and search-and-rescue applications, where we investigate the related achievable data rate performance.
- We highlight potential limitations of RIS-enabled UAV networks and sketch the road-map toward future research directions.

2 Chapter Outline

This chapter is organized as the following. In Sect. 3, we present the fundamentals of RIS technology, an in-depth discussion about metasurfaces, and a thorough comparison between RIS-enabled and relaying networks. We further present the path-loss modeling, including the 3GPP model, of RIS-assisted wireless networks, for terrestrial and non-terrestrial scenarios. Section 4 extensively presents the basic principles, advantages, and limitations of the integration of RIS into UAV networks, with considering two scenarios, namely, RIS-assisted and RIS-equipped. The efficiency of adopting RIS-enabled UAVs as an enabler for public safety networks is demonstrated in Sect. 4, in which simulation results are presented. The chapter is concluded in Sect. 5 in which we highlight major challenges in RIS-enabled UAVs for public safety networks, and point out potential future research directions.

3 Reconfigurable Intelligent Surface

The ongoing deployment of the fifth generation (5G) wireless networks has raised serious debates on whether 5G networks will be capable of delivering the promising vision built over the last few years. Particularly, it has become evident that the advancements offered by 5G networks follow similar trends as the ones brought by their predecessors [1]. This means that, albeit the remarkable performance enhancement introduced, in terms of data rate, spectral and energy efficiency, connected devices, coverage, and capacity, to name a few, 5G wireless networks have failed to realize breakthrough technological trends that promised to capture the ever-growing stringent requirements of future wireless networks, which aim to enable ubiquitous, secure, unified, self-sustainable, and fully-intelligent platforms. Through the solidification process of the 5G standardization and commercialization, the lights were shed on the development of enhancing technologies for improved signals transmission and reception, with emphasis on the design of novel transmitters and receivers. Meanwhile, due to the highly stochastic nature of wireless channels, the propagation environments remain unlikely amenable to control. However, such randomness causes severe signal fluctuation and uncontrollable interference attributed to signals scattering, reflection, and diffraction, rendering it a critical limiting factor in the design of future wireless networks. In light of this, academic and industrial efforts have been initiated in order to explore the potentials of 6G wireless networks, which are envisioned to enable two main principles, namely, softwarization and virtualization, with the aim to conceptualize smart and adaptive radio environment paradigms [5]. In smart radio scenarios, the propagation environment are anticipated to be aware of the undergoing signals transmission, enabling self-optimization and adaptation functionalities.

With the revolutionary solid-state progression and the visualization of software-defined networks (SDNs), RISs, a.k.a intelligent reflective surfaces, have recently

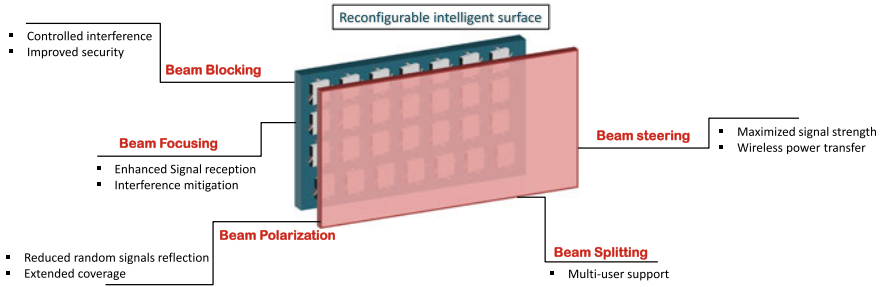


Fig. 1 Enabled functionalities by an RIS

emerged as a disruptive energy and spectrally efficient technology and an appealing candidate for 6G wireless networks [6–8]. In particular, RIS has been promoted as an innovative paradigm that is capable of offering a programmable control over the wireless propagation environment. Such features can be realized by employing an array of reconfigurable elements, referred as Metasurfaces, which enjoy unique electromagnetic (EM) properties, allowing them to enable desirable reactions when interacting with incident wireless signals. Specifically, based on the system requirements, the RIS can enable a number of engineered functionalities, including beam focusing, absorption, imaging, scattering, and polarization [9], as depicted in Fig. 1. These functionalities can be exploited to achieve particular network goals. For example, beam splitting can be utilized to enable multi-user support, while beam blocking can assist with enhancing the security and maintaining a controlled level of interference. Furthermore, beam focusing and steering can play a role in enhancing the received signal strength, mitigating interference, and enabling wireless power transfer. Extended coverage and controlled random signals reflection can be achieved by beam polarization functionality. Owing to these proactive features, RIS has become an attractive point of interest, which, according to research, can offer the following advantages. (i) Simple and flexible deployment, due to the exploitation of near-passive elements and given the fact that these smart surfaces can be mounted on building facades, aerial platforms, vehicles, etc. (ii) Spectral efficiency, (iii) energy efficiency, and (iv) compatibility [10].

3.1 Metasurfaces: The Building Block of Intelligent Surfaces

While signals reflection through a regular reflective surface follows Snell’s law, the key principle of RIS follows the generalized Snell’s law, where the angles of reflection do not necessarily match the angles of arrival. Rather, an RIS manipulates the incident signal phase in order to direct/split/polarize/focus the impinging signal into a desired direction with an adjusted amplitude [6]. Such alteration in the EM properties of wireless signals establishes a novel link between the physical dimension and the digital

world, rendering RIS an attractive technology for future wireless communications. In the following, we detail the fundamentals that enable such intelligent surfaces to manipulate the wireless signals in a man-made manner. Reconfigurable intelligent surfaces are made of a number of metasurfaces, which enjoy sub-wavelength thickness and can potentially function over a wide range of frequencies, spanning from the microwave band to the visible light [11]. A metasurface is regarded as a two-dimensional artificially structured array of metallic or dielectric substrates, enabling them to exhibit unique EM behavior, at the macroscopic level, and therefore, transform the impinging EM signals in various ways [5]. In particular, the RIS interaction with the incident EM waves relies on the design of the meta-atoms (which are the basis of metasurfaces), as well as the arrangement of the substrates, in which they can be organized in patches, strips, or crosses. In more details, meta-atoms experience customized and featured permittivity and permeability characteristics, that are not observed in materials found in the nature. Meta-atoms can be classified into static and dynamic designs, where the latter is equipped with an external switching element. Note that even with a simple ON/OFF switches, dynamic meta-atoms architecture is still capable of enabling an attractive range of functions. In general, the response of the meta-atoms is determined based on the inducted current when an EM wave arrives at the metasurface. In a static architecture, the resultant current pattern at the metasurface is defined by the meta-atoms geometry and composition. Similar factors affect the current patterns in dynamic architectures, in addition to the switches states [12]. Therefore, a more adaptive and fully controllable metasurface can be realized by the dynamic design of the meta-atoms, which can be achieved by properly adjusting the switches, in order to manipulate the meta-atoms permittivity and permeability, and hence, achieve the required macroscopic EM behavior [12].

3.2 *RIS Versus Relaying Systems*

Generally speaking, RIS can be regarded as an enhanced AF relay, in which power amplifiers are eliminated, and therefore, incident signals can be amplified/adjusted without consuming high energy, rather, by employing a large number of REs. In particular, from an energy efficiency perspective, it was proven that RIS can act as a full-duplex multiple-input multiple-output (MIMO) relay, whereas from the spectral efficiency angle, the performance of RIS is comparable with a half-duplex relay. However, self-interference experienced in full-duplex relays does not exist in the RIS, rendering RIS as an energy efficient alternative to relaying networks [13]. On a different note, by recalling that RISs comprise passive or semi-passive elements, RIS enjoys higher deployment flexibility, compared to relaying networks. Furthermore, it was demonstrated that, under the assumption that the LoS component is unavailable, the RIS outperforms AF relays, in terms of average signal-to-noise ratio (SNR), outage probability, and ergodic capacity, even when employing a few number of REs [14]. Nevertheless, with respect to average error rate, the performance of an RIS and AF relay was shown to be comparable, when employing a single RE. For a significant

enhancement to the system reliability, a larger number of REs can be leveraged with the aim to improve the achievable diversity order, and hence, remarkably reduce the average error rate.

On a different manner, it was revealed that a decode-and-forward (DF) relay would require less transmission power in order to achieve low rate, compared to an RIS. This is particularly observed when the RIS has a low number of REs [15]. Yet, as the number of REs increases and the receiver becomes closer to the transmitter or the RIS, the required transmit power for RIS-enabled networks becomes comparable to the DF relay scenario. On the other hand, in order to achieve higher rates when the transmitter-receiver distance is short, the DF relay consumes higher energy, compared to an RIS. Therefore, it can be concluded that for the case of a DF relay, the key is the number of reconfigurable elements. In specific, an RIS can outperform a DF relay when hundreds of reconfigurable elements are employed. In this regard, it is worth highlighting that, even with hundreds of elements, the RIS will be physically small, given that each element has a sub-wavelength size [15].

3.3 Path Loss Modeling in RIS-Enabled Systems

The utilization of RIS is particularly appealing for the cases when direct links between transmitters and receivers are blocked or weak. Therefore, the employment of a RIS introduces a reliable link to support and strengthen direct transmissions or to establish a reliable communication when the direct link is unavailable.

Recent research studies have demonstrated that large-scale fading in RIS-assisted networks can be modeled as free-space path-loss, in which the effect of scattering, reflection, and shadowing are neglected [10], and under the assumption that the RIS is either electrically large or small, i.e., the size of the RIS with respect to the wavelength [16–18]. In particular, the proposed models in the literature are intended to capture the relationship between the path-loss and the RIS size and distance from the transmit/receive nodes. In the following, we present the path-loss model of two scenarios, namely, near-field and far-field. Note that near-field scenario represents the case when the RIS is close to both the transmitter and receiver, or its dimensions are relatively large, i.e., width and length are 10 times larger than the wavelength (λ). On the other hand, far-field denotes a small RIS scenario, or when both the transmitter and receiver or one of them is far from the RIS. Hence, assuming W and L denote the width and the length of an RIS comprises N REs, the n th end-to-end path-loss for a near-field scenario, with respect to the RIS dimensions, can be given by [18]

$$PL_{\text{near}} = \sqrt{G_t G_r} \left(\frac{\lambda}{4\pi d_0} \right) \left[\left(\frac{d_0}{d_{\text{tr}}} \right)^{\frac{\alpha}{2}} + \left(\frac{d_0}{d_{\text{tn}} + d_{\text{nr}}} \right)^{\frac{\alpha}{2}} \rho_n \exp[-j(\theta_i + \theta_r)] \right] \quad (1)$$

where G_t and G_r denote the transmit and receive antennas gains, and d_0 and α account for the reference distance and path-loss exponent, respectively. Also, d_{tr} , d_{tn} and d_{nr} represent the transmitter-receiver, transmitter- n th RE and n th RE-receiver distances, respectively. The n th RE response is represented by the gain ρ_n , while the incident and reflection angles are given by θ_i and θ_r , respectively. Assuming perfect signal reflection with ideal phase-shift, the n th RE reflection gain can be normalized to unity, i.e., $\rho_n = 1$, while the n th phase-shift can be set to zero, $\theta_i + \theta_r = 0$. Note that for the near-field scenario, the RIS acts as an anomalous reflector, and therefore, the path-loss is affected by the summation of the traveling distances of the two links. On the other hand, for the the far-field scenario, in which each RE acts as a scatterer, the end-to-end path-loss is affected by the cascaded distances over the two links. The far-field path-loss through the n th RE can be modeled as the following

$$PL_{\text{far}} = \sqrt{G_t G_r} \left(\frac{\lambda}{4\pi d_0} \right)^2 d_0^\alpha \left(\frac{\rho_n \exp[-j(\theta_i + \theta_r + \phi_n)]}{(d_{tn} d_{nr})^{\alpha/2}} \right) \quad (2)$$

where ϕ_n denotes the adjusted phase-shift at the n th RE.

3GPP Path-Loss Model In RIS-assisted wireless networks, the RIS can be placed at the building facades, advertisement signs, traffic signals, etc. Therefore, in the following, we present the 3GPP path-loss model of RIS-assisted wireless transmission in urban environments. The total path-loss experienced over the BS-RIS link can be evaluated as the following [19]

$$PL_{i-j} = \mathcal{P}^{\text{LoS}} PL_{i-j}^{\text{LoS}} + (1 - \mathcal{P}^{\text{LoS}}) PL_{i-j}^{\text{NLoS}}, \quad (3)$$

where \mathcal{P}^{LoS} is the LoS probability, PL_{i-j}^{LoS} and PL_{i-j}^{NLoS} are the associated losses in the LoS and NLoS conditions between communicating devices i and j , such that $(i, j) \in \{\text{BS}, \text{RIS}\}$.

Assuming that the RIS devices equipping the building are installed below 23 m (i.e., up to 7 floors buildings), the LoS probability between devices i and j can be expressed by [19, Table 7.4.2-1]

$$\mathcal{P}^{\text{LoS}} = \begin{cases} 1 & \text{if } d_{i-j}^{2D} \leq 18 \text{ m} \\ \left(\frac{18}{d_{i-j}^{2D}} + \exp\left(-\frac{d_{i-j}^{2D}}{63}\right) \left(1 - \frac{18}{d_{i-j}^{2D}}\right) \right) & \\ \times \left(1 + f(h_j) \frac{5}{4} \left(\frac{d_{i-j}^{2D}}{100}\right)^3 \exp\left(-\frac{d_{i-j}^{2D}}{150}\right)\right) & \text{if } d_{i-j}^{2D} > 18 \text{ m}, \end{cases} \quad (4)$$

where d_{i-j}^{2D} is the 2D separating distance (projected on the ground) between devices i and j in m, $(i, j) \in \{\text{BS}, \text{RIS}\}$, and $f(h_j)$ is given by

$$f(h_j) = \begin{cases} 0 & \text{if } h_j \leq 13 \text{ m} \\ \left(\frac{h_j-13}{10}\right)^{1.5} & \text{if } 13 \text{ m} < h_j \leq 23 \text{ m}, \end{cases} \quad (5)$$

while the path-loss for LoS and NLoS communication links are written by [19, Table 7.4.1-1]:

$$PL^{\text{LoS}} = 28 + 22 \log(d_{i-j}) + 20 \log(f) + X \quad (6)$$

and

$$PL^{\text{NLoS}} = \max\left(PL^{\text{LoS}}, \bar{P}L^{\text{NLoS}}\right) \quad (7)$$

where

$$\bar{P}L^{\text{NLoS}} = 13.54 + 39.08 \log(d_{i-j}) + 20 \log(f) - 0.6 (h_j - 1.5) + X, \quad (8)$$

d_{i-j} is the 3D distance between devices i and j in m, f is the carrier frequency in GHz, and h_j is the RIS altitude (measured from the middle point for RIS). Also, X represents a log-normal random variable denoting the shadow fading, with standard deviation equals to $\sigma = 4$ dB and $\sigma = 7.8$ dB for LoS and NLoS, respectively.

Finally, assuming that the UAV flying altitude is regulated under 150m, the link between the RIS and the UAV can be represented by the air-to-ground 3GPP model [20]

$$PL_{\text{RIS-UAV}} = 28 + 22 \log_{10}(d_{\text{RIS-UAV}}) + 20 \log_{10}(f) + X_{\text{UAV}}, \quad (9)$$

where X_{UAV} is the normally distributed shadow fading with deviation $\sigma = 4.64 e^{-0.0066 h_{\text{UAV}}}$ in the urban environment.

4 Integration of RIS into UAV Networks: A Review

As studied in [8], RIS is capable of improving the received SNR and the latter increases quadratically when the number of RIS reflecting elements doubles. Such interesting performances, combined with the small payload of RIS compared to active communication equipment has motivated the integration of RIS in aerial platforms, in particular with UAVs. This integration can be identified in two types: First, RIS-assisted UAVs, where RIS mounted on objects, such as buildings facades, vehicle roofs, and towers, can be used to assist UAVs to sustain their beyond visible LoS (BVLoS) communications, i.e., UAVs are controlled without a direct command and control (C&C) link between the pilot and the UAV, to bypass obstacles in their communications with ground users/devices, or to secure such communication links [21–23]. Second, A UAV can be equipped with an RIS in order to reduce on-board payload and save battery usage, while providing efficient communications to ground devices [18, 24–26]. These types are further explained below.

4.1 RIS-Assisted UAV Systems

Assisting UAV communications through RIS has received a lot of attention recently. In [21], the authors investigated the joint problem of UAV trajectory and RIS's passive beamforming design aiming to maximize the average received data rate at a ground user served through the RIS and UAV in a multi-hop fashion. As in [21], the authors of [27] focused on UAV trajectory design and phase shifts optimization, targeting to maximize the sum data rate of a group of ground users. Due to the non-convexity of the problem, an alternating optimization (AO) method, which decomposes the problem into two sub-problems, is developed. Given optimal phase shifting, UAV trajectory design is solved using the successive convex approximation method. Results validate the superiority of the proposed approach compared to benchmarks. Moreover, Yang et al. studied in [22] a similar system, where they derived the analytical expressions of outage probability and average bit error rate (BER). Obtained results demonstrate the advantageous use of the RIS to improve the coverage and reliability of the UAV communication system. Also, authors of [28] extended the previous works to the use of multiple RIS devices and in the mmWave frequency band. Given predefined UAV flying trajectory and minimum QoS requirements, they jointly optimized the deployment, user scheduling, and phase shifting of RIS. An AO-based approach is developed, which is shown to provide superior sum data rate performance than deployments without RIS/UAV optimization. In addition to communication purposes, RIS can be used to assist mobile edge computing (MEC) services in the sky, i.e., by allowing MEC-enabled UAVs to provide computation to ground users through the RIS. In that matter, Mei et al. investigated in [29] the related problem of joint UAV-trajectory, task/cache design, and phase shifts optimization, aiming to maximize the energy-efficiency of the MEC system. The non-convex problem is solved using a sub-optimal successive convex approximation (SCA), and numerical results showed a substantial performance increase compared to benchmarks. Liu et al. developed in [30] an RIS/UAV integration framework, where RIS is deployed to assist a UAV in serving ground users through the non-orthogonal multiple access (NOMA) scheme. Energy minimization problem was formulated, where UAV trajectory, RIS phase shifting, and NOMA power allocation are jointly optimized. Due to the non-convexity of the problem, the authors proposed a reinforcement learning solution, based on decaying deep-Q-network. Through simulations, they demonstrated that their method converges faster than conventional Q-learning. Also, UAV's energy consumption is significantly reduced by integrating RIS into the system. Finally, dynamically optimizing the NOMA decoding order and power allocation allows to decrease energy consumption by 11.7% compared to the benchmark without NOMA. Finally, from the security perspective, Li et al. investigated in [23] the maximization of the average worst-case secrecy rate, defined as the difference in data rates between the communication of a legitimate user and that of an eavesdropper. The authors studied the joint design of the UAV trajectory, RIS phase shifting, and transmit powers of legitimate ground users. Due to the non-convexity of this problem, an AO approach is proposed, where three sub-problems

were formulated and solved using the SCA, \mathcal{S} -Procedure, and semi-definite relaxation (SDR), respectively. Obtained results confirmed the robustness of the proposed solution, and showed its significant average secrecy rate gain compared to baseline algorithms. These works are summarized in Table 1.

4.2 *RIS-Equipped UAV Systems*

The idea of equipping UAVs with RIS, called RIS-UAV, is mainly driven by the UAV motion flexibility to establish strong LoS links with ground devices, thus saving transmit power. Also, due to the typically limited payload and power of UAVs, which may not be able to carry and operate efficiently heavy radio-frequency (RF) transceivers, using RIS instead allows to reduce energy costs. This vision has been first proposed in [25] where it was demonstrated that an RIS-UAV can extend the coverage area of terrestrial BSs, thus filling the coverage holes and meeting users' high-speed broadband needs. In such scenarios, a ground control station is responsible for sending the required configurations allowing the onboard RIS controller to configure RIS phase shifts and direct signals towards the targeted receivers. The same authors conducted in [18] a rigorous link budget analysis for RIS-mounted aerial platforms, including UAVs, high-altitude platforms (HAPS), and low-earth orbit (LEO) satellites. Their results draw insights and guidelines about the use of RIS in aerial platforms. Specifically, it was shown that (1) the RIS-UAV performance is independent from the operating frequency when maximal number of REs is used, (2) with high receiver antenna gain, RIS-UAV data rate is close to that of other platforms, and (3) best data rates are achieved when the RIS-UAV is close to the ground transmitter or receiver. The RIS-UAV vision has been further studied in [31, 32], where novel use cases, challenges, and opportunities were identified and explained. In [26], the authors used the RIS-UAV to maximize cellular coverage within a geographical area. Specifically, they jointly optimize RIS-UAV phase shifting and BS beamforming problem, aiming to maximize the worst received SNR, while taking into account practical flight effects, i.e., undesired RIS-UAV oscillations due to adverse atmospheric conditions. Results proved the robustness and reliability of the flight effects combating method, and its gain of about 25 dB over state-of-the-art schemes. Finally, regarding such systems' security, the authors of [24] proposed to use an RIS-UAV to secure the uplink communications between ground users and a BS. They focused on maximizing the secrecy energy efficiency, defined as the ratio of the secrecy rate and consumed power, through the joint optimization of UAV trajectory, RIS phase shifting, user association, and transmit power. The problem is tackled with an AO-based approach, then, simpler schemes were proposed to solve the RIS phase shifting and UAV trajectory sub-problems. Simulation results illustrated the fast convergence of the proposed method, and the improvement in the secrecy energy efficiency by up to 38% compared to schemes without RIS. Alternatively, RIS has been used in [33] to mitigate jamming signals by accurately optimizing the phase shifts and RIS-UAV location. The aforementioned works are summarized in Table 2.

Table 1 Related works (RIS-assisted UAV systems)

References	Focus	Objective	Findings
[21]	Joint UAV trajectory and RIS phase-shift design	Max. avg. achievable rate	<ul style="list-style-type: none"> – Locally optimal solution obtained using SCA – Proposed algorithm increases avg. achievable rate compared to heuristic benchmarks
[27]	Joint UAV trajectory and RIS phase-shift design	Max. sum data rate of ground users	<ul style="list-style-type: none"> – Optimal solution obtained using AO – RIS enhances the quality of UAV communications – Proposed approach outperforms heuristic UAV trajectory designs
[22]	Analytical modeling of RIS-assisted UAV communication links	Derivation of outage probability and avg. BER expressions	– RIS improves coverage probability, avg. capacity, and system reliability
[28]	Joint optimization of multiple RIS deployment, user scheduling, and phase shifting	Max. sum data rate of ground users	<ul style="list-style-type: none"> – Sub-optimal solution obtained using AO – Proposed solution is superior to benchmarks without RIS phase-shifting and/or UAV trajectory optimization
[29]	Joint UAV trajectory, task/cache placement, and RIS phase shift design	Max. energy efficiency of RIS-assisted MEC-enabled UAV system	<ul style="list-style-type: none"> – Sub-optimal solution obtained using SCA – Proposed solution is superior to static cache/task placement and non-optimized RIS designs
[30]	Joint optimization of UAV trajectory, RIS phase shifts, and NOMA power	Min. energy consumption of RIS-assisted UAV NOMA downlink	<ul style="list-style-type: none"> – A reinforcement learning based solution is developed – Dynamic optimization of NOMA order/power reduces energy consumption compared to non NOMA benchmarks
[23]	Joint design of UAV trajectory, RIS phase shifts, and legitimate users' transmit power	Max. avg. secrecy rate	<ul style="list-style-type: none"> – Sub-optimal solution obtained using AO – Proposed approach is robust against channel uncertainties and outperforms heuristic baselines

Table 2 Related works (RIS-equipped UAV systems)

References	Focus	Objective	Findings
[25]	Control architecture design and case studies of RSS-equipped aerial platforms	Extend coverage of terrestrial BSs	<ul style="list-style-type: none"> – Proposed control architecture is viable – With a fixed number of reflectors, the UAV achieves the best receive power performance
[18]	Link budget analysis of RIS-equipped UAV communication links	Derivation of receive power expressions and maximal achievable data rates	<ul style="list-style-type: none"> – RIS-equipped UAV performance is independent from the operating frequency – With high receive antenna gain, RIS-equipped UAV's data rate is close to that of other platforms – The best performance is obtained when the RIS-equipped UAV is close to the ground transmitter or receiver
[31, 32]	Case studies and challenges discussion of RIS-equipped UAV systems	Shedding light on potential uses and opportunities of RIS-equipped UAV systems	<ul style="list-style-type: none"> – Overview of applications enabled by RIS-equipped UAV systems – Introduction of research, implementation, and experimentation guidelines for RIS-equipped UAV systems
[26]	Joint optimization of BS beamforming and RIS phase shifting	Max. worst received SNR	<ul style="list-style-type: none"> – Proposed approach is guarantees robust coverage against UAV oscillations and outperforms the agnostic benchmark
[24]	Joint optimization of UAV trajectory, RIS phase shifts, user association, and transmit power	Max. secrecy energy efficiency	<ul style="list-style-type: none"> – Sub-optimal solution obtained using AO – Proposed method converges fast and is superior by 38% to non-RIS baselines
[33]	Joint optimization of UAV location and RIS phase shifts	Max. legitimate user data rate	<ul style="list-style-type: none"> – An AO-based solution is proposed – Proposed method effectively compensates jamming and outperforms the non-RIS benchmark

4.3 Use Cases and Performance Evaluation

Clearly, RIS-assisted and RIS-equipped UAV communications have a significant potential use in public safety networks. For instance, by relying on the RIS over building facades or other objects, and on the motion flexibility of UAVs, FR communications can benefit from frequent LoS links, and thus sustain communications while dealing with emergency situations. Moreover, in a hard-to-reach area, the concurrent use of dedicated emergency communication channels from the closest BS combined with an accurate deployment of an RIS-UAV enables temporary communication/computing services for the time to deal with the emergency. Such a deployment can be punctual, recurrent, or periodic in order to ensure surveillance of critical assets.

In order to acquire an understanding about the potential use of RIS-assisted and RIS-mounted UAV systems, we present below public safety use cases with their corresponding link budget analysis and performances.

RIS-Assisted UAV Systems Assisting UAVs with RIS is an interesting feature that would allow extended coverage, higher capacity, and flexible spectrum sharing, for public safety services such as search and rescue, disaster response, and surveillance. For instance, by relying on multiple RIS devices along the path separating the BS from the controlled UAV, the action area of the latter can be significantly increased, which allows for fast and efficient response to threatening incidents within the covered region.

In line with the aforementioned example, we consider a UAV deployed for surveillance purposes in a predefined region. Due to the lack of cellular coverage due to blockages or weak signals, we assume that K RIS devices are deployed in the area to strengthen signals incoming from a BS in a multi-hop fashion, i.e., the BS's signals are forwarded among RIS devices until they reach the UAV, as depicted in Fig. 2. Also, we assume that the RIS devices are numbered from 1 to K , such that RIS_1 is the closest to the BS, while RIS_K is the closest to the UAV, and that RIS_k is equipped with N_k reflecting elements, $k = 1, \dots, K$. In terrestrial environments, an RIS is typically installed on a facade of a building, mainly in an urban environment. Subsequently, the 3GPP model presented in (3)–(5) can be used to model path-loss. Given that in this section we consider K RISs, nodes i and j are set such that $(i, j) \in \{(\text{BS}, \text{RIS}_1), (\text{RIS}_k, \text{RIS}_{k+1}); k = 1, \dots, K - 1\}$.

Subsequently, assuming perfect phase shifting, the link budget of the RIS-assisted UAV communication can be given by

$$P_r = P_t + G_t + G_r - PL_{\text{BS-RIS}_1} - \sum_{k=1}^{K-1} PL_{\text{RIS}_k\text{-RIS}_{k+1}} - PL_{\text{RIS}_K\text{-UAV}} + 20 \sum_{k=1}^K \log(N_k), \quad (10)$$

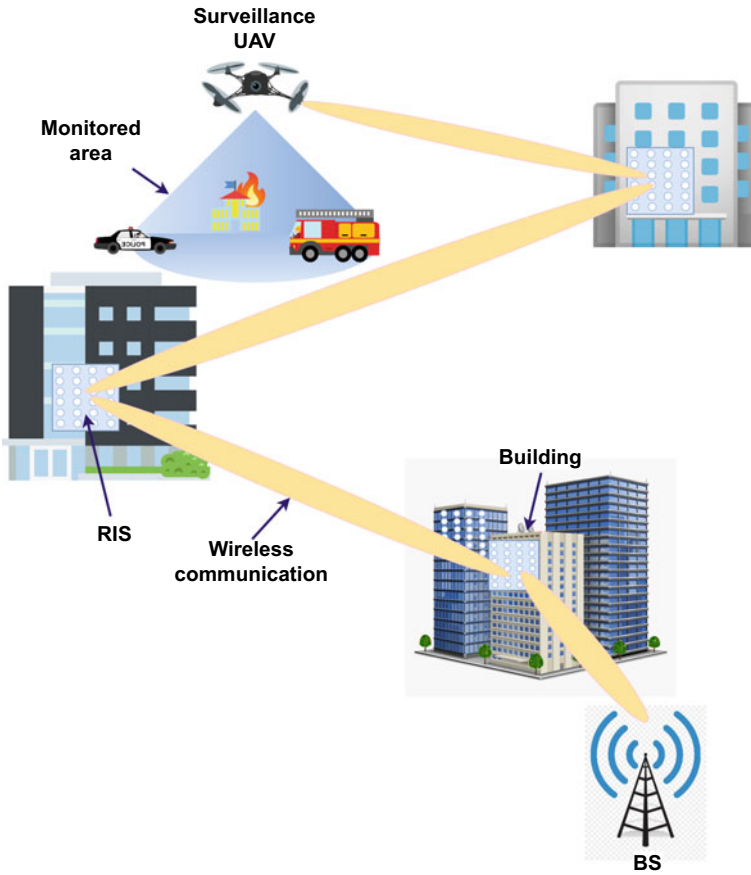


Fig. 2 RIS-assisted UAV communication for surveillance

where P_r is the received power at UAV, P_t is the transmit power of the BS, and G_t and G_r are the transmit and receive gains of the BS and UAV respectively.

The related data rate can be expressed by

$$R = B \log_2 \left(1 + \frac{P_r}{P_n} \right), \tag{11}$$

where B is the transmission bandwidth and P_n is the noise power, defined as

$$P_N = k T B F, \tag{12}$$

where $k = 1.38 \times 10^{-23} \text{J} \cdot \text{K}^{-1}$ is the Boltzmann constant, T is the temperature in $^{\circ}\text{K}$, and F is the noise figure.

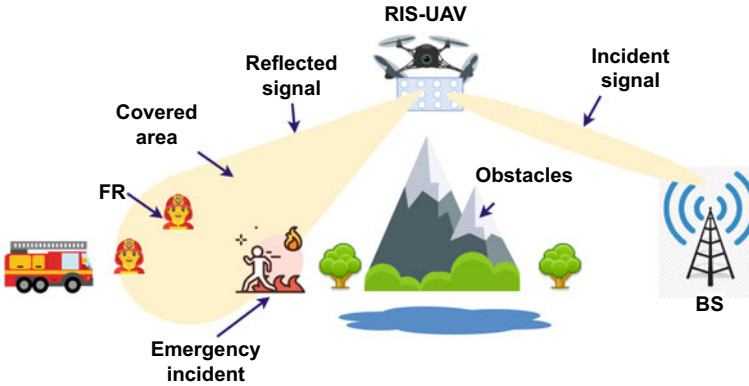


Fig. 3 RIS-UAV assisted communication for search and rescue

RIS-Equipped UAV Systems Unlike the previous use case, an RIS can be mounted on a UAV, thus providing more placement flexibility, which is expected to improve communications' quality of service. Assuming a search and rescue where FR teams (FRs) have to reach an endangered area where victims have been located, RIS-UAVs can be deployed over selected areas to provide connectivity to ground teams. For the sake of simplicity, we consider that a BS communicates with the FR in the targeted area via one RIS-UAV, deployed for the occasion, as illustrated in Fig. 3.

Assuming the 3GPP air-to-ground channel model, it is plausible to assume that communication links are all in LoS. Hence, path-loss in rural and urban environments can be expressed by [20]

$$PL_{BS-UAV}^{\text{rural}} = \max(23.9 - 1.8 \log_{10}(h_{UAV}), 20) \log_{10}(d_{BS-UAV}) + 20 \log_{10}\left(\frac{40\pi f}{3}\right) + X_{UAV}, \quad (13)$$

$$PL_{UAV-FR}^{\text{rural}} = \max(23.9 - 1.8 \log_{10}(h_{FR}), 20) \log_{10}(d_{UAV-FR}) + 20 \log_{10}\left(\frac{40\pi f}{3}\right) + X_{FR}, \quad (14)$$

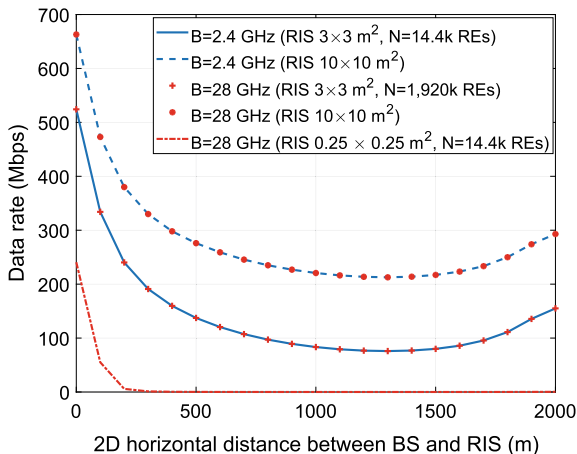
$$PL_{BS-UAV}^{\text{urban}} = 28 + 22 \log_{10}(d_{BS-UAV}) + 20 \log_{10}(f) + X_{UAV}, \quad (15)$$

and

$$PL_{UAV-FR}^{\text{urban}} = 28 + 22 \log_{10}(d_{UAV-FR}) + 20 \log_{10}(f) + X_{FR}, \quad (16)$$

where h_i , d_{i-j} , and X_{UAV} are defined as in the previous subsection, while X_j is the normally distributed shadow fading with deviation as in (8) for the urban environment and with deviation $\sigma = 4.2 e^{-0.0046 h_j}$ for the rural environment.

Fig. 4 Impact of the location of the RIS on the data rate ($K = 1$)



Given ideal phase shifting, the link budget of the RIS-UAV assisted communication can be given by [18]

$$P_r^k = P_t + G_t + G_r - PL_{BS-UAV}^k - PL_{UAV-FR}^k + 20 \log(N), \quad k \in \{\text{rural, urban}\} \tag{17}$$

where P_r^k is the received power at FR in the urban or rural environment. Finally, the data rate can be expressed using (11).

Performance Evaluation We evaluate here the achieved data rate performance for the described use cases above, where the impact of key parameters is also investigated.

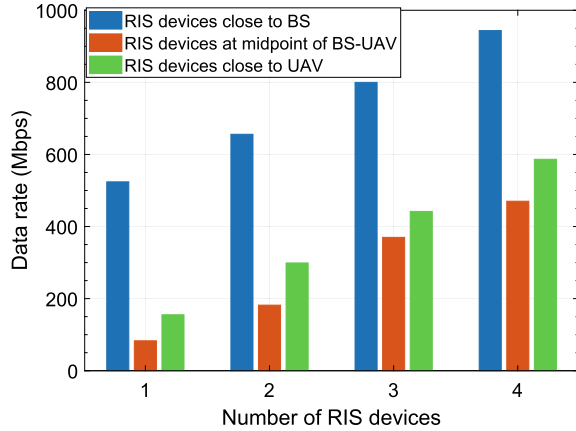
For the first use case (RIS-assisted UAV surveillance), we assume that the system parameters are set as follows: The altitudes of the BS, RIS devices on buildings’ facades, and UAV are set to $h_{BS} = 25$ m, $h_{RIS_k} = 10$ m, $\forall k = 1, \dots, K$, and $h_{UAV} = 100$ m, respectively. Also, the transmit power of the BS is $P_t = 35$ dBm, the transmit and receive gains $G_t = 8$ dBi, and $G_r = 5$ dBi, the frequency $f = 2.4$ GHz, and the bandwidth $B = 20$ MHz [19]. Finally, the area of RIS devices is $A_k = 3 \times 3$ m², $\forall k = 1, \dots, K$ and the number of hosted reflecting elements in the RIS is calculated by [18]

$$N_k = \frac{A_k f^2}{(0.2v)^2}, \quad \forall k = 1, \dots, K, \tag{18}$$

where $v = 3 \times 10^8$ m/s is the speed of light, and 0.2 is the minimal separation between reflecting elements, considering the scattering paradigm [18].

In Fig. 4, given $K = 1$, we depict the data rate performance as a function of the 2D distance between the BS and RIS. As it can be seen, the best performance is achieved when the RIS is the closest to the BS. When the RIS is located about half-way from the UAV, the performance is the lowest due to the degraded incident and reflected signals through the RIS. However, when the RIS is close to the UAV, the data rate slightly increases. This is due to the improved quality of the RIS-UAV channel.

Fig. 5 Impact of the number of RIS devices on the data rate



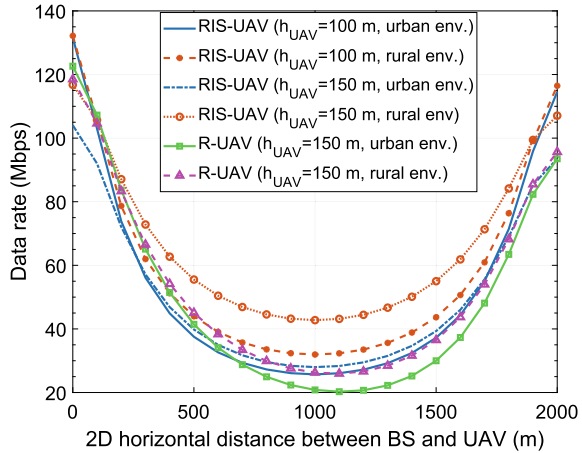
Also, we notice that the performance is insensitive to the used frequency band, for the same RIS area. For instance, given RIS with $A = 9 \text{ m}^2$ and $f = 2.4 \text{ GHz}$, the RIS is equipped with $N = 14.4\text{k}$ reflecting elements according to (18), while $N = 1,960\text{k}$ reflecting elements for $B = 28 \text{ GHz}$ within the same RIS area. It means that the RIS compensates the use of a higher frequency band, which degrades the transmission performance, by the deployment of a larger number of reflecting elements. Finally, when the same number of reflecting elements is used for different frequencies, we found that the higher the frequency, the worst is the data rate performance. This is expected since higher frequencies experience significant environment attenuation, which reduces its efficacy.

Clearly, assisting UAVs in their operation with high data rates would require the use of a sufficiently large RIS regardless of the operating frequency. Nevertheless, the best performances are obtained when placing the RIS closer to the BS.

Figure 5 shows the performance of the multi-hop system, where several RIS devices are used to forward the signals from the BS to the UAV. We distinguish three different cases, where each one corresponds to clustered RIS devices close to either the BS, the middle point between BS-UAV, or close to the UAV. First, we see that forwarding signals in a multi-hop fashion does improve significantly the data rate, conditioned on the same distribution of RIS devices. However, if the RIS locations are inadequate, one would strategically forward the signal through a single or at most two optimally located RIS devices in order to enhance the data rate. Finally, the best performance is achieved for RIS devices close to the BS, which agrees with the results of the previous Figure. Consequently, it is recommended to have RIS devices deployed on the facades of buildings close to the BS, which allows to bypass blockages within the surroundings.

For the second use case (RIS-UAV search and rescue), we consider the following parameters values: Altitudes of BS, RIS-UAV, and FR are set to $h_{BS} = 25 \text{ m}$, $h_{RIS-UAV} = 100 \text{ m}$ or 150 m , and $h_{FR} = 1.5 \text{ m}$, respectively. Also, the transmit power, transmit and receive gains, frequency, and bandwidth are set exactly as in

Fig. 6 Impact of the location of the RIS-UAV on the data rate



the previous use case. Finally, the area of the RIS device mounted on the RIS-UAV is $A_{RIS-UAV} = 0.25 \times 0.25 \text{ m}^2$, thus the number of hosted reflecting elements is $N_{RIS-UAV} = 100$ [18].

In Fig. 6, we present the data rate performance as a function of the 2D distance between the BS and RIS-UAV, and for different RIS-UAV altitudes. Moreover, we compare the proposed RIS-UAV system to the conventional amplify-and-forward UAV relay, denoted R-UAV [34]. Clearly, the best performance is achieved when the UAV (either RIS-UAV or R-UAV) is the closest to the BS, while the worst is obtained at or close to) the midpoint between the BS and FR. When the RIS-UAV is close to the FR, the data rate enhances significantly, but remains at a lower level than in the case of RIS-UAV close to the BS. Also, for the same RIS-UAV altitude, the achieved data rate is better in the rural environment than in the urban one. This is mainly due to stronger communication links with better LoS conditions, which strengthens the received signal at the FR. However, for the same environment conditions, the RIS-UAV altitude has an important impact on the performance. Specifically, we notice that a lower $h_{RIS-UAV}$ achieves better performances when deployed close to the BS or to the FR. In contrast, a higher altitude provides better data rates when the RIS-UAV is located somewhere between the BS and the FR. Indeed, a higher altitude would favor more LoS links, which compensates for the degraded communications to/from the RIS-UAV when located in-between the BS and FR. Clearly, as a RIS-UAV would be deployed and handled by the FR team on the ground, it is more likely that it would achieve a satisfying data rate. Nevertheless, a careful altitude optimization would be needed to obtain the best performance When compared to the R-UAV system at $h_{UAV} = 150 \text{ m}$, we notice that in the rural environment the RIS-UAV and R-UAV performances are almost the same for a UAV placed very close to the BS (under 100 m), while RIS-UAV outperforms R-UAV when the UAV is placed farther. In the urban environment, RIS-UAV is superior to R-UAV only when it is away from the BS

by at least 650m. We conclude that the use of RIS-UAV is mostly relevant for rural long range communications, as the case in wide areas search-and-rescue missions.

4.4 Limitations of RIS-Enabled UAV Networks

Despite the promising potentials realized when integrating RIS into UAV networks, the performance of such integration is constrained by several factors. First, although higher number of REs implies enhanced performance and improved coverage, due to the limited size of UAVs, and in order to guarantee flexible and stable flight, particularly in turbulence scenarios, several constraints are imposed on the sizes of RISs implemented on UAVs. Furthermore, the relatively high mobility and wobbling effect of UAVs requires frequent channel state information (CSI) acquisition and, hence, continuous RIS reconfiguration. Therefore, an increased overhead is resulted, imposing new challenges on the deployment of on-demand and fast RIS-enabled UAV communications in public safety networks. Moreover, joint trajectory design and resource allocation optimization represents a challenging factor in the implementation of RIS-enabled UAVs for public safety networks. Specifically, the joint optimization is required to ensure maximized coverage while maintaining high energy efficiency, in order to meet the needs of public safety networks under the limitations imposed by the constrained UAV capabilities.

5 Challenges and Future Directions

In this section, we outline the main challenges and the associated potential future research opportunities, with the aim to pave the way for the successful realization of efficient public safety networks through the utilization of RIS-enabled UAVs.

- **RIS response optimization:** Given that UAVs hover at relatively high speeds, this necessitates more frequent CSI acquisition, and subsequently, an increased number of RIS re-configuration rounds. These extensive operations introduce additional signaling overhead on the flying UAVs, in order to achieve the optimum RIS configuration, and therefore, efficiently accomplish the assigned missions pertaining to emergency cases in public safety networks. This calls for the design of reliable CSI estimation and RIS configuration in RIS-empowered UAVs for public safety networks.
- **Constrained RIS size in RIS-equipped UAVs:** In order to leverage the flight flexibility, as well as to maintain a stable UAV motion, the size of an RIS mounted on a UAV is limited by several constraints. Such constraints might have direct impact on the performance of the RIS, and can potentially limit the functionalities applied by the RIS. This is particularly pronounced when the UAVs are experienc-

- ing turbulence. This constraint can be loosen for RIS-assisted UAVs, depending on the considered use case and the underlying system model.
- **Channel Modeling:** Although large-scale and small-scale channel modeling has been extensively tackled in the literature, and a number of authors have proposed diverse channel modeling frameworks for near-field and far-field scenarios, the available models in the literature are still lack the comprehension. In more details, most of the reported results have primarily focused on the characterization of large-scale and small-scale fading under ideal unrealistic assumptions. There is still a compelling need for a comprehensive framework to demonstrate the RIS-enabled UAV channel models under practical scenarios, including high mobility as well as UAV wobbling. It should be highlighted that UAV wobbling constitute a major challenge on the design of accurate channel models, as it has a high impact on the quality of the UAV-RIS links, rendering channel modeling for RIS-enabled UAVs an open research topic.
 - **Incorporating Machine Learning Algorithms:** It is foreseen that the integration of RIS and UAV networks for the sake of accomplishing resilient public safety communication would necessitate a sophisticated level of organization, in order to coordinate the UAV trajectory, flying time, energy consumption, as well as optimizing the RIS configuration. In this regard, machine learning is deemed as an enabler for such networks, in which advanced machine learning algorithms can be developed and utilized in order to orchestrate the operation in RIS-enabled UAVs for public safety network. It is worth highlighting that such topic is barely touched in the literature, hence, it represents a potential future research direction.
 - **Physical Layer Security of Public Safety Communications** As the significance of the physical layer security (PLS) is more pronounced in highly dynamic networks, such as UAV networks, it is essential to develop enhanced PLS schemes for RIS-enabled UAV networks that fulfill the security requirements of public safety networks. It is worth highlighting that public safety networks are vulnerable to several physical layer attacks, particularly jamming and spoofing attackS, which have critical impact on such networks, resulting on serious consequences, including humans death. Motivated by this, it is of paramount importance to introduce novel PLS mechanisms to ensure reliable and secure public safety communication, in the context of RIS-enabled UAVs.
 - **Integration with other Non-terrestrial Networks** The emergence of the concept of integrated satellite-aerial-terrestrial (SAT) networks was inspired by the several advantages offered by such networks, including enhanced throughput, coverage, and resilience, which are key components in realizing efficient public safety communications. Yet, the adoption of integrated SAT networks introduces novel challenges pertaining to the heterogeneity and the time-variability nature of these networks. Therefore, to realize the full potential of integrated SAT networks as a key enabler for efficient public safety communication, thorough investigation should be conducted to quantify the performance of such networks, and to point out the major limitations for the development of resilient solutions.

6 Conclusion

In this chapter, we overviewed the fundamentals, design aspects, and applications of RIS as an enabling technology of future wireless services. Specifically, we studied the integration of RIS into UAV technology by focusing on RIS-assisted UAV networks and RIS-equipped UAV systems. To demonstrate their feasibility and potential, we developed two use cases related to public safety, namely aerial surveillance and search-and-rescue UAV missions. Through analysis and simulation results, we illustrated the achievable data rate performances, which validate the relevance of RIS-enabled UAV networks. Finally, we listed the current limitations of this integration and provided valuable insights about the future research directions to further develop RIS-enabled UAV systems.

References

1. Bariah L, Mohjazi L, Muhaidat S, Sofotasios PC, Kurt GK, Yanikomeroglu H, Dobre OA (2020) A prospective look: key enabling technologies, applications and open research topics in 6G networks. *IEEE Access* 8:174 792-174 820
2. Jaafar W, Yanikomeroglu H (2021) Dynamics of laser-charged UAVs: a battery perspective. *IEEE IoT J* 8(13):10 573-10 582
3. Long H, Chen M, Yang Z, Wang B, Li Z, Yun X, Shikh-Bahaei M (2020) Reflections in the sky: joint trajectory and passive beamforming design for secure UAV networks with reconfigurable intelligent surface. [arXiv:2005.10559](https://arxiv.org/abs/2005.10559)
4. Bariah L, Muhaidat S, Sofotasios PC, El Bouanani F, Dobre OA, Hamouda W (2021) Large intelligent surface-assisted nonorthogonal multiple access for 6G networks: performance analysis. *IEEE IoT J* 8(7):5129–5140
5. Gong S, Lu X, Hoang DT, Niyato D, Shu L, Kim DI, Liang Y-C (2020) Toward smart wireless communications via intelligent reflecting surfaces: a contemporary survey. *IEEE Commun Surveys Tuts* 22(4):2283–2314
6. Di Renzo M, Debbah M, Phan-Huy D-T, Zappone A, Alouini M-S, Yuen C, Sciancalepore V, Alexandropoulos GC, Hoydis J, Gacanin H et al (2019) Smart radio environments empowered by reconfigurable AI meta-surfaces: an idea whose time has come. *EURASIP J Wireless Commun Netw* 1:1–20
7. Latva-aho M, Leppänen K (2019) Key drivers and research challenges for 6G ubiquitous wireless intelligence. White Paper, University of Oulu
8. Basar E, Di Renzo M, De Rosny J, Debbah M, Alouini M-S, Zhang R (2019) Wireless communications through reconfigurable intelligent surfaces. *IEEE Access* 7:116 753-116 773
9. Mohjazi L, Zoha A, Bariah L, Muhaidat S, Sofotasios PC, Imran MA, Dobre OA (2020) An outlook on the interplay of artificial intelligence and software-defined metasurfaces: an overview of opportunities and limitations. *IEEE Veh Technol Mag* 15(4)
10. Liu Y, Liu X, Mu X, Hou T, Xu J, Di Renzo M, Al-Dhahir N (2021) Reconfigurable intelligent surfaces: principles and opportunities. *IEEE Commun Surveys Tuts*
11. Abumarshoud H, Mohjazi L, Dobre OA, Di Renzo M, Imran MA, Haas H (2021) LiFi through reconfigurable intelligent surfaces: a new frontier for 6G? [arXiv:2104.02390](https://arxiv.org/abs/2104.02390)
12. Liaskos C, Nie S, Tsioliaridou A, Pitsillides A, Ioannidis S, Akyildiz I (2018) A new wireless communication paradigm through software-controlled metasurfaces. *IEEE Commun Mag* 56(9):162–169

13. Gu Q, Wu D, Su X, Jin J, Yuan Y, Wang J (2021) Performance comparison between reconfigurable intelligent surface and relays: theoretical methods and a perspective from operator. [arXiv:2101.12091](https://arxiv.org/abs/2101.12091)
14. Boulogeorgos A-AA., Alexiou A (2020) Performance analysis of reconfigurable intelligent surface-assisted wireless systems and comparison with relaying. *IEEE Access* 8:94 463–94 483
15. Björnson E, Özdogan Ö, Larsson EG (2019) Intelligent reflecting surface versus decode-and-forward: how large surfaces are needed to beat relaying? *IEEE Wireless Commun Lett* 9(2):244–248
16. Tang W, Chen MZ, Chen X, Dai JY, Han Y, Di Renzo M, Zeng Y, Jin S, Cheng Q, Cui TJ (2020) Wireless communications with reconfigurable intelligent surface: path loss modeling and experimental measurement. *IEEE Trans Wireless Commun* 20(1):421–439
17. Danufane FH, Di Renzo M, De Rosny J, Tretyakov S (2021) On the path-loss of reconfigurable intelligent surfaces: an approach based on green’s theorem applied to vector fields. *IEEE Trans Commun*
18. Alfattani S, Jaafar W, Hmamouche Y, Yanikomeroglu H, Yongaçoglu A (2021) Link budget analysis for reconfigurable smart surfaces in aerial platforms. *IEEE Open J Commun Soc* 2:1980-1995. <https://doi.org/10.1109/OJCOMS.2021.3105933>
19. Study on channel model for frequencies from 0.5 to 100 GHz, 3GPP TR 38.901 V14.3.0 (2018)
20. Study on enhanced LTE support for aerial vehicles, 3GPP TR 36.777 V1.0.0 (2017)
21. Li S, Duo B, Yuan X, Liang Y-C, Di Renzo M (2020) Reconfigurable intelligent surface assisted UAV communication: joint trajectory design and passive beamforming. *IEEE Wireless Commun Lett* 9(5):716–720
22. Yang L, Meng F, Zhang J, Hasna MO, Renzo MD (2020) On the performance of RIS-assisted dual-hop UAV communication systems. *IEEE Trans Veh Technol* 69(9):10 385–10 390
23. Li S, Duo B, Di Renzo M, Tao M, Yuan X (2021) Robust secure UAV communications with the aid of reconfigurable intelligent surfaces. *IEEE Trans Wireless Commun*, p 1
24. Long H, Chen M, Yang Z, Wang B, Li Z, Yun X, Shikh-Bahaei M (2020) Reflections in the sky: joint trajectory and passive beamforming design for secure UAV networks with reconfigurable intelligent surface
25. Alfattani S, Jaafar W, Hmamouche Y, Yanikomeroglu H, Yongaçoglu A, Dao ND, Zhu P (2021) Aerial platforms with reconfigurable smart surfaces for 5G and beyond. *IEEE Commun Mag* 59(1):96–102
26. Mursia P, Devoti F, Sciancalepore V, Costa-Pérez X (2021) RISE of flight: RIS-empowered UAV communications for robust and reliable air-to-ground networks. *IEEE Open J Commun Soc* 2:1616–1629
27. Li J, Liu J (2020) Sum rate maximization via reconfigurable intelligent surface in UAV communication: phase shift and trajectory optimization. In: *Proceedings of IEEE/CIC international conference on communications in China (ICCC)*, pp 124–129
28. Jiang L, Jafarkhani H (2021) Reconfigurable intelligent surface assisted mmwave UAV wireless cellular networks. In: *Proceedings of IEEE international conference on communications*, pp 1–6
29. Mei H, Yang K, Shen J, Liu Q (2021) Joint trajectory-task-cache optimization with phase-shift design of RIS-assisted UAV for MEC. *IEEE Wireless Commun Lett* 10(7):1586–1590
30. Liu X, Liu Y, Chen Y (2021) Machine learning empowered trajectory and passive beamforming design in UAV-RIS wireless networks. *IEEE J Sel Areas Commun* 39(7):2042–2055
31. Abdalla AS, Rahman TF, Marojevic V (2020, Dec) UAVs with reconfigurable intelligent surfaces: applications, challenges, and opportunities. [arXiv preprint arXiv:2012.04775](https://arxiv.org/abs/2012.04775)
32. You C, Kang Z, Zeng Y, Zhang R (2021) Enabling smart reflection in integrated air-ground wireless network: IRS meets UAV
33. Tang X, Wang D, Zhang R, Chu Z, Han Z (2021) Jamming mitigation via aerial reconfigurable intelligent surface: passive beamforming and deployment optimization. *IEEE Trans Veh Technol* 70(6):6232–6237
34. Levin G, Loyka S (2010) Amplify-and-forward versus decode-and-forward relaying: which is better? In: *Proceedings of international Zurich seminar communications*, pp 1–5

UAVs Path Planning by Particle Swarm Optimization Based on Visual-SLAM Algorithm



Umair Ahmad Mughal, Ishtiaq Ahmad, Chaitali J. Pawase,
and KyungHi Chang

Abstract Intelligent 3-D path planning is a crucial aspect of an unmanned aerial vehicle's (UAVs) autonomous flight system. In this chapter, we propose a two-step centralized system for developing a 3-D path-planning for a swarm of UAVs. We trace the UAV position while simultaneously constructing an incremental and progressive map of the environment using visual simultaneous localization and mapping (V-SLAM) method. We introduce a corner-edge points matching mechanism for stabilizing the V-SLAM system in the least extracted map points. In this instance, a single UAV performs the function using monocular vision for mapping an area of interest. We use the particle swarm optimization (PSO) algorithm to optimize paths for multi-UAVs. We also propose a path updating mechanism based on region sensitivity (RS) to avoid sensitive areas if any hazardous events are detected during the execution of the final path. Moreover, the dynamic fitness function (DFF) is developed to evaluate path planning performance while considering various optimization parameters such as flight risk estimation, energy consumption, and operation completion time. This system achieves high fitness value and safely arrives at the destination while avoiding collisions and restricted areas, which validates the efficiency of proposed PSO-VSLAM system as demonstrated by simulation results.

Keywords Visual-SLAM · PSO · Path planning · Autonomous aerial vehicles · UAV

1 Introduction

The ability of an autonomous aerial vehicle to navigate in an unknown environment while simultaneously building a progressive map and localizing itself is a prominent research topic in robotics. Because of the practical uses of simultaneous localization and mapping (SLAM), research has been conducted [1]. Advances in vision-based

U. A. Mughal · I. Ahmad · C. J. Pawase · K. Chang (✉)
Department of Electrical and Computer Engineering, INHA University, Incheon 22212, South Korea
e-mail: khchang@inha.ac.kr

© The Author(s), under exclusive license to Springer Nature Singapore Pte Ltd. 2022
Z. Kaleem et al. (eds.), *Intelligent Unmanned Air Vehicles Communications for Public Safety Networks*, Unmanned System Technologies,
https://doi.org/10.1007/978-981-19-1292-4_8

SLAM algorithms assess the robot's position and generate the terrain as the robot of interest moves [2]. Many SLAM systems in the literature include a diverse set of sensors, including Laser Range Finders (LRF), inertial measurement units (IMU), GNSS receivers, magnetometers, optical flow sensors (OFS), barometers, and Light Detection and Ranging (LiDAR) [3, 4]. Single camera SLAM systems, on the other hand, have gained in popularity in recent years due to their light weight, low cost, and variety of applications in complex environments [5, 6]. In this regard, monocular visual-SLAM has gotten attention for UAV applications since it provides fully autonomous systems in a range of challenging settings without the usage of external positioning systems. UAVs are commonly used for traffic monitoring, health services, search and rescue, security, and surveillance [7–9]. UAVs enhance wireless network coverage, capacity, and efficiency by serving as base stations [10].

Path planning algorithms are designed to find the optimum path based on a set of constraints and objectives (such as terrain constraints and collision avoidance, energy consumption, flight risk, etc.). As a result, path planning must take into account not only limitations and objectives, but also the possibility of dangerous events that occurred unexpectedly along the UAV's path. We propose the region sensitivity (RS) to reduce unconditional hazards by allowing the UAV to recognize an unsafe region and optimize its path to the destination. The focus of this research is to provide a framework for determining the best path to take using monocular vision maps. A visual-SLAM (VSLAM) approach builds an incremental map of the environment while continuously tracking the camera's position. Following that, the resulting map is analyzed and used as input for an optimization algorithm.

The PSO framework is easier to implement and requires less time to compute than other metaheuristic search algorithms. It is also better at handling nonlinear challenges than other heuristic algorithms like ant colony optimization (ACO), Genetic algorithm (GA), and an evolutionary technique (EA). Because the GA is fundamentally discrete, i.e., it encodes to design discrete variables, it has a high computing cost, whereas the PSO is inherently continuous and can be easily modified to handle discrete design variables. As a result, we utilize PSO since it converges efficiently in a dynamic environment. The particle is treated as an integrated individual in the PSO framework, representing a candidate solution. As a result, the performance of all particles defines the global best particle. To analyze a feasible path, the PSO planner evaluates the quality of the entire path rather than a single waypoint.

1.1 Main Contributions

This chapter aims to develop a system that generates the best paths for multiple UAVs to safely arrive at their destinations, even when GPS is unavailable. To build an incremental and progressive map of the surrounding environment, we designed a two-step centralized system based on visual-SLAM. The constructed terrain map in the form of a points cloud is loaded into the proposed multiple-path UAVs optimization planner. To stabilize the system in the least textured environment, we use

the Canny and Harris detectors at the same time. We proposed a dynamic fitness function (DFF) as a joint cost determinant, which contains multiple optimization indexes, such as flight risk estimation, energy consumption, operation completion time, and numerous constraints, such as UAV constraints, which consider the physical limitations of the UAVs, and environmental constraints, which also consider the surrounding conditions. To address unexpected hazardous events, we've presented a path-updating system based on the RS, which allows the UAV to identify an unstable location and optimize its path accordingly. Based on the RS and DFF, the proposed optimization planner utilizes the PSO to compute the fitness of each path. All of these factors contribute to the practicality of our proposed methodology for path planning of multiple UAVs.

1.2 Related Work

SLAM and PSO technologies are often used in research involving underwater, interior, and outdoor environments. The authors of [11] utilize active SLAM for deep reinforcement learning-based robot path planning. The convolutional residual network is used to detect obstacles in the path. The suggested approach employs the Dueling DQN algorithm for obstacle avoidance while also employing the FastSLAM technique to create a 2D map of the surrounding area. Similarly, the authors of [12] use stereo vision-based active SLAM to locate, navigate, and map their environment. To avoid obstacles and complete the task effectively, the cognitive-based adaptive optimization algorithm is introduced. The main focus of the approaches in [11, 12] is on the complete robot task while detecting and avoiding the environment's obstacles.

In [13], the author recommends using a visual-SLAM technique to build an incremental map of the terrain for surveillance. For path planning, the author offers the Cognitive-based Adaptive Optimization (CAO) algorithm. A monocular-inertial SLAM is proposed in [14]. To augment the monocular camera's sensing cues with inertial measurement unit (IMU). PSO method was used in a hazard exploration scenario for a network of UAVs in [15]. The new and improved PSO is proposed as dynamic PSO for UAV networks (dPSO-U). UAVs use delay tolerant networking (DTN) for sharing information. The solution simply evaluates the optimum UAV combinations to thoroughly explore the environment. The 5G network is enhanced with multiple UAVs in [16]. The UAVs serve as a link between the users and the cellular base station. The designed approach's major goal is to position the UAVs in the best possible position to maximize the communication coverage ratio. The authors offer per-drone iterated PSO (DI-PSO) system that utilizes PSO to find the optimum position for each drone. In our method, the UAVs function as individual PSO particle. A group of unmanned aerial vehicles (UAVs) tackles a forest fire in [17]. Before the mission begins, the target locations are assumed to be known. Using an auction-based algorithm, the UAVs were assigned to the various fire areas. The UAVs then employ the centralized PSO algorithm, as well as the parametrization and

time discretization (CPTD) algorithm, to compute the best paths to the designated fire sites.

In [18], an improved PSO algorithm is used for real-time path planning of a single UAV. Work falls under the low-level category of trajectory planning because it involves avoiding moving obstacles. The NBVP [19] is relevant to this paper. Within the planning loop, it employs the RRT technique. A tree node is used to retrieve visual data from the depth sensor. During planning, a small fraction of the best view is executed in each iteration, enabling the trajectory to be adapted to the plan between iterations as a new explored map.

Our previous work [20] examined the environmental and physical characteristics of the surroundings. However, we present a dynamic fitness function (DFF), which involves various optimization factors to handle environmental constraints including terrain limitations, restricted areas, collision avoidance, etc. Moreover, we propose RS to tackle any unexpected hazardous event during UAV flight. To find the optimal DFF and RS system designs, we employ a monocular vision-based SLAM technique. In [21] authors developed an enhanced PSO (IPSO) for robot path planning. The authors evaluate three alternatives in two different environments: PSO, artificial potential field (APF), and IPSO. In [22], the authors developed the adaptive selection mutation limited differential evolution method for path planning in disaster environments. A single objective evolutionary technique, based on reference points, is presented in [23]. The author also developed a hybrid grey wolf optimization technique for UAV path planning in [24]. In the literature, different system parameters were generated from various system philosophies and objectives [25].

Challenges of 3-D UAV placement, such as resource and power allocation, trajectory optimization, and user association are discussed in [26]. This challenge becomes considerably more complicated as the height of the UAV changes, changing the channel conditions and reducing coverage due to severe co-channel interference. The authors proposed optimizing the 3-D UAV placement and path-loss compensation factor for various UAV deployment heights in the suburban setting in order to provide a solution. The authors of [27] suggested a rapid K-means-based user clustering model and jointly optimum power and time transfer-ring allocation that can be used in the real system by deploying UAVs as flying base stations for real-time network recovery and maintenance during and after disasters. Nguyen et al. [28] presented a unique approach based on deep reinforcement learning for finding the best solution for energy-harvesting time scheduling in UAV-assisted D2D communications. The article [29] investigated wireless systems by using a full-duplex (FD) unmanned aerial vehicle (UAV) relay to allow two adjacent base stations to communicate with users and are far distant. In order to increase user performance, non-orthogonal multiple access (NOMA) aided networks and multiple-antenna user design are also investigated. For delay-sensitive communication in UAVs, a disaster resilient three-layered architecture for PS-LTE (DR-PSLTE) is presented in [30].

2 Visual-SLAM Framework

Most vision-based SLAM systems employ a corner features detector, such as the Harris corner detector. In a non-textured scene, the corner detector cannot identify enough feature points. As a solution, we present the corner-edge point system, which employs edge points as well. The edge-point is the detected point on the edge segment. Our method recognizes corner and edge points by comparing the 3D points of the next image and estimating the camera's position by comparing the 3D points of the next image. In this method, the camera's trajectory and a 3D map are produced. In addition to robustness, it provides a detailed representation of the object, which improves the modeling process of surface detection and reconstruction.

2.1 Approach

Correspondence between the points may lead to multiple matches, including outliers. Random sampling consensus (RANSAC) [31] handles inliers, outliers, dividing data using perspective projection [32]. The large matching errors are eliminated by the progressive sample consensus PROSAC algorithm [33]. In the beginning, we estimate the trajectory of the camera with small detected points, and afterwards, we use a coarse-to-fine approach to refine the trajectory and feature point correspondence by progressively increasing the points. The overall approach to constructing a map using the visual-SLAM system can be seen in Fig. 1.

2.1.1 Keypoint Matching

Most computer vision applications require Structure from Motion (SfM), Multi-view Stereo (MvS), image registration, and image retrieval. The technique begins with keypoint detection and description and then proceeds on to keypoint matching. A descriptor is a multidimensional vector that denotes the keypoints in space. As a result, the keypoint is identified, which is then projected on the images from two different perspectives. First, we apply acceleration segment characteristics to find keypoints (FAST). The edge locations are then determined using the well-known Harris Corner detector [34] and Canny edge detector [35]. To eliminate outliers, the robust independent elementary features (BRIEF) descriptor is oriented around the gradient. Due to their lower processing complexity and higher accuracy compared to other detectors and descriptors [36]. The SIFT has the lowest matching rate of 31.8% in 0.25 s, while the ORB combines FAST and BRIEF to have the highest matching rate of 49.5% in 0.02 s.

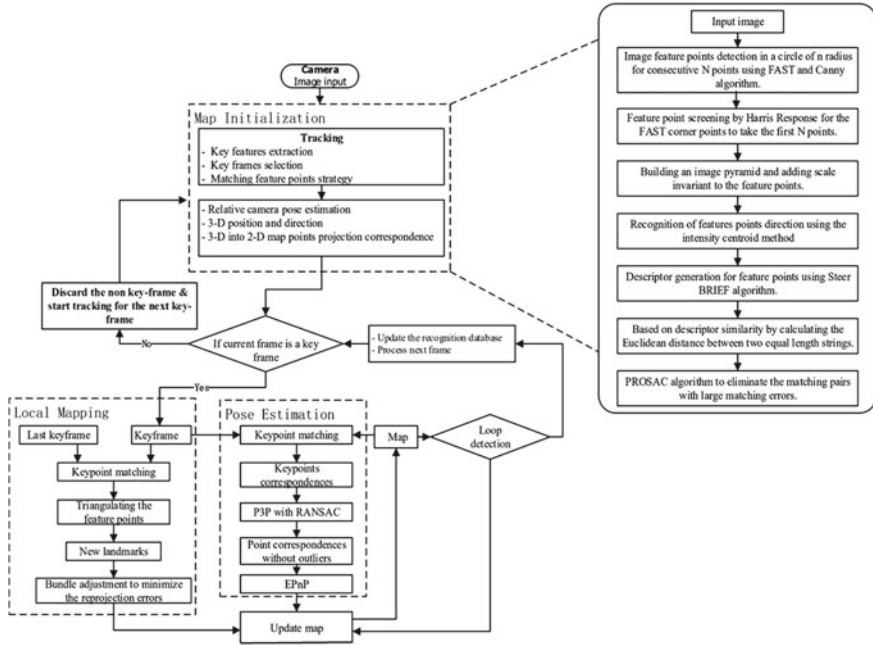


Fig. 1 Flowchart of map construction using Visual-SLAM

2.1.2 Keypoint Reconstruction

A 3D point from consecutive images is calculated using the following equation:

$$P_e = \left(\frac{b(x_1 + x_r)}{2(x_1 - x_r)}, \frac{by}{(x_1 - x_r)}, \frac{bf}{(x_1 - x_r)} \right)^T \tag{1}$$

where, b indicates baseline, and f is the focal length, $y = y_l = y_r$, while (x_l, y_l) represents the points on one image, and (x_r, y_r) represents the point on the consecutive next image. We set $u = (x_l, y_l, x_r, y_r)$ and $P_c = S(u)$, and therefore, the covariance of the edge point (P_c) is calculated as

$$\sum P_e = \frac{\delta S}{\delta u} \sum u \frac{\delta S^T}{\delta u} \tag{2}$$

Now, we assume $(\sum u = \text{diag} \sigma_{x_1}^2, \sigma_{y_r}^2, \sigma_{y_r}^2)$ and, for the implementation, we take $\sigma_{x_r} = \sigma_{y_l} = \sigma_{y_r} = 0 : 5 [Pixels]$. The correlation between σ_{y_l} and σ_{y_r} is assumed to be very strong.

2.1.3 Camera Motion Estimation

The trajectory of the camera can be estimated by successfully matching the points from time $t-1$ to t when the points are reconstructed in frame $I_t - 1$, and the points are detected at frame I_t . Let v_t be a camera pose at time t , where P_{t-1}^i is a i -th reconstructed 3D point at $t - 1$. Similarly, P_{t-1}^i is a point that was taken as a projection of P_{t-1}^i on the image at I_t . The point P_{t-1}^i is termed a map point because it is stored for map generation, and therefore, point P_{t-1}^i can be represented as $P_{t-1}^i = k(P_{t-1}^i, v_t)$, where k indicates the function of perspective projection:

$$K = N_t^{-1}(P_{t-1}^i - M_t)$$

$$k(P_{t-1}^i, v_t) = \left(f \frac{K_x}{K_z}, f \frac{K_y}{K_z} \right)^T \quad (3)$$

where, M_t and N_t are the translation and rotation matrices of vector v_t . Let g_t^i is a point on the image corresponding to P_{t-1}^i , so the cost function, C can be defined as

$$C(v_t) = \sum_{i=1}^n q(g_t^i, P_{t-1}^i) \quad (4)$$

where $q(g_t^i, P_{t-1}^i)$ represents the penalty that depends on the Euclidean distance between points g_t^i and P_{t-1}^i . We use the perpendicular distance between the point P_{t-1}^i and the segment containing the point g_t^i in image [37, 38]. We estimate the motion using pose vector v_t at time t , and the correspondence between the points from decreasing cost function $C(v_t)$. This can be achieved by utilizing the gradient descent method, setting the initial value of vector v_t to v_{t-1} , and setting closest point g_t^i to its closest corresponding point, P_{t-1}^i , by calculating the Euclidean distance. This process of point matching repeats, which decreases $C(v_t)$, and the optimal pose vector v_t , and thus, point correspondences are achieved.

2.1.4 Map Construction

We build an incremental 3D map of the environment based on camera pose vector v_t by transforming the 3D points into world coordinates from the camera coordinates. Let us take the camera coordinates and P_e^i as the i -th 3D point, so the location of this point in the camera coordinates can be represented as follows:

$$P^i = c(P_e^i, v_t) = N_t P_e^i + M_t \quad (5)$$

We integrate the identified 3D points based on their correspondences, which decreases the depth error. Based on the covariance, we integrate the location of all the identified 3D points. We take the average location of the identified 3D points between the keyframes, which increases the efficiency. The created 3D points indicate the map, and estimate the trajectory of the camera, between the keyframes.

2.1.5 Camera Motion Update

Camera motion is updated by extracting the keyframe from the sequence of images with interval d , and then, we refine the motion using the RANSAC algorithm between the keyframes. As expected, the camera motion is relatively large between the keyframes, so to avoid the local minima, we initialize the value of a keyframe to I_d from the estimated camera motion by each keyframe $I_t + 1$. Every 3D point P_{t-d}^i taken upto keyframe I_{t-d} is supposed to project onto keyframe I_t and match to the 3D point q_t^i in the image [39].

Uncertainty is evaluated by calculating the covariance matrix of camera poses. We use \bar{v}_t and \sum_{v_t} to represent the mean and covariance, in which \bar{v}_t is calculated from the keyframe, whereas \sum_{v_t} is calculated with the following mechanism. Let s_t represents the vector of multiple points in the image at time t where w_t indicates the vector of 3D points, which are matched with s_t . We can indicate s_t as $s_t = h(w_t, v_t) + n_t$, where n_t is noise having zero mean and zero covariance, \sum_{n_t} , and s_t can be obtained with the Taylor expansion, as follows:

$$s_t \approx k(\bar{w}_t, \bar{v}_t) + \frac{\delta k}{\delta w_t}(w_t - \bar{w}_t) + \frac{\delta k}{\delta v_t}(v_t - \bar{v}_t) + n_t \quad (6)$$

We can calculate the covariance of camera trajectory utilizing Eq. 6, as follows:

$$\sum v_t = \left(J_{v_t}^T \left(\sum_{n_t} + J_{w_t} \sum_{w_t} J_{w_t}^T \right)^{-1} J_{v_t} \right)^{-1} \quad (7)$$

where, $J_{v_t} = \frac{\delta k}{\delta v_t}(\bar{w}_t, \bar{v}_t)$, $J_{w_t} = \frac{\delta k}{\delta w_t}(\bar{w}_t, \bar{v}_t)$ and \sum_{w_t} represents the covariance matrix of the 3D points that match s_t . The size of the \sum_{w_t} depends on the number of 3D points and if the number of points is large, which makes \sum_{w_t} computation intractable.

We assume that the location of all the 3D points that are reconstructed from the same frame have a strong correlation. To overcome the complexity, we divide all 3D points into two parts, w_a and w_b , where w_a indicates the 3D points reconstructed from the last keyframe, I_{t-d} , and w_b represents the reconstructed 3D points from the past key frames, I_1 to I_{t-2d} . we can approximate each group covariance to the mean covariance of all 3D points. Considering all the assumptions, we have the following:

$$\begin{aligned}
 J_{wt} \sum_{wt} J_{wt}^T &= \frac{1}{|w_a|} \sum_{P \in w_a} J_P \sum_P J_P^T + \frac{1}{|w_b|} \sum_{P \in w_b} J_P \sum_P J_P^T \\
 J_P &= \frac{\delta k}{\delta P} (\bar{P}, \bar{v}_t)
 \end{aligned} \tag{8}$$

where, J_P and \sum_P represent the Jacobian and covariance matrix of a 3D point, respectively. This supposition decreases the computational complexity of the system.

2.1.6 Map Update

We construct the 3D map according to section II-A4. We fuse the matched 3D points with weights according to their covariance. The 3D point explained in section II-A4 can also be expressed as

$$P_t^i = c(P_{e,t}^i, v_t) \tag{9}$$

As mentioned above, we are ignoring correlation term \sum_{wt} , and therefore, we calculate the covariance matrix of each 3D point. Let $\overline{P_t^i}$ and $\sum_{P_t^i}$ represent the mean and covariance of a 3D point, respectively. Using the Taylor expansion, we have the following:

$$P_t^i \approx c(\overline{P_{e,t}^i}, \bar{v}_t) + \frac{\delta c}{\delta P_{e,t}^i} (P_{e,t}^i - \overline{P_{e,t}^i}) + \frac{\delta c}{\delta v_t} (v_t - \bar{v}_t) \tag{10}$$

The covariance of 3D point P_t^i can be calculated using Eq. 10 as follows:

$$\overline{\sum_{P_t^i}} = \frac{\delta c}{\delta P_{e,t}^i} \sum P_{e,t}^i \frac{\delta c}{\delta P_{e,t}^i}^T + \frac{\delta c}{\delta v_t} \sum v_t \frac{\delta c}{\delta v_t}^T \tag{11}$$

We update the location and covariance of a 3D point by fusing Eq. 11 with the point at t-d, as follows:

$$\begin{aligned}
 \overline{P_t^i} &= \overline{P_{t-d}^i} + \sum P_{t-d}^i \left(\sum_{P_{t-d}^i} + \overline{\sum_{P_t^i}} \right)^{-1} (P_t^i - \overline{P_{t-d}^i}) \\
 \sum_{P_t^i} &= \left(\sum_{P_{t-d}^i}^{-1} + \overline{\sum_{P_t^i}^{-1}} \right)^{-1}
 \end{aligned} \tag{12}$$

3 Swarm-Based Path Planning Approach

In this section, we introduce the proposed path planning scheme based on particle swarm optimization. The elevation map generated by the visual-SLAM algorithm is used as input terrain information for the optimization algorithm to plan the optimum path. The data set we used in our system is very diverse, and provides information on the terrain. There are multiple system constraints, which must be satisfied before planning the path from source to destination and meeting the multiple objectives we desire in order to obtain the maximum value. In this regard, we propose the DFF to derive the optimal trajectory of the UAVs while considering all the constraints and objectives of the system.

3.1 Working Principle of Particle Swarm Optimization

PSO is a heuristic search algorithm. It was first developed by Kennedy and Eberhart in 1995 to introduce a method for optimization of a nonlinear function [40]. It is a nature-inspired set of computational methodologies to resolve complex real-world problems. PSO computes the number of particles to look for the best solution. Each particle moves in accordance with both its previous best particle in the group and the swarm's global best particle. Each particle changes its velocity and location in real time using information from the prior velocity and best position obtained by any particle in the group, as well as the global swarm's best position.

3.2 PSO Formulation

The mathematical formulation for each particle's velocity and position are stated as follows. Let the total number of particles in a swarm be P , the total iterations is N , and the 3D dimension of each particle is D . Therefore, for the particle, position x and velocity v can be represented as:

$$\begin{aligned} x_i &= (x_{i1}, x_{i2}, \dots, x_{iD}) \\ v_i &= (v_{i1}, v_{i2}, \dots, v_{iD}) \end{aligned} \quad (13)$$

The position for the best particle, $p_{i,best}$, in the group and the global best swarm particle, s_{best} , can be computed as follows:

$$\begin{aligned} p_{i,best} &= (p_{i1,best}, p_{i2,best}, \dots, p_{iD,best}) \\ s_{best} &= (s_{1,best}, s_{2,best}, \dots, s_{D,best}) \end{aligned} \quad (14)$$

Because p_{best} and s_{best} are termed cost values for PSO, once a cost function is defined, then the position and velocity are updated as follows:

$$\begin{aligned} x_{ij}^{t+1} &= x_{ij}^t + v_{ij}^{t+1} \\ v_{ij}^{t+1} &= \chi v_{ij}^t + ar_1(p_{i,j,best} - x_{ij}^t) + br_2(s_{j,best} - x_{ij}^t) \\ \text{For } i &= 1, 2, 3, \dots \text{ P } j = 1, 2, 3 \dots \text{ D } t = 1, 2, 3, \dots \text{ N} \end{aligned} \quad (15)$$

where, a and b are the self-cognitive acceleration property and the social knowledge parameter of the swarm, respectively, which represent the inheritance characteristics of the personal particle and the whole swarm; and are random values in the range $[0-1]$, and χ represents the inertia of an individual particle, which induces an effect on the velocity from one iteration to next iteration. The authors in [41] suggested optimum values of $a = b = 1.496$ and $\chi = 0.7298$ for PSO performance.

4 Proposed Dynamic Fitness Function

In order to derive the optimal trajectories, the DFF computes the fitness of the trajectory considering optimization parameters, which are divided into two groups, namely, objectives and constraints. The former consist of risk estimation, energy consumption, and operation completion time; the latter are further divided into two parts depending upon the UAV's physical constraints (flying slope and turning angle) and the physical limitations of the environment (region sensitivity, restricted areas, and terrain constraints). The working flow of the DFF can be observed in Fig. 2. The DFF can be formulated as seen in equation:

$$DFF_{fitness} = F_{objectives} + F_{constraints} \quad (16)$$

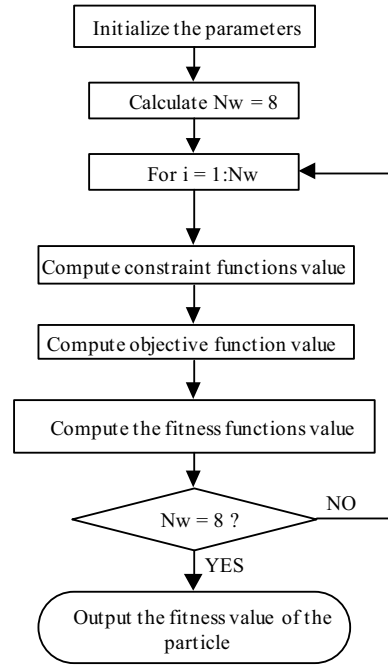
where, $F_{objectives}$ indicates the objectives function on which we focus to gain the maximum value, whereas $F_{constraints}$ indicates the UAV physical and environmental restrictions, which must be fulfilled before planning the trajectory.

4.1 Objectives Design

We have set optimization parameters, and the objectives were constructed to improve the quality of path planning. The objectives can be represented as weighted components of risk estimation, energy consumption, and operation completion time, as follows:

$$F_{objectives} = w_1 O_{RE} + w_2 O_{EC} + w_3 O_{OT} \quad (17)$$

Fig. 2 Flowchart to compute dynamic fitness function



where, w_1, w_2, w_3 denote the weights of the objective components [39], which are chosen to derive the importance of each component while planning the path, and O_{RE}, O_{EC}, O_{OT} are functions from which values are taken in the range $[0, 1]$. We aim to derive the optimum path with less risk, energy, and time.

4.1.1 Risk Estimation

Some flight restrictions should be implemented. In harsher weather conditions, such rain, snow, or strong winds, small UAVs are susceptible to damage. The UAV altitude while doing the work should be moderate; winds at higher altitudes are stronger. The UAV also faces risks because of dense clouds that impede its ability to focus. Based on the above risks, we identify the following two types of risk.

1. Environmental Risk

The environment has a wide range of characteristics, and therefore, it is difficult to make a model that precisely measures the environmental risk. Therefore, for simplicity, an environmental value is generated randomly, $r_{i,i+1}^e$, that represents the risk from the i -th waypoint to waypoint $(i + 1)$. The summation of the risk values would be considered the environmental risk.

2. Altitude Risk

The altitude risk is actually an absolute difference in altitude between two waypoints, and therefore, we formulate altitude risk $r_{i,i+t}^a$ as follows:

$$r_{i,i+t}^a = k * (z_{i+1} - z_i) \quad (18)$$

where, k represents a constant parameter for control. Because risk analysis depends on location, it will change according to weather conditions and the UAV's altitude at the same instant during flight. Therefore, the total risk can be formulated as follows:

$$O_{RE} = \frac{\sum_{i=1}^{N_w-1} RE_i}{maxRE} \quad (19)$$

$$RE_i = w_E Rr_{i,i+t}^e + w_{AR} r_{i,i+t}^a \quad (20)$$

RE_i shows the total risk from the i -th waypoint to waypoint $(i + 1)$, while w_{ER} and w_{AR} are the weight factors of the environmental and altitude risks, respectively. N_w denotes the total number of waypoints from source to destination, and $maxRE$ is a normalized value of the risk, which can be computed as follows:

$$maxRE = (N_w - 1) * [w_{ER} * Z * w_{AR} (2 * maxr^e)] \quad (21)$$

where, $maxr^e$ indicates the maximum value instigated by the environment risk, and Z is the altitude of the UAV during flight.

4.1.2 Energy Consumption

Fuel is essential to UAV missions. If the UAV does not arrive on time, the mission is said to have failed. A simple method that uses less energy (EC) should be the priority. We assume the UAV velocity stays constant during flight. We define EC as follows:

$$O_{EC} = \frac{\sum_{i=1}^{N_w-1} FC_i}{maxFC} \quad (22)$$

$$FC_i = P_u * t_{i,i+1} \quad (23)$$

$$t_{i,i+1} = \frac{d_{i,i+1}}{v} \quad (24)$$

$$d_{i,i+1} = \sqrt{(x_{i+1} - x_i)^2 + (y_{i+1} - y_i)^2 + (z_{i+1} - z_i)^2} \quad (25)$$

where, FC_i represents the fuel burned in flying from the i -th waypoint to waypoint $(i + 1)$. P_u is the power of the UAV at velocity v , while $t_{i,i+1}$ is the total time taken by the UAV to fly from the i -th waypoint to waypoint $(i + 1)$; $d_{i,i+1}$ indicates the Cartesian distance of a flight from the i -th waypoint to waypoint $(i + 1)$, and $maxFC$ is a normalized value for fuel consumption, which can be formulated as follows:

$$maxFC = (N_w - 1) * P_u * \frac{d_{max}}{v} \quad (26)$$

where, $d_{max} = \sqrt{X^2 + Y^2 + Z^2}$ where X, Y, Z indicate the three dimensions of the UAV, i.e., the X-axis, Y-axis, and Z-axis, respectively, during flight time.

4.2 Constraints Design

To optimize possible flight paths Constraints are 0 when satisfied, otherwise a penalty is applied. Applying a penalty Q assures that the path from source to destination is always feasible. Considering the physical restrictions on the UAV and the environment's limits, we can formulate the constraints as follows:

$$F_{Constraints} = UAV_{constraints} + Environment_{constraints} \quad (27)$$

4.2.1 UAV Constraints

The UAVs have physical properties that cause these constraints. The UAV's behavior during maneuvering should be treated as a priority, as it offers smoothness in flight. In this regard, we care for the most crucial aspects of a UAV: slope and rotation. UAV limitations are therefore defined as follows:

$$UAV_{constraints} = TA + FS \quad (28)$$

1. Turning Angle

The turning angle indicates a UAV's maneuverability in the horizontal direction, i.e. the angle taken during flight from the previous and current directions. The turning angle should be less than the maximum tolerable threshold for turning, thus we calculate it as follows:

$$TA = 0, TA = \sum_{i=2}^{N_w-1} TA_i$$

where,

$$T A_i = \begin{cases} Q, & \text{if } \theta > \theta_{max} \\ 0, & \text{otherwise} \end{cases} \quad (29)$$

where, θ defines the turning angle of the UAV in 3D directions (x_i, y_i, z_i) , and θ_{max} maximum tolerable angle. The authors in [34] provided the formulation to calculate turning angle θ_i as follows:

$$\theta = \arccos\left(\frac{(p_{x_i}, p_{y_i})(p_{x_{i+1}}, p_{y_{i+1}})^T}{\|p_{x_i}, p_{y_i}\|_2 \|p_{x_{i+1}}, p_{y_{i+1}}\|_2}\right) \quad (30)$$

where, $p_{x_i} = x_i - x_{i-1}$, $p_{x_{i+1}} = x_{i+1} - x_i$, $p_{y_i} = y_i - y_{i-1}$, $p_{y_{i+1}} = y_{i+1} - y_i$ and $\|x\|_2$ is a vector norm for a vector x .

2. Flying Slope

The flying slope is defined as the mobility of a UAV while gliding and while climbing. During flight, the UAV's slope is along the horizontal from one waypoint to the next. Given the permissible gliding and ascending angles, the slope of a UAV is derived as:

$$FS = 0, FS = \sum_{i=2}^{N_w} FS_i$$

where,

$$FS_i = \begin{cases} Q, & \text{if } f_i \notin [\tan(\alpha_{max}), \tan(\beta_{max})] \\ 0, & \text{otherwise} \end{cases} \quad (31)$$

where, FS_i is the flying slope from one waypoint to the i -th waypoint; α_{max} and β_{max} represent the maximum tolerable gliding and climbing angles, and f_i can be formulated, according to [34], as follows:

$$f_i = \frac{z_i - z_{i-1}}{\|x_i - x_{i-1}, y_i - y_{i-1}\|_2} \quad (32)$$

where, f_i is the flying slope taken by the UAV from the i -th waypoint $(x_i; y_i; z_i)$.

4.2.2 Environment Constraints

Due to the external environment, the UAV must follow specific rules. Restricted areas such as military sites, key government institutions, etc., should be taken into consideration. Therefore, a system should be planned to avoid these limited locations. Likewise, unforeseen events can occur in which the UAV encounters a flying toy, for example, an unregistered aerial vehicle, or birds in flight. Regional sensitivity is used to handle these types of circumstances. This deals with randomly generated sensitive regions where the UAV recognizes a threat and computes a safe path to avoid them. Furthermore, the terrain restricts flight. Environmental constraints can be expressed as follows. We divide the path into a 20×20 grid, and the UAV can sense four cells around itself.

$$Environment_{constraints} = RA + RS + TL + ML + CA \quad (33)$$

1. Restricted Area

There are some specific areas that UAVs are not permitted to fly through due to restrictions, such as cantonments, restricted government territories, and so on, and hence the feasible path to the destination should be a legal one that avoid those regions. For simplicity, we consider a restricted area to be a rectangle. Formulation of a restricted region as follows:

$$RA = 0, RA = \sum_{i=1}^{N_w} RAC_i \quad (34)$$

where,

$$RAC_i = \begin{cases} Q, & \text{if waypoint in Range}(x_r, y_r) \\ 0, & \text{otherwise} \end{cases}$$

where, $Range(x_r, y_r) = \{m_x \leq x_r \leq n_x\} \cap \{m_y \leq y_r \leq n_y\}$ and m_x and n_x represent the lower and upper bounds, respectively, for x coordinates of the r-th restricted area at the i-th waypoint, whereas m_y and n_y indicate the lower and upper bounds, respectively, of y coordinates of the r-th restricted area at the i-th waypoint.

2. Region Sensitivity

Unconditional and unexpected events might occur during flight. Thus, all hazardous events in the path of a UAV are randomly generated. It notices the hazard and constructs a path to avoid them. This can be formulated as follows:

$$Rs = 0, Rs = \sum_{i=1}^{N_w} Rs_i(t) \quad (35)$$

where

$$\begin{aligned}
 Rs_i &= \sum_{cellx \in N(i)} v_{cellx}(t) \\
 Rs_i &= \begin{cases} Q, & \text{if } Rs_i > Rs_{th} \\ 0, & \text{otherwise} \end{cases}
 \end{aligned} \tag{36}$$

where, $Rs_i(t)$ is the value for sensitivity at the i -th waypoint during the flight at time t , and $v_{cellx}(t)$ is the cell value at flight time t . $N(i)$ is the set of neighbor cells for the i -th waypoint. The UAV checks the values of the cells at every waypoint, and if any cell has a sensitivity value greater than the threshold, penalty Q will be given. It checks the values of the set of neighbor cells for $N(i)$ to avoid that region to satisfy the constraint.

3. Terrain Limits

During flight, a UAV should take into consideration the limitations of the terrain so that the UAV always flies above it and avoids collisions (for example, with mountains). To adhere to a terrain constraint, the algorithm gives penalty Q to provide the feasible path. This constraint can be formulated as follows:

$$TL = 0, TL = \sum_{i=1}^{N_w} TL_i \tag{37}$$

where,

$$TL_i = \begin{cases} Q, & \text{if } z_i \leq \text{map}(x_i, y_i) \\ 0, & \text{otherwise} \end{cases}$$

where, $\text{map}(x_i, y_i)$ is a function that returns the altitude of the terrain location at point (x_i, y_i) , which finds the number of points inside that location.

4. Map Limits

For a feasible path, the UAV must stay inside the mission space to avoid uncertainties. Therefore, the algorithm applies penalty Q to the points of a trajectory that are off the map limits. This constraint ensures the space of a mission can be formulated as follows:

$$ML = \sum_{i=1}^{N_w} ML_i \tag{38}$$

where,

$$ML_i = \begin{cases} 0, & \text{Inmap}(x_i, y_i) \\ Q, & \text{Otherwise} \end{cases}$$

$$\text{Inmap}(x_i, y_i) = (x_l^m \leq x_i \leq x_u^m) \wedge (y_l^m \leq y_i \leq y_u^m) \quad (39)$$

where, x_l^m and x_u^m are the lower and upper bounds, respectively, for the x coordinate, and y_l^m and y_u^m are the lower and upper bounds, respectively, for the y coordinate. The minimum value to satisfy the map constraint is $ML = 0$.

5. UAV Collision Avoidance

When calculating paths for multiple UAVs, the planner must ensure that the UAVs do not get too close to each other, increasing the possibility of a collision while following their individual paths. To keep a safe distance between them, the limitation can be expressed as follows:

$$CA = \sum_{i=1}^{N_w^u} \sum_{j=1}^{N_w^u} CA_i \quad (40)$$

where,

$$CA_i = \begin{cases} Q, & \text{if } d_{ij}^{uv} < d_{min} \\ Q, & \text{otherwise} \end{cases}$$

$$d_{min}^{uv} = \sqrt{(x_i^u - x_j^v)^2 + (y_i^u - y_j^v)^2 + (z_i^u - z_j^v)^2} \quad (41)$$

where, d_{min} is the minimum distance between the UAVs to avoid a collision, and d_{ij}^{uv} is the distance between the i-th waypoint and the j-th waypoint of the u-th UAV trajectory and the j-th UAV trajectory, respectively.

5 Operation of the Proposed Path Planner

In this section, we explain the working mechanism of the proposed multiple UAV–path planner, which is based on visual-SLAM, PSO, and the DFF explained in Sects. 2, 3, and 4, respectively. The proposed planner first utilizes the elevation map generated by visual-SLAM and fed into the PSO planning algorithm to derive the optimum trajectory for each UAV to the defined destinations, in which the DFF optimizes all the possible waypoint sequences to reach destinations considering all constraints and objectives, along with satisfying the collision avoidance condition. If all conditions are satisfied, the planner will output the optimum trajectory for each UAV to its destination.

In our proposed system, the path from source to destination consists of waypoints and line segments. We opted for an eight-waypoint trajectory-generation system. For clear understanding, we divided the whole operation area into cells and determine the estimated flight time to the destination. Next, we initialize the PSO algorithm to plan the optimum path for each UAV, which can be seen in Fig. 3 from step 5–33. In the quest to attain the optimum trajectory for each UAV, at first, the planner randomly generates the velocity and position vectors of particle PN. Next, using Eq. (15), the velocity and position vectors of each particle are updated.

After that, the proposed DFF is applied to the updated particle as shown the working flowchart of the DFF in Fig. 2. Considering all the constraints and objectives,

Algorithm 1 Pseudocode of proposed UAVs Path Planner	
1:	Set flight time = T_{flight} ;
2:	Initialize the cell values;
3:	for $i = 1: T_{flight}$
4:	{
5:	while (CA is not satisfied)
6:	{
7:	Set UAV number = N ;
8:	for $j = 1: N$
10:	Set iteration number = N_{iter} ;
11:	Set particle number = P_n ;
12:	for $k = 1: N_{iter}$
13:	{
14:	for $t = 1: P_n$
15:	{
16:	Randomly initialize x_t and v_t ;
17:	Initialize $P_{t,best} = x_t, S_{best} = x_{Pn}$;
18:	Update x_t and v_t using the updating formula (15);
19:	Compute the fitness value of x_t using formulas (16) -(39);
20:	if (fitness (x_t) > fitness ($P_{t,best}$))
21:	{ $P_{t,best} = x_t$; }
22:	if (fitness ($P_{t,best}$) > fitness (S_{best}))
23:	{
24:	$S_{best} = P_{t,best}$;
25:	$Opt_fitness = fitness (S_{best})$;
26:	}
27:	Sense the sensitive region using formula (36);
28:	if ($RS(i) < RS(th)$)
29:	$Opt_fitness = fitness (S_{best})$;
30:	else
31:	return to step 19;
32:	}
33:	}
34:	Evaluation collision among multi-UAVs using formula (40);
35:	}
36:	Output the collision-free trajectories for multiple UAVs
37:	}
38 :	Output T_{flight} flight time path planning results;

Fig. 3 Pseudocode of the proposed path planner

the DFF optimizes each particle and finally outputs the best particle, pibest and the global best particle in the swarm, sbest, which is explained in Sect. 4. The DFF output is based on the fitness value acquired by each particle. Then, we store the optimum path for the first UAV and set the iteration number to N_t . Before initializing the other UAVs, we aim to derive a collision-free path, and therefore, we check collision avoidance condition CA. If CA is satisfied, the planner outputs optimum trajectories for all UAVs; otherwise, it goes back to step 5 if the CA is not satisfied. Finally, when the flight time reaches, the planner will output the optimum paths for all UAVs to their respective destinations. The process of the proposed planner is represented in the pseudocode algorithm shown in Fig. 3.

6 Simulation Results

In this section, we develop a Matlab-based operational environment to evaluate the working performance of the proposed two-step UAV path-planning system. The main simulation parameters are listed in Table 1. In our implementation, we used a data set [42] that was collected by a monocular camera installed at the quad-copter, in different environments. The data set is publicly available, and more details can be found at midair.ulg.ac.be. The data set was utilized as input to the optimization algorithm for multiple-UAV path planning algorithm. We used different types of test sequences, which can be seen in Figs. 4 and 5 in our system to construct an online map of the environment. Figure 6a indicates the features in the consecutive scenes that were matched to simultaneously build an incremental map, which can be seen in Fig. 6b. The points cloud map contains information on the x, y, z positions and normal at every point. The terrain representations from the points cloud can be seen in Fig. 7. We utilized a triangulation algorithm [43] to reconstruct the terrain from

Table 1 Simulation parameters

Parameter	Value
No. of UAVs	2
Speed	10 m/s
Power	20
Iteration number	32, 64, 128, 256, 512
Sensitivity threshold	10
Turning angle threshold	85°
Gliding angle threshold	-30°
Climbing angle threshold	30°
Minimum distance threshold	0.2
Initial environmental risk	1-5
Flight time threshold	2
Grid size	20 × 20

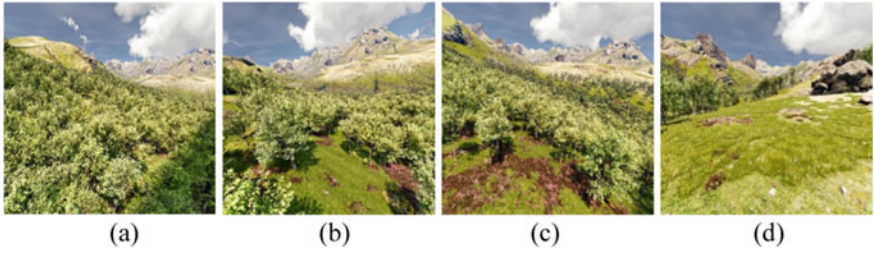


Fig. 4 Flight path (sequence 0005)

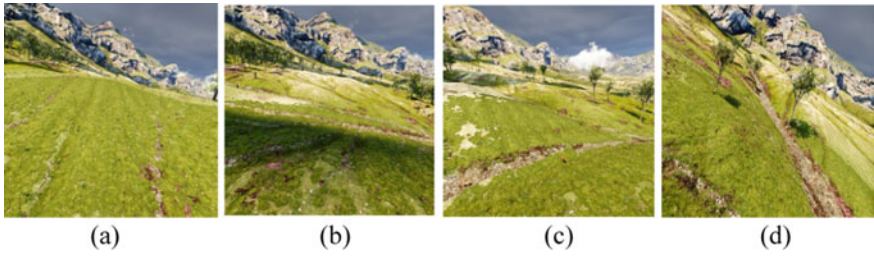


Fig. 5 Flight path (sequence 0012)

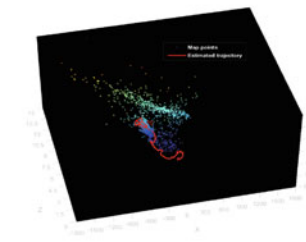
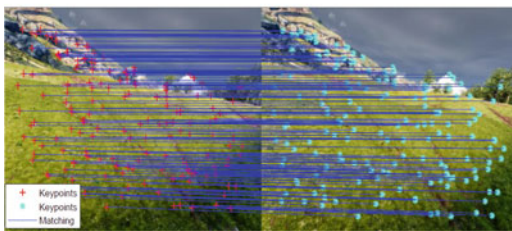
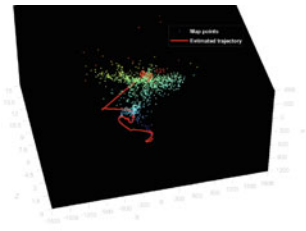


Fig. 6 a Image registration between consecutive scenes and b Map construction by VSLAM to be used for path planning

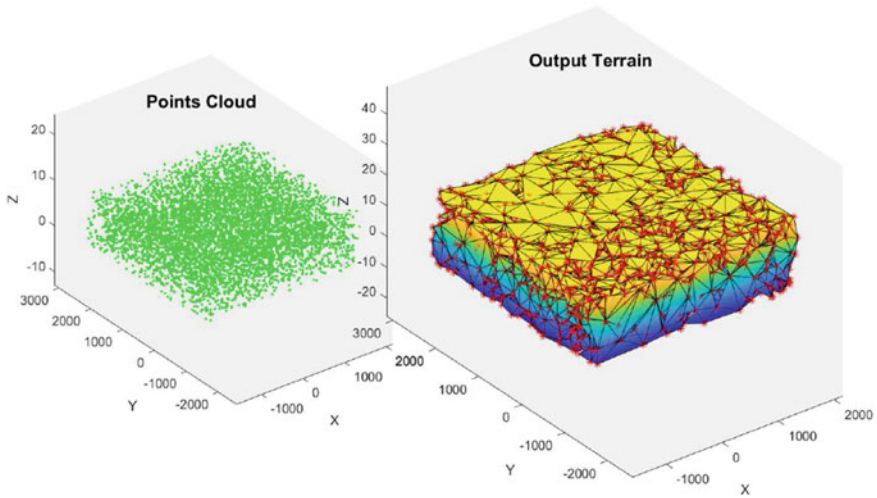


Fig. 7 Terrain representation from the points cloud of sequence 0012

the points cloud.

Figure 8 shows the effect of different numbers of particles on the optimal fitness value of the proposed DFF. We can clearly see that the fitness value of the proposed DFF converges to a stable value faster as the number of particles and iterations

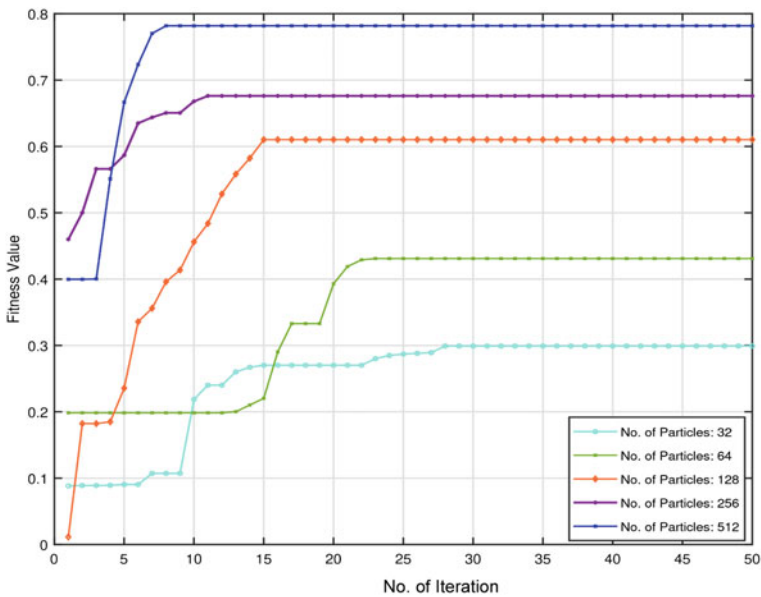


Fig. 8 Optimal fitness values for different numbers of optimization particles

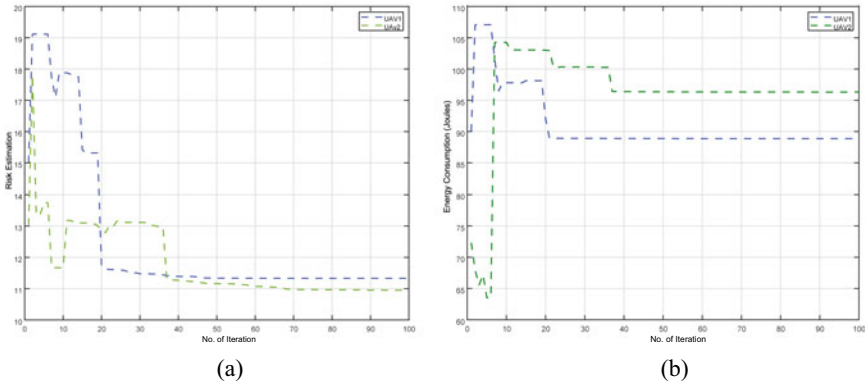


Fig. 9 Optimization of the PSO path planner performance in terms of **a** risk estimation and **b** energy consumption

increases. The optimization performance of the path planner in terms of energy consumption and flight risk estimation can be observed in Fig. 9. We utilized 128 particles in our system. As the number of iterations increased, the values of energy consumption and flight risk estimation converged to a stable value. Moreover, the difference between the optimum value of energy consumption, where both UAVs converge, is less than five, and the values of flight risk estimation for both UAVs is similar, which depicts the effectiveness of the proposed path planner by ensuring fairness between the generated paths for both UAVs.

Figure 10 shows the optimal paths followed by UAV 1 and UAV 2 from source to destination while avoiding sensitive regions and restricted areas, respectively, for the first three flights. The small red 1×1 rectangles have a sensitivity greater than the threshold, while the black 2×2 rectangles indicate restricted areas where UAVs are not allowed to fly.

The sensitive regions generate randomly, indicating a hazardous event, so the proposed planner optimizes the path until hazardous free paths to the destinations

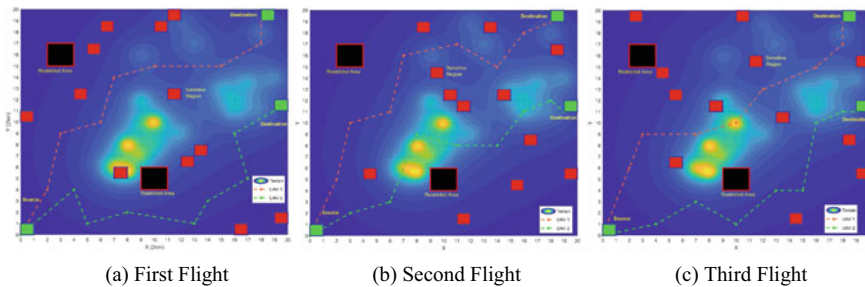


Fig. 10 Optimal trajectories of the UAVs from source to destination using proposed algorithm

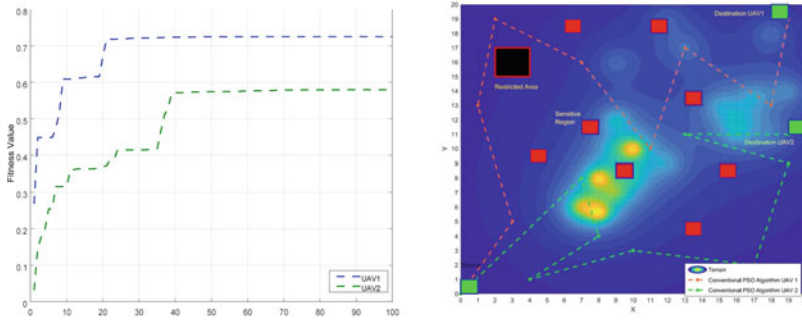


Fig. 11 a Optimal fitness values attained and, b UAVs Flight using Conventional PSO Algorithm

are determined. We can observe that the trajectories generated for each flight time avoids all the sensitive regions and reach the destination safely.

The proposed algorithm also ensures that the multiple UAVs do not collide with each other. The green 1×1 rectangles represent the source and destination. In Fig. 10, the yellow highlighted areas are high elevations. We can also see that the trajectory waypoints generated do not overlap, and a UAV reaches the destination by following the shortest path, which indicates the high efficiency of the proposed planner. Therefore, Fig. 11a indicates the high fitness value attained by each UAV driven by the proposed path planner.

Figure 11b indicates the trajectories generated by the conventional PSO. As the defined environment is dynamically complex due to which conventional PSO is incompatible with adapting the situation; therefore, it takes very high computational time to converge. Considering the incompatibility of the conventional PSO in our environment, we choose to make the environment less complicated and convenient to converge. The computational time for the conventional PSO for the simple environment is higher than our proposed algorithm in the dynamic and complex environment. The conventional PSO takes 1,767 s while our proposed algorithm takes 739.8 s.

The same computer is used to run the both algorithms. The Table 2 indicates the flight statistics of both algorithms for the first flight. The conventional PSO algorithm for both UAVs reaches the destination following the long path. It takes more travel time while our proposed algorithm reaches the destination for both UAVs following the shortest path and in optimal travel time in a highly complex environment. The distance covered from one waypoint to another and the corresponding flight times for both UAVs can be seen in Fig. 12a, b.

The total distances from the source to destination covered by UAVs during the first flight were 3,062.4369 m and 3,065.0706 m. Likewise, the times taken to reach the destinations for both UAVs were almost the same i.e., 307 s. Similarly, Fig. 12c, d indicates the distance covered and corresponding flight time for both UAVs from one waypoint to another using the conventional PSO algorithm. We can observe that the distance and time taken at each waypoint is greater than the proposed algorithm. The total distance covered by the UAVs for the first flight is 5,571.9591 (m) and

Table 2 Distance and Time comparison with the conventional PSO

Parameter	Value
(a) Flight dynamics of first flight using proposed algorithm	
Distance covered by UAV 1	3,062.4369 (m)
Distance covered by UAV 2	3,065.0706 (m)
Travel time by UAV 1	307.2542 (s)
Travel time by UAV 2	307.4481 (s)
(b) Flight dynamics of first flight using conventional PSO algorithm	
Parameter	Value
Distance covered by UAV 1	3,062.4369 (m)
Distance covered by UAV 2	3,065.0706 (m)
Travel time by UAV 1	307.2542 (s)
Travel time by UAV 2	307.4481 (s)

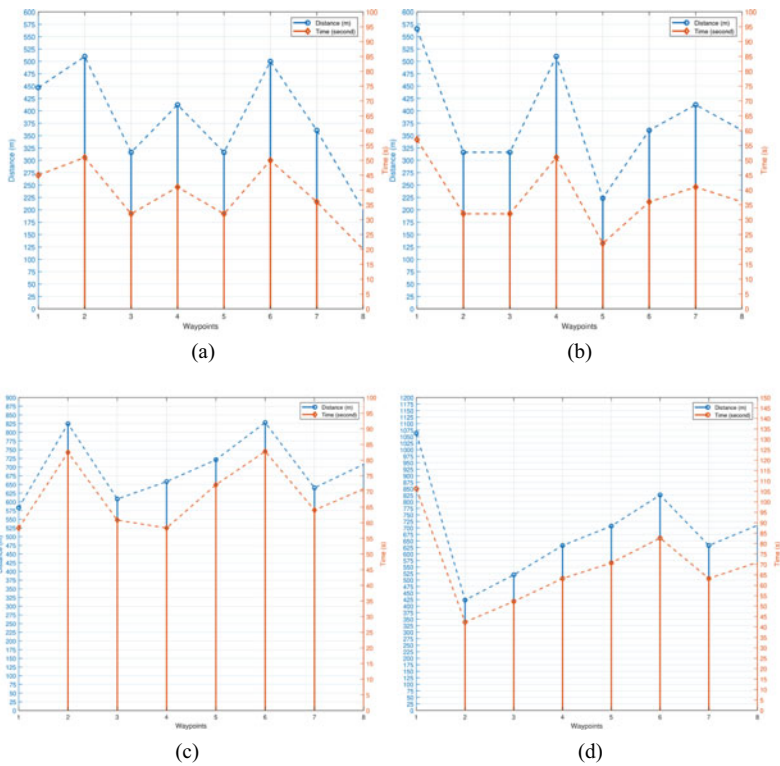
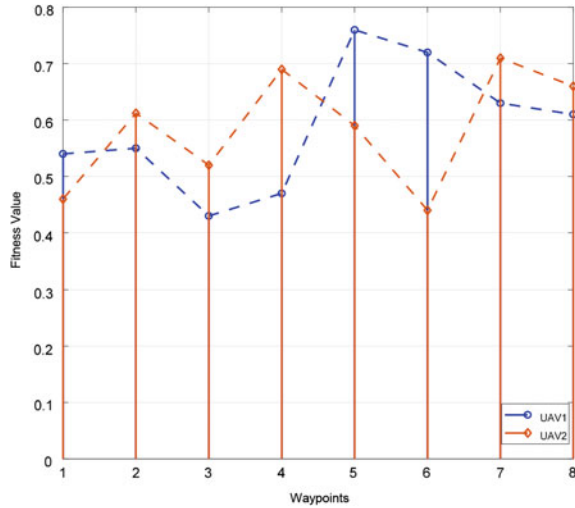


Fig. 12 UAV flight dynamics in terms of distance and time using proposed algorithm for **a** UAV 1 and **b** UAV 2 and using conventional PSO algorithm **c** UAV 1 and **d** UAV 2

Fig. 13 Fitness values attained at each waypoint during the flight by proposed algorithm



6,065.0706 (m). Similarly, the total time consumed by UAV1 and UAV2 is 551.6796 (s) and 549.7633 (s), respectively. In Fig. 13, we show the fitness values attained at each waypoint by both UAVs during their flights. We sum up the optimal fitness values of all waypoints for UAV 1 and UAV 2. The total optimal fitness for all the waypoints of UAV 1 and UAV 2 were 5.52 and 5.51, respectively, which are virtually the same and which depict the fairness of our proposed two-step path planner.

7 Conclusions

In this paper, we designed a two-step, centralized system to construct a map using state-of-the-art visual-SLAM. We introduce corner-edge points matching mechanism to stabilize the system with the least extracted map points. The proposed algorithm effectively detects the keypoints in different environments and successfully registers the features. The constructed map is processed as an input mean for the particle swarm optimization algorithm to plan UAVs' optimum path. We proposed a dynamic fitness function considering different optimization objectives and constraints in terms of UAV flight risk estimation, energy consumption, and maneuverability for the operational time. We also proposed a path updating mechanism based on region sensitivity to avoid sensitive regions if any hazardous and unexpected event detects in UAVs' paths. The system effectively avoids the sensitive regions and returns collision-free paths to reach UAV to the destinations safely. The simulation results validate the effectiveness of our proposed PSO-VSLAM system. We currently consider two UAVs over different flight times to evaluate our proposed PSO-VSLAM system's performance, and it successfully outputs the collision-free trajectories and proves high adaptability towards the complex dynamic environment. Therefore, we plan to consider more than

two UAVs in our future work and implement machine learning algorithms because our proposed system effectively achieves the collision-free trajectories for two UAVs while adapting to the highly dynamic and complex environment.

Acknowledgement This work was supported by the National Research Foundation of Korea (NRF) grant funded by the Korea Government (MSIT) under Grant NRF-2019R1F1A1061696.

References

1. Cadena C, Carlone L, Carrillo H, Latif Y, Scaramuzza D, Neira J, Reid I, Leonard JJ (2016) Past, present, and future of simultaneous localization and mapping: toward the robust-perception age. *IEEE Trans Rob* 32(6):1309–1332
2. Trujillo JC, Munguia R, Guerra E, Grau A (2018) Cooperative monocular-based SLAM for multi-UAV systems in GPS-denied environments. *Sensors* 18(5):1351
3. Du H, Wang W, Xu C, Xiao R, Sun C (2020) Real-time onboard 3D state estimation of an unmanned aerial vehicle in multi-environments using multi-sensor data fusion. *Sensors* 20(3):919
4. Ramezani M, Tinchev G, Iuganov E, Fallon M (May 2020) Online LiDAR-SLAM for legged robots with robust registration and deep-learned loop closure. In: 2020 IEEE international conference on robotics and automation (ICRA), pp 4158–4164
5. Stentz A, Fox D, Montemerlo M (2003) Fastslam: a factored solution to the simultaneous localization and mapping problem with unknown data association. In: Proceedings of the AAAI national conference on artificial intelligence
6. Loo SY, Mashohor S, Tang SH, Zhang H (2020) DeepRelativeFusion: dense monocular SLAM using single-image relative depth prediction. arXiv:2006.04047
7. Shakhathreh H, Sawalmeh AH, Al-Fuqaha A, Dou Z, Almaita E, Khalil I, Othman NS, Khreishah A, Guizani M (2019) Unmanned aerial vehicles (UAVs): a survey on civil applications and key research challenges. *IEEE Access* 7:48572–48634
8. Mughal UA, Xiao J, Ahmad I, Chang K (2020) Cooperative resource management for C-V2I communications in a dense urban environment. *Veh Commun* 26:100282
9. Mughal UA, Ahmad I, Chang K (2019) Virtual cells operation for 5G V2X communications. In: Proceedings of KICS, pp 1486–1487
10. Shakoor S, Kaleem Z, Baig MI, Chughtai O, Duong TQ, Nguyen LD (2019) Role of UAVs in public safety communications: energy efficiency perspective. *IEEE Access* 7:140665–140679
11. Wen S, Zhao Y, Yuan X, Wang Z, Zhang D, Manfredi L (2020) Path planning for active SLAM based on deep reinforcement learning under unknown environments. *Intell Serv Robot* 1–10
12. Kalogeiton VS, Ioannidis K, Sirakoulis GC, Kosmatopoulos EB (2019) Real-time active SLAM and obstacle avoidance for an autonomous robot based on stereo vision. *Cybern Syst* 50(3):239–260
13. Doitsidis L, Weiss S, Renzaglia A, Achtelik MW, Kosmatopoulos E, Siegwart R, Scaramuzza D (2012) Optimal surveillance coverage for teams of micro aerial vehicles in GPS-denied environments using onboard vision. *Auton Robot* 33(1):173–188
14. Alzugaray I, Teixeira L, Chli M (May 2017) Short-term UAV path-planning with monocular-inertial SLAM in the loop. In: 2017 IEEE international conference on robotics and automation (ICRA), pp 2739–2746
15. Sánchez-García J, Reina DG, Toral SL (2019) A distributed PSO-based exploration algorithm for a UAV network assisting a disaster scenario. *Futur Gener Comput Syst* 90:129–148
16. Shi W, Li J, Xu W, Zhou H, Zhang N, Zhang S, Shen X (2018) Multiple drone-cell deployment analyses and optimization in drone assisted radio access networks. *IEEE Access* 6:12518–12529

17. Ghamry KA, Kamel MA, Zhang Y (June 2017) Multiple UAVs in forest fire fighting mission using particle swarm optimization. In: 2017 International conference on unmanned aircraft systems (ICUAS), pp 1404–1409
18. Cheng Z, Wang E, Tang Y, Wang Y (2014) Real-time path planning strategy for UAV based on improved particle swarm optimization. *JCP* 9(1):209–214
19. Bircher A, Kamel M, Alexis K, Oleynikova H, Siegwart R (May 2016) Receding horizon “next-best-view” planner for 3d exploration. In: 2016 IEEE international conference on robotics and automation (ICRA), pp 1462–1468
20. Teng H, Ahmad I, Msm A, Chang K (2020) 3D optimal surveillance trajectory planning for multiple UAVs by using particle swarm optimization with surveillance area priority. *IEEE Access* 8:86316–86327
21. Pattanayak S, Choudhury BB (2021) Modified crash-minimization path designing approach for autonomous material handling robot. *Evol Intel* 14(1):21–34
22. Yu X, Li C, Zhou J (2020) A constrained differential evolution algorithm to solve UAV path planning in disaster scenarios. *Knowl-Based Syst* 204:106209
23. Dasdemir E, Köksalan M, Öztürk DT (2020) A flexible reference point-based multi-objective evolutionary algorithm: an application to the UAV route planning problem. *Comput Oper Res* 114:104811
24. Qu C, Gai W, Zhang J, Zhong M (2020) A novel hybrid grey wolf optimizer algorithm for unmanned aerial vehicle (UAV) path planning. *Knowl-Based Syst* 194, 105530
25. Atencia CR, Del Ser J, Camacho D (2019) Weighted strategies to guide a multi-objective evolutionary algorithm for multi-UAV mission planning. *Swarm Evol Comput* 44:480–495
26. Shakoor S, Kaleem Z, Do DT, Dobre OA, Jamalipour A (2020) Joint optimization of UAV 3D placement and path loss factor for energy efficient maximal coverage. *IEEE Internet Things J* 9776–9786
27. Do-Duy T, Nguyen LD, Duong TQ, Khosravirad S, Claussen H (2021) Joint optimisation of real-time deployment and resource allocation for UAV-Aided disaster emergency communications. *IEEE J Sel Areas Commun* 1–14
28. Nguyen KK, Vien NA, Nguyen LD, Le MT, Hanzo L, Duong TQ (2020) Real-time energy harvesting aided scheduling in UAV-assisted D2D networks relying on deep reinforcement learning. *IEEE Access* 9:3638–3648
29. Do DT, Nguyen TTT, Le CB, Voznak M, Kaleem Z, Rabie KM (2020) UAV relaying enabled NOMA network with hybrid duplexing and multiple antennas. *IEEE Access* 8:186993–187007
30. Kaleem Z, Yousaf M, Qamar A, Ahmad A, Duong TQ, Choi W, Jamalipour A (2019) UAV-empowered disaster-resilient edge architecture for delay-sensitive communication. *IEEE Network* 33(6):124–132
31. Zhou H, Zhang T, Jagadeesan J (2018) Re-weighting and 1-point RANSAC-Based P \$ n \$ n P solution to handle outliers. *IEEE Trans Pattern Anal Mach Intell* 41(12):3022–3033
32. Chum O, Matas J (June 2005) Matching with PROSAC-progressive sample consensus. In: 2005 IEEE computer society conference on computer vision and pattern recognition (CVPR’05), vol 1, pp 220–226
33. Bellavia F, Tegolo D, Valenti C (2011) Improving Harris corner selection strategy. *IET Comput Vision* 5(2):87–96
34. Canny J (1986) A computational approach to edge detection. *IEEE Trans Pattern Anal Mach Intell* 6:679–698
35. Karami E, Prasad S, Shehata M (2017) Image matching using SIFT, SURF, BRIEF and ORB: performance comparison for distorted images. [arXiv:1710.02726](https://arxiv.org/abs/1710.02726)
36. Ohta Y, Kanade T (1985) Stereo by intra- and inter-scanline search using dynamic programming. *IEEE Trans Pattern Anal Mach Intell* 2:139–154
37. Lowe DG (1991) Fitting parameterized three-dimensional models to images. *IEEE Trans Pattern Anal Mach Intell* 13(5):441–450
38. Zheng C, Li L, Xu F, Sun F, Ding M (2005) Evolutionary route planner for unmanned air vehicles. *IEEE Trans Rob* 21(4):609–620

39. Kennedy J, Eberhart R (Nov 1995) Particle swarm optimization. In: Proceedings of ICNN'95-international conference on neural networks, vol 4, pp 1942–1948
40. Roberge V, Tarbouchi M, Labonté G (2012) Comparison of parallel genetic algorithm and particle swarm optimization for real-time UAV path planning. *IEEE Trans Industr Inf* 9(1):132–141
41. Fonder M, Van Droogenbroeck M (2019) Mid-air: a multi-modal dataset for extremely low altitude drone flights. In: Proceedings of the IEEE/CVF conference on computer vision and pattern recognition workshops, pp 0–0
42. Guo X, Chen S, Lin H, Wang H, Wang S (July 2017) A 3D terrain meshing method based on discrete point cloud. In: 2017 IEEE international conference on information and automation (ICIA), pp 12–17
43. Kneip L, Scaramuzza D, Siegwart R (2011) A novel parametrization of the perspective-three-point problem for a direct computation of absolute camera position and orientation. *CVPR* 2011:2969–2976

UAV-Assisted Cooperative Routing Scheme for Dense Vehicular Ad hoc Network



Omer Chughtai, Muhammad Naeem, and Kishwer Abdul Khaliq

Abstract Intelligent transportation system (ITS) has enormous potential and has been able to extend the transportation systems to more sustainable, secure, and manageable communicating systems. Particularly, a Vehicular ad hoc network (VANET) plays an imperative part to preserve and oversee the features of ITS. Since VANET provides a highly dynamic environment, where disseminating messages to the intended destination in a scenario with high node-density without any interruption is a critical strategy. Existing data dissemination techniques using single-radio devices do face degradation in terms of an increase in end-to-end (ETE) delay and decrease in throughput because of the inefficient spectrum utilization. To deal with this, techniques that use assistance from other channels that are generally referred to as dual-radio multi-channel have been proposed, which can efficiently use the spectrum in a cooperative manner; however, due to the cross-channel interference in the same band, the network performance degrades. Considering these facts, getting assistance from another network is one of the solutions to increase the performance of the network. Therefore, a UAV-assisted Cooperative Routing Scheme (UCRS) has been proposed, where a Flying ad hoc network (FANET) aids VANET. Each node in UCRS creates an Allied Node Table (ANT) based on the vehicles in the forwarding zone. The best node among several nodes available in ANT is selected in an ETE route through which the data traffic is forwarded to the intended destination. With connection/communication disturbance due to congestion or gap between the vehicles during data exchange, UCRS attempts local repair up to two hops; in case of failure to recover the route, assistance from UAV is carried out. The performance

O. Chughtai (✉) · M. Naeem

Department of Electrical and Computer Engineering, COMSATS University Islamabad, Wah Campus, Rawalpindi 47040, Pakistan

e-mail: omer.chughtai@cuiwah.edu.pk

K. A. Khaliq

School of Electronic and Electrical Engineering, University of Leeds, Leeds, England

e-mail: K.A.Khaliq@leeds.ac.uk

evaluation is performed using the network simulator (ns-2.31) and the analysis shows that UCRS achieved better performance as compared to U2RV and AODV with an increase in node density.

Keywords Routing · UAV-assistance · Vehicular Ad hoc Network · Dense environment · Cooperative routing

1 Introduction

Vehicular Ad hoc Network (VANET) empowers vehicles to communicate with each other with any central control through various wireless communication technologies. One of the main issues with respect to the expanded utilization of private vehicles is an increase in the number of fatalities that happen due to mishaps on the roads and related threats which have been recognized as genuine issues being stood up in modern societies. One of the solutions is to have a coordination with other networks to get assistance e.g., FANET. FANET and VANET support different routing algorithms than MANET. Primarily, VANET provides Vehicle-to-vehicle (V2V) and Vehicle-to-Infrastructure (V2I) communications. One of its goals is to optimize data transmission with increased throughput and reduced delays. VANET protocols are generally designed to address variable traffic density with rapid topological changes. To cater to the new wireless communication with respect to vehicles, IEEE has standardized vehicular communication as the IEEE 802.11p standard.

The IEEE 802.11p of VANET is also referred to as WAVE (Wireless Access for Vehicular Environments) and DSRC (Dedicated Short Range Communication). VANET is the integral technology of an Intelligent transportation system (ITS) and is capable to provide services for high-speed data dissemination and autonomous driving [1]. The rapid increase in vehicles and their technical growth has become dynamic [2]. In order to meet the Quality of service (QoS) requirements and to have a reliable connection, the vehicular network has been amalgamated with emerging technologies like fifth generation (5G) networks, software-defined networks (SDN), and Internet of things (IoT), which generally referred as the Internet of Vehicles (IoV). These emerging technologies are integrated with VANET to enhance the overall functionality, quality, scalability, versatility, and adaptability. However, due to issues of security, exorbitant cost, and heterogeneity, the performance of the SDN controller still needs improvement. Additionally, the automobile manufacturing industries have deployed Wi-Fi-based DSRC in their recent vehicles and are looking forward to 5G and (D2D) device-to-device communication technology as discussed in [3]. Along with the aforementioned technologies, which have been integrated with VANET, another emerging concept, that considers multi-dimensional integrated systems which are capable to control processes and integrate information, and along with this, it provides real-time monitoring with high reliability, security and efficiency are vehicular to anything (V2X). V2X is also an important entity in emerging technologies of ITS and has numerous advantages over conventional ITS.

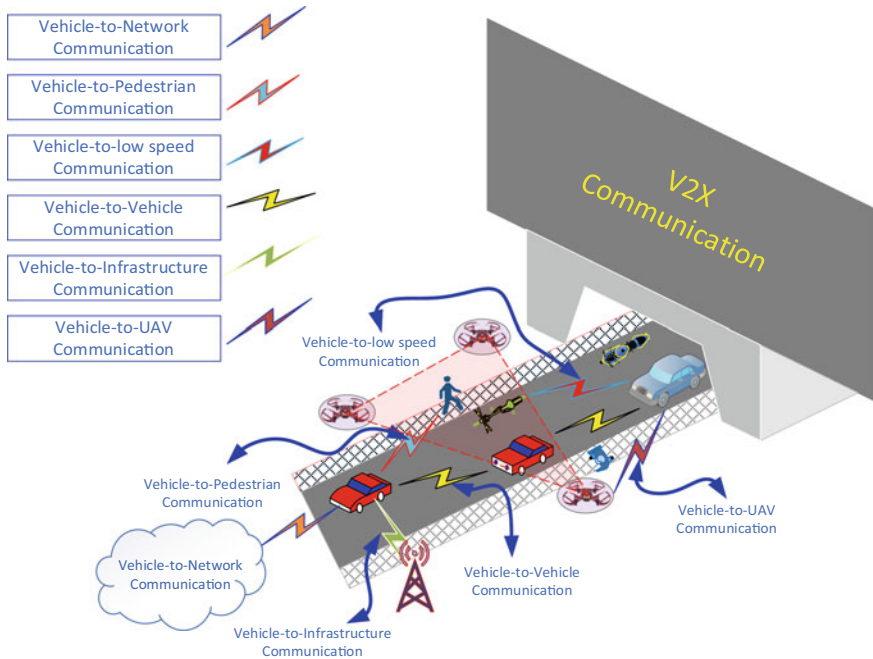


Fig. 1 V2X Communication in an ad hoc manner with available entities in the network

For example, V2X communication is operated in a dynamic environment, with high mobility and low latency.

With V2X communication, communicating nodes can exchange real-time and secure information with the capacity to upgrade for future assistance. There are various types of wireless communications that can be carried out by vehicles in V2X communication, i.e., V2V (vehicle to vehicle), V2R (vehicle to the roadside unit), V2I (vehicle to infrastructure), V2P (vehicle to pedestrian), and V2U (vehicle to UAV) as depicted in Fig. 1 and discussed in [4]. V2X communication requires extremely low end-to-end delay and very high reliability, which cannot be achieved by using the conventional cellular network [5]. The problem of dis-connectivity and untimely dissemination of data traffic in VANET is due to the gap between the vehicles. Additionally, the problem might be due to the inefficient spectrum utilization and alternately switching among various service channels using the single-radio device. This increases the ETE delay and decreases throughput. In contrary to this, the dual-radio devices can efficiently use the spectrum; however, due to the cross-channel interference of the same band, the network performance degrades. Furthermore, the network performance deteriorates because of the inappropriate selection of path or next-hop node in the network. By considering the above-stated problems, VANET requires an efficient routing mechanism and may need to have assistance from another network with a distinctive band, which might help to increase the connectivity and

may route the desired information reliably to the intended destination in a timely manner.

The rest of the paper is organized as follows: Sect. 2 of this research presents the background knowledge of V2X communication and the effectiveness of getting assistance from another channel or from another network. Section 3 discusses the proposed mechanism of routing in UAV-assisted VANET. Section 4 presents the simulation results with a detailed analysis and Sect. 5 contains the conclusion.

2 Literature Review

VANET mainly consists of Roadside Units (RSUs) and On-Board Units (OBUs). OBUs are installed on vehicles while RSUs are deployed by the trusted authority. RSU deployment schemes can influence OBU's short time certificate update [6]. Location and density of RSU estimate the effectiveness of VANETs [7]. In order to deploy the RSUs, several features are taken into consideration to achieve an optimal solution. Different techniques can be used i.e., BIP (Binary integer programming) and BEH (Balloon expansion heuristic). Multi channels i.e., control channel CCH and service channels SCH are supported by IEEE standard 1609.4. CCH is responsible to transmit control information as well as safety, while SCH is responsible to transmit service data [8]. However, data exchange among heterogeneous networks can be very complicated, where the issues like security, privacy, authenticity, data transmission rate, and latency can rise, and need to be addressed well in time. In the literature, there are notable examples from the works of [9–11] regarding the mobility model, channel characterization model, and routing protocols in heterogeneous networks. V2X communication intended to be one of the indispensable modes of communication for future self-sufficient vehicles, which are getting closer to reality with every passing day. Diverse communication technologies have been consolidated to frame a heterogeneous V2X system to help data merger. However, data reliance models are yet intended to cater for single-use cases [12] which are not covered by Cooperative Intelligent Transport Systems (C-ITS). Car applications incorporate a wide arrangement of utilization cases, going from crash avoidance to high platooning, and to exceptionally self-governing driving; each having various prerequisites as far as network types and traffic designs are concerned. Specifically, the advancements in V2X communication should be backward-compatible with a vehicle to infrastructure (V2I), vehicle to vehicle (V2V), vehicle to pedestrian (V2P), and vehicle to UAV.

UAVs are viewed as a significant component of IoT, which are furnished with dedicated sensors with specialized communication gadgets. UAVs offer different administrative tasks, for example, low height reconnaissance, post-catastrophe salvage, coordination, and communication. In addition, the abilities of drones to assist broadband remote communication, particularly shaping FANETs by communicating with ground nodes, have been evaluated by simulations and approved through field tests in [13]. Compared with vehicles and their structures, drones fly in the sky with a higher likelihood to interface ground vehicles and with different UAVs by means

of a line of sight (LOS), which encourages profoundly reliable transmission [14]. In [15], the author presents the UAV (drone) assisted vehicular networks DVN, which gives a pervasive connection with vehicles by integrating network technologies and communication of UAVs with associated vehicles. In particular, the author initially proposed the architecture of the DVN and highlighted its services. It has been accentuated that by coordinating with infrastructure and vehicles, UAVs are capable to improve vehicle-to-vehicle communication, data collection ability, coverage, and interworking efficiency of the network.

One of the most important subjects in the field of communication in ad hoc networks is the increasing demand of available routes [16]. All Key point indicators (KPIs) in routing depend upon the basic algorithm of a routing protocol. FANET is one of the desired solutions and is used as a relay between disconnected VNs [17]. Moreover, UAVs with high stability and effective residual energy can increase network life by selecting efficient routes using artificial intelligence (AI) based algorithms that adopt a reinforced learning approach [18]. An adaptive UAV-assisted geographic routing with Q-Learning is presented in [19]. Here, the presented routing scheme is divided into aerial component and depth-first search (DFS) algorithm. The first part is used to determine the global routing path using the fuzzy logic and the second component is used to gather information like the global road traffic. The gathered information is then forwarded to the ground requesting vehicle. In order to improve the quality of service (QoS) of each end-user (EU) UAV can select its trajectory based on the location of EU [20]. Looking into the needs of the future, the author in [21] has proposed the Internet of UAVs over a cellular network with 6G to facilitate UAVs to everything U2X using dynamic routing protocols and reinforcement learning.

To enhance communication in VANET by means of optimization, UAVs have been utilized in order to investigate the relay selection problem in [22, 23]. In [10], the author has also selected FANET to assist VANETs, whenever disconnection occurs. Due to the flexible mobility of UAVs, they immediately act as a relay to re-establish the connection. However, the protocol used by the author cannot tolerate even a few seconds of disconnection. To overcome this issue another author in [24] has proposed a protocol that built the routing paths gradually combining three parameters i.e. traffic density, connectivity, and distance between connecting nodes. Nevertheless, this protocol lacks the information about the location of vehicles in the routing path. In [4], the authors overcome the drawbacks of [24] and exploited UAVs to calculate the exact location of vehicles by the exchange of HELLO messages. However, UAVs are under-utilized as they are only used when the other routing paths between vehicles are disconnected. In urban cities, UAVs are considered to be a suitable choice to provide VANET connectivity [25]. To get the assistance from UAV in an area where either the disaster takes place or public safety missions are required, a work presented in [26] was considered, that uses the resource allocation scheme in emergency scenarios for UAV-aided relay systems. UAVs can avoid obstacles to ensure the reliable delivery of data. Therefore in [27, 28], the process of route discovery is based on flooding and on-demand route request. While route reply (RREP) is sent back by the destination including information of all discovered paths to the

source node. However, the destination node needs to wait for multiple paths in [27]; this creates a high end-to-end (ETE) delay. In [29], it has been highlighted that the usage of just V2V communication does not perform well in a high mobility scenario with intermittent connections. Therefore, the authors have proposed a mechanism to increase the network scalability through a 3D-routing concept for VANETs, using a position-based routing to improve the routing performance in VANET.

3 UAV-Assisted Cooperative Routing Scheme (UCRS)

The Vehicular Ad hoc Network (VANET) considered in this research work consists of a set of wireless nodes that are deployed randomly on a flat surface along with the road structure. Each vehicle in the network has built-in wireless transceivers and is pre-programmed to identify itself through a unique node identifier. All the vehicles are assumed to have equal characteristics in terms of processing capabilities, sensing range, and memory. However, the destination is assumed to have higher capabilities and is considered as a base/ground station. Additionally, each node (Vehicle/UAV) is equipped with the Global positioning system (GPS) to monitor the geographical position and is capable to maintain its own tables used to perform routing. Energy constraint is neglected in this model, and it is supposed that each node is equipped with enough battery.

In the model depicted in Fig. 2, communication among vehicles is shown which can take assistance from Flying ad hoc network (FANET). A dense vehicular network environment has been considered, which may reflect the scenario of congestion. UAVs deployed in a dense urban environment can act as a relay node between vehicles whenever a disconnection in VANET is predicted [30]. UAVs receive commands from ground stations regarding the disconnected areas, the nearest UAV will move toward the desired location, the vehicle will take assistance from the UAV and will provide information about the destination location. UAVs present in the FANET will transmit the data packet to the final destination. This is how a UAV assisted VANET is established. Each vehicle in VANET determines two different zones based on the position of its neighboring nodes. All vehicles which are available in front of a particular vehicle based on its vicinity are retained in the front-zone and all those nodes which are behind a particular vehicle and are within the vicinity of a particular node are retained in the behind-zone. The less congested vehicles amongst the nodes available in the front-zone are stored in Allied Node Table (ANT). All the nodes in ANT have enough resources to be part of the reliable route. However, the best node or vehicle among all the nodes in ANT is selected based on the composite metric during the route reply procedure.

Whenever a particular vehicle along the route from source to a destination becomes congested or link failure occurs during the course of data communication, it needs to take assistance. For that purpose, FANET has been used and each node (UAV) in FANET covers a larger coverage area as compared to the vehicles used in VANET. Thus, assistance from FANET provides an extra benefit of coverage enhancement

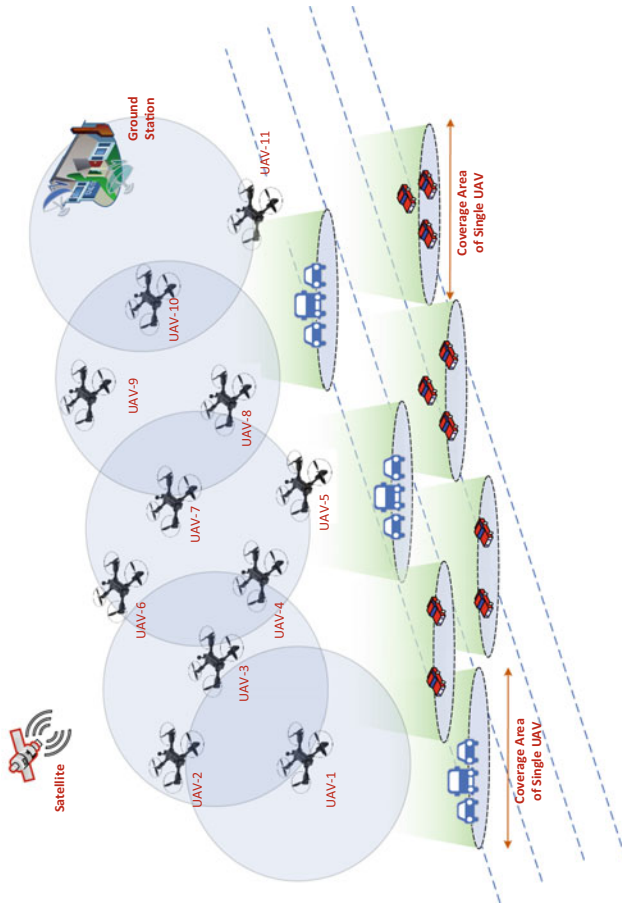


Fig. 2 System model used in UAV-assisted cooperative routing scheme (UCRS)

as well as reduces the latency with a smaller number of hop count. It is assumed that UAVs fly at low altitudes. Low altitude restriction ensures the safety and avoids collision with other aircraft [31].

3.1 Direction Towards Destination

It is assumed that every node is well aware of the destination node and its geographical position. With the consideration of this assumption, the direction towards a destination can be estimated easily. Additionally, certain criteria are established for categorizing front and behind zones. The nodes in the front zone of a specific node are selected by considering the relative speed and direction towards the destination. The forwarding angle is computed as follows and is also used in [28].

$$\theta = \cos^{-1} \frac{d_{rn_d} - d_{lh-rn}}{\sqrt{(d_{lh_d} - d_{lh-rn})^2} - \sqrt{(d_{rn_d} - d_{lh-rn})^2}}, \quad \therefore \theta \leq 180^\circ \quad (1)$$

where; d_{rn_d} is the distance of reference node from destination node. d_{lh-rn} is the distance of last hop from reference node d_{lh_d} is the distance of last hop from destination node. The forward angle is used to determine the nodes in the front-zone as well as behind zone. If the angle between the last hop (lh) and reference nodes (rn) is less than 180° . Then the reference node is in the forward zone of the last hop in the direction towards the destination node (d).

3.2 Speed of Node

The speed of a node is computed in relevance with the speed of other nodes present in the front zone. Whenever a node selects the next-hop node, its speed is also taken into account. Node with comparable relevant speed is allowed to be the part of the route from source to destination and is computed below:

$$V_i = \frac{V_{lh} - V_{rn}}{V_{max}} \quad (2)$$

In Eq. (2), V_i is the relative velocity of node “i”, V_{lh} is the speed of forwarding node, V_{rn} is the speed of next hop node, while V_{max} is the maximum speed of the node in the vicinity, which is assumed as 120 km/h.

3.3 Traffic Load or Congestion-Level

Each node in the network maintains the traffic flows that are passing through the node. These flows are identified through the flooding ID, which is determined through the source and the broadcast identifiers. The nodes which accommodate a greater number of flows are more prone to congestion so that is why such nodes are represented as congested nodes. Currently, it is assumed that an intermediate node can have a maximum of seven flows in the network.

3.4 Composite Metric

Composite metric comprises of three different parameters, i.e., relative speed, signal strength, and congestion level. Using this composite metric, the best node among the available nodes from ANT is selected. Composite metric is calculated at each hop during Cooperative Route Response (CRRS) along the way from destination towards the source. However, while disseminating the Cooperative Route Request (CRRQ) message, if Time to live (TTL) value approaches 32 hops, which is also used in AODV [32], then further, CRRQ will not be disseminated in the network. Composite metric uses the weighted sum of unit-less quantities that are relative speed, signal strength, and congestion level, as shown below;

$$CM = \alpha \times V_i + \beta \times S_{rx_thi} + \gamma \times T_{fi} \quad (3)$$

In Eq. (3), α , β and γ are constants with equal weights.

To establish a cooperative route from source to destination in VANET, along with the periodic messages to populate the ANT, a broadcast message, which is referred to as Cooperative Route Request (CRRQ)—generated by the source node to discover the destination in the network. Additionally, if the destination found through the dissemination of CRRQ messages received by the nodes, then the destination requires to send the response by generating a Cooperative Route Response (CRRS) towards the source. The following text shows the description of ANT, CRRQ, and CRRS. In UCRS, the Allied node table (ANT) is populated based on the entries received during the 1-hop Hello broadcast message dissemination. As each node in the network periodically sends the 1-Hop Hello messages. In this message, three important parameters aforementioned above are included.

3.5 Working Principle of UCRS

The working principle of the proposed work is depicted through a flow chart in Fig. 3 and elaborated with the scenario shown in Fig. 4a. Initially, all the nodes in vehicular

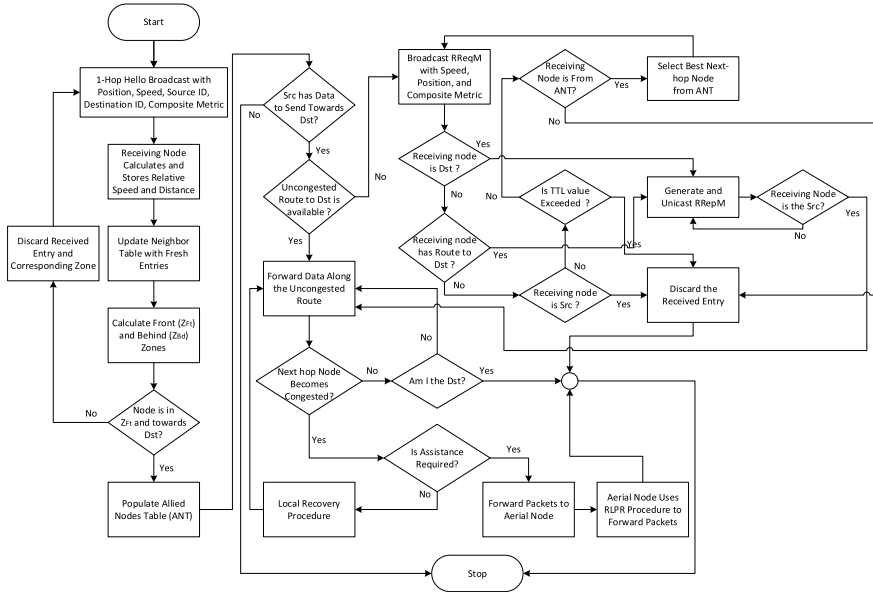
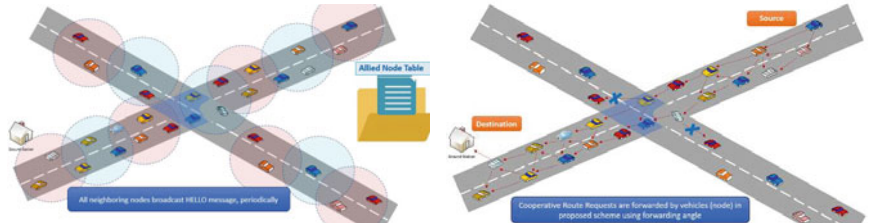
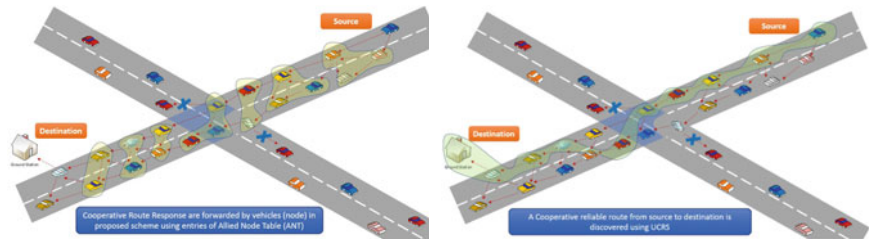


Fig. 3 UCRS working based on flow chart to populate allied node table and route discovery along with data traffic transmission



(a) Periodic 1-Hop HELLO message broadcast (b) Cooperative route request (CRRQ) dissemination procedure in VANET



(c) Cooperative route response (CRRS) (d) End-to-End (ETE) Cooperative Route dissemination procedure in VANET

Fig. 4 A scenario depicting the working principle of UCRS

network broadcast 1-Hop Hello messages, periodically, and share a set of information including node position, number of traffic flows as congestion-level, relative speed, and angle—to determine the front and behind zone. In contrast to this, the node when receives a Hello message, calculates a signal strength. All the information that is received and determined in 1-Hop Hello message is maintained in the table. Each node segregates its neighbors in front zone and behind zone and populate allied node table based on uncongested suitable nodes. Source or the originator node broadcasts the CRRQ packet to all the nodes in its vicinity, if it does not have the route to the destination; and the nodes in the front zone shall further rebroadcast the request based on ANT entries. Nodes that are not in the front zone or moving away from destination will simply discard the CRRQ message as shown in Fig. 4b. Once the Cooperative route request reaches the destination, it will select the best node out of allied nodes based on the unicast Cooperative route response message (CRRS).

Destination Node, when receives the first CRRQ, sends a unicast reply to the node from where it receives the CRRQ as depicted in Fig. 4c. The node that receives the CRRS needs to compute the best node from ANT based on the value of composite metric. This procedure continues until the CRRS reaches to the source node. At this stage, the ETE cooperative route is discovered as shown in Fig. 4d. Once the CRRS packet reaches the main originator node for a particular flow, it starts to transmit data packets to the discovered route. During the course of data communication, whenever a disconnection occurs or link failure detected between the nodes which are available in the active route, the node that discovers this failure, initiates a local recovery procedure to re-establish the path. In case local recovery could not resolve the issue, the node then tries to seek assistance from the other network i.e., FANET, and shown in Fig. 5. Now data will travel via aerial nodes until it reaches the destination node.

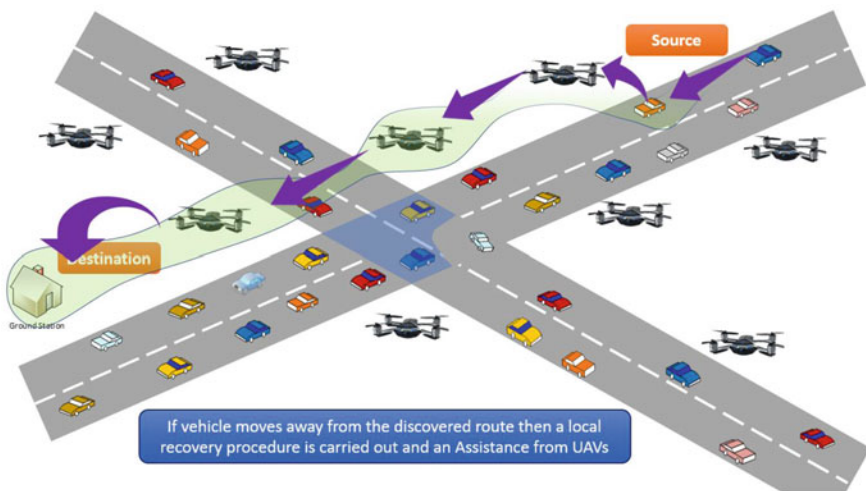


Fig. 5 Getting assistance from UAVs during the course of data communication in VANET

Table 1 Simulation parameters used to evaluate and compare with state-of-the-art techniques

Simulation parameter	Value
Frequency	2.4 GHz
CS_Thresh_	5.01E-12
RX_Thresh_	3.65E-10
Channel type	Wireless channel
Propagation model	Two ray ground (VANET) Free space (FANET)
MAC type	IEEE 802.11p
Interface queue type	DropTail
Max packet in queue	50
Routing protocol	AODV U2RV UCRS

4 Simulation Results and Discussion

The simulation model is designed to describe the UCRS protocol in comparison with various routing protocols like AODV and U2RV. Simulation parameters are defined in Table 1 and the algorithm of UCRS is already described in previous section. However, the performance evaluation of UCRS in comparison with AODV and U2RV is carried out based on varying node density.

Impact of Varying Node Density

The node density generally refers to the number of neighbors of a particular node in the network. With a higher node density, the channel acquisition time to send the traffic increases. This increases the delay to forward the data packets. Figure 6 shows

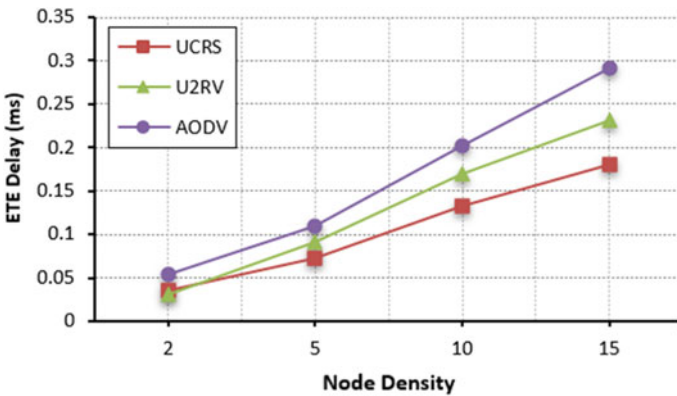


Fig. 6 Impact of node density on ETE Delay with 7 different number of sources

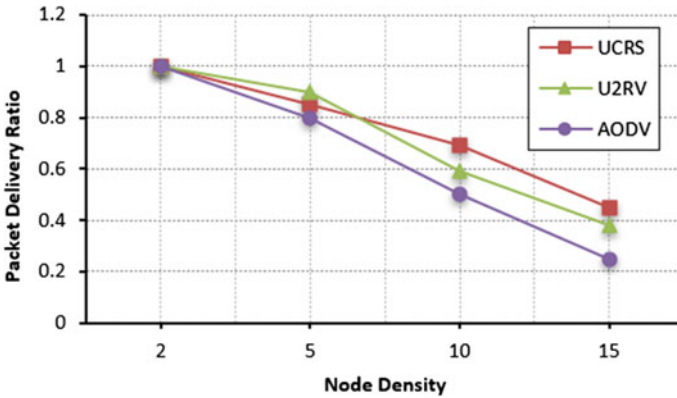


Fig. 7 Impact of node density on packet delivery ratio with 7 different number of sources

that ETE delay as compared to an increase in the node density. It has been observed that with a smaller number of neighboring nodes, the ETE delay is less in all the protocols. However, with the increase in the node density, UCRS shows 35% less ETE delay as compared to AODV while 16% less ETE delay as compared to U2RV. This is because, in UCRS, only allied nodes within the front zone are allowed to grab the channel so the nodes have a high probability to acquire the channel for data packets. In contrary to this, in U2RV and in AODV, all the neighboring nodes are required to acquire the channel for route discovery messages so the probability of acquiring the channel for data packets decreases. This decreases the ETE delay as the nodes need to queue the packets.

In Fig. 7, the PDR shows a decreasing trend with the increase in the number of neighboring nodes in the network. It has been observed that with 2 node-density, the PDR is 100% in a network with 100 nodes. However, as the node density increases,

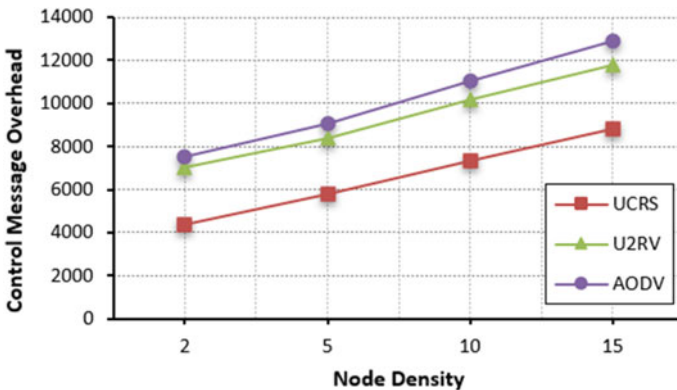


Fig. 8 Impact of node density on control message overhead with 7 different number of sources

the PDR decreases. This decrease is smaller in UCRS as compared to U2RV and AODV because of the selection of those nodes which are towards the destination and are uncongested. In contrary to this, U2RV and AODV, show a higher decrease in PDR. This is because, with higher node density, the nodes become congested, and due to congestion, the packet loss increases, and this decreases the PDR in the network. Additionally, with the increases in node density, the control message overhead increases in U2RV and AODV. Figure 8 shows that the control message overhead in UCRS is 36% less than AODV while 31% less than U2RV.

5 Conclusions

Routing in VANET is one of the major aspects to increase the performance of the network. Albeit the highly dynamic environment in VANET, where disseminating messages with high node density to the intended destination without any interruption is a critical task. Existing data dissemination techniques using single-radio devices do face degradation in network performance especially with the increase in end-to-end (ETE) delay and decreased throughput because of the inefficient spectrum utilization. To deal with this, techniques that used assistance from other channels that generally referred as dual-radio multi-channel have been proposed, which can efficiently use the spectrum; however, due to the cross-channel interference in the same band, the network performance degrades. Therefore, in this work, a UAV-assisted Cooperative Routing Scheme (UCRS) has been proposed, where Flying ad hoc network (FANET) provides assistance to VANET. The simulation analysis showed that UCRS experienced 35% less ETE delay as compared to AODV while 16% less ETE delay as compared to U2RV. Additionally, the control message overhead in UCRS is 36% less than AODV while 31% less than U2RV.

References

1. Fan X, Huang C, Fu B, Wen S, Chen X (2018) Uav-assisted data dissemination in delay-constrained vanets. *Mobile Inf Syst* 2018
2. Al-Heety OS, Zakaria Z, Ismail M, Shakir MM, Alani S, Alsariera H (2020) A comprehensive survey: benefits, services, recent works, challenges, security, and use cases for sdn-vanet. *IEEE Access* 8:91028–91047
3. Senouci O, Harous S, Aliouat Z (2020) Survey on vehicular ad hoc networks clustering algorithms: Overview, taxonomy, challenges, and open research issues. *Int J Commun Syst* 33(11):e4402
4. Oubbati OS, Lakas A, Lagraa N, Yagoubi MB (2016) Uvar: an intersection uav-assisted vanet routing protocol. In: 2016 IEEE wireless communications and networking conference, pp 1–6. IEEE
5. Filippi A, Moerman K, Daalderop G, Alexander PD, Schober F, Pfliegl W (2016) Ready to roll: why 802.11 p beats lte and 5g for v2x. NXP Semiconductors, Cohda Wireless and Siemens White Paper

6. Sun Y, Lin X, Lu R, Shen X, Su J (2010) Roadside units deployment for efficient short-time certificate updating in vanets. In: 2010 IEEE international conference on communications, pp 1–5. IEEE
7. Aslam B, Amjad F, Zou CC (2012) Optimal roadside units placement in urban areas for vehicular networks. In: 2012 IEEE symposium on computers and communications (ISCC), pp 000423–000429. IEEE
8. Almohammed AA, Noordin NK, Sali A, Hashim F, Balfaqih M (2017) An adaptive multi-channel assignment and coordination scheme for IEEE 802.11 p/1609.4 in vehicular ad-hoc networks. *IEEE Access* 6:2781–2802
9. Oubbati OS, Lakas A, Zhou F, Güneş M, Lagraa N, Yagoubi MB (2017) Intelligent uav-assisted routing protocol for urban vanets. *Comput Commun* 107:93–111
10. Zhou Y, Cheng N, Lu N, Shen XS (2015) Multi-uav-aided networks: aerial-ground cooperative vehicular networking architecture. *IEEE Veh Technol Mag* 10(4):36–44
11. Messous M-A, Senouci S-M, Sedjelmaci H (2016) Network connectivity and area coverage for uav fleet mobility model with energy constraint. In: 2016 IEEE wireless communications and networking conference, pp 1–6. IEEE
12. Han QIU, Meikang QIU, Zhihui LU, Memmi G (2019) An efficient key distribution system for data fusion in v2x heterogeneous networks. *Inf Fusion* 50:212–220
13. Gupta L, Jain R, Vaszkun G (2015) Survey of important issues in uav communication networks. *IEEE Commun Surv & Tutor* 18(2):1123–1152
14. Bor-Yaliniz I, Yanikomeroglu H (2016) The new frontier in ran heterogeneity: multi-tier drone-cells. *IEEE Commun Mag* 54(11):48–55
15. Shi W, Zhou H, Li J, Wenchao X, Zhang N, Shen X (2018) Drone assisted vehicular networks: architecture, challenges and opportunities. *IEEE Netw* 32(3):130–137
16. Khan IU, Qureshi IM, Aziz MA, Cheema TA, Shah SBH (2020) Smart iot control-based nature inspired energy efficient routing protocol for flying ad hoc network (fanet). *IEEE Access* 8:56371–56378
17. Lakew DS, Sa'ad U, Dao N-N, Na W, Cho S (2020) Routing in flying ad hoc networks: a comprehensive survey. *IEEE Commun Surv & Tutor* 22(2):1071–1120
18. Khan MF, Yau K-LA (2020) Route selection in 5g-based flying ad-hoc networks using reinforcement learning. In: 2020 10th IEEE international conference on control system, computing and engineering (ICCSCCE), pp 23–28. IEEE
19. Jiang S, Huang Z, Ji Y (2020) Adaptive uav-assisted geographic routing with q-learning in vanet. *IEEE Commun Lett* 25(4):1358–1362
20. Liu Q, Shi L, Sun L, Li J, Ding M, Shu F (2020) Path planning for uav-mounted mobile edge computing with deep reinforcement learning. *IEEE Trans Veh Technol* 69(5):5723–5728
21. Zhang S, Zhang H, Song L (2020) Beyond d2d: full dimension uav-to-everything communications in 6g. *IEEE Trans Veh Technol* 69(6):6592–6602
22. He Y, Zhai D, Jiang Y, Zhang R (2020) Relay selection for uav-assisted urban vehicular ad hoc networks. *IEEE Wireless Commun Lett* 9(9):1379–1383
23. He Y, Zhai D, Wang D, Tang X, Zhang R (2020) A relay selection protocol for uav-assisted vanets. *Appl Sci* 10(23):8762 Dec
24. Oubbati OS, Lakas A, Lagraa N, Yagoubi MB (2015) Cruv: connectivity-based traffic density aware routing using uavs for vanets. In: 2015 International conference on connected vehicles and expo (ICCVE), pp 68–73. IEEE
25. Wang X, Luoyi F, Zhang Y, Gan X, Wang X (2016) Vdnet: an infrastructure-less uav-assisted sparse vanet system with vehicle location prediction. *Wireless Commun Mobile Comput* 16(17):2991–3003
26. Do-Duy T, Nguyen LD, Duong TQ, Khosravirad S, Claussen H (2021) Joint optimisation of real-time deployment and resource allocation for uav-aided disaster emergency communications. *IEEE J Selected Areas Commun*
27. Oubbati OS, Lakas A, Zhou F, Güneş M, Yagoubi MB (2017) A survey on position-based routing protocols for flying ad hoc networks (fanets). *Veh Commun* 10:29–56

28. Usman Q, Chughtai O, Nawaz N, Kaleem Z, Khaliq KA, Nguyen LD (2021) A reliable link-adaptive position-based routing protocol for flying ad hoc network. *Mobile Netw Appl* 1–20
29. Sehgelmeble YC, Fischer S (2020) A different perspective in routing for vanets. In: 2020 international symposium on networks, computers and communications (ISNCC), pp 1–4
30. Sedjelmaci H, Messous MA, Senouci SM, Brahmi IH (2018) Toward a lightweight and efficient uav-aided vanet. *Trans Emerg Telecommun Technol* 30(8):e3520
31. Oubbati OS, Chaib N, Lakas A, Lorenz P, Rachedi A (2019) Uav-assisted supporting services connectivity in urban vanets. *IEEE Trans Veh Technol* 68(4):3944–3951
32. Perkins C, Belding-Royer E, Das S (2021) Request for comment (rfc) 3561: Ad hoc on-demand distance vector (aodv) routing, 2003, accessed the RFC on Feb 2021